

## PROMPT FISSION NEUTRON SPECTRA

The following States are Members of the International Atomic Energy Agency:

AFGHANISTAN	GUATEMALA	PAKISTAN
ALBANIA	HAITI	PANAMA
ALGERIA	HOLY SEE	PARAGUAY
ARGENTINA	HUNGARY	PERU
AUSTRALIA	ICELAND	PHILIPPINES
AUSTRIA	INDIA	POLAND
BELGIUM	INDONESIA	PORTUGAL
BOLIVIA	IRAN	ROMANIA
BRAZIL	IRAQ	SAUDI ARABIA
BULGARIA	IRELAND	SENEGAL
BURMA	ISRAEL	SIERRA LEONE
BYELORUSSIAN SOVIET	ITALY	SINGAPORE
SOCIALIST REPUBLIC	IVORY COAST	SOUTH AFRICA
CAMEROON	JAMAICA	SPAIN
CANADA	JAPAN	SUDAN
CEYLON	JORDAN	SWEDEN
CHILE	KENYA	SWITZERLAND
CHINA	KHMER REPUBLIC	SYRIAN ARAB REPUBLIC
COLOMBIA	KOREA, REPUBLIC OF	THAILAND
COSTA RICA	KUWAIT	TUNISIA
CUBA	LEBANON	TURKEY
CYPRUS	LIBERIA	UGANDA
CZECHOSLOVAK SOCIALIST	LIBYAN ARAB REPUBLIC	UKRAINIAN SOVIET SOCIALIST
REPUBLIC	LIECHTENSTEIN	REPUBLIC
DENMARK	LUXEMBOURG	UNION OF SOVIET SOCIALIST
DOMINICAN REPUBLIC	MADAGASCAR	REPUBLICS
ECUADOR	MALAYSIA	UNITED KINGDOM OF GREAT
EGYPT, ARAB REPUBLIC OF	MALI	BRITAIN AND NORTHERN
EL SALVADOR	MEXICO	IRELAND
ETHIOPIA	MONACO	UNITED STATES OF AMERICA
FINLAND	MOROCCO	URUGUAY
FRANCE	NETHERLANDS	VENEZUELA
GABON	NEW ZEALAND	VIET-NAM
GERMANY, FEDERAL REPUBLIC OF	NIGER	YUGOSLAVIA
GHANA	NIGERIA	ZAIRE, REPUBLIC OF
GREECE	NORWAY	ZAMBIA

The Agency's Statute was approved on 23 October 1956 by the Conference on the Statute of the IAEA held at United Nations Headquarters, New York; it entered into force on 29 July 1957. The Headquarters of the Agency are situated in Vienna. Its principal objective is "to accelerate and enlarge the contribution of atomic energy to peace, health and prosperity throughout the world".

Printed by the IAEA in Austria

October 1972

PANEL PROCEEDINGS SERIES

## PROMPT FISSION NEUTRON SPECTRA

PROCEEDINGS OF A CONSULTANTS' MEETING  
ON PROMPT FISSION NEUTRON SPECTRA  
ORGANIZED BY THE  
INTERNATIONAL ATOMIC ENERGY AGENCY  
AND HELD IN VIENNA, 25-27 AUGUST 1971

INTERNATIONAL ATOMIC ENERGY AGENCY  
VIENNA, 1972

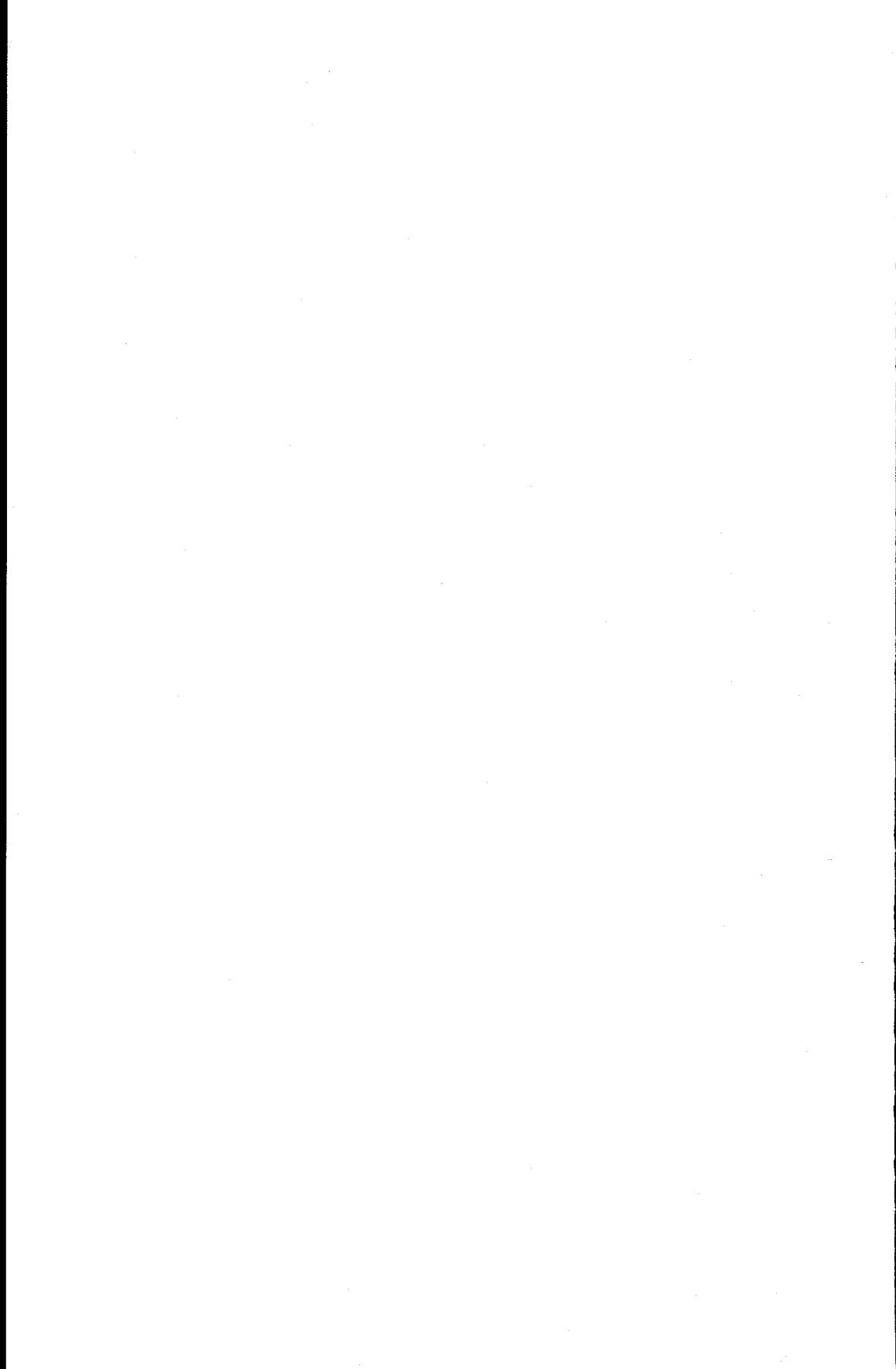
PROMPT FISSION NEUTRON SPECTRA  
IAEA, VIENNA, 1972  
STI/PUB/329

## FOREWORD

The fission neutron spectrum occupies a key position among the nuclear data required for application in reactor design. A detailed knowledge of fission spectra is important not only for reliable prediction of the physics characteristics of fast power breeder reactors, but also for other applications. The increasing use of 'integral' data measurements with critical assemblies for the adjustment of evaluated data is one factor that focuses the interest on fission spectra. Several cases of discrepancies between differential data and data measured as averages over fission spectra need clarification. For several categories of nuclear data either  $^{252}\text{Cf}$  or  $^{235}\text{U}$  fission spectra serve as standards.

Upon the recommendation of the International Nuclear Data Committee, the IAEA held a Consultants' Meeting on the Status of Prompt Fission Neutron Spectra on 25-27 August 1971 at its Headquarters in Vienna. The consultants' group was called together within the framework of the nuclear data review program of the Nuclear Data Section of the Agency. Similar experts' meetings have been held in the past to review well-defined and important nuclear data problems, for example the capture-to-fission ratio of  $^{239}\text{Pu}$ , the report of which was included in the proceedings of the Second International Conference on Nuclear Data for Reactors held by the IAEA in Helsinki in 1970.

This report is one result of the Consultants' meeting. It contains the papers presented at the meeting, together with the resultant recommendations. As a further consequence of the meeting a number of experimental investigations and critical reviews of new and old data will be motivated and influenced by the Recommendations, which were established as the consensus of opinion of the experts present at the meeting and were drawn up and annotated by the Chairmen.



# CONTENTS

Introduction .....	1
A.T.G. Ferguson, A.B. Smith	
Fission neutron spectra: Perspective and suggestion .....	3
A.B. Smith	
A review of prompt fission neutron spectrum data for $^{235}\text{U}$ and $^{239}\text{Pu}$ neutron-induced fission and $^{252}\text{Cf}$ spontaneous fission .....	19
A. Koster	
Brief review of integral measurements with fission spectrum neutrons .....	29
J.A. Grundl	
Discrepancies between integral and differential measurements of the prompt fission neutron energy spectrum .....	33
C.G. Campbell, J.L. Rowlands	
Fission neutron energy spectra induced by fast neutrons on $^{238}\text{U}$ , $^{235}\text{U}$ and $^{239}\text{Pu}$ .....	41
H.-H. Knitter, M. Coppola, M.M. Islam, N. Ahmed, B. Jay	
A measurement of the prompt fission neutron spectrum of $^{235}\text{U}$ at 0.5-MeV incident neutron energy: Tentative results .....	59
P.I. Johansson, E. Almén, B. Holmqvist, T. Weidling	
Fission neutron spectra measurements of $^{235}\text{U}$ , $^{239}\text{Pu}$ and $^{252}\text{Cf}$ .....	65
H. Werle, H. Bluhm	
Fission neutron spectrum measurement of $^{252}\text{Cf}$ .....	81
L. Jéki, Gy. Kluge, A. Lajtai, P.P. Dyachenko, B.D. Kuzminov	
Delayed neutrons from spontaneous fission of $^{252}\text{Cf}$ .....	89
V.N. Nefedov, A.K. Melnikov, B.I. Starostov	
Difference of microscopic integral cross-section ratios in the $^{235}\text{U}$ and $^{239}\text{Pu}$ thermal fission neutron spectra .....	97
A. Fabry	
Measurement of the average fission cross-section ratio, $\bar{\sigma}_f(^{235}\text{U})/\bar{\sigma}_f(^{238}\text{U})$ , for $^{235}\text{U}$ and $^{239}\text{Pu}$ fission neutrons .....	107
J.A. Grundl	
Integral check of fission neutron spectrum through average cross-sections for some threshold reactions .....	113
I. Kimura, K. Kobayashi, T. Shibata	
The influence of fission neutron spectra on integral nuclear quantities of fast reactors .....	129
E. Kiefhaber, D. Thiem	
Prompt fission neutron spectra .....	149
Gy. Kluge	
Remarks on neutron fission related to the relative importance of the symmetric and asymmetric fission modes .....	161
Ghislaine de Leeuw-Gierts, S. de Leeuw	
Conclusions and recommendations .....	169
List of participants .....	175

\_\_\_\_\_



## INTRODUCTION

A. T. G. FERGUSON

AERE Harwell,  
Didcot, Berks,  
United Kingdom

A. B. SMITH

Argonne National Laboratory,  
Argonne, Ill.,  
United States of America

Prompt fission-neutron emission was observed more than three decades ago. Soon thereafter a number of microscopic measurements showed that the energy spectrum of these neutrons was an 'evaporation' distribution with an average energy of  $\sim 2.0$  MeV. This observation was consistent with the theoretical concept of neutron emission from a highly excited and rapidly moving fragment.<sup>1</sup> In retrospect, these early studies of fission neutron spectra were remarkably descriptive of the phenomena. More recent microscopic measurements employing the best available contemporary technology have substantiated the qualitative features of the earlier results and extended our knowledge over a wider mass-energy range. Much of the recent work emphasized the relation of the spectrum to fission kinetics, neutron emission probabilities, angular correlations and to the possible existence of energy-dependent structure. These detailed results were not always consistent and had minor impact on contemporary nuclear energy programs, which were largely associated with thermal reactor concepts. The performance of thermal reactor systems is not particularly sensitive to the details of the fission spectra and, generally, the available information was sufficient for the applied development programs. However, discrepancies between microscopic and macroscopic observations did exist; notably in the interpretation of solid-metal critical experiments, and the understanding of 'age' and certain macroscopic indexes such as fission ratios. Some of these discrepancies did not withstand careful examination, others were attributed to uncertainties in associated fast neutron data and some simply remained. Thus stood the matter of fission neutron spectra until relatively recently.

As it became clear that long-term energy requirements would likely be met with the development of the fast reactor, fast neutron properties including the fission neutron spectrum became of increased importance. The experimental and theoretical understanding of fast reactor neutronics and of basic fast neutron cross-sections rapidly improved. However, certain critical discrepancies between calculated and measured fast reactor performance remained troublesome and were attributed to an uncertain knowledge of microscopic fast neutron properties including prompt fission neutron spectra, particularly those of  $^{238}\text{U}$  and  $^{239}\text{Pu}$ . In addition, the results of more accurate determinations of macroscopic spectral indexes

---

<sup>1</sup> It is interesting to note the validity of very early understanding of the fission process and fission neutron spectra as given, for example, in the papers by: J. Wheeler (Phys. Rev., 1940), L. Turner (Rev. Mod. Phys., 1940) and R. Peierls, Energy Distribution of Fission Neutrons, MS-65.

were often inconsistent with 'known' cross-section information or with the microscopically measured prompt-fission-neutron spectra. Many of the macroscopic interpretations indicated that the average prompt fission-neutron energy was significantly higher (~10%) than reported from microscopic measurement and that the distribution deviated from a simple 'evaporation' form. This conclusion was not entirely unambiguous as a number of possibly uncertain neutron parameters enter into the interpretations of, particularly, fast reactor neutronics. However, uncertainty in the fission neutron spectrum was strongly suggested and, if true, was an appreciable source of error in the development of major world-wide nuclear energy programs.

The importance of a precise knowledge of fission-neutron spectra was widely recognized by those responsible for fast reactor development and for the provision of nuclear data for applied programs. The INDC, the EACRP, the EANDC and a number of regional reactor and data groups gave detailed attention to the problem. Previous experimental results were critically reviewed and a number of new macroscopic and microscopic measurements implemented. Preliminary results from some of the latter were reported at the IAEA Conference on Nuclear Data for Reactors (Helsinki, 1970). Now, a year later, far more definitive results are emerging and a contemporary review of the status of prompt fission neutron spectra is warranted. This is recognized by the INDC and the IAEA in the convening of this consultants meeting gathering together active workers in fields from throughout the world. The objectives are to: (a) assay past and present microscopic and macroscopic knowledge of prompt fission neutron spectra; (b) summarize the present status of the field with such conclusions as warranted by the available information; and (c) to make such recommendations as are judged useful for guiding future efforts into a most productive course. Subsequent portions of these Proceedings deal in detail with these charges. Section 3 contains the individual papers contributed by the various consultants. These range from general contemporary reviews of the field, through comprehensive reports of new and precise experimental results to detailed plans for future work many of which have already been implemented. Collectively, these papers form a uniquely comprehensive summary of the current status of the field and give an indication of future results. From these contributions and discussions of the consultants, both generally and as subgroups, summary conclusions and recommendations are drawn and set forth in section 4. It is hoped that these will be of particular value in guiding future work and that they will assist the evaluator and other users in assaying the validity of the basic information utilized in applied calculations.

The consultants are indebted to the Agency for the opportunity to carry out these productive discussions in an important area of common interest and for the hospitality and services extended during their visit. The Chairmen thank all participants for so freely contributing the time and knowledge requisite to the productive meeting.

# FISSION NEUTRON SPECTRA: PERSPECTIVE AND SUGGESTION\*

A.B. SMITH  
Argonne National Laboratory,  
Argonne, Ill.,  
United States of America

## Abstract

FISSION NEUTRON SPECTRA: PERSPECTIVE AND SUGGESTION.

Recently reported macroscopic and spectrum-average measurements and the analysis of fast-critical experiments have suggested an uncertain knowledge of prompt-fission-neutron spectra. These suggestions re-kindled the author's long-term interest in the fission spectrum. Specifically, the applied importance of these uncertainties stimulated additional work at this Laboratory with the objective of testing certain of the postulates put forth as the result of the macroscopic studies. In preparation for new experimental work the status of prompt-fission-neutron spectra was assayed and the results of that survey have received a limited distribution. The pertinent experimental work at this Laboratory is now complete. Essentially concurrently a number of new experimental results have become available at other laboratories. In the following resumé the present status of prompt-fission-neutron spectra is outlined inclusive of both the new and the older results. Primary emphasis is given to basic microscopic information with attention to associated experimental problems and limitations.

## I. Macroscopic Characteristics

### A. Fission-Neutron Spectra

Current uncertainties arise, to a large extent, from the results of recent macroscopic studies employing various reaction indices<sup>1-5</sup> and from the detailed analysis of fast critical assemblies.<sup>5-8</sup>

The interpretation and adjustment of basic data from the analysis of fast critical experiments is difficult. However, from such analyses Campbell and Rowlands suggest that average-fission-neutron spectrum energy is 5-10% higher than indicated by microscopic measurement and that the spectrum shape may differ from a Maxwellian form.<sup>6</sup> Similar uncertainties have been discussed in relation to the fast critical assemblies ZEBRA-2 and ZPR-3 by Okrent et al.<sup>7</sup> The details of the fast critical analyses are too complex for description here. However, it appears that most of the calculations give no consideration to the dependence of the fission-neutron energy and/or spectrum on the energy of the fission-inducing incident neutron. This dependence may be significant, particularly in very fast assemblies.<sup>16</sup>

Some reaction-rate measurements in fission-neutron spectra tend to support the suggestions resulting from critical-assembly studies.<sup>1-5</sup> However, the interpretation is again neither simple nor unique as a number of uncertain physical parameters are involved in addition to

---

\* This document constitutes a summary of a working paper submitted to the Working Group and is contemporary with pre-meeting status. The full text of the paper is available as INDC(USA)-37/G and contains details and recommendations not provided in this summary. Many of the latter recommendations are essentially the same as those of the Working Group set forth elsewhere in these Proceedings.

Table 1. Macroscopic Fission Spectrum Parameters.

Isotope	E(ave), MeV <sup>a</sup>	E(in), MeV <sup>b</sup>	Ratio <sup>c</sup>	Reference
U-233	1.998	TH	0.982	21
	-----	TH	1.015	19
	-----	TH	1.021 +- 0.005	4
	-----	TH	1.020 +- 0.005	24
	1.960			20 ENDF
U-235	2.100 +- 0.100	FAST CRIT.	-----	6
	2.034	TH	-----	21
	1.950	TH	-----	17
	1.950 - 2.025	FAST	-----	1
	2.200	TH	-----	4
	2.240	TH	-----	2
	2.060	TH	-----	22
	2.025	TH	-----	18
	1.950			20 ENDF
Pu-239	2.077	TH	1.021	21
	-----	TH	1.040	19
	-----	TH	1.039 +- 0.002	4
	-----	TH	1.025 +- 0.0062	24
	2.115			20 ENDF
Pu-240	1.738	SP	0.854	21
Cf-252	2.050	SP	1.007	21
	2.085 +- 0.06	SP	-----	23

## Footnotes:

- Average fission neutron energy as given or deduced from the basic reference. Errors are omitted when not directly available.
- Incident neutron energy. TH=Thermal, Fast or Fast Crit.= Fast Critical spectrum, SP=Spontaneous fission.
- Ratio E(ave-X)/E(ave-235) is given when directly measured or deduced from same experimental set.

the inherent experimental error. The interpretation of such reaction-rate studies has recently been reviewed by Fabry et al.<sup>1</sup> and by Grundl.<sup>4</sup> The status of available macroscopic results is outlined in Table 1. The recent reaction-rate results of Refs. 2, 4 and 1 (to a lesser extent) all tend to indicate a larger average-fission-neutron energy than microscopic measurements. However, a number of other reaction-rate results are consistent with microscopic values including the recent work of Refs. 17 and 18. Generally the uncertainties in the macroscopic average tend to be large. In contrast some ratios of average energies are given to within very small (fractional %) errors. The ratio values appear to be the more reliable, as is true in most microscopic measurements. Thus the fact that the macroscopic values is particularly disturbing.

Over a number of years Fabry and co-workers<sup>1</sup> have experimentally studied the response of a wide range of detectors (mostly threshold reactions) in fission-spectrum environments. Apparently the initial

work was similar to that of Depuydt and Neve de Mevergnies.<sup>25</sup> In any case, the fission-spectrum measurements were made with an "in-cavity" arrangement. The early Fabry results indicated a 15-20% harder fission neutron spectrum than is usually obtained from microscopic measurements. Fabry concluded that his results were consistent with those of Grundl<sup>4</sup> and of Leachman and Schmidt.<sup>26</sup> The results were sensitive to the exact microscopic cross sections used in the interpretation. This critical matter is extensively discussed by Fabry in Ref. 1.

Grundl<sup>4,5</sup> carefully studied reaction rates using both a mono-energetic neutron source (Van deGraaff) and a fission source. His work has the merit of careful relative detector calibration free of many cross section-associated uncertainties. However, Grundl points out the importance of an accurate absolute energy scale and notes that uncertainties in energy of as little as 150 keV can lead to gross errors in subsequently determined average-fission-neutron energy values. The importance of careful calibrations should not be underestimated.

Grundl, like Fabry, used an "in-cavity" arrangement for producing a fission-neutron spectrum. Forty percent of the return flux from the surrounding material (a D<sub>2</sub>O water tank) was above 0.1 MeV. Grundl considered in detail this cavity perturbation using DSN calculations. However, the return-flux correction may not have been perfect and it is noted that the same laboratory went to considerable trouble to hang GODIVA (a bare metal critical) well above the ground to obtain a high-fidelity leakage spectrum. The cavity problem has been serious since Chadwick's time and it remains so.

Grundl deduced ratios of the average-fission-neutron energies of U-233 and Pu-239 to that of U-235 (see Table 1). The associated errors are very small. The Grundl ratios are very similar to other macroscopic ratio values; for example those of Bonner,<sup>21</sup> Harris<sup>19</sup> and Kovalev et al.<sup>24</sup> However, macroscopic-ratios remain seriously discrepant with those deduced from the majority of microscopic measurements. Grundl indicates an average-fission neutron energy for U-235 of  $\sim 2.2$  MeV, appreciably higher than that deduced from the majority of the microscopic and macroscopic measurements. He further suggests that the spectrum at low neutron energies is less intense than that given by a Maxwellian form in contrast to the opposite trend in some microscopic measurements.<sup>27,28,41</sup>

McElroy<sup>2,3</sup> has extensively analyzed reaction-rate measurements, primarily those of Grundl<sup>4</sup> and of Fabry.<sup>1</sup> He employs an iterative procedure with the computation code SAND-II and a library of selected microscopic cross sections to deduce detailed spectral distributions from the measured reaction rates. He suggests an average U-235 fission-neutron energy of  $\sim 2.24$  MeV, similar to that proposed by Grundl. In addition the spectrum deduced by McElroy is 20-40% lower than that indicated by a Maxwellian distribution at neutron energies of  $\sim 800$  keV. This is a large difference in a region where microscopic measurements are reliable. Indeed, a recent specifically designed microscopic experiment failed to verify the McElroy spectrum at these low energies.<sup>13</sup> To what extent the large discrepancy is due to uncertainties in the SAND-II procedures, the cross section library or the respective measurements is a moot question. However, it has been suggested that the SAND results are sensitive to small and essentially unknown sub-threshold reaction cross sections.<sup>29</sup>

B. Fission-Neutron Cross Section of U-238 in a U-235 Fission-Neutron Spectrum.

The quantity  $\sigma_f(X_{235}^{238}\text{U})$  is frequently cited as an index of the fission-neutron spectrum and of  $\sigma_f(238)$ . Representative experimental and calculated values are outlined in Table 2. The experimental values of Leachman and Schmidt,<sup>26</sup> of Richmond<sup>31</sup> and of Nikolaev et al.<sup>30</sup> are in the range 310-315 mb. The measured results of Fabry et al.<sup>1</sup> are somewhat larger. All of the experimental values are appreciably larger than the result calculated by Grundl<sup>4</sup> using microscopic spectra and selected U-238 fission cross sections. However, the calculated result of Campbell and Rowlands<sup>6</sup> based upon the data of Hart<sup>32</sup> is in reasonable agreement with the measurements. The results depend on the fission cross section of U-238 in the MeV region where recent microscopic measurements<sup>33</sup> indicate larger values than found in widely used evaluations.<sup>20</sup>

$\sigma_f(X_{235}^{238}\text{U})$  measurements have generally employed steady-state neutron beams or fluxes. This is in contrast to precision microscopic fission cross section measurements which employ pulsed-neutron sources and fast timing techniques to control background effects.

C. Age to Indium Resonance in H<sub>2</sub>O

The study of the age of U-235 fission neutrons to indium resonance in H<sub>2</sub>O has not received the attention warranted by its basic importance and relation to the fission-neutron spectrum. The measured and calculated results are outlined in Table 3. Experimental values prior to 1961 tend to be large; 27-31 cm<sup>2</sup>.<sup>35</sup> More recent experimental results are in the range 26-28 cm<sup>2</sup>.<sup>36,37</sup> The experiments did not generally use point sources but rather combinations of plane and other complex reactor-driven sources. As a consequence the deduction of the fundamental parameter from the measured values entailed considerable correction. Recent theoretical calculations based upon microscopic fission-neutron spectra<sup>22,38</sup> yield calculated ages very close to the later experimental values. Further, from age considerations, Story<sup>18</sup> concluded that the average-fission-neutron energy is very similar to the microscopic value. Harris<sup>19</sup> has pointed out that

Table 2. Measured and Calculated Values of  $\bar{\sigma}_f(X_{235}^{238}\text{U})$ .

Ref.	$\bar{\sigma}_f$ , mb
<u>Measured</u>	
Fabry et al. <sup>1</sup>	353 ± 30, 374 ± 30
Nikolaev et al. <sup>30</sup>	310 ± 10
Leachman and Schmidt <sup>26</sup>	313 ± 5
<u>Calculated</u>	
Grundl <sup>4</sup>	273 - 282 ± 5 <sup>a</sup>
Campbell and Rowlands <sup>6</sup>	301

<sup>a</sup>The lower value was obtained with a Maxwellian temperature = 1.29 MeV. The higher value from the Cranberg expression<sup>34</sup>.

Table 3. Age to Indium Resonance in  $H_2O$ .

Ref.	Age ( $cm^2$ )
<u>Measured</u>	
Summary of pre-1961 values <sup>35</sup>	27 - 31
Doerner et al. <sup>36</sup>	$27.9 \pm 0.1$
Paschall <sup>37</sup>	$26.6 \pm 0.3$
<u>Calculated</u>	
Dunford and Alter <sup>22</sup>	$26.46 \pm 0.32$
Staub et al. <sup>38</sup>	$25.4 \pm 26.4$
Story <sup>18</sup>	Deduces Average fission energy to be $\sim 2.025$ MeV

Table 4. Microscopic Fission Spectrum Parameters.

Isotope	E(ave), MeV <sup>a</sup>	E(in), MeV <sup>b</sup>	Ratio <sup>c</sup>	Reference
Th-229	$1.860 \pm 0.060$	TH	-----	41
Th-232	2.250	14.0	1.068	42
U-233	$1.870 \pm 0.080$	TH	$0.960 \pm 0.03$	11
	Exp. Decade	TH	-----	43
	=ABOUI 4.2 MeV			
	$2.300 \pm 0.120$	14.0	1.108	42
U-235	$2.010 \pm 0.00$	TH	-----	40
	$1.956 \pm 0.013$	TH	-----	27
	$2.020 \pm 0.025$	TH	-----	27
	$2.110 \pm 0.150$	0.03-0.4	-----	13
	$1.900 \pm 0.200$	TH	-----	44
	2.000	TH	-----	45
	Exp. Decade	TH	-----	46
	=3.900 $\pm$ 0.2 MeV			
	2.060	0.03	-----	34
	$1.946 \pm 0.045$	0.1	-----	47
	$1.800 \pm 0.100$	TH	-----	48
	$1.905 \pm 0.019$	0.95	-----	49
	$1.860 \pm 0.060$	0.04	-----	50
	$1.860 \pm 0.060$	1.5	-----	50
	$2.040 \pm 0.060$	14.3	-----	51
	$2.075 \pm 0.090$	14.0	-----	42
	1.982	TH	-----	52
U-238	$1.927 \pm 0.045$	2.09	-----	47
	$2.133 \pm 0.048$	4.09	-----	47
	$1.935 \pm 0.030$	1.35	-----	49
	$2.190 \pm 0.070$	14.3	-----	51
	$2.320 \pm 0.120$	14.0	1.118	42
	$2.019 \pm 0.080$	1.9	-----	69
	$1.850 \pm 0.080$	2.3	-----	69
Pu-238	$2.025 \pm 0.060$	TH	-----	41

Table 4. (Cont.)

Isotope	E(ave), Mev	E(in), MeV	Ratio	Reference
Pu-239	2.136 $\pm$ 0.024	TH	1.092 $\pm$ 0.014	27
	2.075 $\pm$ 0.017	TH	1.028 $\pm$ 0.012	27
	-----	0.03 - 0.4	1.075 $\pm$ 0.02	13
	Exp. Decade =4.3 $\pm$ 0.2	TH	-----	53
	2.110 $\pm$ 0.044	0.13	1.084 $\pm$ 0.03	47
	2.010 $\pm$ 0.060	0.04	1.080 $\pm$ 0.04	50
	2.025 $\pm$ 0.060	TH	-----	54
	1.815	0.3-1.5	-----	55
	2.175 $\pm$ 0.070	+1.9	-----	56
	2.120 $\pm$ 0.070	1.5	-----	57
	2.180 $\pm$ 0.060	1.9	-----	57
	2.280 $\pm$ 0.060	2.3	-----	57
	2.270 $\pm$ 0.100	4.0	-----	57
	2.530 $\pm$ 0.090	4.5	-----	57
	2.420 $\pm$ 0.100	5.0	-----	57
	2.420 $\pm$ 0.080	5.5	-----	57
	2.375 $\pm$ 0.120	14.0	1.144	42
Pu-241	2.002 $\pm$ 0.051	TH	1.027	10
Pu-242	1.810 $\pm$ 0.11	SP	-----	54
Am-242M	2.130 $\pm$ 0.050	TH	-----	41
Cm-244	2.055 $\pm$ 0.060	SP	-----	54
	2.070 $\pm$ 0.060	TH	-----	41
	2.187 $\pm$ 0.093	SP	-----	58
Cm-245	2.250 $\pm$ 0.070	TH	-----	41
Cf-249	2.320 $\pm$ 0.060	TH	-----	41
Cf-252	2.220 $\pm$ 0.050	SP	-----	41
	2.350 $\pm$ 0.100	SP	-----	12
	2.348 $\pm$ 0.100	SP	-----	28
	2.155 $\pm$ 0.024	SP	1.102 $\pm$ 0.014	27
	2.130 $\pm$ 0.022	SP	1.054 $\pm$ 0.015	27
	2.080	SP	-----	59
	2.340 $\pm$ 0.050	SP	-----	60
	2.085 $\pm$ 0.060	SP	1.120 $\pm$ 0.050	50
	2.100	SP	-----	61
	2.220 $\pm$ 0.040	SP	-----	41

Footnotes:

- Average fission neutron energy as given or deduced from the basic reference. Errors are omitted when not directly available.
- Incident neutron energy. TH=Thermal, Fast or Fast Crit.= FAST CRITICAL SPECTRUM, SP=Spontaneous fission.
- Ratio E(ave-X)/E(ave-235) is given when directly measured or deduced from same experimental set.



age is sensitive to changes in the average-fission-neutron energy; a 10% change in age corresponding to a  $\sim 200$  keV change in average energy at 2.0 MeV. He further concludes that  $\bar{E}(\text{Pu-239})/\bar{E}(\text{U-235}) \sim 1.04$ , a value similar to other macroscopic results.

## II. Microscopic Characteristics

### A. Average-Fission-Neutron Energies and their Ratios.

More than sixty microscopic measurements of fission-neutron spectra are reported in the literature. These results are outlined in Table 4 with the associated references giving an indication of method, range, quality and unusual properties.<sup>39</sup> More than thirty of the measurements pertain to U-235 and Pu-239 with the remainder distributed over the mass region  $A = 229 - 252$ . The incident neutron energy range extends from thermal to 14.3 MeV with additional spontaneous fission processes, principally Cf-252. The experimental techniques employed generally fall into three categories; 1) time-of-flight (TOF) using proton-recoil or reaction detectors, 2) proton-recoil spectrometers either in the form of counters or emulsions, and 3) reaction spectrometers such as Li-6 and He-3 counters. The measurements are most straightforward when obtained with thermal or low-energy ( $< 1.0$  MeV) neutron-induced or spontaneous fission. At higher incident neutron energies the observed spectrum is complicated by contributions from other neutron emitting processes, such as inelastic scattering, and the requisite corrections lead to greater uncertainties.

A qualitative inspection of Table 4 reveals several general characteristics. 1) No thermal or low-energy-neutron-induced fission spectrum for  $A \leq 244$  has been microscopically observed to have an average energy as large as the  $\sim 2.2$  MeV ascribed to some of the macroscopic results. 2) Uncertainties assigned to the average-energy values are not consistent with the discrepancies between measurements. The experimentalists have apparently been optimistic with a certain affinity for errors of 40-60 keV. 3) The ratio  $\bar{E}(\text{Pu-239})/\bar{E}(\text{U-235})$  deduced from microscopic measurements is, with one exception, consistently larger than the comparable macroscopic value. The exception is in doubt as the same group obtained a larger value using an alternate technique.<sup>27</sup> 4) There may be some tendency for microscopic  $\bar{E}$  values to grow with time but probably by less than 50-100 keV at most.

The average-neutron energies of U-235 thermal and low-energy neutron-induced fission are outlined in Table 5. The weighted average is 1.979 MeV with an RMS deviation of 4.3%. This average is not consistent with the larger macroscopic results. A similar outline of the average-fission-neutron energies of Pu-239 is given in Table 6. Two values of this Table are lower than the rest of the set with that of Ref. 50 being from a generally low set of values. The weighted average of Table 6 is 2.084 MeV or 2.093 MeV if the low value of Ref. 50 is omitted. The ratio of the average values of Tables 5 and 6 is  $\bar{E}(\text{Pu-239})/\bar{E}(\text{U-235}) = 1.053 \pm 0.050$ . The relatively large error does not make a comparison with the macroscopic results particularly rewarding and the explicitly measured ratios of Table 7 are strongly preferred for definitive comparisons. The average of

Table 5. U-235 AVE-Energy (Thermal and Low Energy Fission).

E-AVE(MeV)	ERROR	REF.
2.010	.060	40
1.956	.013	27
2.020	.025	27
2.110	.150	13
1.900	.200	44
2.000	.060	45*
2.060	.060	34*
1.946	.045	47
1.800	.100	48
<hr/>		
AVE(MeV)=	1.979201 <sup>a</sup>	RMS DEV.= .086094

Table 6. Pu-239 AVE-Energy (Thermal and Low Energy Fission).

E-AVE(MeV)	ERROR	REF.
2.136	.024	27
2.075	.017	27
2.110	.044	47
2.025	.060	54
2.010	.060	50
<hr/>		
AVE(MeV)=	2.084073 <sup>a</sup>	RMS DEV.= .049855

Table 7. Ratio Pu-239/U-235 AVE-Energy (Thermal and Low Energy Fission).

E-AVE(MeV)	ERROR	REF.
1.092	.014	27
1.075	.020	13
1.084	.030	47
1.080	.040	50
<hr/>		
AVE(MeV)=	1.084119 <sup>a</sup>	RMS DEV.= .006369

Table 8. Cf-252 AVE-Energy (Spontaneous Fission).

E-AVE(MeV)	ERROR	REF.
2.348	.100	28
2.350	.100	12
2.155	.024	27
2.130	.022	27
2.080	.150	59*
2.340	.050	60
2.085	.060	50
2.100	.200	61
2.220	.040	30
<hr/>		
AVE(MeV)=	2.188953 <sup>a</sup>	RMS DEV.= .110669

\* Error estimate by author; a. weighting factor = 1/error.

the directly measured values is  $\bar{E}(\text{Pu-239})/\bar{E}(\text{U-235}) = 1.084 \pm 0.006$ . This average is not inclusive of the exceptionally low value of Ref. 27 (which could not be verified by other work at the same institution). Thus the directly measured microscopic Pu-239/U-235 ratios are significantly higher than the comparable macroscopic values given in Table 1. This is disturbing as the measured ratios should be experimentally reliable and, as was pointed out in Ref. 13, the results are not particularly dependent on the spectral shape.

Of the spontaneous-fission-neutron spectra that of Cf-252 has been the most extensively studied. The results are outlined in Table 8. The spread in the experimental values is, in part, the consequence of weak sources available for some of the early work (for example Ref. 61). However, more recent values obtained with stronger sources differ by far more than their respective errors. It has been suggested by Jéki et al.<sup>72</sup> that backgrounds have seriously perturbed experimental Cf-252 average energies generally reducing the true values by 100-200 keV. Some values of the ratio  $\bar{E}(\text{Cf-252})/\bar{E}(\text{U-235})$  have been determined (see Table 4). These ratios are generally associated with measurements giving lower Cf-252 average-energy values. The discrepancies between the various Cf-252 results present a serious problem. Accurate Cf-252 results are important to the determination of an easily used "standard" fission-neutron spectrum and they effect the determination of other important quantities such as Nu-bar. The Cf-252 results strongly influence the determination of spectral dependence on Nu-bar and, indirectly, on incident neutron energy.

#### B. Spectrum Shape and Structure.

The observed fission-neutron spectra are usually described by either the "Watt"<sup>45</sup> expression

$$N(E)dE \sim \exp(-bE) \sinh \sqrt{cE} dE \quad (1)$$

or a Maxwellian distribution

$$N(E)dE \sim \sqrt{E} \exp(-E/T). \quad (2)$$

The latter was theoretically proposed by Terrell<sup>62</sup> from consideration of neutron evaporation from the moving fragment described by a Weisskopf "temperature",  $T$ . As noted by Weisskopf,<sup>63</sup> the temperature concept is only qualitative and one could reasonably expect considerable deviation from this simple approximation when dealing with the complex fission process. Indeed, experiment indicates that some of the fission neutrons are emitted at the actual scission rather than subsequently from the moving fragments.<sup>64</sup> Furthermore, the fragments are very highly excited and measurements indicate that multiple emission with varying temperatures does occur.<sup>14,60</sup> Despite these complexities, either of the above forms has been shown to be qualitatively descriptive of microscopic measurements. From a pragmatic point of view the difference between the two spectral forms is small; less than 5% below 6 MeV. At 10 MeV the difference is 25% but at this energy the spectral intensity has decreased by more than two orders of magnitude from the most probable value and as a consequence the relatively poor experimental statistical accuracy cannot clearly differentiate between the two above expressions. From the standpoint of numerical manipulation the Maxwellian is probably to be preferred.

Neither Eq. (1) or (2) fully describe all of the experimental results. Several measurements indicate an abundance of low energy neutrons well above that predicted by either expression.<sup>28,41,70</sup> The low-energy excess is particularly evident in Cf-252 fission as measured by Meadows<sup>28</sup> and by Zamyatin et al.<sup>41</sup> A careful inspection of a number of other measured spectra reveals a consistent tendency for a low-energy neutron excess for several of the fission processes. Good examples are the spectra of U-235, Pu-239 and Cf-252 shown in Ref. 27. Furthermore, some fast critical studies have suggested a similar low-energy excess.<sup>65</sup>

Neutron emission from highly excited fragments can be complex and a small portion of the emitted neutrons may arise from (f;x,n) processes. These could give a structure to the fission-neutron spectrum. Indeed, Zamyatin et al.<sup>41</sup> and Nefedov<sup>71</sup> reported a structure in the measured Cf-252 and U-235 fission neutron spectra. Nefedov associates this structure with specific fragment energies. This structure has escaped notice in other detailed work such as that of Meadows.<sup>28</sup> Furthermore, no structure was observed in a search of a number of U-235 and Pu-239 fission spectra by Smith<sup>13</sup> and it seems unlikely that the phenomena is peculiar to Cf-252. Structure of the type reported in Ref. 41 should be cautiously considered as a number of experimental artifacts can contribute to the observed effect and have done so in similar processes such as n-n' scattering.

Several measurements<sup>14,60</sup> observed the fission-neutron spectra in correlation with the mass and direction of motion of the fission fragments. The results are largely explained in terms of evaporation postulates with a light/heavy fragment neutron-emission ratio approximately 1.2 - 1.4. The results are not particularly sensitive to any reasonable anisotropy of the neutron emission from the moving fragment. The direction of fission fragment motion is known to be correlated with incident-neutron direction at some incident-neutron energies dependent upon the particular fission channels involved. The correlation is particularly pronounced near threshold, for example in U-238 fission. In these selected regions one would expect a correlation between the incident neutron direction and the fission spectrum if the evaporation hypothesis holds true. A possible indication of such an effect has been observed in U-238 by Knitter et al.<sup>69</sup> However, the incident neutron energies of the Knitter and of other work do not exactly correspond to those of a strong incident-neutron to fragment correlation and the incident resolutions employed in the fission spectrum measurements are usually coarse compared to the energy dependence of the fragment correlations. An incident-neutron to fission-neutron angular correlation could contribute to an anomalous structure observed in some measurements made at selected incident energies and reaction angles. This possible effect was, of course, avoided in the more detailed studies such as those of Refs. 13 and 49 where the spectrum was observed at a number of reaction angles. In any case, an angular correlation, localized in incident energy, will not be of appreciable applied significance.

### C. Spectral Dependence on Nu-bar and Incident Energy.

There are a number of microscopic results obtained at incident neutron energies well above thermal (see Table 4). However, as noted above, some of these results are open to considerable question as the measured values may be heavily contaminated with neutrons

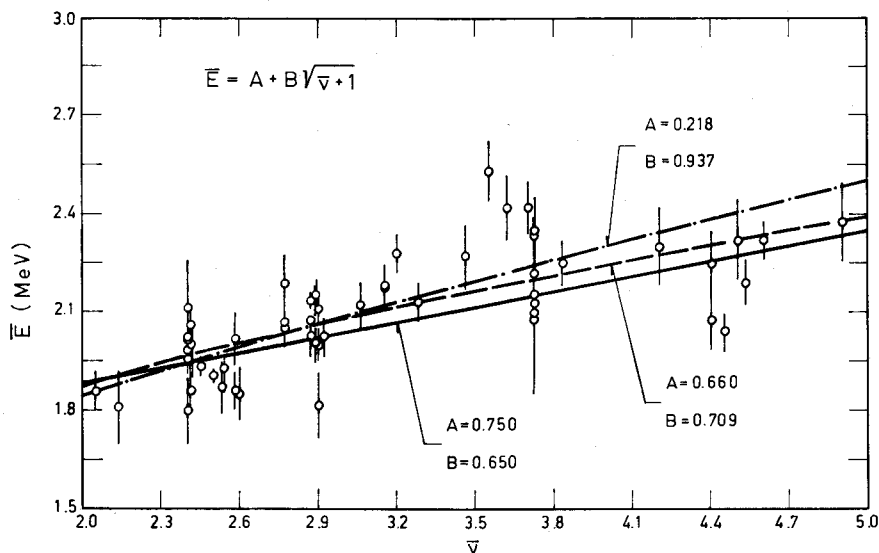


FIG.1. Dependence of average fission neutron energy,  $\bar{E}$ , on  $\text{Nu-bar}$ . Data points are from Table 4. Curves indicate the Terrell [62] expression with various parameter choices as described in the text.

originating in processes other than fission. The number of measurements at high incident energies where the fission origin of the neutrons is assured is too limited for a good definition of spectral dependence on incident neutron energy. However, there are a number of spontaneous fission results available, notably for Cf-252. These are not as subject to ambiguous interpretation and span a wide range of  $\text{Nu-bar}$  values.  $\text{Nu-bar}$  is fairly well known both for spontaneous fission and as a function of incident neutron energy. Therefore the dependence of microscopic fission-neutron spectra on  $\text{Nu-bar}$  and, indirectly, on incident neutron energy can reasonably be examined. The  $\text{Nu-bar}$  route is that followed here.

From basic considerations of kinetics and the equation-of-state Terrell<sup>62</sup> relates the average-fission-neutron energy,  $\bar{E}$ , to  $\text{Nu-bar}$  through the relation

$$\bar{E} = A + B \sqrt{\text{Nu-bar} + 1} \quad (3)$$

where  $A = 0.75$  and  $B = 0.65$ .

The values of  $A$  and  $B$  were determined from a comparison with experimental results. The expression of Eq. 3 is compared with the experimental values of Table 4 in Fig. 1. The requisite  $\text{Nu-bar}$  values were taken primarily from the IAEA tabulations and the work of Soleihac et al.<sup>66</sup> and from a few additional sources where necessary.  $\bar{E}$  is not a strong function of  $\text{Nu-bar}$  and thus the comparison is not appreciably influenced by the relatively small uncertainties in  $\text{Nu-bar}$ .

The data of Fig. 1 is grouped about the thermal neutron-induced fission of U-235 and Pu-239 and the spontaneous fission of Cf-252. The remainder of the points correspond to a limited number of recent

spontaneous fission results, primarily from Ref. 41, and various measurements made with incident neutrons with energies up to 14.3 MeV. The Terrell expression is indicated by the solid curve. A least-squares fit to all of the data, weighted by  $1/\text{error}^2$ , gives the dashed curve. The dashed-dotted curve was obtained by a similar fitting procedure but omitting those values possibly contaminated with non-fission neutrons. Generally, the slope of the curve rises as the basic data becomes more comprehensive and then more selective. However, none of the curves are consistent with the microscopic measurements of the ratio  $\bar{E}(\text{Pu-239})/\bar{E}(\text{U-235})$  (for example, the Terrell ratio = 1.04 and that of Table 7 = 1.084). Further, none of the curves are consistent with the higher  $\bar{E}(\text{Cf-252})$  values nor with many of the  $\bar{E}$  values corresponding to the Nu-bar range 2.65 - 3.70. The conclusion is that a number of experimental values are systematically in error or that Eq. 3 is not quantitatively descriptive of the physical phenomena; or both.

#### D. Comments on Flux Normalization and Detector Efficiency

Microscopic fission-spectrum measurements seek to determine the relative energy distribution of a continuum-temperature spectrum over the extended energy range 1 keV to 10 MeV or more. The discrepancies between measured values are of the order of 1-10%. Measurements of this nature are exceedingly difficult requiring detailed attention to the calibration of the detector response regardless of the specific method. Some indication of the difficult nature of the problem is to be found in similar x-n spectral measurements which generally do not provide temperature distributions for nuclear processes approaching the accuracies sought in fission-spectrum measurements.

Many of the fission measurements are directly or indirectly based upon the n-p cross section. This cross section is known to suitable accuracy<sup>67</sup> but its utilization in the laboratory often leaves much to be desired. Little attention is given to the effects of multiple processes or to the presence of carbon in the hydro-carbons often employed as detectors. The latter may be a source of anomalous structure as carbon scattering is resonant over much of the range of interest. The sensitivity of the detection system is often deduced only from calculation. Such calculations have not proven outstandingly reliable in fast-neutron-flux determinations. In some instances the detection efficiency is "verified" by observation of some "known" source reaction such as D(d,n). It is not clear that these source distributions are sufficiently well known to serve as a standard.

The above indicates that the microscopic measurement of fission spectra is a difficult flux measurement problem and that greatly increased attention should be given to the quantitative calibration of the detectors employed using the n-p cross section over the entire energy range and/or the carbon scattering cross section at lower energies (below 1.8 MeV). Any measurement without such careful calibration of the detection system using a well controlled mono-energetic neutron source may be subject to systematic uncertainties.

The above statements are not as applicable to spectrum-ratio measurements wherein the detection efficiency does not directly relate to the result.

### III. Concluding Remark

The above is a resumé of current knowledge of fission-neutron spectra with emphasis on microscopic quantities. Clearly, there is a discrepancy between some macroscopic results and the microscopic values which, on the average, have remained relatively static for a number of years. The discrepancy is by no means universal nor is it becoming more acute with time. It should be stressed that microscopic knowledge of the fission-neutron-spectrum is good in the context of the difficult nature of the problem and in comparison with our understanding of other neutron processes. For example, few per cent differences between the "Watt" and Maxwellian forms or between measured  $\bar{E}(\text{Pu-239})/\bar{E}(\text{U-235})$  ratios are no larger than current discrepancies in fast-fission cross sections of U-235; one of the most basic cross sections. It will not be easy to grossly improve the already relatively good quality of the microscopic information.

It has been suggested that an evaluation of the basic data is now in order. The contemporary merit of such an effort can be questioned. Many of the available results, though of good quality, are old and poorly documented. As a consequence the evaluator may tend to equate newness with goodness to the detriment of physical fact. At present an evaluation can massage and renormalize to remove some of the more glaring discrepancies between, for example, average energies and ratios; but it is unlikely that it will resolve the basic issue--the difference between some macroscopic deductions and microscopic values. It is here suggested that an evaluation would be more pregnant several years hence when, hopefully, the concepts and criticisms of this and similar meetings have born fruit. Until that time, in this author's opinion, the fission-neutron spectra stands as indicated by the microscopic results outlined above.

### References

1. A. Fabry et al., Helsinki Conference, IAEA-CN-26/39 (1970). Threshold detector studies. Possibly non-maxwellian shape; see also, Nukleonik 10, 280 (1967).
2. W. McElroy, Nucl. Sci. Eng. 36, 109 (1969). Deduced from threshold detector studies. Shape very different from maxwellian.
3. W. McElroy et al., Nucl. Sci. Eng. 36, 15 (1969).
4. J. Grundl, Nucl. Sci. Eng. 31, 191 (1968). See also; Proc. Symposium on Neutron Standards and Flux Normalization, Argonne National Laboratory (1970). Threshold detector studies.
5. J. Grundl, Nucl. Sci. Eng. 30, 39 (1967).
6. C. Campbell and J. Rowlands, Helsinki Conference, IAEA-CN-26/116 (1970), values deduced from fast critical data adjustment.
7. D. Okrent et al., Nucl. Applications and Tech. 9, 454 (1970).
8. Discussion of EACRP (1969), et seq.
9. L. Stewart, INDC(US)-17U (1970).

10. A. B. Smith et al., Phys. Rev. 123, 2140 (1961). Relative to  $\bar{E}(235) = 1.95$  MeV. TOF and emulsion techniques to  $\sim 7.0$  MeV. Maxwellian shape with some excess at low energies.
11. A. B. Smith et al., Phys. Rev. 114, 1351 (1959). Relative to  $\bar{E}(235) = 1.95$  MeV. TOF and emulsion techniques to  $\sim 7.5$  MeV. Maxwellian with large excess at low energies.
12. A. B. Smith et al., Phys. Rev. 108, 411 (1957). TOF and emulsion techniques. Maxwellian shape.
13. A. B. Smith, Nucl. Sci. Eng. 44, 439 (1971). TOF methods to  $\sim 7$  MeV. Ratio 239/235 in interval 0.3 - 7.5 MeV. 235 spectra to 1.6 MeV only.
14. A. B. Smith et al., New York Meeting of the American Physical Society (1959).
15. A. B. Smith, INDC(US)-16G (1970).
16. B. Leonard, Private Communication. Also see Proc. of Knoxville Conference (1971).
17. M. Najzer et al., Helsinki Conference, IAEA-CN-26/6 (1970).
18. J. Story, Helsinki Conference, IAEA-CN-26/110 (1970).
19. D. Harris, ANS Trans. 9, 453 (1966). Deduced from macroscopic analysis. Tabulated values are relative to  $\bar{E}(235) = 1.935$  MeV.
20. Evaluated Nuclear Data File-B (ENDF/B), National Neutron Cross Section Center, Brookhaven National Laboratory.
21. T. Bonner, Nucl. Phys. 23, 116 (1961). Sphere transmission techniques.
22. C. Dunford and H. Alter, AI-AEC-MEMO-12915 (1971). Monte-Carlo age calculations.
23. L. Green, Nucl. Sci. Eng. 37, 232 (1969). Transmission techniques assuming Maxwellian form.
24. V. Kovalev et al., JETP 33, 1069 (1957). Threshold detectors, ratio relative to  $\bar{E}(235) = 2.0$  MeV.
25. H. Depuydet and M. Neve de Mevergnies, J. Nucl. Energy, 16, 447 (1952).
26. R. Leachman and H. Schmidt, J. Nucl. Energy 4, 38 (1957).
27. H. Werle and H. Bluhm, Report to the EACRP (1971). Proton recoil and He-3 spectrometer results to  $\sim 8.0$  MeV. The two methods are discrepant. Generally an excess of low energy neutrons relative to a Maxwellian. Somewhat revised values with the same general results have been presented to this meeting.
28. J. Meadows, Phys. Rev. 157, 1076 (1967). Li-6 and proton recoil counters with TOF techniques. Large excess above Maxwellian at low energies. Results consistent with L. Jeki et al., Helsinki Conference, IAEA-CN-26/4 (1970).



29. W. McElroy, Private Communication.
30. Nikolaev et al., JETP 7, 517 (1958).
31. R. Richmond as quoted by Allen and Henkel, Progress in Nucl. Energy, Sec. I, 2, Pergamon Press (1957).
32. W. Hart, AHSB(S) R124 (1967).
33. W. Poenitz, Private Communication.
34. L. Cranberg et al., Phys. Rev. 103, 662 (1956). TOF and emulsion techniques to  $> 10$  MeV, Watt form.
35. See for example: H. Goldstein et al., Proc. 2nd Inter. Conference on Peaceful Uses of Atomic Energy, Vol. 16, Geneva (1958).
36. R. Doerner et al., Nucl. Sci. Eng. 9, 221 (1961)
37. R. Paschall, Nucl. Sci. Eng. 20, 436 (1964); see also 23, 256 (1965).
38. A. Staub et al., Nucl. Sci. Eng. 34, 272 (1968).
39. In formulating this resume continued reference was made to the recent review of A. H. Jaffey, Argonne National Laboratory Report ANL-7747 (1970). It is recommended to the reader.
40. I. C. Richards, Thesis, University of London (1971), Li-6 spectrometer. Results quoted by Campbell and Rowlands to EACRP (1971).
41. Yu. S. Zamyatin et al., Helsinki Conference, IAEA-CN-26/90 (1970). TOF method, maxwellian form, structure at low energies, range 0.5-6.0 MeV with CF-252 to few keV. Relative to U-235 = 1.935 MeV.
42. Iu. S. Zamiatnin et al., Sov. J. At. Energy 4, 443 (1958). Emulsion techniques  $\sim 0.6 - 5.0$  MeV.
43. K. Henry and M. Hayden, ORNL-2081 (1956). Proton recoil spectrometer, poor statistics.
44. Mukhin as given in Physics of Nuclear Fission, Pergamon Press (1958). This volume generally describes early USSR work most of which is of the Maxwellian shape.
45. B. Watt, Phys. Rev. 87, 1037 (1952). See also D. Hill, Phys. Rev. 87, 1032 (1952). Recoil methods above 500 keV to 10 MeV.
46. N. Nereson, Phys. Rev. 85, 600 (1952). Same general experiment as Ref. 53, below.
47. E. Barnard et al., Nucl. Phys. 71, 228 (1965). TOF methods  $\sim 300$  keV to 7 MeV, Maxwellian shape.
48. K. Skarsvag and K. Berghiem, Nucl. Phys. 45, 72 (1963), TOF methods  $\sim 0.4 - 11.8$  MeV.
49. E. Almen et al., Progress Report S-426 Neutron Physics Section, Aktiebolaget Atomenergi, (1971), TOF techniques. No angle effects. Maxwellian distributions 1.0 - 10 MeV. See also Helsinki Conference IAEA-CN-26/57 (1970).

50. H. Conde and G. During, Arkiv for Fysik 29, 313 (1965). TOF methods to 7 MeV. Maxwellian shape.
51. Yu. A. Vasiliv et al., JETP 38, 671 (1960). TOF techniques in interval  $\sim 0.5 - 5.0$  MeV.
52. Frye et al., LA-1670 (1954). Photo-plate technique. Data is probably redundant with Ref. 34, above.
53. N. Nereson, Phys. Rev. 88, 823 (1952). Emulsion techniques above  $\sim 1.0$  MeV. Results given only as exponential fall rate.
54. L. Belov et al., INDC-260-E (1969). TOF techniques with Maxwellian shapes. See also Yadern. Fiz. 9, (4), 727 (1969).
55. D. Boyce et al., AERE-PR/NP-14 (1968). TOF techniques in conjunction with scattering measurements. Incident energies  $< 1.5$  MeV, spectrum range  $< \sim 7.0$  MeV.
56. R. Batchelor and K. Wyld, AWRE-0-55/69 (1969). TOF techniques  $\lesssim 7$  MeV.
57. H. Knitter and M. Coppola, Zeits fur Physik 228, 286 (1969). TOF techniques over range  $\sim 1 - 7$  MeV. Maxwellian shape.
58. T. R. Herold, Savannah River Laboratory Report DP-949 (1969). He-3 spectrometer,  $0.5 - 6.0$  MeV.
59. Hjalmer et al., Phys. Rev. 100, 1542 (1955). Emulsion techniques  $\sim 1 - 7$  MeV, poor statistics, Maxwellian shape.
60. H. Bowman, Phys. Rev. 126, 2120 (1962). TOF methods to  $\sim 7$  MeV.
61. E. Hjalmar et al., Arkiv for Fysik 10, 357 (1956). Emulsion data. Poor statistics, Watt form.
62. J. Terréll, Physics and Chemistry of Fission, Vol. II, IAEA (1965).
63. J. Blatt and V. Weisskopf, Theoretical Nuclear Physics, J. Wiley and Sons, New York (1952).
64. Kapoor et al., Phys. Rev. 131, 283 (1963).
65. W. Loewenstein, Private Communication.
66. Soleihac et al., J. Nucl. Energy 23, 257 (1969).
67. See Proceedings of the Symposium on Neutron Standards and Flux Normalization, Argonne National Laboratory (1970).
68. J. Pilcher and F. Brooks, Annual Report of Southern Universities Nuclear Institute, SUNI-14, Faure, Republic of South Africa (1970).
69. H. Knitter et al., Private Communication.
70. L. Jeki et al., Helsinki Conference, IAEA-CN-26/4 (1970). Qualitative TOF results indicate low-energy excess from Maxwellian.
71. V. N. Nefedov, NIIAR-P52 (1969).
72. L. Jeki et al., KFKI-71-9 (1970).

# A REVIEW OF PROMPT FISSION NEUTRON SPECTRUM DATA FOR $^{235}\text{U}$ AND $^{239}\text{Pu}$ NEUTRON-INDUCED FISSION AND $^{252}\text{Cf}$ SPONTANEOUS FISSION

A. KOSTER  
International Atomic Energy Agency,  
Vienna

## Abstract

A REVIEW OF PROMPT FISSION NEUTRON SPECTRUM DATA FOR  $^{235}\text{U}$  AND  $^{239}\text{Pu}$  NEUTRON-INDUCED FISSION AND  $^{252}\text{Cf}$  SPONTANEOUS FISSION.

The report reviews the major differential measurements of prompt fission neutron spectra and gives an estimate of the average energy of the spectra of  $^{235}\text{U}$  and  $^{239}\text{Pu}$  for thermal neutron fission and of  $^{252}\text{Cf}$  for spontaneous fission. Only for  $^{235}\text{U}$  were enough experimental data available to allow a fitting by an orthogonal polynomial function. Discrepancies in the existing data are pointed out particularly for  $^{252}\text{Cf}$ .

## INTRODUCTION

The aim of this paper is to review the major differential measurements of prompt fission neutron spectra and, on this basis, to estimate the average energy of the spectra of  $^{235}\text{U}$  and  $^{239}\text{Pu}$  for thermal neutron fission and of  $^{252}\text{Cf}$  for spontaneous fission. Californium has, of course, been included because of its use as a standard reference nuclide for  $\bar{\nu}$  and fission spectrum measurements. The work is not intended to be a comprehensive evaluation of all experiments performed to date, but only a concise summary to serve as a background document for the IAEA Consultants Meeting on the Status of Prompt Fission Neutron Spectra. Experiments using threshold detectors for determining spectrum temperatures were excluded because otherwise a critical assessment of all cross-sections involved would be required, which would entail considerable effort in addition to what appears possible at present.

The most extensively studied fission spectrum is that of  $^{235}\text{U}$ ; numerous experiments using various methods have been performed since 1942. From the beginning the standard procedure to obtain the spectrum temperature from a differential measurement has been to fit some function derived from nuclear evaporation theory to the data. Almost without exception the function chosen has been either a Maxwellian or the so-called Watt spectrum [1]. The Maxwell spectrum is the simplest:

$$N_M(E) = C_M \sqrt{E} e^{-E/T} \quad (1)$$

with average energy

$$\bar{E}_M = \frac{3}{2} T \quad (2)$$

TABLE I.  $^{235}\text{U}$ , PUBLISHED DATA

Ref.	Year	Incident energy (MeV)	Secondary energy range (MeV)	Type of function fitted to obtain E or T	Results		Method	Sample	Detector	Comments
					(Values in parentheses were not given explicitly by authors but obtained here)	$\bar{E}$				
[2]	1971	Thermal	0.1-9.5	Numerical integr. Maxwell	$1.946 \pm 0.12$	(1.298)	Proton recoil	$5.1 \times 5.1 \times 0.15$ cm, 99% Ni coated	Prep. counter	Preliminary. Possibly overestimating systematic errors.
[3]	1971	0.035 and 0.400	< 1.6	Maxwell	$1.932 \pm 0.13$	(1.293)	TOF at 8 angles	Cylinder, h = 2 cm, d = 2 cm, 94% enr.	Proton recoiling scintill. detectors	Corrections made are difficult to assess.
					$(2.11 \pm 0.21)$	(1.41 $\pm$ 0.14)				
[4]	1969	Thermal	2-11	Maxwell	(1.978)	$1.318 \pm 0.005$	TOF	Near-critical sphere (APFA-III)	Li-glass	Spectrum was considered pure fission above 2 or 3 MeV.
[5]	1967	Thermal	6-20	Maxwell	(1.950)	$1.30 \pm 0.02$	Proton recoil leakage spectrum from reactor	(Reactor fuel)	Counter telescope	Little information on corrections (e.g. fast fission?).
[6]	1965	0.1	0.3-4.0	Maxwell	(1.945)	$1.297 \pm 0.030$	TOF at 90°	Disc, d = 20 cm, h = 0.7 cm	Scintill. disc, d = 20 cm, h = 2.5 cm	Error given very small; no allowance for systematic error.
[7]	1965	Thermal	0.7-6.0	Watt	1.980	(1.321)	TOF at 90°	Citrate on foil, 2 mg/cm <sup>2</sup>	Stibene crystal	Scanty information on experimental details and on corrections.
[8]	1965	0.04	0.3-7.5	Maxwell	(1.889)	$1.24 \pm 0.04$	TOF at 70°	Sphere d = 2.0 cm	Plastic scintill.	Very low temperature may be due to underestimate of wall effect and inelastic scatt. of secondary neutrons.
[9]	1961	Thermal	< 4	Maxwell	(1.996)	$1.332 \pm 0.030$	Sphere moderation	Foils, th = 0.025 - 0.05 cm	Bramblett counter (sphere moderation)	

TABLE I (cont.)

[10]	1956	0.005-0.08	(a) 0.35-12.0 (b) 0.175-4.14	Watt and Maxwell	(1.930)	1.288	(a) Photogr. plate (b) TOF	Foil 11.4 x 15.2 x 0.08 cm 1 g $^{235}\text{U}$ on Pt	(a) Photogr. plate (b) Plastic scintill.	Possible normalization error when combining the two experiments. Possibly an error caused by delayed gammas in TOF exp.
[11]	1952	Thermal	3.3-17.2	Watt	2.00	(1.333)	Proton recoil	Discs: 1: th = 0.43 cm, 28.5 g and 31: th = 0.025 cm, total 54.1 g	Prop. counters	Fitted data include those of Hill [11].
[12]	1952	Thermal	0.4-6.4	Watt	(Included, Ref.[1])		Proton recoil combined with absorbers for range deter- mination	Natural and en- riched uranium plates, th = 0.5 cm	3 coinc. and 1 anti-coinc. counters	Many corrections were needed. Results appear unreliable.
[13]	1949	Thermal	0.075-0.60	Watt	2.00	(1.333)	Proton recoil	7.5 x 25 x 0.025 cm	Cloud chamber	(n, p) cross-section needs updating. Systematic errors may be appreciable.
[14]	1944	Thermal	0.39-7.02	Watt	2.00	(1.333)	Proton recoil	10 mil $^{235}\text{U}$ oxide on Al	Photogr. plate	Poor energy resolution and large errors at low energy.
[15]	1944	Thermal	1-4	Watt	2.00	(1.333)	Proton recoil	Discs of 2930 g, 243 g (nat.) and 2 g (enriched)	Ion chamber Photogr. plate	No correction for inelastic scattering in thick samples.
[16]	1965	1.5	0.3-7.5	Maxwell	(1.875)	1.35 ± 0.04	TOF at 90°	0.5 mg/cm <sup>2</sup> $^{235}\text{U}$ on Pt.	Plastic scintill.	Possible underestimate of scattering in walls.
[17]	1968	3.9	> 4	-	T (3.9 MeV)/T (th) = 1.05 ± 0.03		Threshold detector	Spher. shell	$^{24}\text{Mg}(n, p)$ and $^{107}\text{Ag}(n, 2n)$	Ratio only.
[18]	1969	14.3	0.4-5.0	Watt + evap. spectrum	(2.040)	1.36 ± 0.04	TOF	2 mg/cm <sup>2</sup> $^{235}\text{U}$ coating inside fission chamber	Toluene scintill.	No mention of (n, 2n) corr.

TABLE II. RESULTS FOR  $^{239}\text{Pu}$ 

Ref.	Year	Incident energy (MeV)	Secondary energy range (MeV)	Type of function fitted to obtain T or $\bar{E}$	Results (Values in parentheses were not given explicitly by the authors but calculated here)		Method	Sample	Detector	Comments
					$\bar{E}$ (MeV)	$T_M$ (MeV)				
[2]	1971	Thermal	0.1-9.5	Numerical integr. Maxwell	$2.145 \pm 0.12$ $2.107 \pm 0.13$	(1.429) (1.406)	Proton recoil	$5.1 \times 5.1 \times 0.137$ cm, 92% 0.01 cm steel coating	Prop. counter	Preliminary. Possibly overestimating systematic errors.
[3]	1971	0.035 and 0.400	< 1.6		$(239)/(235) = 1.075 \pm 0.09$ (2.13)		TOF at 8 angles	Cylinder $d = 2$ cm, $h = 2$ cm	Proton recoil Scintill. det.	Very large scatter in data. Accuracy of 2% seems high.
[20]	1968	Thermal	0.1-9.5	Maxwell	(2.05)	1.35	TOF	(no info.)	(no info.)	(Insufficient info.)
[6]	1965	0.130	0.26-5.0	Maxwell	(2.13)	$1.407 \pm 0.020$	TOF at $90^\circ$	Cylinder $d = 1.27$ cm, $h = 2.54$ cm	Scintill. disc, $d = 10$ cm $h = 2.5$ cm	No mention of corr. for scattering in thick sample.
[8]	1965	0.04	0.3-7.5	Maxwell	(2.02)	$1.34 \pm 0.04$	TOF at $70^\circ$	Sphere $d = 2.0$ cm	Plastic scintill.	Corrections applied may be underestimated.
[9]	1961	Thermal	< 4	Maxwell	(2.08)	1.385	Sphere moderation	Foils, $th = 0.025 - 0.05$ cm	Bramblett counter (sphere moderation)	Not corr. for delayed neutrons.
[15]	1958	Thermal	> 4	-	$(239)/(235) = 1.05 \pm 0.03$ (2.08)		Threshold det.	Spher. shell	$^{241}\text{Mg}(n,p)$ $^{109}\text{Ag}(n,2n)$	Ratio only.
[21]	1957	Thermal	(no info.)	-	$(239)/(235) = 1.05 \pm 0.01$ (2.076)		Threshold det.	(no info.)	(no info.)	(?)
[22]	1952	Thermal	0.5-8.0	Watt	2.00	(1.333)	Photogr. plate; proton recoil at $90^\circ$	Disc, $d = 1.25$ cm $h = 0.68$ cm Ni coated	Photogr. plate	Normalization at 1.5 MeV to $^{235}\text{U}$ data.

TABLE II (cont.)

[23]	1970	1.5	1.8-6.5	Maxwell	(2.12 ± 0.07)	1.41 ± 0.05	TOF	Cylinder, d = 1.20 cm h = 2.5 cm 54.8 g; 98.91% <sup>239</sup> Pu	Plastic scintill.	Inelastic contribution derived from low-energy part of data at 1.9 and 2.3 MeV.
		1.9	"	"	(2.18 ± 0.06)	1.45 ± 0.04				
		2.3	"	"	(2.28 ± 0.06)	1.52 ± 0.04				
		4.0	"	Maxwell + inel.	(2.27 ± 0.10)	1.51 ± 0.07				
		4.5	"	"	(2.53 ± 0.09)	1.69 ± 0.06				
		5.0	"	"	(2.42 ± 0.10)	1.61 ± 0.07				
		5.5	"	"	(2.42 ± 0.08)	1.61 ± 0.05				
[15]	1958	4	> 4	"	(239/4MeV)/(235/Th) = 1.09 ± 0.04 (2.155)		Threshold det.	Spher. shell	<sup>24</sup> Mg(n, p) and <sup>10</sup> Ag(n, 2n)	Ratio only.

The spectrum suggested by Watt, on the other hand, is based on the assumptions of isotropic angular and Maxwellian energy distributions in the centre-of-mass system and reads as follows [1]:

$$N_W(E) = C_W e^{-E/T_f} \sinh(2\sqrt{EE_f}/T_f) \quad (3)$$

where  $E_f$  is the average kinetic energy per nucleon of a fragment and

$$\bar{E}_W = E_f + \frac{3}{2} T_f \quad (4)$$

Assuming that  $\bar{E}_W \cong \bar{E}_M$ , we can see, comparing Eqs (2) and (4), that

$$T \cong T_f + \frac{2}{3} E_f \quad (5)$$

Most of the earlier experiments at Los Alamos were fitted to a function of the type (3) with parameters as determined by Watt, i.e.  $T_f = 1.0$  MeV and  $E_f = 0.5$  MeV, which gives a value for  $\bar{E}_W$  of 2.0 MeV.

### 1. THE $^{235}\text{U}$ THERMAL NEUTRON-INDUCED FISSION SPECTRUM

An attempt has been made to collect all published results on the thermal neutron induced fission spectrum of  $^{235}\text{U}$ . Some data are not available, being still classified or never published. These are not included, even though they have been mentioned in other papers. Only those results have been included that have been reported in the available literature so that at least some experimental details and analysis methods can be given. A list of the available measurements together with some relevant experimental details is given in Table I. As can be seen from the values for  $\bar{E}$  and  $T$ , there exists remarkable agreement between the results obtained by different methods and between old and recent measurements. These results are also in agreement with some references to unpublished work [15, 17-19]. The average of 13 measurements of the spectrum, due to thermal (up to 100 keV) neutrons, gives a value of  $1.969 \pm 0.075$  MeV for the average energy  $\bar{E}$ . Excluding the very low value obtained by Condé and During [8], the average energy becomes  $1.978 \pm 0.046$  MeV. The reason for the low value for  $\bar{E}$  obtained by Condé and During is not immediately obvious. The most likely explanation is that the authors underestimated the effects of wall-scattering and scattering in the very thick samples used in the  $^{235}\text{U}$  and  $^{239}\text{Pu}$  measurements. It would probably be more correct to determine a suitably weighted average of the data, taking into account the authors' own error estimates. However, because of the many possibilities of systematic errors in the original data and the different methods of deriving the average energy, proper weighting of these data appears an almost impossible task.

With one exception, all results listed were obtained through fitting a function to the raw data. This assumes an a priori knowledge of the shape of the spectrum, which, however, rests on a shaky theoretical basis. The author who found the average energy through integration [2] used only his own data for this purpose, which entails several drawbacks, including the limited energy range studied.



It appeared therefore that a useful task might be performed if a way could be found of combining several data sets in as wide an energy range as possible and integrating the resultant curve. To this end we collected as many data sets as possible and normalized these sets to a reference set<sup>1</sup>, using the method of equal areas. An orthogonal polynomial function was thereafter fitted to the normalized data.

The resulting expression of the form

$$F(E) = a_0 + a_1 E + a_2 E^2 + \dots + a_n E^n \quad n < 40$$

was integrated over the interval 0 - 20 MeV to obtain

$$\bar{E} = \frac{\int_0^{20} f(E) E \, dE}{\int_0^{20} f(E) \, dE}$$

For this method to work well a large number of data points is desirable. Unfortunately, the response to our request for data was only partly successful, most data older than 5 years being lost and some authors refusing to release their data. Some of the older Los Alamos publications contained the data, which were, however, of doubtful value because of the large scatter of individual data points. Mainly lacking are data points in the higher energy region beyond 10 MeV as the fitting program needs sufficient points there to prevent the function from fluctuating at the higher energies. For  $^{235}\text{U}$  over 200 data points are available, permitting a reasonable fit. Preliminary results for the integral up to 10 MeV for a 12-degree fit give a value for the average energy of  $\bar{E} = 1.97$  MeV. This would appear to validate the use of a simple Maxwellian as an approximation to the fission spectrum of  $^{235}\text{U}$ . More work needs to be done, however, to establish confidence limits for this value. Taking the value for  $\bar{E}$  found this way, several functions can be fitted to the data with the object of seeing which one approaches the real shape more closely.

## 2. THE $^{239}\text{Pu}$ THERMAL NEUTRON-INDUCED FISSION SPECTRUM

The results obtained for  $^{239}\text{Pu}$  are summarized in Table II. Several experiments measured only the ratio of  $T(239)/T(235)$ , including some measurements made with threshold detectors. It is assumed that errors in threshold measurements are likely to cancel in a ratio measurement and these results have therefore been included. The average of 6 results, excluding the ratio results, gives an average energy

$$\bar{E} = 2.071 \text{ MeV}$$

<sup>1</sup> For this preliminary trial the data obtained by Barnard et al. [6] were used as 'standard' to which the others were normalized.

TABLE III.  $^{252}\text{Cf}$ 

Ref.	Year	Secondary energy range (MeV)	Type of function fitted to obtain $\bar{E}$ or T	Results (Values in parentheses were not given explicitly by the authors but calculated here)		Method	Sample (Initial activity)	Detector	Comments
				$\bar{E}$ (MeV)	$T_M$ (MeV)				
[2]	1971	0.1-9.5	Numerical integr. Maxwell	$2.134 \pm 0.17$ (1.423) 2.000 (1.333)	(1.423) (1.333)	Proton recoil	$10^5$ n/s on Pt sheet in steel cylinder	Prop. counter	Preliminary.
[24]	1970	0.04-6		(2.24)	$1.48 \pm 0.03$	TOF		Plastic scintill.	No corr. for delayed gammas. Rel. to $^{235}\text{U}$ $T = 1.29$ $\bar{Y} = 2.426$
[25]	1969			(2.10)	1.39	Manganese bath			
[26]	1967	0.003-15	Maxwell (0.5-15 MeV)	2.348	(1.565) (1.522)	TOF	$8.6 \times 10^5$ fss/min	Li-glass	Deviation from Maxwellian at low energies.
[8]	1965	0.7-7.5	Maxwell	(2.10)	$1.39 \pm 0.04$	TOF	(no inf.)	Li-glass and plastic scintill.	Not corr. for scattered back-ground or delayed gammas.
[27]	1962	0.5-6	Evapor. spectr.	$2.34 \pm 0.05$	(1.56)	TOF	$1.56 \times 10^5$ fss/min on Ni foil	Plastic scintill.	Delayed gammas neglected.
[12]	1961	<4	Maxwell	(2.05)	$1.367 \pm 0.030$	Sphere moderation	$6 \times 10^5$ n/s	Bramblett counter (sphere moder.)	Not corr. for scattered or delayed neutrons.
[15]	1958	>4	-	(252/Spont)/( $^{232}\text{Th}$ ) = $1.11 \pm 0.05$		Threshold det.	(no inf.)	$^{24}\text{Mg}(n,p)$ and $^{100}\text{Ag}(n,2n)$	Ratio only.
[28]	1957		Watt	2.36	(1.57)	(a) TOF (b) Proton recoil	$1.2 \times 10^5$ n/min	(a) Plastic scintill. (b) Photogr. plate	Delayed gammas not considered for TOF meas., which was used for normalization. Separate, the two methods give different results.
[29]	1955	>2	Maxwell	(2.12)	$1.402 \pm 0.09$		30 fss/min	Photogr. plate	Only 281 tracks measured at high energy and low resolution.

Including the ratio measurements and assuming the value of 1.978 MeV obtained in section 1 for the average energy of  $^{235}\text{U}$ , we get

$$\bar{E} = 2.078 \text{ MeV}$$

which implies a ratio  $T(239)/T(235)$  of 1.051.

### 3. THE $^{252}\text{Cf}$ SPONTANEOUS FISSION SPECTRUM

Table III summarizes the available experimental results on  $^{252}\text{Cf}$ . This isotope is of special importance because of its possible use as a standard for all fission spectrum work. It is therefore unfortunate that such large discrepancies exist between the different results. Jéki and his co-workers [30] have made a study of this problem and analysed the main experiments published. They made a study of the different corrections that have to be made in the different techniques used and came to the conclusion that neglect of these corrections will lead to an underestimate of the true value of the temperature. Their observations are, however, also valid for some of the  $^{235}\text{U}$  results, which now agree well to the average energy; this agreement would not necessarily be retained if additional increases in the temperature would appear necessary when introducing further corrections. It would seem that some further studies of systematic errors in measurements on this isotope are desirable. The comments of Jéki et al. have been included in Table III.

The results are distributed in two distinct groups with values for  $\bar{E}$  of about 2.10 and 2.37 MeV respectively. Before this discrepancy is resolved, there is obviously not much sense in calculating a straightforward average of all experiments.

Several authors [26, 30] have observed a substantial discrepancy between the fitted Maxwellian and the experimental points at low energy. This seems to indicate that for spontaneous fission a Maxwellian gives a poorer representation of the spectrum than for neutron-induced fission. A simple integrated average energy might give better agreement amongst different data sets. There again, no data are available to enable this method to be applied.

### REFERENCES

- [1] WATT, B.E., Phys. Rev. 87 (1952) 1037.
- [2] WERLE, H., private communication, 1971.
- [3] SMITH, A.B., Rep. INDC(USA)-27/L (1971).
- [4] NEILL, J., Rep. GA-9753 (1969).
- [5] SHERWOOD, G.G., KING, J.S., Trans. Am. nucl. Soc. 10 (1962) 555.
- [6] BARNARD, E. et al., Nucl. Phys. 71 (1965) 228.
- [7] NEFEDOV, V.N. et al., Atomn. Energ. 20 (1966) 342.
- [8] CONDE, H., DURING, G., Physics and Chemistry of Fission (Proc. Symp. Salzburg, 1965) 2, IAEA, Vienna (1965) 93.
- [9] BONNER, T.W., Nucl. Phys. 23 (1961) 116.
- [10] CRANBERG, L. et al., Phys. Rev. 103 (1956) 662.
- [11] HILL, D., Phys. Rev. 87 (1952) 1034.
- [12] BONNER, T.W. et al., Phys. Rev. 87 (1952) 1032.
- [13] NERESON, N., Phys. Rev. 85 (1962) 600.

- [14] NICODEMUS, D.B., STAUB, H.H., Phys. Rev. 89 (1953) 1288.
- [15] BONDARENKO, I.I. et al., Int. Conf. peaceful Uses atom. Energy (Proc. Conf. Geneva, 1958) 15, UN, New York (1958) 353.
- [16] VASIL'EV, Yu.A. et al., Soviet Phys. JETP 33 (1960) 671.
- [17] MUKHIN, K.N. et al., reported by EROZOLIMSKII, B.G., Phys. nucl. Fission, Atomn. Energ. (1956) Suppl.1.
- [18] BARTON, D.M., reported by LEACHMAN, R.B., Int. Conf. peaceful Uses atom. Energy (Proc. Conf. Geneva, 1958) 2, UN, New York (1958) 193.
- [19] ALMENE, E. et al., reported by WIEDLING (Ref.[28], discussion).
- [20] BELOV, L.M. et al., Rep. INDC-260 E (1969) 94.
- [21] KOVALEV, V.P. et al., Soviet Phys. JETP 33 (1957) 1069.
- [22] NERESON, N., Phys. Rev. 88 (1952) 823.
- [23] COPPOLA, M., KNITTER, H.H., Z. Phys. 232 (1970) 286.
- [24] ZAMYATNIN, Yu.S. et al., Nuclear Data for Reactors (Proc. Conf. Helsinki, 1970) 2, IAEA, Vienna (1970) 183.
- [25] GREEN, L., Nucl. Sci. Engng 37 (1969) 232.
- [26] MEADOWS, J.W., Phys. Rev. 157 (1967) 1076.
- [27] BOWMAN, H.R. et al., Phys. Rev. 126 (1962) 2120.
- [28] SMITH, A.B., FIELDS, P.R., Phys. Rev. 108 (1957) 411.
- [29] HJALMAR, E. et al., Ark. Fys. 10 (1955) 357.
- [30] JÉKI, L. et al., Rep. KFKI-71-9 (1971).

# BRIEF REVIEW OF INTEGRAL MEASUREMENTS WITH FISSION SPECTRUM NEUTRONS

J. A. GRUNDL

National Bureau of Standards,  
Washington, D. C.,  
United States of America

## Abstract

BRIEF REVIEW OF INTEGRAL MEASUREMENTS WITH FISSION SPECTRUM NEUTRONS.

The paper is an edited transcript of the introduction to the discussion of integral measurements of fission cross-sections averaged over fission spectra given by the author at the meeting.

This review deals with the second aspect of measurement that motivates this meeting, a meeting called to ascertain the status of prompt fission neutron spectra. This particular method of observing neutron interactions with matter has a long history and is generally denoted under the title integral measurements. As a practitioner of this art may I say that, without complaint, we take our usual place when we appear at a meeting of differential measurers. We try to tell our tale quickly and minimize the interruptions. Happily, this meeting is somewhat different. One may gather from Dr. Ferguson's remarks that in some way, and recently, integral measurements have achieved the unexpected. They have made the bridge between differential data and integral measurement a bridge with two-way traffic.

In the summary of the last meeting of the EANDC you may find this meeting on fission spectra quite bluntly described as a "confrontation between experimenters of micro- and macro-persuasions". The idea of a crisp interaction between differential and integral measurers is attractive, but I should like to take issue with this description on two points. First, confrontation is worthwhile only if the result is an increase in understanding of what integral measurers are about — even when they do their job poorly. And, more important, confrontation should not jeopardize the pious hope that the chances for useful co-operation between us may be improved. More and more the two types of measurement have a single purpose: the early demonstration of an economical and publicly acceptable fast breeder reactor. My second point of issue is with terminology. Micro and macro, I believe, do not correctly distinguish the two kinds of measurement that are represented at this meeting. A more careful distinction is necessary, it seems to me, because it is precisely with fission spectra that integral measurements are in the domain of measurement that is commonly called microscopic. In what follows I am borrowing from a review paper on fission spectra given at the EANDC Symposium on Neutron Standards and Flux Normalization last fall [1].

Four terms are of concern: microscopic and macroscopic, differential and integral. Macroscopic and microscopic are relatively easy to distinguish if we presume they apply to experimental arrangements and not to techniques of measurement. Macroscopic in this view refers to experimental arrangements in which a dominating feature is neutron transport.

That is, arrangements in which multiple encounters of neutrons with nuclei produce a series of neutron velocity changes, and in important instances new sources of neutrons. The main point is multiple encounters of neutrons with nuclei. Microscopic data as a classification follows simply: microscopic refers to experimental arrangements in which single encounters of neutrons with nuclei predominate. Distinguishing integral and differential methods of measurement is more difficult. Disagreement is unavoidable because the techniques do overlap, and there is a danger of becoming academic. The following formulation is proposed as a useful one because it focuses on the relationship between the two techniques. Integral measurements: measurements that require for their interpretation an integration of point-wise microscopic data over energy and/or space intervals that are not small compared to the range of interest. Differential measurements: measurements for which the integration of point-wise microscopic data is not necessary for interpretation, only for corrections. Thus, microscopic and macroscopic may refer to both differential and integral results, and not every experiment is uniquely classified. Total cross-sections, for example, are generally derived from microscopic arrangements, differential in energy but integral with respect to the differential scattering cross-section. The bulk of neutron cross-section measurements with accelerators are differential microscopic. Critical mass measurements are always integral macroscopic, but the determination of a leakage spectrum from a critical assembly by time-of-flight is a differential macroscopic measurement.

The measurements to be discussed in this part of the program, therefore, are integral microscopic measurements with fission neutrons. The motive to make these measurements is simple, they are a first step validation of nuclear data. As we say in other company, "Are the data that come from differential microscopic measurements any good - what do they do for us?" Well, one of the first things they ought to do for us is to correctly predict a basic fission cross-section averaged over the shape of the fission spectrum. The truth, as you know, is that for  $^{238}\text{U}$  it does not. This is the beginning of our problem and I shall return to it in a minute.

For most of the people around this table the fission spectrum is a fascinating and interesting phenomena; for other people, however, it is a matter of very expensive decisions. I have been asked to speak for those other people who are not here, those other users of the fission spectrum. For them the area of concern is the integrity of reactor fuels and materials. In this problem area neutron detection by activation is the important instrument for spectrum characterization and dosimetry. And no longer is this technique regarded as a stopgap, something to be replaced some day by a reliable in-pile spectrometer. It is almost certain that activation detectors, quite simply foils, are going to be all that we shall ever have for diagnostic work in the prototype and materials test reactors. And unless something quite unexpected happens to the rate at which accurate differential reaction-rate cross-sections become available, the fission spectrum will remain an important calibration base for these detectors.

Now, to be a little more specific. Integral measurements must be done with an accuracy that is not always necessary for differential methods. The leverage for this class of measurement is generally small and the in-

formation to be derived from them often resides within error bands of a few per cent or less. Thus, critical masses for ideal spheres of enriched uranium and plutonium metal have been measured to a few tenths of a per cent, and material replacement measurements in reactors involve reproducing the reactivity of the reactor to better than a few hundredths of a per cent. For average cross-section ratio measurements in basic critical systems, values at the level of 5% are almost worthless, two per cent numbers are required for really valuable checks of computation. To achieve this kind of accuracy we do not deceive ourselves. We simply retreat. We make our measurements in the simplest possible systems, avoid absolute measurements, use simple detecting schemes, and worst of all engage in long-term efforts. The critical mass measurements just mentioned were begun in the early fifties, yet the latest revision of observed spherical critical masses was published only last year. Similarly, spectral indexes for basic critical assemblies, which incidentally display very nearly

TABLE I.  $^{235}\text{U}$  FISSION SPECTRUM AVERAGED FISSION CROSS-SECTION FOR  $^{238}\text{U}$

OBSERVATION	
Absolute determinations	
Leachman and Schmitt (1957)	$310 \pm 4$ mb
Richmond	(310)
Fabry et al. (1970)	$353 \pm 30$ mb
Ratio measurements	
$^{235}\text{U}/^{238}\text{U}$ plus critical mass of $^{235}\text{U}$ metal sphere, Grundl (1968)	$327 \pm 25$ mb (330 mb for $\chi_{49}$ )
Fabry et al. (1970)	$331 \pm 31$ mb
PREDICTION	
Compilations prior to 1965	309 mb
Evaluations after 1965	
Maxwellian form ( $\bar{E} = 1.935$ MeV)	$273 \pm 5$ mb
Watt form ( $\bar{E} = 2.013$ MeV)	$282 \pm 5$ mb
Implications of recent $\sigma_f(E, ^{235}\text{U})$	
White	270 mb
Poenitz	(240 mb)
Discrepancy: $\frac{\text{Observed}}{\text{Predicted}} = 1.13$	

a fission spectrum shape above 1 MeV, have been carried out periodically for nearly 20 years and by nearly a dozen different experimenters.

We have performed integral measurement, therefore, which we take seriously. We find it difficult, however, to reconcile some of these measurements with differential data. A starting point for displaying the difficulties is the so-called Leachman-Schmitt measurement. This experiment is quite simply a measurement of the average fission cross-section of  $^{238}\text{U}$  for fission neutrons arising from  $^{235}\text{U}$ . The significance of the experiment is clear,  $^{235}\text{U}$  fission neutrons drive the fission neutron chain and  $^{238}\text{U}$  is the fuel for that chain. Table I, taken from Ref. [1], shows the situation regarding observed and predicted values for this average cross-section. The value determined by Leachman and Schmitt, 310 mb, was for thermal neutron-induced fission [2]. A second measurement by Richmond is in excellent agreement but unfortunately was never reported. It is a notebook number. A measurement by Fabry reported in 1970 [3] does not quite agree, but importantly it is on the high side of the Leachman-Schmitt value.

As you can see, the array of results for this basic experiment is not large. If some of you would say that we had best wait for more data from the integral measurers before we spend a lot more effort on differential measurement, I might agree. However, the Leachman-Schmitt measurement was carefully done and properly documented and it has withstood more than one attempt to fault it. Also, new measurements with  $^{252}\text{Cf}$  fission neutrons will be undertaken soon. Still, because so few absolute results exist, it is useful to take the route of deriving information from ratio measurements, our most common retreat [1]. The result as shown in the Table agrees with Leachman-Schmitt, but only because of errors considerably larger than those reported by Leachman and Schmitt. I might note here that more precise and redundantly measured average fission cross-section ratios at the centre of metal critical spheres parallel and substantiate the ratio measurements in Table I [4].

The matter of prediction is summarized in the lower section of the Table. The discrepancy with observation is clear — and rather well known now — it stands as a serious obstacle to improved understanding of almost all fission-associated, fast-neutron spectra.

The fission spectrum, then, is the first bridge between differential neutron cross-section data and the design and operation of functional chain reacting systems. With the remaining time assigned to us, Mr. Fabry and myself would like to describe two particular integral measurements in progress at our respective laboratories. The purpose of the presentation will be to show the strengths and the problems of integral microscopic measurements with fission neutrons. Hopefully it will generate some critical discussion.

#### REFERENCES

- [1] GRUNDL, J.A., "Fission-neutron spectra: Macroscopic and integral results", Neutron Standards and Flux Normalization, AEC Symposium Series 23 (1971).
- [2] LEACHMAN, R.B., SCHMITT, H.W., J. nucl. Energy 4 (1957) 38.
- [3] FABRY, A., DECOSTER, M., MINSART, G., SCHEPERS, J.C., VANDEPLAS, P., Nuclear Data for Reactors (Proc. Conf. Helsinki, 1970) 2, IAEA, Vienna (1970) 535.
- [4] GRUNDL, J.A., HANSEN, G.E., Nuclear Data for Reactors (Proc. Conf. Paris, 1966) 1, IAEA, Vienna (1967) 321-36.



# DISCREPANCIES BETWEEN INTEGRAL AND DIFFERENTIAL MEASUREMENTS OF THE PROMPT FISSION NEUTRON ENERGY SPECTRUM

C.G. CAMPBELL, J.L. ROWLANDS  
UKAEA, Reactor Group,  
Winfrith, Dorchester,  
Dorset, United Kingdom

*Presented by A.T.G. Ferguson*

## Abstract

DISCREPANCIES BETWEEN INTEGRAL AND DIFFERENTIAL MEASUREMENTS OF THE PROMPT FISSION NEUTRON ENERGY SPECTRUM.

The results of recent differential measurements of the fission spectra of  $^{235}\text{U}$  and  $^{239}\text{Pu}$  are summarized and discrepancies between these measurements and values deduced from integral measurements are discussed. It is recommended that the differential measurements should be re-evaluated to determine the best shape for the spectrum and the uncertainty in the shape and that the different activation measurements made in a fission spectrum should be evaluated and discrepancies identified. It is also recommended that further measurements of the average value of the  $^{238}\text{U}$  fission cross-section in a  $^{235}\text{U}$  thermal fission spectrum should be made.

## 1. INTRODUCTION

The calculation of reactions with thresholds at MeV energies (such as  $^{238}\text{U}$  fission) and the range of neutron diffusion during moderation requires an accurate knowledge of the fission spectrum shape. Evaluations of the differential measurements have concluded that the spectra are accurately known (the mean energies being accurate to  $\pm 1\%$ ) but a number of integral measurements indicate that the mean energy of the fission spectrum for  $^{235}\text{U}$  thermal fission should be 5 or 10% higher than that given by the differential measurements and an analysis of activation measurements suggests that the shape differs significantly from the Maxwellian form that represents the differential measurements. Integral measurements also give a smaller value for the difference between the mean energies of the  $^{239}\text{Pu}$  and  $^{235}\text{U}$  thermal fission spectra than the value obtained from an evaluation of the differential measurements. A knowledge of this difference is required when relating measurements made in  $^{235}\text{U}$ -fuelled systems to corresponding  $^{239}\text{Pu}$ -fuelled reactors.

One of the most important types of integral measurement relating to the fission spectrum is the value of the  $^{238}\text{U}/^{235}\text{U}$  fission ratio measured in a fission spectrum or a reactor spectrum. Lubitz and Stewart [1] have recently reviewed the differential and integral measurements and they argue that errors in the  $^{238}\text{U}$  and  $^{235}\text{U}$  fission cross-sections used in the analysis could explain the discrepancy between calculation and these integral measurements. However, other integral measurements that do not involve fission cross-sections (such as age measurements) also indicate a higher mean energy. Some preliminary fast reactor spectrum measurements at

MeV energies also suggest that it is the spectrum that is in error rather than the fission cross-sections. A recent review of the differential measurements of fission spectra, made by Jaffey [2], concludes that the spectrum is not well determined by the measurements, which may be subject to systematic errors such as the efficiency calibration of the neutron detector.

Fabry et al. [3] have made a least squares fit to the  $^{235}\text{U}$  fission spectrum activation measurements and found that a good fit can be obtained using the Watt spectrum (which fits the differential measurements). In this fitting there was an 11% error in the  $^{238}\text{U}/^{235}\text{U}$  fission ratio calculated using the conventional values of the cross-sections but ways were suggested in which these cross-sections could be modified to be consistent with the fission spectrum averages and the differential cross-section measurements. A still better fit to the activation of detectors with thresholds in the high MeV range was obtained by using a more general form for the fission spectrum, but the mean energy was still within 3% of 2 MeV, the value obtained from differential measurements.

The object of the present paper is to present a brief summary of the differential and integral measurements and to suggest further work that might resolve the discrepancies.

## 2. DIFFERENTIAL MEASUREMENTS

Barnard et al. [4] have reported measurements of the fission spectra of  $^{235}\text{U}$ ,  $^{238}\text{U}$  and  $^{239}\text{Pu}$  and have evaluated the available differential data. They conclude that the data can be represented by the Maxwellian form and recommend the values for the temperatures and mean energies ( $\bar{E} = \frac{3}{2}T$ ) of the Maxwellian given in Table I. The ratio of the mean energies for the  $^{239}\text{Pu}$  and  $^{235}\text{U}$  spectra is 1.07.

Smith [5] has recently reported preliminary measurements for  $^{235}\text{U}$  and  $^{239}\text{Pu}$ . The object of the measurements was to determine the shape below 1.6 MeV and the ratio of the temperatures for  $^{239}\text{Pu}$  and  $^{235}\text{U}$ . The temperature for the  $^{235}\text{U}$  spectrum measured to 1.6 MeV is consistent with the measurements of Barnard et al. (The best fit to the data corresponds to a temperature of  $1.41 \pm 0.14$  MeV, while the spectrum measured by Barnard et al. below 1.6 MeV corresponds to a temperature of 1.37 MeV. Fitting to the wider energy range in the measurements of Barnard et al.

TABLE I. MEAN ENERGIES AND MAXWELLIAN TEMPERATURES FOR THERMAL FISSION SPECTRA OF  $^{235}\text{U}$  AND  $^{239}\text{Pu}$

		Mean energies (MeV)	Temperatures (MeV)
Maxwellian:			
$^{235}\text{U}$	Thermal fission	$1.95 \pm 0.015$	$1.30 \pm 0.01$
$^{239}\text{Pu}$	Thermal fission	$2.085 \pm 0.015$	$1.39 \pm 0.01$

results in a temperature of 1.29 MeV.) The ratio of temperatures for  $^{239}\text{Pu}$  and  $^{235}\text{U}$  were measured over a wider energy range (up to 8 MeV) and gave a ratio of  $1.075 \pm 2\%$  consistent with the recommendations of Barnard et al.

Recent measurements by Rickard [6] made using a  $^6\text{Li}$  spectrometer, when fitted by a Maxwellian, result in a temperature of  $1.34 \pm 0.04$  MeV for  $^{235}\text{U}$  thermal fission.

The recent measurements, while not inconsistent with the recommendations of Barnard et al., do give higher temperatures. Jaffey's remarks suggest that a re-evaluation of the earlier measurements might result in larger uncertainties being assigned to them. An evaluation of the earlier data and the recent measurements would then result in a temperature a few per cent higher than the Barnard et al. value. A re-evaluation of the earlier data might also show how more accurate measurements could be made.

Possible departures from the Maxwellian form that are consistent with the differential measurements might be significant in reactor calculations. The range of shapes that is consistent with the differential measurements should be evaluated. The significance of this range of shapes could be assessed by calculating the  $^{238}\text{U}/^{235}\text{U}$  fission ratio variation. It is thought that a re-evaluation of the spectrum measurements, taking into account possible departures from a Maxwellian form, might result in a calculated fission ratio about 5% higher than the value obtained using the spectrum recommended by Barnard et al.

### 3. ACTIVATION MEASUREMENTS

Grundl [7] has made activation measurements in a  $^{235}\text{U}$  thermal fission spectrum using a number of detectors. An analysis of these measurements made by McElroy [8] gives a fission spectrum with 20% fewer neutrons below 1.4 MeV and 16% more above (10% more in the range 1.4 to 3 MeV and 30% more in the range 3 to 6 MeV). The mean energy of the spectrum is about 2.2 MeV.

An analysis of activation measurements made by Bresesti et al. [9] shows them to be consistent with the differential measurements of the fission spectrum. The measured activation cross-sections are renormalized by the factor 1.14 to give a best fit to the Watt spectrum. The measured and calculated activation cross-sections then differ by up to about 7%, with an average difference of 3%. The peak deduced from Grundl's measurements between 3 and 6 MeV is not consistent with Bresesti's measurements, and the discrepancy found for  $^{238}\text{U}$  fission by Fabry et al. is not apparent in this analysis.

The studies made by Fabry et al. indicate that the activation measurements and the differential measurements can be reconciled by making changes to the standard  $^{238}\text{U}$  and  $^{235}\text{U}$  fission cross-section evaluations. An attempt should be made to verify these changes by differential cross-section measurements. They also show that a more general form than the Maxwellian form is required to give a good fit to the activation measurements. A simultaneous fit to the differential spectrum measurements and the activation detector measurements would be a logical extension of the work, although the good fit to the activation measurements obtained using the Watt

TABLE II.  $^{238}\text{U}$  CROSS-SECTION IN THE  $^{235}\text{U}$  FISSION SPECTRUM

	Cross-section (mb)
Fabry et al.	$353 \pm 30$ and $374 \pm 30$
Leachman and Schmidt; Richmond	$313 \pm 5$
Nikolaev et al.	$310 \pm 10$
Calculation	301

spectrum implies that the spectra derived by fitting to the activation detectors (with modified  $^{238}\text{U}$  and  $^{235}\text{U}$  data) should also fit the differential measurements.

There is a need to resolve discrepancies between the activation measurements made by Grundl, Boldeman, Bresesti and Fabry and between the different analyses.

#### 4. $^{238}\text{U}$ FISSION CROSS-SECTION IN A FISSION SPECTRUM

The average value of the  $^{238}\text{U}$  fission cross-section in a fission spectrum has been measured by Fabry et al., Leachman and Schmidt [10], Richmond [11] and Nikolaev [12]. Their values are given in Table II, together with the value calculated using the recommended fission spectrum and the  $^{238}\text{U}$  fission cross-section evaluated by Hart [13]. This is a more valuable integral measurement than the  $^{238}\text{U}/^{235}\text{U}$  fission ratio in a fission spectrum because it is closely related to the  $^{238}\text{U}$  fission rate per fission in a reactor (and removes one source of uncertainty — the  $^{235}\text{U}$  fission cross-section). Further measurements of this quantity would be valuable.

#### 5. AGE TO THE INDIUM RESONANCE

Measurements of the second moment of the spatial distribution of reactions in indium resulting from a fission neutron source in a moderator (the age to the indium resonance) provide information on the mean lethargy of the fission spectrum. The uncertainties in the cross-sections of carbon,  $\text{H}_2\text{O}$  and  $\text{D}_2\text{O}$  are small. Story [14] has made an analysis of the age measurements in these moderators and reached the preliminary conclusion that a fission spectrum with a Maxwellian temperature of  $1.35 \pm 0.02$  MeV gives a best fit to the measurements (a mean energy of  $2.025 \pm 0.03$  MeV).

#### 6. ANALYSIS OF $^{238}\text{U}/^{235}\text{U}$ FISSION RATES IN FAST REACTOR SPECTRA

Campbell and Rowlands [15] have described a cross-section adjustment study made to fit a wide range of integral measurements. The mean energy

TABLE III. RATIO OF THE MEAN ENERGIES OF THE FISSION SPECTRA OF  $^{239}\text{Pu}$  AND  $^{235}\text{U}$ 

Barnard et al.	Differential	$1.07 \pm 0.02$
Smith	Differential	$1.075 \pm 0.02$
Grundl	Integral	$1.039 \pm 0.002$
Bonner	Integral	$1.040 \pm 0.003$
Kovalev et al.	Integral	$1.04 \pm 0.01$

of the fission spectrum was included as a variable. The mean energy of the  $^{235}\text{U}$  fission spectrum was increased by  $8\% \pm 5\%$ , to  $2.10 \pm 0.10$  MeV, the assumed standard deviation being  $\pm 10\%$ . The  $^{238}\text{U}/^{235}\text{U}$  fission ratio measurements made in reactor spectra were the quantities that determined the adjustment. When a smaller uncertainty was assumed a smaller adjustment resulted.

#### 7. INTEGRAL MEASUREMENTS OF THE RATIO OF THE MEAN ENERGIES OF $^{239}\text{Pu}$ AND $^{235}\text{U}$ FISSION SPECTRA

Integral measurements of the ratio of the mean energies of the fission spectra for  $^{239}\text{Pu}$  and  $^{235}\text{U}$  have been made by Grundl [16], Bonner [17] and Kovalev et al. [18] and their results are compared with the values derived from differential measurements by Barnard et al. and by Smith in Table III. The two types of measurement make a different type of averaging over the fission spectrum. The difference could be explained if the  $^{239}\text{Pu}$  fission spectrum departs from the Maxwellian form in a different way to the  $^{235}\text{U}$  spectrum.

#### 8. REACTOR SPECTRUM MEASUREMENTS

Lubitz and Stewart have summarized a number of reactor spectrum measurements, both differential measurements made with nuclear emulsions and measurements made with activation detectors. These measurements are more consistent with the differential fission spectrum measurements than the spectrum derived from Grundl's activation measurements.

Rickard has made  $^6\text{Li}$  spectrometer measurements in the Zebra 8H assembly and concludes that the 12% underestimate of the  $^{238}\text{U}/^{235}\text{U}$  fission rate is caused by an underestimation of the spectrum above the  $^{238}\text{U}$  fission threshold, rather than an underestimate of the  $^{238}\text{U}$  fission cross-section.

#### 9. CONCLUSIONS

A new evaluation of the differential measurements is required in which the best form (not necessarily Maxwellian or Watt) is selected and the

TABLE IV. MEAN ENERGIES AND MAXWELLIAN TEMPERATURES FOR THE  $^{235}\text{U}$  FISSION SPECTRUM

Authors	Type of measurement	Form of fit	Mean energy (MeV)	Maxwellian temperature (MeV)
Barnard et al.	Differential	Maxwellian	$1.95 \pm 0.015$	$1.30 \pm 0.01$
	Differential (below 1.6 MeV)	Maxwellian		(1.37 )
Smith	Differential (below 1.6 MeV)	Maxwellian		$(1.41 \pm 0.14)$
Rickard	Differential ( $^6\text{Li}$ )	Maxwellian	$2.01 \pm 0.06$	$1.34 \pm 0.04$
Grundl and McElroy	Activation detectors	5 groups	$\sim 2.2$	
Bresetti et al.	Activation detectors	Watt	2.00	
Fabry et al.	Activation detectors	Watt and other forms	1.948 to 2.024	
Story	Age measurements	Maxwellian	$2.025 \pm 0.03$	$1.35 \pm 0.02$
Campbell and Rowlands	Reactor measurements	Maxwellian	$2.10 \pm 0.10$	$1.40 \pm 0.07$

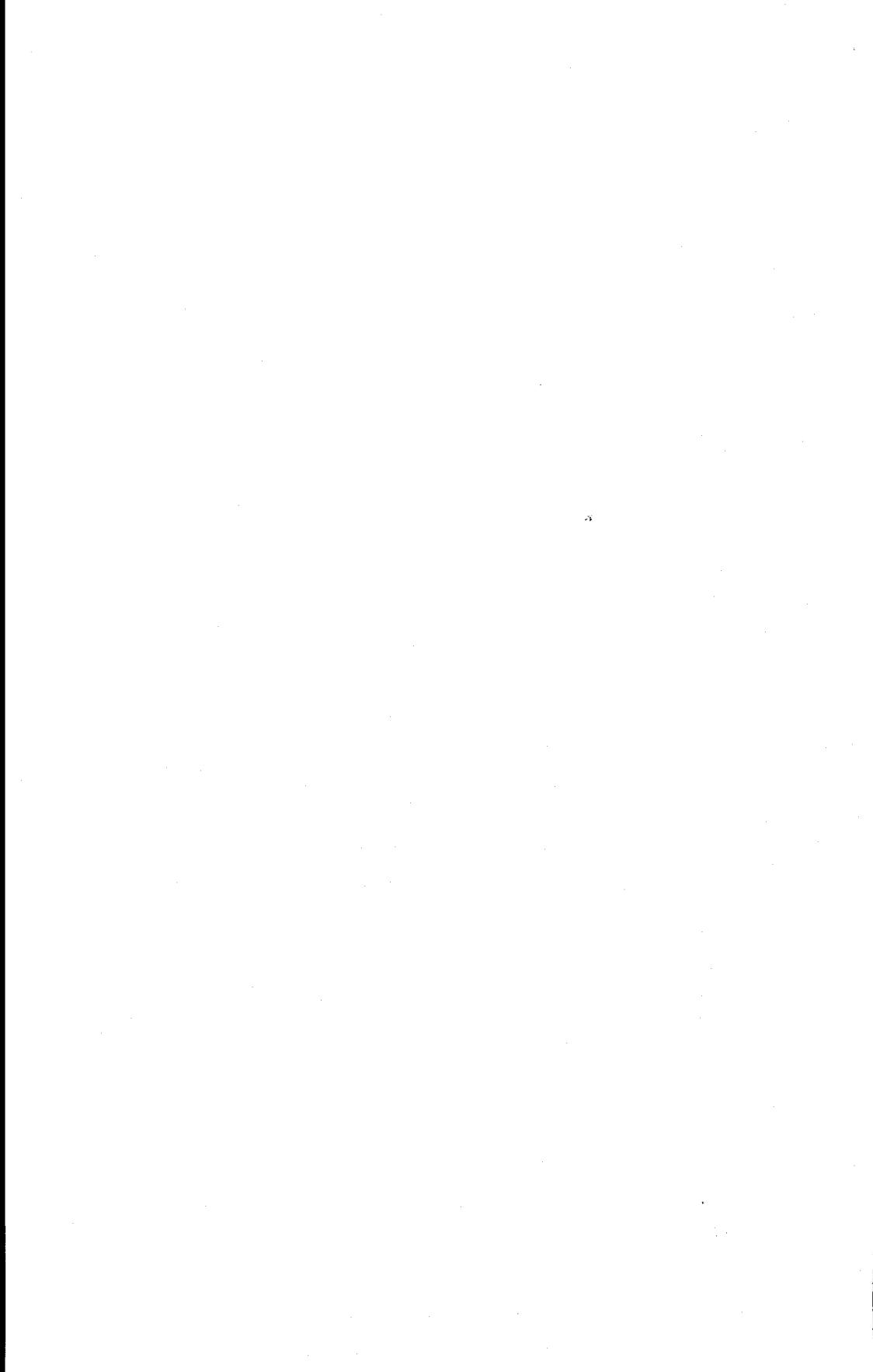
uncertainties in the mean energy and in the shape are assessed. The evaluation should include an assessment of the measurements of the  $^{239}\text{Pu}$  spectrum relative to the  $^{235}\text{U}$  spectrum.

Fission spectrum activation measurements should be evaluated and discrepancies identified. There is a large discrepancy between the measurements of the  $^{238}\text{U}$  fission cross-section in a fission spectrum. Further measurements of this important integral quantity are desirable. An attempt should be made to resolve the discrepancies between the different analyses of activation measurements. For example, Fabry et al. and Bresesti et al. find that the Watt spectrum gives a good fit to the measurements, but McElroy deduces a quite different shape. Fabry finds a large discrepancy for the  $^{238}\text{U}$  fission activation whereas Bresesti finds it to be consistent with the Watt spectrum.

The different values derived for the mean energy of the  $^{235}\text{U}$  thermal neutron fission spectrum, or the temperature of the Maxwellian, are summarized in Table IV.

#### REFERENCES

- [1] LUBITZ, C.R., STEWART, L., Remarks on the Neutron-Induced Fission Spectrum, Rep. EANDC(US)-139/L.
- [2] JAFFEY, A.H., Prompt-neutron Spectra and Delayed-neutron Spectra from Fission: Some Comments on Current Knowledge, Rep. ANL-7747 (1970).
- [3] FABRY, A., De COSTER, M., MINSART, G., SCHEPERS, J.C., VANDERPLAS, P., "Implications of fundamental integral measurements on high energy nuclear data for reactor physics", Nuclear Data for Reactors, (Proc. Conf. Helsinki, 1970) 2, IAEA, Vienna (1970) 535.
- [4] BARNARD, E., FERGUSON, A.T.G., McMURRAY, W.R., Van HEERDEN, I.J., Time of flight measurements of neutron spectra from the fission of U235, U238 and Pu239, Nucl. Phys. 71 (1965) 228.
- [5] SMITH, A.B., Note on Prompt Fission Neutron Spectra of U235 and Pu239, Rep. EANDC(US)-153/L.
- [6] RICKARD, I.C., The Measurement of Fast Neutron Spectra with Semiconductor Detectors, Ph.D. thesis University of London, 1971.
- [7] GRUNDL, J.A., A study of fission neutron spectra with high energy activation detectors. Part II: Fission spectra, Nucl. Sci. Engng 31 (1968) 191.
- [8] McELROY, W.N., Implications of recent fission-averaged cross-section measurements, Nucl. Sci. Engng 36 (1969) 109.
- [9] BRESESTI, A.M., BRESESTI, M., ROTA, A., RYDIN, R.A., Threshold reaction excitation functions intercalibrated in a pure fission spectrum, Nucl. Sci. Engng 40 (1970) 331.
- [10] LEACHMAN, R.B., SCHMIDT, H.W., J. nucl. Energy 4 (1957) 38.
- [11] RICHMOND, R., results quoted ALLEN, D.W., HENKEL, R.L., Progr. nucl. Energy, Ser. I 2, Pergamon Press, Oxford (1957).
- [12] NIKOLAEV, M.N., GOLUBEV, V.I., BONDARENKO, I.I., Soviet Phys. JETP 7 (1958) 517.
- [13] HART, W., Fission Cross-section Data Files for Th232, U233, U234, U235, U236, U238, Np237, Pu239, Pu241 and Pu242 in the Energy Range 1 keV to 14 MeV, Rep. AHSB(S)-R 124 (1967).
- [14] STORY, J.S., "Neutron cross-section evaluation in the thermal and resonance energy range for nuclides of mass less than 220", Nuclear Data For Reactors (Proc. Conf. Helsinki, 1970) 1, IAEA, Vienna (1970) 721.
- [15] CAMPBELL, C., ROWLANDS, J.L., "The relationship of microscopic and integral data", Nuclear Data For Reactors (Proc. Conf. Helsinki, 1970) 2, IAEA, Vienna (1970) 391.
- [16] GRUNDL, J.A., Dissert. Abstr. 25 11 (1965) 6704.
- [17] BONNER, T.W., Nucl. Phys. 23 (1961) 116.
- [18] KOVALEV, B.P., STAVINSKI, V.S., Soviet J. atom. Energy 5 (1958) 1588.





# FISSION NEUTRON ENERGY SPECTRA INDUCED BY FAST NEUTRONS ON $^{238}\text{U}$ , $^{235}\text{U}$ AND $^{239}\text{Pu}$

H.-H. KNITTER, M. COPPOLA,\* M.M. ISLAM,\*\*  
N. AHMED,† B. JAY  
Central Bureau for Nuclear Measurements,  
EURATOM,  
Geel, Belgium

## Abstract

FISSION NEUTRON ENERGY SPECTRA INDUCED BY FAST NEUTRONS ON  $^{238}\text{U}$ ,  $^{235}\text{U}$  AND  $^{239}\text{Pu}$ .

Measurements of fission neutron energy spectra induced by fast neutrons on  $^{238}\text{U}$ ,  $^{235}\text{U}$  and  $^{239}\text{Pu}$  using time-of-flight technique are presented. The average fission neutron energies have been calculated from the time-of-flight spectra of  $^{238}\text{U}$  at incident neutron energies of 1.9 and 2.3 MeV, of  $^{235}\text{U}$  at 0.14, 0.40, 1.5, 1.9 and 2.3 MeV, and of  $^{239}\text{Pu}$  at 1.5, 1.9, 2.3, 4.0, 5.0 and 5.5 MeV. Their values have been compared with the theoretical predictions of Terrell. The angular distributions of the fission neutrons are also evaluated in some cases to look for any anisotropy in their emission.

## 1. INTRODUCTION

A good knowledge of the parameters of the neutron-induced fission process is of significance for the optimum economical layout of nuclear power plants. For fast breeder reactors one important set of parameters is those that describe the prompt fission neutron spectrum. Despite its importance, only a small amount of effort has been devoted to the accurate determination of fission neutron spectra. There exist for  $^{235}\text{U}$  only measurements of the fission neutron energy spectra for thermal [1-3], slow [4], 40 keV [5], 100 keV [6], 1.5 MeV [5] and 14.3 MeV [7] incident neutron energies. Only measurements at spot energies [6-9] have been made on  $^{238}\text{U}$  so far. Measurements exist for  $^{239}\text{Pu}$  at thermal [1, 2, 8, 10-12], 40 keV [5], 130 keV [6] and 2.0 MeV [13] incident neutron energies.

A relevant question is the dependence of the fission neutron spectrum on the incident neutron energy or with  $\bar{\nu}$ , the average number of neutrons produced per fission event. A theoretical study of this problem was undertaken by Terrell [14, 15] who concluded that the fission neutron spectrum in the laboratory reference system should be of Maxwellian shape and derived an equation that gives the variation of the average fission neutron energy  $\bar{E}$  of the Maxwellian spectrum with  $\bar{\nu}$ . One of the cases best suited to a study of the dependence of the average fission neutron energy  $\bar{E}$  on the incident neutron energy  $E_n$  is the neutron-induced fission process on  $^{239}\text{Pu}$ , since for this isotope the dependence of  $\bar{\nu}$  with the incident neutron energy  $E_n$  is rather strong.

\* Present address: CCR, Ispra, Italy.

\*\* Guest collaborator from the Pakistan AEC.

† Present address: Atomic Energy Centre, Dacca, Bangladesh.

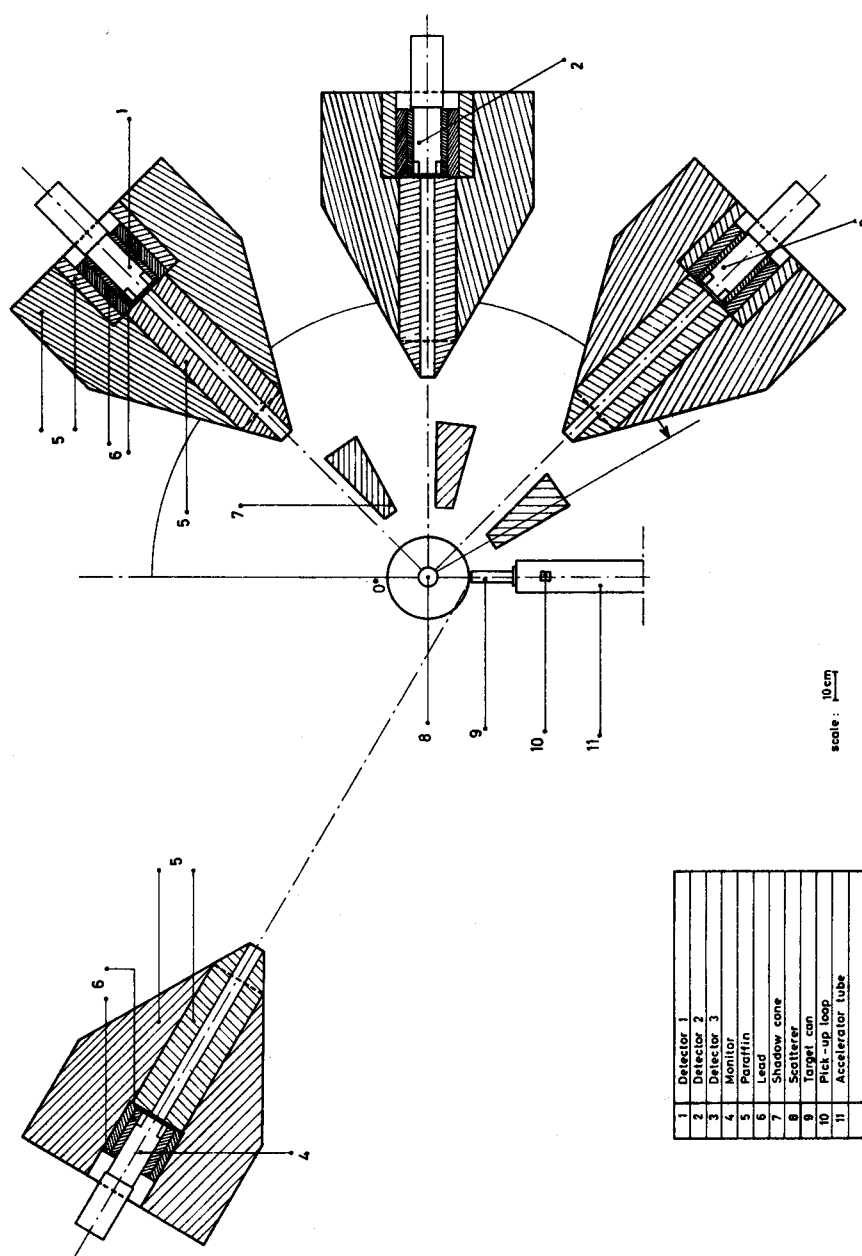


FIG. 1. Layout of the detecting system.

If one also considers in this analysis the value of the average fission neutron energy of the spontaneous fission neutron spectrum of  $^{240}\text{Pu}$ , it is possible to investigate the above dependence on  $\bar{\nu}$  over a large region of  $\bar{\nu}$  starting from the value of 2.19 (see Fig. 12).

In this paper the results of the measurements of fission neutron energy spectra of  $^{238}\text{U}$  at incident neutron energies of 1.9 and 2.3 MeV, of  $^{235}\text{U}$  at 0.14, 0.40, 1.5, 1.9 and 2.3 MeV and of  $^{239}\text{Pu}$  at 1.5, 1.9, 2.3, 4.0, 4.5, 5.0 and 5.5 MeV are presented. For the measurements on  $^{239}\text{Pu}$  and  $^{238}\text{U}$  see also Refs [16] and [17] respectively.

## 2. EXPERIMENTAL EQUIPMENT AND PROCEDURE

The measurements were done at the 3-MV Van de Graaff accelerator of CBNM using the fast neutron time-of-flight technique. The layout of the experimental set-up is shown in Fig. 1. A pulsed ion beam of 1-ns pulse width and 1-MHz repetition rate was focused on the neutron-producing target. For neutron production three different reactions were used. For the measurement at 0.14 MeV neutrons were produced through the  $^7\text{Li}(p, n)^7\text{Be}$  reaction. For the measurements between 0.4 and 2.3-MeV incident neutron energies the neutrons were produced through the  $\text{T}(p, n)^3\text{He}$  reaction and at neutron energies between 4.0 and 5.5 MeV use was made of the  $\text{D}(d, n)^3\text{He}$  reaction in conjunction with a deuterium gas target described elsewhere [18].

The neutrons, emitted around  $0^\circ$  with respect to the direction of the incoming ion beam, were scattered by the sample towards three detectors placed at equal distances from the scatterer and viewing it through their collimating shieldings. Each detector consisted of a cylindrical NE 102A plastic scintillator, 5.0 cm in diameter and 2.5 cm thick, viewed by an AVP 56/03 photomultiplier. The fast outputs of the three detectors gave the start signal for three time-to-pulse height converters. The stop signals were extracted from a pick-up loop before the ion target at about 30 cm distance. The output signals of the time-to-pulse height converters were registered simultaneously in three different sections of a 4096-channel pulse height analyser. The overall time resolution of such a neutron time-of-flight spectrometer, including the ion pulse width of the accelerator, was about 2.3 ns.

The relative neutron fluence was measured with a fourth time-of-flight spectrometer of the same type with the detector inserted in a shielding collimating the neutrons coming from the neutron-producing target. The monitor was placed at  $-20^\circ$  with respect to the ion beam and at a distance of 5 m from the neutron-producing target. By means of a window discriminator, only that part of the neutron time spectrum corresponding to the neutrons from the target was selected to monitor the measurements.

A great effort was made to determine experimentally the relative efficiency of the detectors. Since the angular distributions of neutron source reactions are not known with sufficient accuracy, they cannot safely be used for this special calibration purpose. A much better way to obtain the detector efficiency is to measure the angular distribution of neutrons scattered from hydrogen at one or more incident neutron energies in order to cover with a sufficient number of points all the energy range of interest. Therefore, the neutron scattering from a hydrogenous sample was measured at 2.3 and 5.75-MeV incident neutron energies in angular steps of  $2.5^\circ$  between

TABLE I. SAMPLE USED IN THE INVESTIGATIONS

Sample	External diameter (cm)	Internal diameter (cm)	Height (cm)	Weight (g)	Isotopic abundance (%)
$^{238}\text{U}$	3.50	2.60	2.50	205.09	99.00
$^{235}\text{U}$	3.00	2.10	2.46	161.27	93.15
$^{239}\text{Pu}$	1.20	-	2.50	54.80	98.91

20° and 67.5°. The hydrogenous sample was a hollow polyethylene cylinder of 1.00 cm outside diameter, 0.60 cm inside diameter and 4.00 cm height. Its weight was 1.840 g and the content of hydrogen was  $(14.31 \pm 0.06)\%$ . Corrections for the attenuation of the scattered neutron flux density were applied to the experimental results. They were calculated using the program MAGGIE in the version modified at CBNM [19] and, for comparison, using the method described by Cranberg and Levin [20].

In addition, the efficiency ratios of two of the detectors with respect to the first one were determined experimentally by measuring the direct neutron yield from source reactions in the energy range concerned under the same geometrical conditions for each counter. In this way it was possible to compare the efficiency ratios obtained with two different experimental procedures.

In determining the shapes of the fission neutron spectra it is important to have an accurate determination of the time scale of the time-of-flight spectra. Therefore, deliberately to avoid the use of delay lines, time-of-flight spectra of direct neutrons were recorded at different primary neutron energies between 0.4 and 2.3 MeV. The time interval per channel was then obtained from the positions of the neutron and  $\gamma$ -ray peaks in the spectra, the distance between target and detector and the known primary neutron energies. In this way, the linearity of the time scale was also checked. The non-linearity was found to be smaller than 0.5%.

The specifications of the samples used in the present investigation are given in Table I. The  $^{238}\text{U}$  sample was a hollow cylinder of natural uranium. The  $^{235}\text{U}$  sample consisted of 10 cylindrical rings canned in an aluminium container of 0.2 mm wall thickness. The  $^{239}\text{Pu}$  sample was a solid cylinder canned in a Zircaloy container of 0.2 mm wall thickness. Empty cans of the same materials and of equal weights and shapes were used to subtract the scattering contributions coming from the containers of the samples.

Each sample and the respective can were mounted on a 0.15-mm diameter tungsten wire vertically in front of the neutron-producing target. The distance between the target and the centre of the sample was 15 cm for both the  $^{238}\text{U}$  and  $^{235}\text{U}$  measurements and 10 cm in the  $^{239}\text{Pu}$  case. The distance between the sample and the detectors was always 1.41 m. The measurements were performed with the sample in the addition mode and subsequently with the can in the subtraction mode for the same number of monitor counts. They were alternately repeated until the statistics in the spectra were sufficient. The changing of the sample and the can was done automatically.

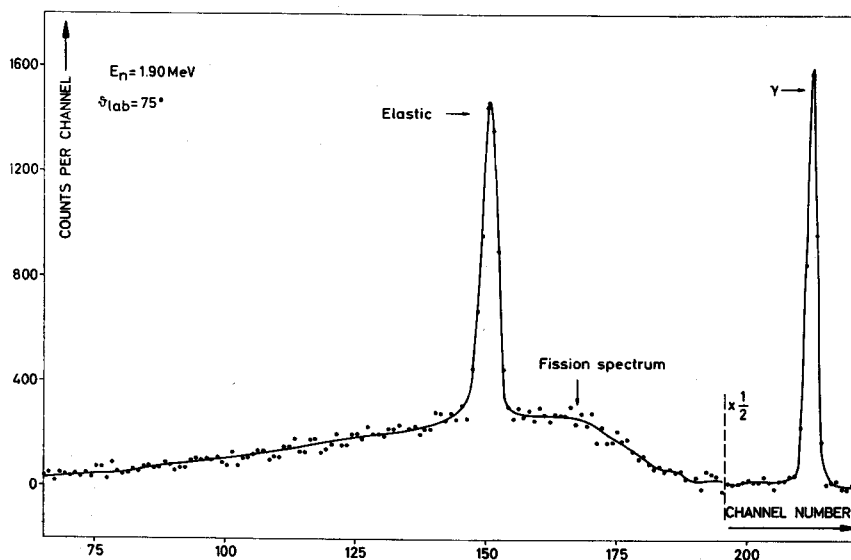


FIG.2. Typical time-of-flight spectrum.

All the measurements for the uranium isotopes were taken, except for the ones at  $E_n = 0.40$  MeV and  $0.14$  MeV for  $^{235}\text{U}$ , at 17 or more angles between  $20^\circ$  and  $150^\circ$ . The measurements between  $20^\circ$  and  $60^\circ$ , between  $70^\circ$  and  $110^\circ$ , and between  $120^\circ$  and  $150^\circ$  were done with the first, second and third counter respectively.

In the case of  $^{235}\text{U}$ , measurements at  $E_n = 0.4$  and  $0.14$  MeV were done at three fixed angles of  $45^\circ$ ,  $90^\circ$  and  $135^\circ$  with the three counters. Only in the  $0.14$ -MeV case was a 'coincidence counter' of low energy threshold used in place of the second counter. For  $^{239}\text{Pu}$  the measurements taken with counter 1 between  $25^\circ$  and  $75^\circ$  were analysed to evaluate the fission neutron spectra [16].

### 3. EXPERIMENTAL RESULTS

A time-of-flight spectrum, typical of all the measurements taken on the two uranium isotopes and on  $^{239}\text{Pu}$ , is shown in Fig.2. Since in this context we want to deal only with fission neutron spectra, the interesting part of the spectrum is the one that appears above the elastic peak. This part shows a pure fission neutron spectrum. The part below the elastic peak is composed of fission neutron events and of events emanating from inelastic neutron scattering.

#### 3.1. Fission neutron spectra of $^{238}\text{U}$

In the case of  $^{238}\text{U}$  the part of the time-of-flight spectra containing purely fission neutrons was investigated for incident neutron energies of  $1.9$

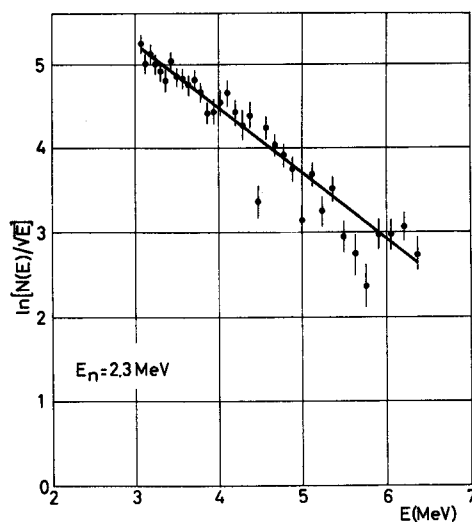


FIG. 3. Sum of the fission neutron spectra of  $^{238}\text{U}$  measured between  $120^\circ$  and  $150^\circ$  at  $E_n = 2.3$  MeV. The solid line represents the best fit through the experimental points.

TABLE II. MAXWELLIAN TEMPERATURE  $T_F$  AND AVERAGE FISSION NEUTRON ENERGY  $\bar{E}$  OF  $^{238}\text{U}$

$E_n$ (MeV)	$T_F$ (MeV)	$\bar{E}$ (MeV)
1.90	1.35	$2.02 \pm 0.08$
2.30	1.23	$1.85 \pm 0.08$

and 2.3 MeV to determine the average fission neutron energy  $\bar{E}$ . If the number of fission neutrons emitted per unit energy interval  $N_F(E)$  in the laboratory system can be represented by a Maxwellian distribution [14] of the form

$$N_F(E) = C_F \cdot \sqrt{E} \exp(-E/T_F) \quad (1)$$

where  $C_F$  is a normalizing constant,  $E$  the emitted neutron energy and  $T_F$  is related to the average fission neutron energy by  $\bar{E} = 3/2 T_F$ , a plot of  $\ln(N_F(E)/\sqrt{E})$  against the emitted neutron energy  $E$  should give values around a straight line. At each primary neutron energy the spectra measured with the same counter at different angles were summed up. The sum spectra were corrected for counter efficiencies, transformed into energy spectra and used to calculate the two parameters  $C_F$  and  $T_F$  of Eq. (1) by the method of least squares. It was found that the experimental points are fairly well distributed around a straight line. An example of the fission neutron sum spectra is shown in Fig. 3. The experimental values of  $\bar{E}$  are given in Table II. The values of the average fission neutron energy  $\bar{E}(E_n)$  determined in this experiment are plotted in Fig. 4 against the incident neutron energy  $E_n$ .

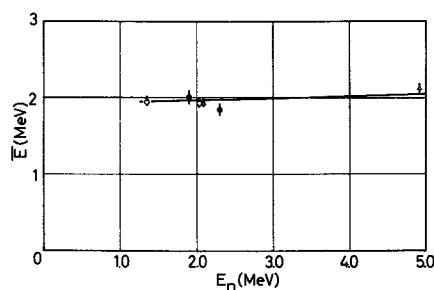


FIG. 4. Variation of the average fission neutron energy  $\bar{E}$  of  $^{238}\text{U}$  with the incident neutron energy  $E_n$ :  $\bullet$  present work;  $\Delta$  Ref. [6];  $\circ$  Ref. [9]. The solid line refers to calculations using Eq. (2).

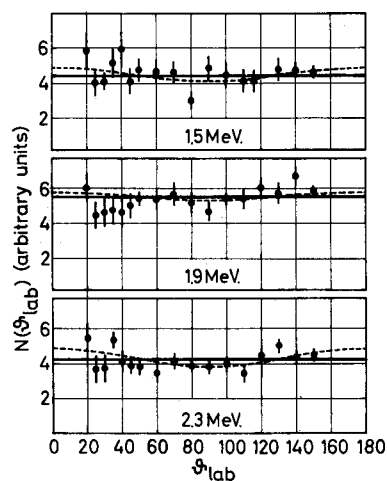


FIG. 5. Fission neutron angular distributions from neutron-induced fission of  $^{238}\text{U}$  with respect to the direction of the incoming neutron beam.

together with the results of other works [6, 9]. A theoretical curve was also calculated following Terrell's assumption [14, 15] that the average energy of the fission neutrons may be related to  $\bar{\nu}(E_n)$ , the average number of neutrons per fission event, by the expression

$$\bar{E}(E_n) = \bar{E}_f + 0.645(\bar{\nu}(E_n) + 1)^{\frac{1}{2}} \quad (2)$$

where  $\bar{E}_f$  is the average fission fragment kinetic energy per nucleon. Its value was taken to be 0.74 MeV [2]. The numerical values of  $\bar{\nu}(E_n)$  are given in Ref. [21]. The agreement between the experimental points and the theoretical curve is good.

The angular distribution of fission neutrons  $N(\theta)$  has also been evaluated from the neutron time-of-flight spectra at incident neutron energies of 1.5, 1.9 and 2.3 MeV. For this purpose the counts per channel in each spectrum were corrected for counter efficiency and summed up between the fission neutron energy limits of 2.14 and 6.30 MeV, 2.62 and 6.28 MeV, and 3.06 and 5.62 MeV at the primary neutron energies of 1.5, 1.9 and 2.3 MeV respectively. The angular distributions obtained are shown in Fig. 5. The

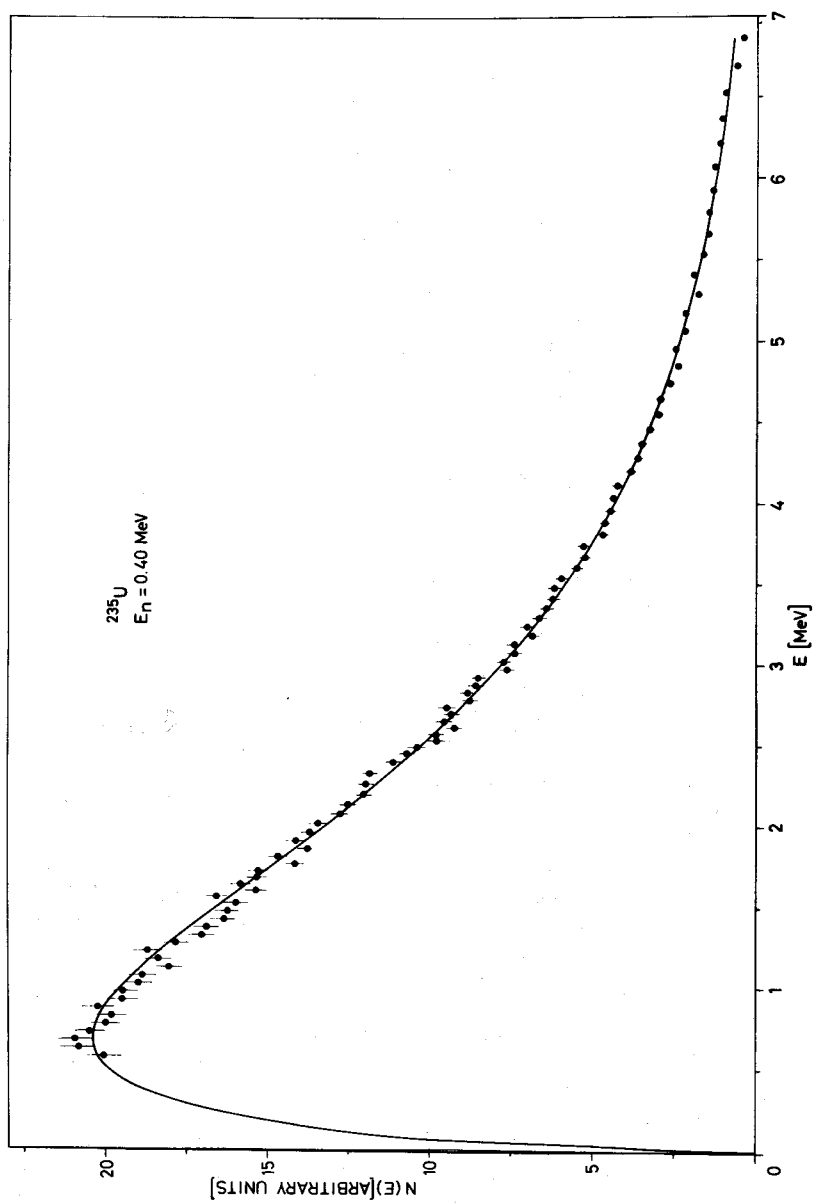


FIG. 6. Preliminary fission neutron spectrum from neutron-induced fission of  $^{235}\text{U}$  at  $E_n = 0.40$  MeV and  $\theta_{\text{lab}} = 135^\circ$ . Solid line represents the least squares fit through the experimental points taken from 1 MeV onwards; dashed curve is an eye-guide through the experimental points below 1 MeV.



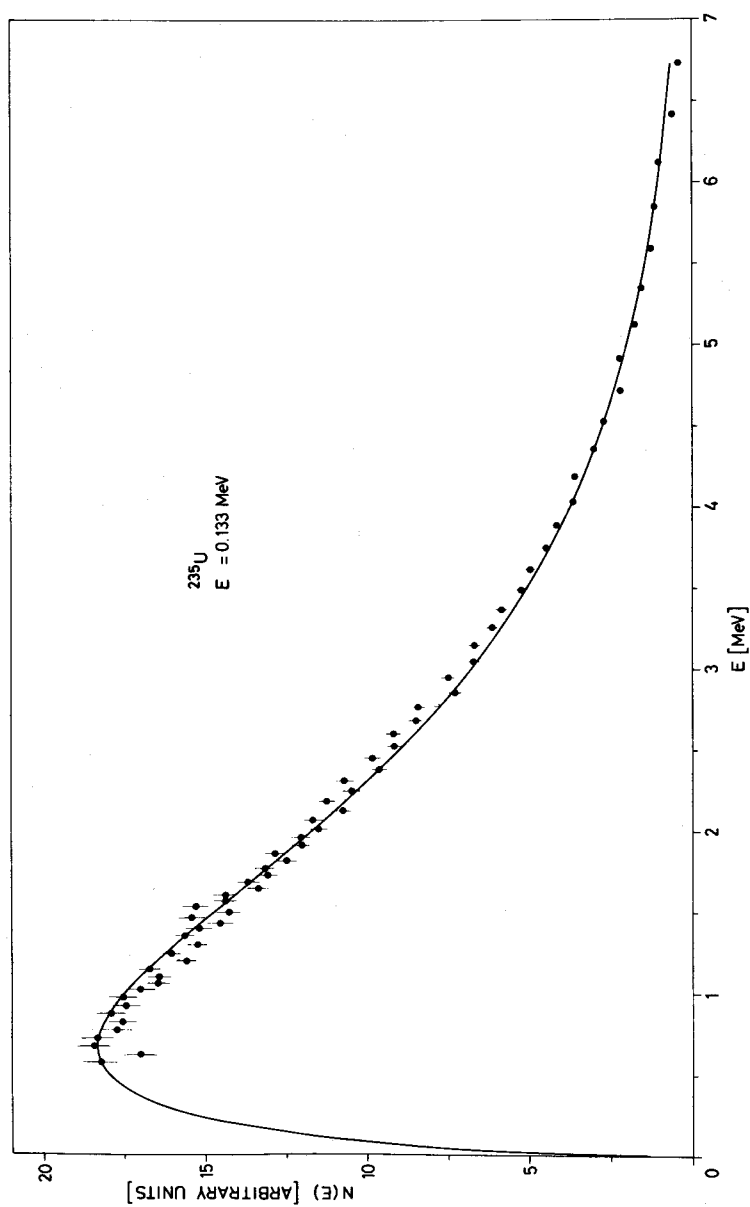


FIG. 7. Preliminary fission neutron spectrum from neutron-induced fission of  $^{235}\text{U}$  at  $E_n = 0.14$  MeV and  $\theta_{\text{lab}} = 135^\circ$ . Solid line represents the least squares fit through the experimental points taken from 1 MeV onwards.

solid lines represent the results of least squares fits assuming isotropy for the fission neutron angular distributions in the laboratory reference system. The dashed curves are the results of the fits assuming an angular dependence of the form  $N(\theta) = A_0 P_0 + A_2 P_2(\cos \theta)$ , where the  $P_i$  are the  $i^{\text{th}}$  order Legendre polynomials. In this case the ratios  $R = N(0^\circ)/N(90^\circ)$  are  $1.19 \pm 0.20$ ,  $1.08 \pm 0.17$  and  $1.27 \pm 0.24$  at the incident neutron energies of 1.5, 1.9 and 2.3 MeV respectively. Due to the uncertainties in the values of  $R$ , these results allow no conclusions with regard to anisotropy for the fission neutron emission, though there seems to be a slight indication of such an effect.

### 3.2. Fission neutron spectra of $^{235}\text{U}$

Fission neutron spectra from this isotope were measured at the incident neutron energies of 0.133, 0.40, 1.5, 1.9, 2.3, 4.0, 4.5, 5.0 and 5.5 MeV. The evaluation of the fission neutron spectra has so far been done only up to 2.3 MeV. The evaluation procedure was essentially the same as that applied in the previous case. However, it was found that a constant background, which is due to an induced activity of the sample, has to be subtracted from the time-of-flight spectra before treating them in the way described. This background was smaller than 1.5% of the counts at the

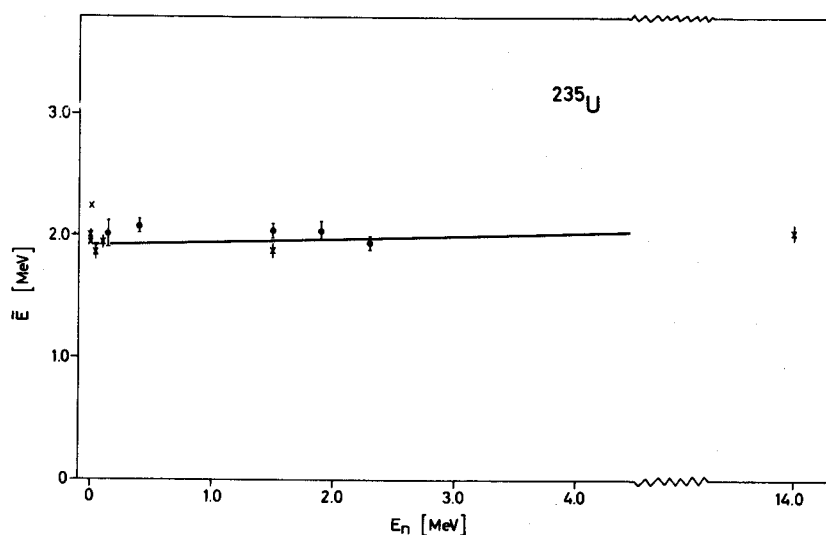
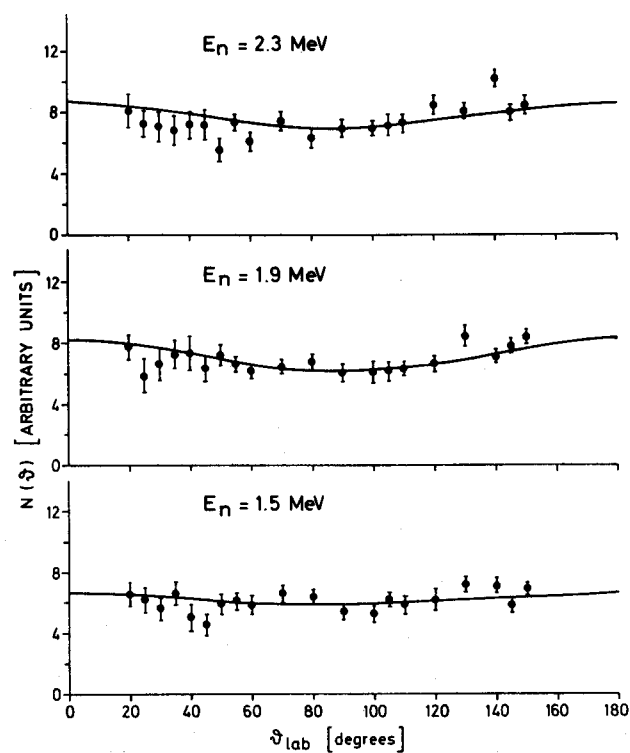


FIG. 8. Variation of the average fission neutron energy  $\bar{E}$  of  $^{235}\text{U}$  with the incident neutron energy  $E_n$ : ● present work; × results from Ref. [9].

TABLE III. MAXWELLIAN TEMPERATURE  $T_F$  AND AVERAGE FISSION NEUTRON ENERGY  $\bar{E}$  OF  $^{235}\text{U}$  (preliminary values)

$E_n$ (MeV)	$T_F$ (MeV)	$\bar{E}$ (MeV)
0.133	1.34	$2.01 \pm 0.05$
0.40	1.36	$2.04 \pm 0.04$
1.50	1.36	$2.04 \pm 0.05$
1.90	1.36	$2.04 \pm 0.08$
2.30	1.29	$1.94 \pm 0.04$

FIG.9. Fission neutron angular distributions from neutron-induced fission of  $^{235}\text{U}$  with respect to the direction of the incoming neutron beam. The integration limits of the fission spectrum are 3.0 and 6.0 MeV.

maximum of the fission neutron time-of-flight spectrum. Two measurements were performed at 0.40 MeV at an interval of four months and with the detectors placed at 45°, 90° and 135°. Both measurements gave the same results. Figure 6 shows the fission neutron sum spectrum of the two measurements taken with the three detectors. The solid line represents a least squares fit through the experimental points with a Maxwellian function. Figure 7 shows the results of the measurements made at 0.133 MeV incident neutron energy. This is also a sum spectrum of two sets of measurements taken with two detectors placed at 45° and 135°. The solid line represents a least squares fit through the experimental points with a Maxwellian function.

Figure 8 shows the average fission neutron energies plotted against the incident neutron energy. The corresponding numerical values are given in Table III. The solid points represent the preliminary results of the present experiment and the crosses give the results of other workers compiled in Ref.[9]. The solid line represents Terrell's theoretical curve. The corresponding  $\bar{v}$  values were taken from Ref.[21].

The fission neutron angular distributions were also evaluated from the measurements performed at 1.5, 1.9 and 2.3 MeV. Figure 9 shows the results of this work. The full circles represent the angular distributions of the fission neutrons corresponding to an integration interval of the spectra between 3.0 and 6.0 MeV. The curves represent the least squares fits through the experimental points with the same Legendre polynomial expansion as used in the previous case. The ratios  $N(0^\circ)/N(90^\circ)$  are  $1.11 \pm 0.14$ ,  $1.32 \pm 0.12$  and  $1.25 \pm 0.15$  at the incident neutron energies of 1.5, 1.9 and 2.3 MeV respectively. Here again, because of uncertainties in the R-values, no definite conclusion can be made about the anisotropy in the fission neutron angular distributions.

### 3.3. Fission neutron spectra of $^{239}\text{Pu}$

Temperatures of the neutron-induced fission neutron evaporation process were determined at incident neutron energies of 1.5, 1.9, 2.3, 4.0, 4.5, 5.0 and 5.5 MeV. At the energies up to 2.3 MeV the evaluation was made in a similar way to that described for the  $^{238}\text{U}$  case. Figure 10 shows as an example the fission neutron spectra obtained at 1.9 and 2.3 MeV. In this semilogarithmic plot the experimental points must be distributed around a straight line if the fission neutron spectrum has a Maxwellian shape.

At incident energies above 2.3 MeV it is no longer possible to extract the parameters of the fission neutron energy distribution from the part of the spectrum left above the elastic peak because of the shift of the elastic peak towards the high-energy part of the spectrum. In fact the useful energy range in this part of the spectrum and the number of counts in it become too small for this purpose. One can try, nevertheless, to use the part of the continuous neutron energy spectrum below the elastic peak to extract the parameters of the inelastic and the fission neutron energy distributions. For this analysis, under the assumption of independence of the shape of the fission plus inelastic neutron spectra from the measuring angle, the

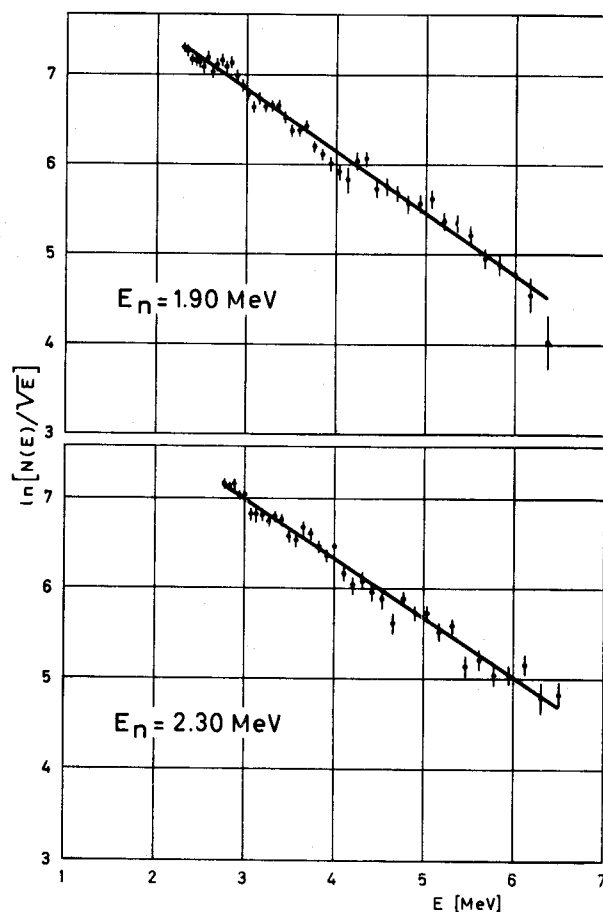


FIG.10. Fission neutron energy spectra of the neutron-induced fission process on  $^{239}\text{Pu}$  at incident neutron energies of 1.9 and 2.3 MeV. The solid lines represent the best fits through the experimental points.

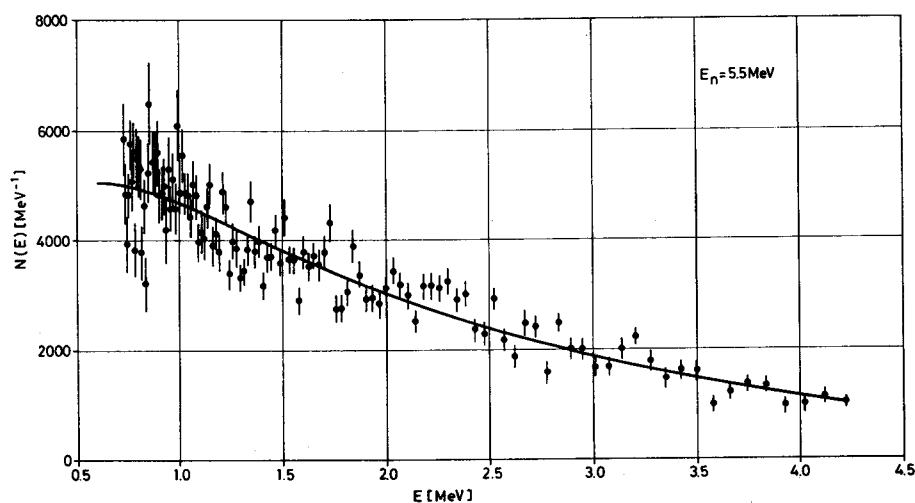
measurements made at the angles  $25^\circ$ ,  $30^\circ$ ,  $35^\circ$ ,  $45^\circ$ ,  $60^\circ$  and  $75^\circ$  were summed up. After subtracting the gamma-ray background, the experimental spectra (after the proper transformations had been made) were fitted with the expression

$$N(E) = C_F \cdot \sqrt{E} \exp(-E/T_F) + C_I \cdot E \cdot \exp(-E/T_I) \quad (3)$$

where the second term, deduced from the Fermi gas model, represents the energy distribution of the inelastic neutrons;  $T_I$  is the temperature of the inelastic neutron evaporation process and  $C_I$  is a normalization constant. The other parameters have the same meaning as in Eq. (1). The numerical values of  $T_F$  obtained and of the average fission neutron energy  $\bar{E}$  corresponding to  $T_F$  are given in Table IV.

TABLE IV. MAXWELLIAN TEMPERATURE  $T_F$  AND AVERAGE FISSION NEUTRON ENERGY  $\bar{E}$  OF  $^{239}\text{Pu}$ 

$E_n$ (MeV)	$T_F$ (MeV)	$\bar{E}$ (MeV)
1.50	1.41	$2.12 \pm 0.07$
1.90	1.45	$2.18 \pm 0.06$
2.30	1.52	$2.28 \pm 0.06$
4.00	1.51	$2.27 \pm 0.10$
4.50	1.69	$2.53 \pm 0.09$
5.00	1.61	$2.42 \pm 0.10$
5.50	1.61	$2.42 \pm 0.08$

FIG. 11. Fission and inelastic neutron energy spectrum of  $^{239}\text{Pu}$  at an incident neutron energy of 5.5 MeV. The solid line represents the best fit through the experimental points.

As an example, the experimental neutron energy distribution measured at  $E_n = 5.5$  MeV is shown in Fig. 11. The solid line represents the best fit through the experimental points using Eq. (3). The error bars represent only the statistical error of the measured points.

In Fig. 12 the fission neutron temperatures are plotted against  $\bar{\nu}$ , the average number of neutrons per fission event. The full circles are the fission neutron temperatures obtained in the present measurements, the crosses are the ones determined by other workers as compiled in Ref. [9]

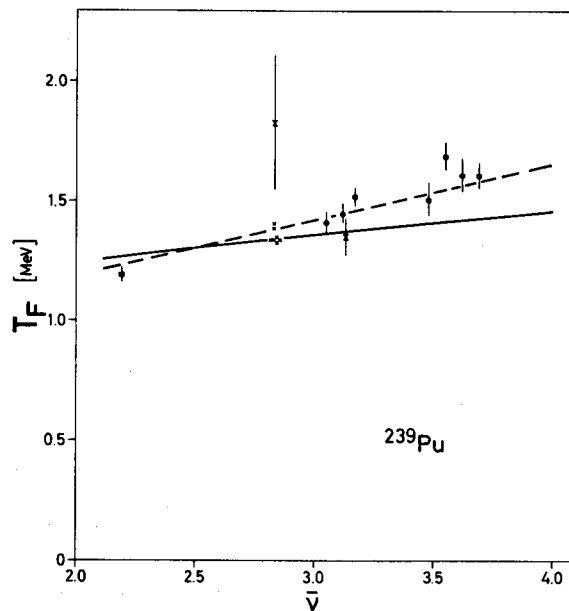


FIG.12. Variation of the Maxwellian temperature of the fission neutron evaporation process,  $T_F$  with the average number of neutrons emitted in a fission event  $\bar{\nu}$ :  $\bullet$  Ref.[16];  $\times$  Ref.[9];  $\blacksquare$  from spontaneous fission of  $^{240}\text{Pu}$ , Ref.[1]. The solid and dashed lines represent the results of the calculations using Eqs (4) and (5) respectively.

and the square represents the fission neutron temperature of the spontaneous fission process of  $^{240}\text{Pu}$ . The solid line is calculated according to Terrell's expression [15],

$$\bar{E} = 0.74 + 0.645(\bar{\nu} + 1)^{\frac{1}{2}} \quad (4)$$

$\bar{\nu}$  was taken as determined by Soleilhac et al. [22]. The dashed curve is calculated according to the Eq. (2),

$$\bar{E} = 0.74 + 0.35(\bar{\nu} + 1) \quad (5)$$

assuming linear dependence of the average fission neutron energy on  $(\bar{\nu} + 1)$ . The coefficient of the last term is chosen to match the thermal neutron-induced fission temperature of  $^{235}\text{U}$  ( $\bar{E} = 1.935$  MeV,  $\bar{\nu} = 2.43$ ). This latter assumption appears to be in much better agreement with the experimental data of  $^{239}\text{Pu}$  compared to the Terrell curve using Eq. (4).

#### 4. CONCLUSIONS

The dependence of the temperature of the fission neutron evaporation process on the incoming neutron energy as determined in the present

measurements on  $^{238}\text{U}$  and  $^{235}\text{U}$  agree reasonably, within the error, with the results of other measurements. The agreement with the Terrell curve is also good. However, for the  $^{239}\text{Pu}$  case the Terrell curve does not fit our data. Rather, the experimental results show linear dependence on  $(\bar{\nu} + 1)$ , including the one of the spontaneous fission of  $^{240}\text{Pu}$ .

The fission neutron energy spectra above 1-MeV incident energy in the present investigation agree with a Maxwellian shape, as suggested by Terrell [14, 15], assuming that the fission neutrons are generated from the fission fragments. But the measurements at lower energies on  $^{235}\text{U}$  at 0.40 and 0.14 MeV show clearly a deviation from the Maxwellian distribution in the energy range below 1-MeV fission neutron energy, though the data are only preliminary. At incident neutron energies above about 1 MeV this deviation cannot be seen because of the superposition of elastically and inelastically scattered neutrons in that part of the fission spectrum where this deviation occurs. Because of this uncertainty in the shape of the fission neutron spectra, the inelastic cross-sections calculated from the time-of-flight spectra are bound to be overestimated. This was shown by Batchelor and Wyld [13] in their measurements on  $^{235}\text{U}$  and  $^{239}\text{Pu}$  at  $E_n = 2.0$  MeV. The reason for the excess of fission neutrons over the Maxwellian distribution is not clear. One reason may be that the fission neutrons are not solely emitted by the fission fragments, rather there is a large emittance of neutrons at the time of scission of the parent nucleus into the fragments. While the high-energy part (above 1 MeV) of the fission neutron spectra at all the incident neutron energies can be fitted well with the Maxwellian distribution with the corresponding fission temperatures in agreement with the theory, the excess of neutrons appears only below about 1 MeV. It would be interesting to study the fission neutron spectra below 1 MeV, preferably down to 100 - 200 keV fission neutron energies. Some theoretical considerations in this perspective will be also necessary.

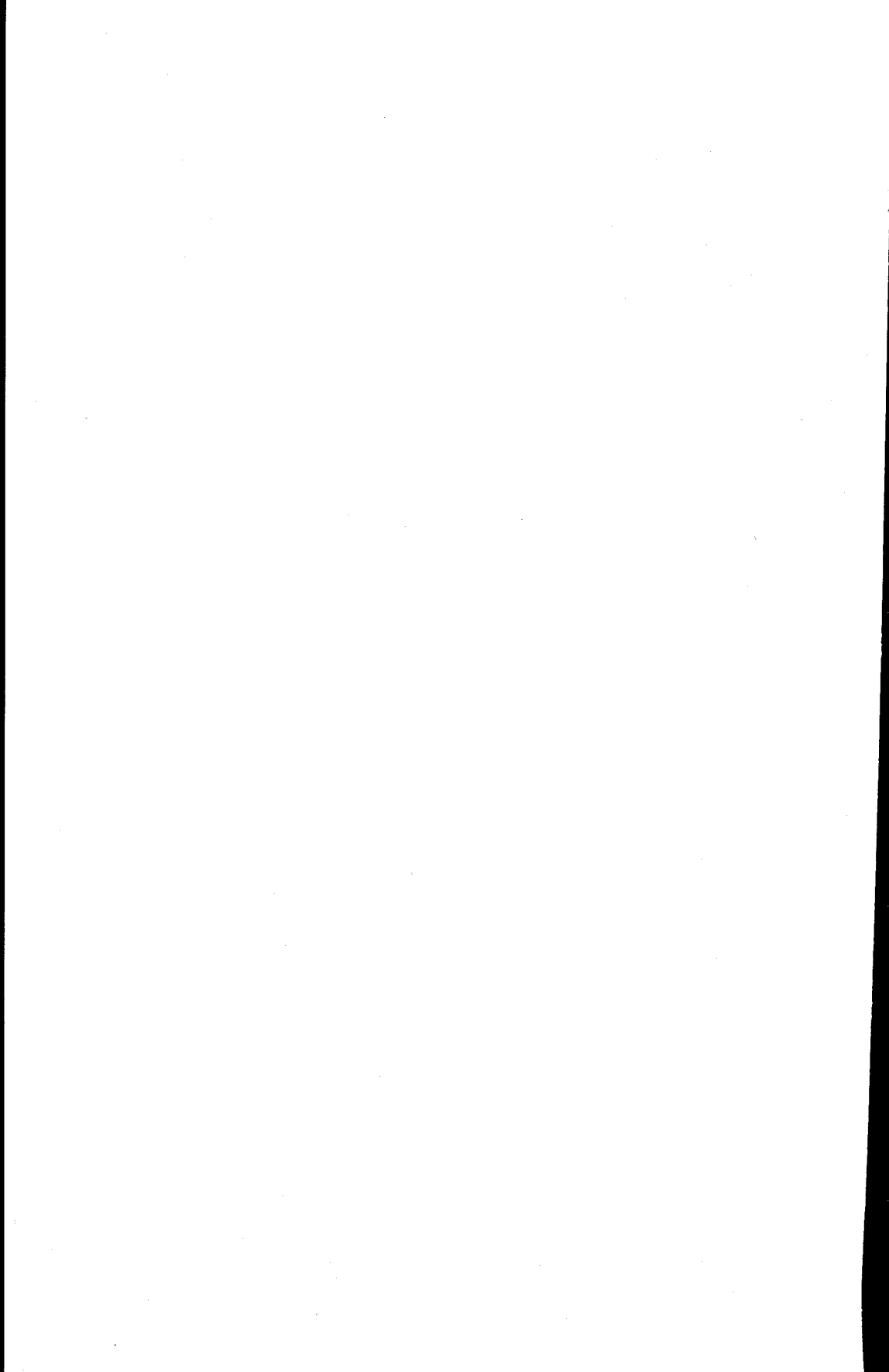
The angular distributions of the fission neutrons presented here show that they are isotropic within the error, though the evidence for anisotropy cannot be completely ruled out. It would be worthwhile to calculate the shape of the angular distribution of the fission neutrons as a function of the anisotropy of the fragment angular distribution. If the fission neutrons are emitted solely by the fragments, this will also give a check on the shape of the fission neutron angular distributions.

## REFERENCES

- [1] BONNER, T.W., Nucl. Phys. **23** (1961) 116.
- [2] GRUNDL, J.A., Nucl. Sci. Engng **31** (1968) 191.
- [3] McELROY, W.N., Rep. BNWL-SA-1794 (1968).
- [4] CRANBERG, L., FRYE, G., NERESON, N., ROSEN, L., Phys. Rev. **103** (1956) 662.
- [5] CONDÉ, H., DURING, G., Ark. Fys. **29** (1965) 313.
- [6] BARNARD, E., FERGUSON, A.T.G., McMURRAY, W.R., Van HEERDEN, I.J., Nucl. Phys. **71** (1965) 228.
- [7] VASILJEV, Yu.A., ZAMYATNIN, Yu.S., ILJIN, Yu.I., SIROTININ, E.I., TOROPOV, P.V., FOMUSHKIN, E.F., Soviet Phys. JETP **11** (1960) 483.
- [8] DIDIER, D., MOUHAYRAT, G., PERRAULT, F., Int. Conf. Nuclear Structure Study with Neutrons, Antwerp, 1965.
- [9] ALMÉN, E., HOLMQVIST, B., WIEDLING, T., Nuclear Data for Reactors (Proc. Conf. Helsinki, 1970) **2**, IAEA, Vienna (1970) 93.



- [10] BELOV, L.M., BLINOV, M.V., KAZARINOV, N.M., KRIVOKHATSKY, A.S., PROTOPOPOV, A.N., Rep. INDC-260 E (1969) 94.
- [11] GRUNDL, J.A., NEUER, J.R., Bull. Am. phys. Soc. 1 (1956) 95.
- [12] NERESON, N., Phys. Rev. 88 (1952) 823.
- [13] BATCHELOR, R., WYLD, K., Rep. AWRE 055/69 (1969).
- [14] TERRELL, J., Phys. Rev. 113 (1959) 527.
- [15] TERRELL, J., "Prompt neutrons from fission", Physics and Chemistry of Fission (Proc. Symp. Salzburg, 1965) 2, IAEA, Vienna (1965) 3.
- [16] COPPOLA, M., KNITTER, H.-H., Z. Phys. 232 (1970) 286.
- [17] KNITTER, H.-H., COPPOLA, M., AHMED, N., JAY, B., Z. Phys. 244 (1971) 358.
- [18] KNITTER, H.-H., COPPOLA, M., Z. Phys. 207 (1967) 56.
- [19] HORSTMANN, H., SCHMIDT, H., ENEA program library, Ispra, Rep.087.
- [20] CRANBERG, L., LEVIN, J.S., Rep. LA-2177 (1959).
- [21] BNL 325, 2nd ed. 3 (1965).
- [22] SOLEILHAC, M., FREHAUT, J., GAURIAN, J., J. nucl. Energy 23 (1969) 257.



# A MEASUREMENT OF THE PROMPT FISSION NEUTRON SPECTRUM OF $^{235}\text{U}$ AT 0.5-MeV INCIDENT NEUTRON ENERGY: TENTATIVE RESULTS

P.I. JOHANSSON, E. ALMÉN, B. HOLMQVIST, T. WIEDLING  
Atomic Energy Company,  
Studsvik, Nyköping,  
Sweden

## Abstract

A MEASUREMENT OF THE PROMPT FISSION NEUTRON SPECTRUM OF  $^{235}\text{U}$  AT 0.5-MeV INCIDENT NEUTRON ENERGY: TENTATIVE RESULTS.

The shapes of fission neutron spectra are of interest for power reactor calculations. Recently it has been suggested that the neutron-induced fission spectrum of  $^{235}\text{U}$  should be harder than was earlier assumed. For this reason measurements of the neutron spectra of some fissile isotopes are in progress at this laboratory. The report presents results from a current study of the energy spectra of the neutrons emitted in the neutron-induced fission of  $^{235}\text{U}$ .

The measurements were performed at an incident neutron energy of 0.53 MeV by using time-of-flight techniques together with pulse shape discrimination in the neutron detector system to suppress the gamma background. The detector was calibrated with respect to energy and efficiency from 0.5 to 14 MeV, which enabled the fission spectrum to be analysed over a much larger energy range than in any previous investigation of the  $^{235}\text{U}$  spectrum. Corrections for the effect of neutron attenuation in the uranium sample were calculated by using a Monte Carlo program. The fission neutron spectrum was analysed on the basis of energy distributions according to Maxwell and Watt, and it was shown that Watt's distribution is more useful than Maxwell's for describing the spectrum.

## 1. INTRODUCTION

The shapes of prompt fission neutron spectra of the main fissile and fertile isotopes have recently attracted great interest, although previously it had been assumed that these spectra had been measured with satisfactory precision. This renewed interest was initiated by results from macroscopic measurements, which indicated appreciably harder spectra than those calculated from microscopic experiments. The differences between the results obtained by these two groups of methods gave the impulse to carry out new microscopic experiments using fast incident neutron energies at Studsvik. Thus, measurements have been performed on  $^{235}\text{U}$  at a primary neutron energy of 0.95 MeV and on  $^{238}\text{U}$  at 1.35 and 2.02 MeV, using a time-of-flight technique in combination with a plastic scintillation detector [1, 2]. The parameter usually chosen to characterize a fission neutron spectrum shape is the Maxwellian temperature; it was found that the values for this temperature agreed with previously published results from microscopic measurements, within the limits of experimental error. Thus the findings here did not support the results from the macroscopic data.

A review of microscopic fission spectrum measurements was recently published [3]. An inspection of the data in this review shows that most spectrum analyses have been made in a relatively limited energy region,

ranging from about 0.5 up to 7 MeV. The lower energy limit is set by the problems that often arise because of the difficulty of determining the response function of the detector with high precision. The upper limit is probably set by neutron intensity considerations related to the rapid falling off in the yield of fission neutrons with increasing energy. Furthermore, the scatter in the results of many of the previous prompt fission neutron spectrum measurements illustrates the need for more accurate information on most fissionable nuclei. This should be obtained using the most sophisticated and reliable techniques, with the emphasis on bringing down the systematic uncertainties.

This investigation is concerned with the fission neutron spectrum from  $^{235}\text{U}$  measured at an input energy of 0.53 MeV. The experiment used a time-of-flight technique. A comparatively large liquid scintillator was chosen as a detector element to get high efficiency over a large energy range, good time resolution and the possibility of using pulse shape discrimination to suppress the gamma background. This experimental technique has given very positive results in that it has enabled the recording of a fission neutron spectrum with very satisfactory statistics from about 0.5 MeV up to the highest fission neutron energy. The background conditions were extremely good, even up in the high energy range, thus giving extraordinary accuracy for an experiment of this type.

The experimental details and tentative results will be discussed fully in the following sections.

## 2. EXPERIMENTAL ARRANGEMENTS AND PROCEDURE

The fission spectrum measurements were made by using a time-of-flight technique in conjunction with a 6-MeV pulsed Van de Graaff accelerator. An ion pulse width of 1.5 ns at a repetition rate of 1 Mc has been used throughout the experiments. The neutron detector consisted of a liquid scintillator with pulse shape discrimination properties (Nuclear Enterprises, NE213; 13 cm in diameter and 5 cm thick) viewed by a fast photomultiplier. The detector arrangements were located in a large shielding of lithium paraffin, iron and lead [4]. The distance between the uranium sample and the detector was 300 cm.

Neutrons of 0.53-MeV energy were produced by the  $^7\text{Li}(p, n)^7\text{Be}$  reaction with a target consisting of lithium metal evaporated on to a thin tantalum backing. The proton energy used (2.26 MeV) is well below the threshold energy (2.378 MeV) for production of neutrons by the  $^7\text{Li}(p, n\gamma)^7\text{Be}$  reaction [5]. The thickness of the target was 26 keV as measured. The mean proton current was about 4  $\mu\text{A}$ . The relative neutron flux was monitored with a direction sensitive long counter.

The  $^{235}\text{U}$  measurements were made at a detector angle of  $90^\circ$  relative to the incident neutron beam. The uranium sample (height 3.00 cm, outer diameter 1.80 cm and inner diameter 0.95 cm) contained 93%  $^{235}\text{U}$ . Polythene scattering samples (height 3.00 cm, outer diameter 0.95 cm and inner diameter 0.65 cm and height 5.00 cm and diameter 1.00 cm, respectively) were used to measure the response function of the neutron detector.

The effect of room-scattered neutrons interacting with the sample was studied with a tantalum scatterer. The measurements were repeated both with the tantalum and uranium samples and without any scatterer.

It is very important in measurements of this type, requiring accurate determinations of intensities in different energy intervals covering a large energy range, that the energy scale as well as the energy dependence of the neutron detector should be known with high accuracy. The energy calibration of the time-to-pulse-height converter of the neutron spectrometer was performed by observing neutron groups from the reactions  $\text{T}(p, n)^3\text{He}$  and  $^9\text{Be}(d, n)^{10}\text{C}$  and the neutron scattering from hydrogen, carbon and nickel. The energy range covered was 0.5 to 21 MeV. The finite dimensions of the target-scatterer-detector system introduce, however, a spread in the scattering angle of the detected neutrons. This effect, together with the fact that the energy of the scattered neutrons is strongly dependent upon the scattering angle, makes the (n, p) process less useful at large angles for energy calibrations. Consequently, neutron scattering from hydrogen was only used for energy calibrations at angles smaller than about  $35^\circ$ .

The relative efficiency of the neutron detector was determined by observing neutron scattering from hydrogen at different primary energies and at different angles. The (n, p) cross-sections compiled by Horsley [6] were used to derive the response function by a simple normalization procedure. Thus the energy range from 1 to 14 MeV was covered. The low-energy part of the efficiency curve, i. e. from 0.4 to 4 MeV, has also been measured by detecting neutrons from the  $\text{T}(p, n)^3\text{He}$  reaction [7, 8].

### 3. EXPERIMENTAL RESULTS, DATA ANALYSIS AND CORRECTIONS

At fast primary neutron energies the analysis of fission neutron spectra recorded by time-of-flight techniques becomes somewhat complicated because of the interference between the continuous fission spectrum and neutrons emitted in competing elastic and inelastic scattering processes. With the present technique and energy resolution it is difficult to resolve the close-lying neutron groups from inelastic scattering events and to observe that part of the fission spectrum on which they are superposed.

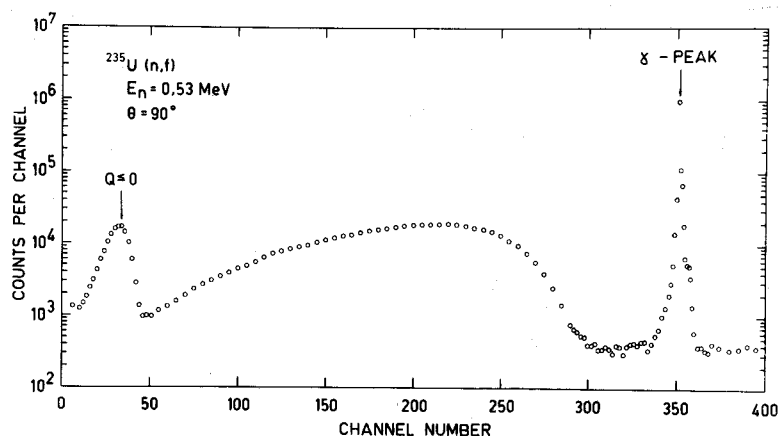


FIG. 1. Time-of-flight spectrum from fission in  $^{235}\text{U}$  induced by 0.53-MeV neutrons.

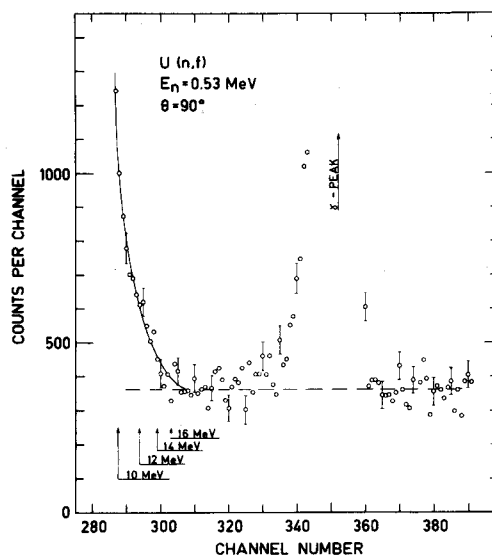


FIG.2. High-energy part of the fission neutron spectrum of  $^{235}\text{U}$ .

The high-energy end of the fission spectrum may also be somewhat influenced by the low-energy tail of the peak from sample gammas incident on the detector. The distortion of the high-energy region of the neutron spectrum by the gamma peak has been drastically diminished by pulse shape discrimination together with a lead absorber (thickness 0.8 cm) positioned in front of the detector. The absorber introduced only a small reduction (less than 20 per cent) in the neutron detection efficiency.

The time-of-flight spectrum from fission in  $^{235}\text{U}$  induced by 0.53-MeV neutrons is shown in Fig. 1. A peak due to gamma radiation is also visible as is a peak from unresolved neutron elastic and inelastic scattering events. The high-energy part of the fission spectrum is plotted in Fig. 2 and shows the contribution of fission neutrons at energies above 10 MeV.

The fission neutron spectrum has been analysed by the method described in Ref. [2]. Thus the contributions to the fission spectrum caused by the high-energy tail of the elastic peak and the low-energy tail of the gamma peak were taken care of by subtracting neutron scattering spectra recorded with a  $^{181}\text{Ta}$  sample. Tantalum is convenient for this purpose since, on the one hand, it is rather heavy and on the other, like  $^{235}\text{U}$ , it has many low-lying excited states. The resulting fission spectrum was analysed up to 14 MeV.

The importance of the corrections for flux attenuation and source-to-sample geometry for the uranium sample has been studied earlier [2] on the basis of Monte Carlo technique. The correction factor was found to vary very little with increasing fission neutron energy, i.e. between 1.19 and 1.17. Thus the fission spectrum is corrected by roughly the same factor over the entire energy region.

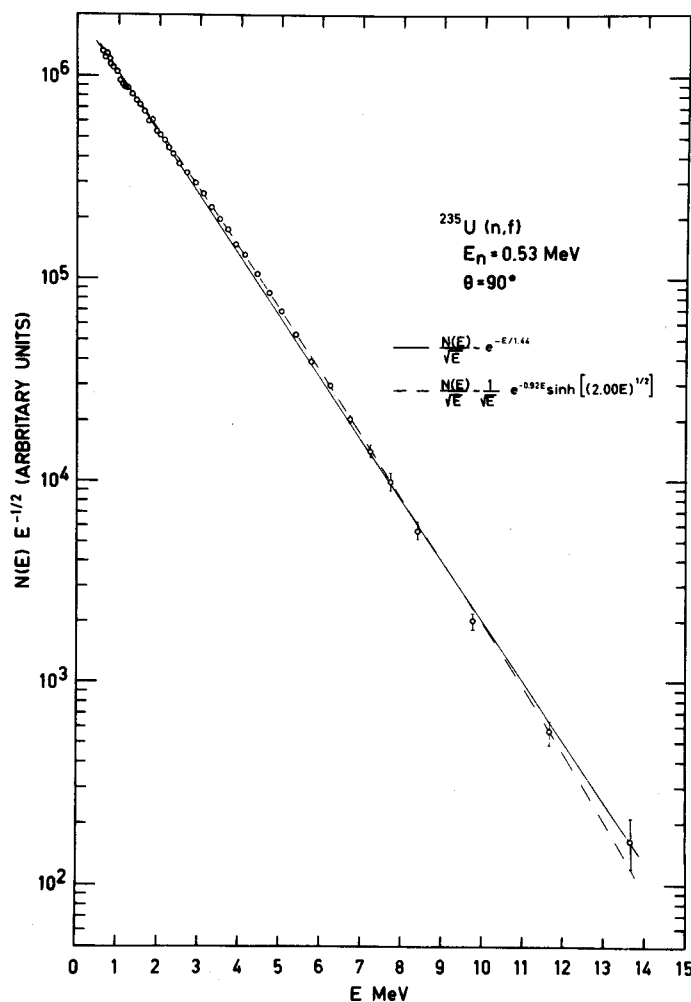


FIG. 3. Fission neutron spectrum from  $^{235}\text{U}$  obtained at 0.53-MeV incident energy. The line and the dashed curve are least squares fits to the experimental points assuming energy distributions according to Maxwell and Watt, respectively.

#### 4. DISCUSSION

The prompt fission neutron spectrum is usually interpreted on the basis of a Maxwellian distribution  $N(E) \sim E^{1/2} \exp(-E/T_m)$  where  $T_m$  is the temperature. This approach has also been tried for describing the present experimental data. The fission spectrum has been plotted on a semi-logarithmic scale as shown in Fig. 3. The line has been calculated with the Maxwellian expression, using a least squares procedure which gives a temperature of 1.44 MeV. It is evident from the figure that the fission

spectrum is not well represented by a Maxwellian distribution. This trend has already been observed in the authors' earlier fission spectrum measurements of  $^{235}\text{U}$  and  $^{238}\text{U}$  [2]. The shape of fission neutron spectra is also frequently represented by an expression  $N(E) \sim e^{-AE} \sinh[(BE)^{1/2}]$ , as proposed by Watt [9]. This distribution has been fitted to the experimental points and it is represented by the dashed curve in Fig. 3. The coefficients are  $A = 0.92 \text{ MeV}^{-1}$  and  $B = 2.0 \text{ MeV}^{-1}$ . It is clear that Watt's distribution is more useful than Maxwell's distribution for describing the measured fission spectrum.

The analysis of the experimental data is still in progress. Thus the results reported here are to be considered only as tentative.

#### REFERENCES

- [1] ALMÉN, E., HOLMQVIST, B., WIEDLING, T., Nuclear Data for Reactors (Proc. Conf. Helsinki, 1970) 2, IAEA, Vienna (1970) 93.
- [2] ALMÉN, E., HOLMQVIST, B., WIEDLING, T., Neutron Energy Spectra from Neutron-Induced Fission of  $^{235}\text{U}$  at 0.95 MeV and of  $^{238}\text{U}$  at 1.35 and 2.02 MeV, Rep. AE-429 (1971).
- [3] WIEDLING, T., "Fission neutron spectra, microscopic results", EANDC Symp. Neutron Standards and Flux Normalization, Argonne National Laboratory, 1970.
- [4] HOLMQVIST, B., Ark. Fys. 38 (1968) 403.
- [5] MARION, J.B., FOWLER, J.L., Fast Neutron Physics, Monographs and Texts in Physics and Astronomy, Vol. IV, Part 1 (1960) 133.
- [6] HORSLEY, A., Nuclear Data 2A (1966) 243.
- [7] Data of PERRY, J.E. et al., Los Alamos Scientific Laboratory, private communication.
- [8] PAULSEN, A., LISKIEN, H., Nuclear Data for Reactors (Proc. Conf. Paris, 1966) 1, IAEA, Vienna (1967) 217.
- [9] WATT, B.E., Phys. Rev. 87 (1952) 1037.



# FISSION NEUTRON SPECTRA MEASUREMENTS OF $^{235}\text{U}$ , $^{239}\text{Pu}$ AND $^{252}\text{Cf}$

H. WERLE, H. BLUHM

Institut für Neutronenphysik und Reaktortechnik,  
Kernforschungszentrum Karlsruhe,  
Federal Republic of Germany

## Abstract

FISSION NEUTRON SPECTRA MEASUREMENTS OF  $^{235}\text{U}$ ,  $^{239}\text{Pu}$  AND  $^{252}\text{Cf}$ .

The fission neutron spectra of  $^{235}\text{U}$ ,  $^{239}\text{Pu}$  and  $^{252}\text{Cf}$  were studied experimentally using proton-recoil proportional counters and  $^3\text{He}$  semiconductor sandwich spectrometers. The spectra and the average energies determined with both techniques agree within the experimental errors and the spectra are described quite well by Maxwellian distributions. The average energies are consistent with most previously reported microscopic results and amount to 1.956 (2.020), 2.136 (2.075) and 2.155 (2.130) MeV for  $^{235}\text{U}$ ,  $^{239}\text{Pu}$  and  $^{252}\text{Cf}$ , the numbers in brackets refer to the  $^3\text{He}$ -spectrometer values. An unexplained disagreement exists between the proton-recoil (1.092) and the  $^3\text{He}$ -spectrometer (1.028)  $^{239}\text{Pu}/^{235}\text{U}$  average energy ratio.

## 1. INTRODUCTION

Recent integral studies of the thermal neutron-induced fission of  $^{235}\text{U}$  and  $^{239}\text{Pu}$  with activation detectors [1, 2] indicate that (1) the average energy of the prompt  $^{235}\text{U}$  fission neutrons is about 10% higher; and (2) the average energy of the  $^{239}\text{Pu}$  fission neutrons is remarkably closer to that of the  $^{235}\text{U}$  fission neutrons than previously deduced from differential spectrum measurements [1, 3, 4]. These differences have a noticeable influence on some important fast reactor parameters [5]. Therefore, we found it useful to remeasure the fission spectra of  $^{235}\text{U}$ ,  $^{239}\text{Pu}$  and  $^{252}\text{Cf}$ , using two independent methods, one based on proton-recoil scattering and the other on the  $^3\text{He}(n, p)\text{T}$  reaction.

## 2. EXPERIMENTS

### 2.1. Experimental set-up

The measurements were performed at a tangential beam hole of the Karlsruhe research reactor FR2. The geometrical arrangement is shown in Fig. 1. A beam of thermal neutrons, extracted from the thermal column, struck the fissile samples placed at a distance of about 40 cm outside the walls of the biological shield. For safety reasons, sample and detectors had to be surrounded with a shield of 30 cm lithium-paraffin and 10 cm lead. This gave rise to a relatively large amount of back-scattered neutrons, especially with the proton-recoil counters, which had to be placed some tens of centimetres away from the sample.

The  $^{235}\text{U}$  and  $^{239}\text{Pu}$  fissile samples were square platelets,  $51 \times 51 \times 1.5$  mm ( $^{235}\text{U}$ ) and  $51 \times 51 \times 1.37$  mm ( $^{239}\text{Pu}$ ). The  $^{235}\text{U}$  sample consists of 93% enriched uranium metal and is coated with a thin layer of

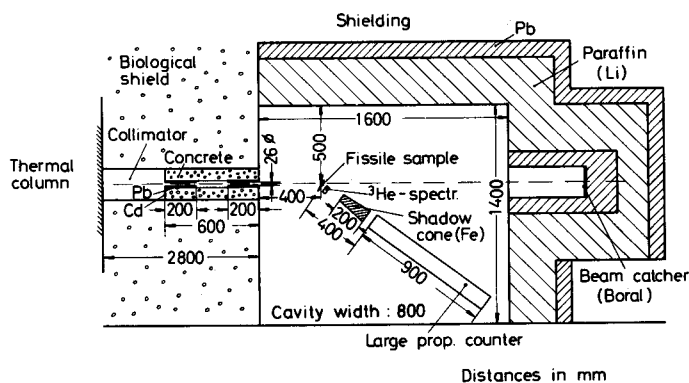


FIG. 1. Experimental set-up of sample, detectors and shielding.

nickel, while the  $^{239}\text{Pu}$  sample, also metallic, consists of 92%  $^{239}\text{Pu}$  (8%  $^{240}\text{Pu}$ ) and is clad with 0.1 mm steel. The  $^{252}\text{Cf}$  spontaneous fission source consisted of about  $0.5 \mu\text{g}$   $^{252}\text{Cf}$ , which was distributed on a thin platinum sheet enclosed in a steel cylinder (diam. 7 mm, height 18 mm). The source strength amounted to about  $10^6$  n/s.

The detectors were outside the beam and the normal of the platelets was somewhat inclined to the direction of the beam. The platelets were covered with sheets of 0.5 mm Cd containing circular holes (10 to 30 mm diam.) to concentrate the fission source into a small area. Source strengths between  $10^7$  and  $10^8$  (n/s) were used for the  $^{235}\text{U}$  and  $^{239}\text{Pu}$  measurements, the variation being accomplished by changing the hole diameter in the Cd sheets and in the lead collimators. The source strength was constant to within 1% over each measuring period of several days.

## 2.2. Proportional counter measurements

Small proton-recoil proportional counters have been used successfully for several years for neutron spectrum measurements in the energy range below about 1.5 MeV. It has been shown by test measurements with monoenergetic neutrons and by comparisons with results of other techniques that large cylindrical counters filled with high stopping-power gases ( $\text{CH}_4$  and  $\text{CH}_4 + \text{Kr}$  mixtures) can be used for measurements up to 10 MeV in beam geometry [6].

Above 200 keV these large cylindrical counters were used in beam geometry. In addition, for energies below 500 keV we applied three small spherical counters at a distance of about 5 cm from the source. For counters filled with methane only the energy range above 1.2 MeV was evaluated, where carbon recoil distortions are small (2% at 1.2 MeV, 1% at 1.4 MeV) and decrease rapidly with increasing energy. Instead of  $\gamma$ -n-discrimination, a series of counters and fillings with widely overlapping energy ranges were used (Table I).

TABLE I. PROTON-RECOIL COUNTER DATA

No.	Type	Dimensions: active length × diameter (mm)	Distance source from side of detector (mm)	Filling	Energy range (MeV)
1	Cylindrical	835×90	400	2 atm Kr <sup>+</sup> 2 atm CH <sub>4</sub>	3 - 10
2	Cylindrical	835×90	400	3 atm CH <sub>4</sub>	1,2 - 5
3	Cylindrical	335×42	300	4 atm H <sub>2</sub>	0,2 - 1.2
4	Cylindrical	335×42	300	2 atm H <sub>2</sub>	0,1 - 0,7
5	Spherical	Diameter 39,4	50	1,2,4 atm H <sub>2</sub>	0,1 - 0,6

The results of both types of cylindrical counters were related to each other without arbitrary constants by the dimensions of the counters, the distance from the source and the number of protons per cm<sup>3</sup>, whereas the results of the spherical counters were normalized to those of the cylindrical counters to give the same total flux in the energy range between 0.25 and 0.45 MeV.

The energy calibration was carried out with the 764-keV thermal peak of the  $^3\text{He}(n, p)\text{T}$  reaction. The amount of  $^3\text{He}$  (some  $10^{-2}$  Torr) was chosen such that outside the thermal neutron beam the disturbance of the proton distribution caused by the peak was small. The position of the 764-keV calibration peak was checked with monoenergetic neutrons. The proton recoil distributions measured were evaluated with a code similar to that described in Ref.[7] by unfolding the differentiated proton spectra with differentiated response functions. We used calculated response functions that had been checked experimentally by monoenergetic neutrons.

The background of room-scattered neutrons was corrected for by evaluating the difference spectrum from measurements with and without a shadow cone between source and detector. The iron cone was 200 mm long and was formed and installed in such a way that it just shadowed the active part of the counter against source neutrons. Figure 2 shows the spectrum of wall-scattered neutrons deduced from the  $^{235}\text{U}$  measurements with shadow cone. The mean energy lies somewhat above 1 MeV, which is about a factor of two lower than the mean energy of the source neutrons. The dip in the spectrum around 430 keV is probably caused by the strong  $^{16}\text{O}$  scattering resonance. Also shown is the ratio of wall-scattered and source spectra for various counters. The measurements drawn with dashed lines were rejected. At the low energy limit (1.4 MeV) of counter 2 the intensity of wall-scattered neutrons amounts to about 40% of the source intensity, the corresponding value of counter 3 (4) is 66% (at 0.4 MeV), and for the spherical counters it is estimated from measurements at different distances from the source to be about 4% at 100 keV. It should be mentioned that the proton recoil  $^{252}\text{Cf}$  measurements were also performed in the cavity shown in Fig.1.

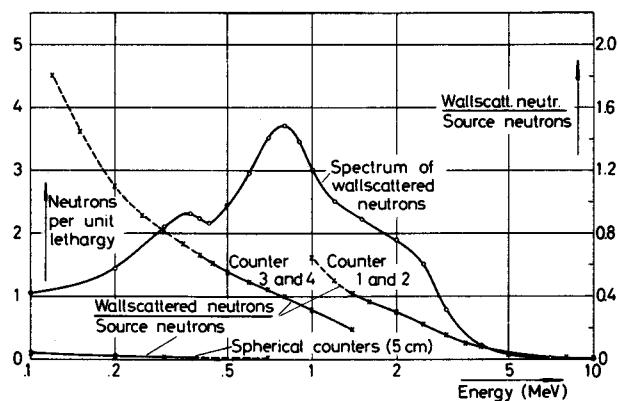


FIG. 2. Spectrum and relative number of wall-scattered neutrons for the proton-recoil measurements.

The normal procedure, measuring with one counter both the  $^{235}\text{U}$  and the  $^{239}\text{Pu}$  sample before the next counter is installed, should have minimized any reproducibility errors in the deduced ratio of the  $^{239}\text{Pu}$  to  $^{235}\text{U}$  spectra. Detailed considerations concerning systematic errors in the measured spectra are given elsewhere [6]. To summarize, the main contributions to the systematic errors in the high-energy region originate from wall-effect corrections, whereas in the low-energy region the background of wall-scattered neutrons contributes the main part. It is estimated that the measured spectra deviate from the 'true' spectra (both normalized at 2 MeV) not more than  $\pm 13\%$  above 7 MeV,  $\pm 3\%$  between 7 and 5 MeV,  $\pm 2\%$  between 5 and 0.8 MeV,  $\pm 10\%$  between 0.8 and 0.2 MeV and  $\pm 20\%$  below 0.2 MeV. The overall systematic error for the mean energy of the spectra amounts to about 6%, where 3% result from the spectrum uncertainties specified above and another 3% from possible errors in the energy calibration. The error in the mean energy due to the fact that the measurements are limited to the energy range between 0.1 and 10 MeV is estimated to be well below 0.5%.

### 2.3. $^3\text{He}$ semiconductor sandwich spectrometer measurements

Secondly, we used a  $^3\text{He}$  semiconductor sandwich spectrometer, which had recently been developed and tested [8]. This spectrometer differs from the  $^3\text{He}$  sandwich spectrometer used by other authors (1) by a discrimination possibility against gamma-background; and (2) by the possibility to correct for energy losses of the protons and tritons in the  $^3\text{He}$  gas. It is, therefore, possible to extend its useful energy range down to 100 keV.

The space between the two circular Si surface barrier detectors separated by 1 cm (0.6 cm) with sensitive areas of 450 mm<sup>2</sup> (200 mm<sup>2</sup>) and depletion depth of 400  $\mu\text{m}$  (200  $\mu\text{m}$ ) is used as proportional counter. A 40- $\mu\text{m}$  thick counting wire fixed in the midplane between the two semiconductor diodes forms the anode. The spectrometer is filled with

2.5 atm  $^3\text{He}$  and 10 Torr  $\text{CH}_4$ . The proportional counter is operated at rather low voltages (around 500 V) leading to moderator gas multiplication factors.

The spectrometer only accepts those events that have produced pulses both in the semiconductor detectors and in the proportional counter, the amplitudes of which exceed certain levels introduced by the electronic system. The possibility of discrimination against gamma background is based on the fact that the specific ionization of Compton electrons (mainly produced in the Si diodes) is much smaller than that of protons or tritons. Correspondingly, the energy losses of the latter in the  $^3\text{He}$  gas are considerably larger than those of electrons with the same energy. The electronic system of the spectrometer is shown in Fig. 3. Its fast coincidence unit (resolving time 200 ns), which opens a linear gate, considerably reduces the number of semiconductor pulses before adding up the proportional counter pulses. Therefore, pile-up between the broad proportional counter pulses (shaping time  $2\text{ }\mu\text{s}$ ) and the summed semiconductor pulses stretched to  $3\text{ }\mu\text{s}$  is strongly reduced. The threefold sum is multiplied by the proportional counter pulse in a logarithmic computer. The product is generally considerably larger for proton-triton pairs than for electrons. Therefore, proton-triton pulses can be separated from electron pulses by a single-channel analyser.

The energetic resolution of the whole system was nearly identical for both spectrometers and amounted to about 60 keV FWHM. This good resolution is mainly achieved by the addition of the proportional counter pulses, which improves it from about 200 keV to 60 keV. The calibration of the semiconductor diodes was carried out with a  $^{233}\text{U}$   $\alpha$ -source deposited on a thin VYNS foil [9] and placed in an evacuated spectrometer of similar design. By means of this energy calibration the position (channel number) of the thermal peak of the  $^3\text{He}(n, p)\text{T}$  reaction was determined and then the amplification to the proportional counter was changed until the experimental position agreed with the calculated one in order to get the right correction for the energy losses in the gas.

From each measured pulse height spectrum such events resulting from  $(n, p)$  and  $(n, \alpha)$  reactions in the Si diodes had to be subtracted. This was achieved by another measurement where the  $^3\text{He}$  gas in the spectrometer was replaced by  $^4\text{He}$ . Because of the high efficiency of the spectrometer, this background was less than 15% over the whole energy range.

To calculate the neutron spectrum from the measured pulse height distribution it is necessary to know both the  $^3\text{He}(n, p)\text{T}$  cross-section and the geometrical efficiency of the spectrometer [8]. The geometrical efficiency has been calculated by a Monte Carlo program and the results of this program were checked for various neutron beam entrance directions and various energies between 100 keV and 2 MeV. The agreement between measurement and calculation was satisfactory. The relatively small distance between fission source and spectrometer led to variation in the angular distribution and in the absolute value of the neutron flux across the spectrometer dimension. This has been taken into account in the Monte Carlo program. The  $^3\text{He}(n, p)\text{T}$  cross-section used for the evaluation of the fission spectra is that recommended by Als-Nielsen [10], which has been confirmed recently by direct measurements.

Difficulties arose from the large gamma background and the high thermal neutron flux entering the spectrometer. Pile-up between these

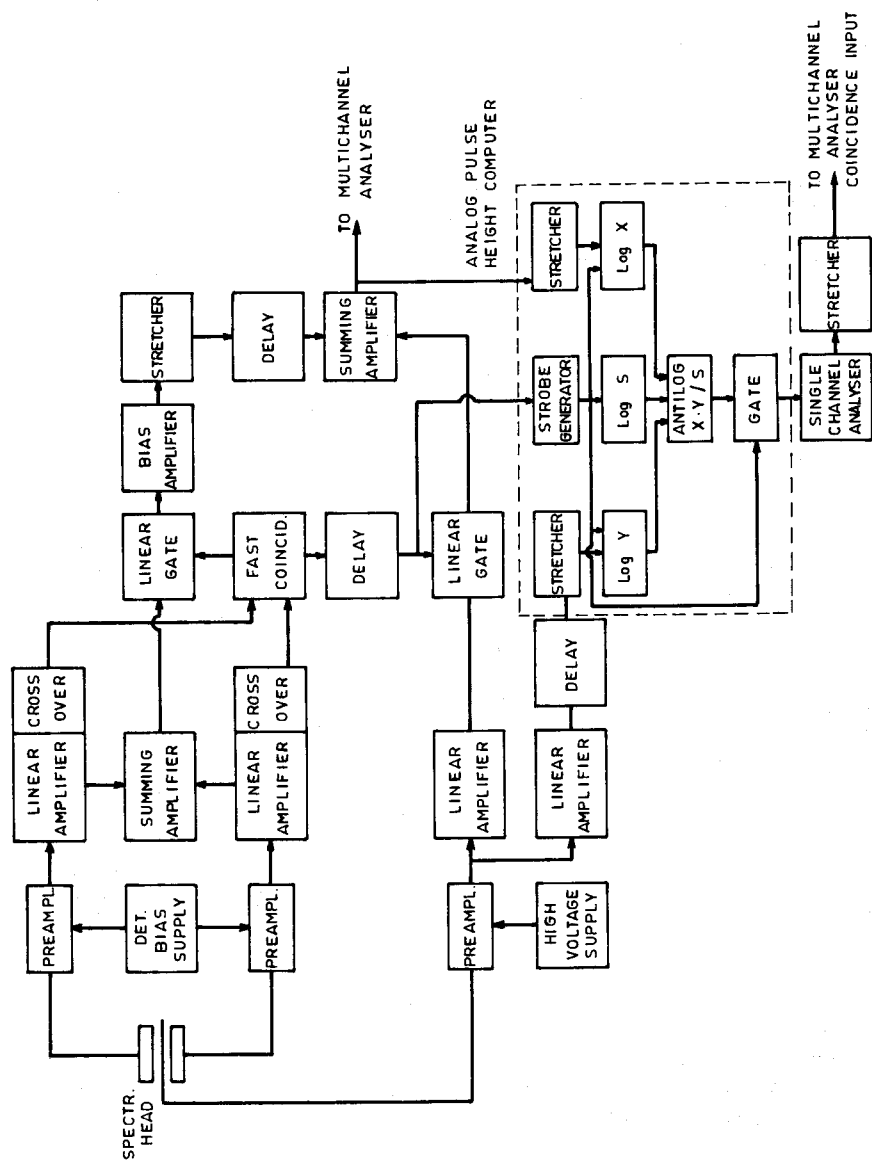


FIG. 3. Block diagram of the  $^3\text{He}$ -spectrometer electronics.

TABLE II. MEASURED FISSION NEUTRON SPECTRA  $\chi_u(E)$   
PER UNIT LETHARGY

Proton recoil spectrometer results				$^3\text{He}$ -spectrometer results				
Mean energy (MeV)	$^{239}\text{Pu}$	$^{235}\text{U}$	$^{252}\text{Cf}$	Mean energy (MeV)	$^{239}\text{Pu}$	$^{235}\text{U}$	Mean energy for Cf (MeV)	$^{252}\text{Cf}$
0.104	0.026	0.021	0.018	0.115	0.016	0.039	0.104	0.018
0.115	0.026	0.031	0.024	0.148	0.039	0.063	0.133	0.033
0.128	0.031	0.033	0.028	0.181	0.075	0.091	0.163	0.055
0.142	0.034	0.038	0.033	0.214	0.093	0.112	0.193	0.069
0.157	0.041	0.049	0.037	0.247	0.097	0.136	0.222	0.081
0.175	0.048	0.061	0.046	0.280	0.126	0.162	0.252	0.101
0.196	0.059	0.067	0.072	0.313	0.145	0.173	0.282	0.119
0.218	0.067	0.083	0.093	0.346	0.159	0.197	0.311	0.131
0.241	0.077	0.099	0.107	0.379	0.189	0.209	0.341	0.159
0.267	0.086	0.115	0.090	0.412	0.227	0.232	0.371	0.186
0.297	0.104	0.123	0.102	0.445	0.194	0.236	0.400	0.197
0.331	0.115	0.147	0.134	0.478	0.221	0.238	0.430	0.217
0.368	0.131	0.162	0.152	0.511	0.259	0.254	0.460	0.227
0.408	0.163	0.182	0.181	0.544	0.262	0.292	0.490	0.261
0.454	0.168	0.225	0.202	0.596	0.277	0.302	0.519	0.243
0.510	0.203	0.245	0.288	0.669	0.305	0.330	0.549	0.256
0.572	0.253	0.280	0.277	0.750	0.312	0.320	0.579	0.274
0.637	0.260	0.309	0.378	0.841	0.351	0.352	0.608	0.316
0.705	0.296	0.344	0.298	0.944	0.355	0.362	0.669	0.322
0.795	0.322	0.386	0.298	1.059	0.405	0.416	0.750	0.356
0.895	0.348	0.374	0.411	1.188	0.456	0.462	0.841	0.358
0.995	0.378	0.419	0.444	1.334	0.482	0.493	0.944	0.401
1.110	0.401	0.442	0.449	1.496	0.513	0.528	1.059	0.451
1.235	0.428	0.444	0.459	1.678	0.559	0.549	1.188	0.499
1.370	0.454	0.490	0.546	1.883	0.567	0.568	1.334	0.531
1.520	0.485	0.504	0.527	2.125	0.566	0.553	1.496	0.575
1.690	0.512	0.534	0.606	2.370	0.547	0.543	1.678	0.593
1.880	0.546	0.561	0.610	2.660	0.521	0.524	1.883	0.628
2.090	0.562	0.557	0.622	2.985	0.487	0.470	2.125	0.623
2.320	0.559	0.564	0.609	3.350	0.450	0.437	2.370	0.619
2.575	0.571	0.540	0.637	3.760	0.384	0.377	2.660	0.582
2.860	0.534	0.509	0.583	4.220	0.331	0.321	2.985	0.534

TABLE II (cont.)

Proton recoil spectrometer results				<sup>3</sup> He-spectrometer results				
Mean energy (MeV)	<sup>239</sup> Pu	<sup>235</sup> U	<sup>252</sup> Cf	Mean energy (MeV)	<sup>239</sup> Pu	<sup>235</sup> U	Mean energy for Cf (MeV)	<sup>252</sup> Cf
3.175	0.511	0.467	0.591	4.730	0.279	0.254	3.350	0.503
3.525	0.459	0.414	0.528	5.310	0.221	0.206	3.760	0.461
3.920	0.419	0.353	0.491	5.950	0.166	0.147		
4.455	0.348	0.287	0.390	6.660	0.113	0.122		
5.050	0.277	0.222	0.317					
5.615	0.201	0.162	0.234					
6.220	0.151	0.118	0.175					
6.900	0.104	0.079	0.122					
7.680	0.065	0.049	0.084					
8.540	0.039	0.029	0.035					
9.495	0.024	0.016	0.005					

two background components would have an influence mainly on the low-energy part of the measured spectra. To minimize these perturbations the spectrometer was taken out of the thermal neutron beam (Fig. 1) and surrounded by a 1 mm Cd sheet. The fission rate was reduced to a reasonable compromise between count rate and gamma intensity. Owing to the small dimensions of the shielded room containing the fission samples (<sup>235</sup>U and <sup>239</sup>Pu) and the spectrometers, the number of room-scattered fission neutrons was rather high. An estimate of the relative number of wall-scattered to source neutrons was calculated from measurements at three different positions of the <sup>3</sup>He-spectrometer (2, 4 and 9 cm). From these measurements and from the results of the <sup>252</sup>Cf measurement, which was performed in a clean geometry with large distances to the walls, it was concluded that the effect of roomscatter on the <sup>235</sup>U and the <sup>239</sup>Pu fission spectra may be neglected above 500-keV neutron energy but may increase up to 15 - 20% at energies around 300 keV and even higher at smaller energies. It should be pointed out that these estimates do not agree with the values from the spherical proton recoil counters (Fig. 2). No reasonable explanation could be found for this. The statistical error of the points shown in Fig. 4 is always less than 3% and the systematic error of the <sup>3</sup>He-spectrometer, including uncertainties due to the energy calibration, the geometrical efficiency and the <sup>3</sup>He(n, p)T cross-section has been estimated to  $\pm 20\%$  at 100 keV,  $\pm 12\%$  at 300 keV and  $\pm 10\%$  above 500 keV.



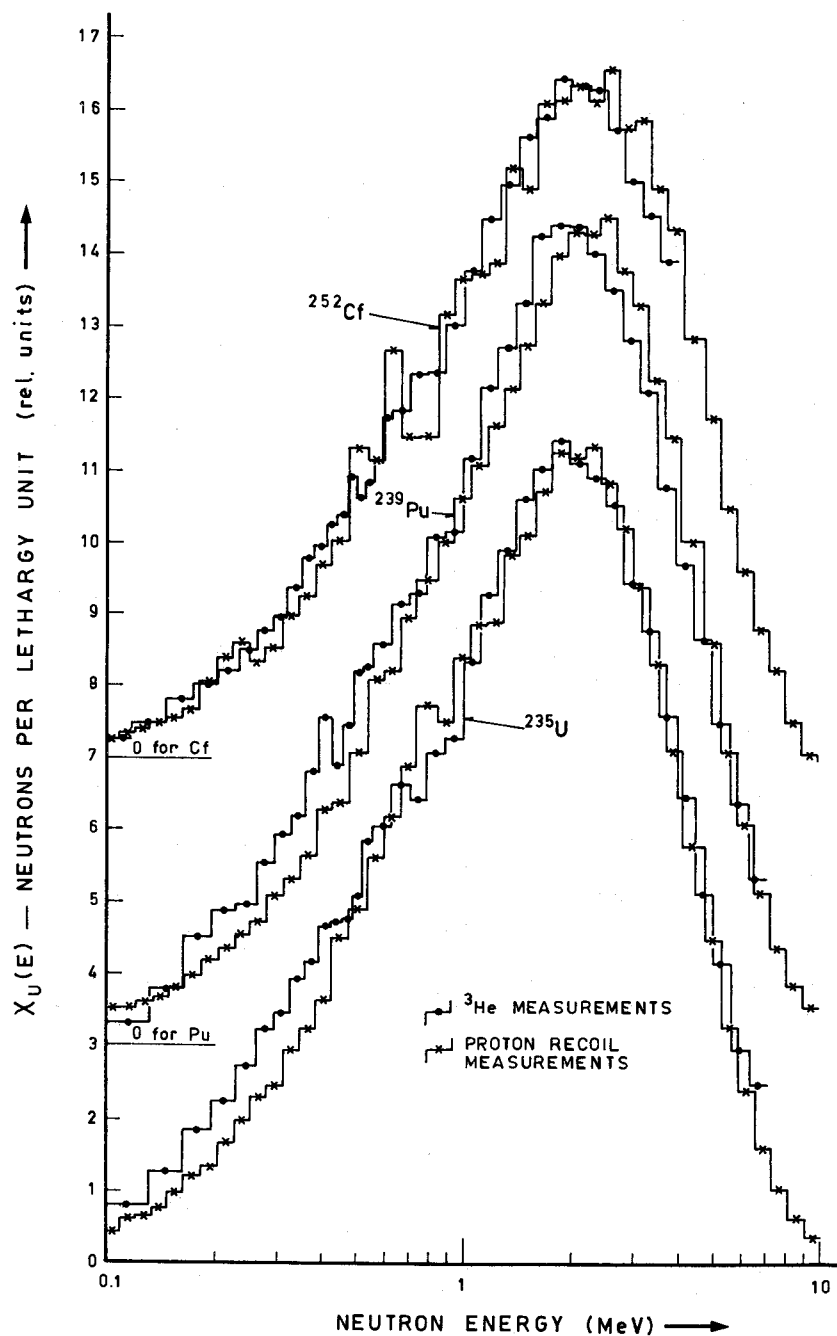


FIG. 4.  $^3\text{He}$  and proton-recoil measured fission spectra. The spectra have been normalized to equal neutrons between 500 keV and 6 MeV for  $^{235}\text{U}$  and  $^{239}\text{Pu}$  and between 500 keV and 4 MeV for  $^{252}\text{Cf}$ .

## 3. RESULTS AND DISCUSSION

The spectra measured here are composed of prompt and delayed neutrons. Above 1 MeV the differences between the prompt spectra and our results are negligible, below 0.4 MeV they amount to about 4% for  $^{235}\text{U}$  and  $^{252}\text{Cf}$  and to 2% for  $^{239}\text{Pu}$ . The average energies calculated from the whole energy range measured (0.1 - 10 MeV) differ from the values calculated from the energy range above 1.5 MeV and from the prompt fission spectra values by 0.5% for  $^{235}\text{U}$  and  $^{252}\text{Cf}$  and by 0.3% for  $^{239}\text{Pu}$ .

The effect of inelastic scattering in the source and in the detector walls (1.5 mm steel) was estimated by one-dimensional  $S_n$  calculations for adjacent slabs of  $^{235}\text{U}$  and Fe, each 1.5 mm thick. Fission neutrons were produced homogeneously in the  $^{235}\text{U}$  slab and the spectrum of neutrons leaking out perpendicularly from the iron slab was assumed to be representative for the measured spectra. The ratio of leakage to fission spectra, both normalized at 2 MeV, was 1.11, 1.07, 1.025 and 0.96 at 0.15, 0.6, 1.1 and 8 MeV respectively. Evaluating the whole energy range measured (0.1 - 10 MeV) the shift in the average energies is 3%, whereas it amounts to 0.5% only if the energy region above 1.5 MeV is analysed.

To summarize, because of the presence of delayed neutrons and because of inelastic scattering, the spectra measured here are softer than the prompt fission spectra. Above 1 MeV the differences are estimated to be smaller than  $\pm 3\%$  and the influence on the average energies deduced from the energy range above 1.5 MeV should be not larger than 0.5%. No corrections for these effects have been applied to the data given in the following.

The measured spectra (per unit lethargy)  $\chi_u$  are listed in Table II and shown in Fig. 4. The spectra are normalized such that  $\int_{0.5 \text{ MeV}}^{E_m} \chi_u du_n = 1$ , with  $E_m = 6 \text{ MeV}$  for  $^{235}\text{U}$  and  $^{239}\text{Pu}$ ,  $E_m = 3.6 \text{ MeV}$  for  $^{252}\text{Cf}$ . Above about 600 keV the spectra measured with both techniques agree rather well. For  $^{239}\text{Pu}$  there seems to be a small shift in the energy scale of both spectra. Below about 500 keV large discrepancies exist for the  $^{235}\text{U}$  and  $^{239}\text{Pu}$  spectra, whereas the  $^{252}\text{Cf}$  spectra are in good agreement. It is supposed that these discrepancies are at least partly caused by the large amount of wall-scattered neutrons and the higher gamma background in the  $^{235}\text{U}$  and  $^{239}\text{Pu}$  measurements.

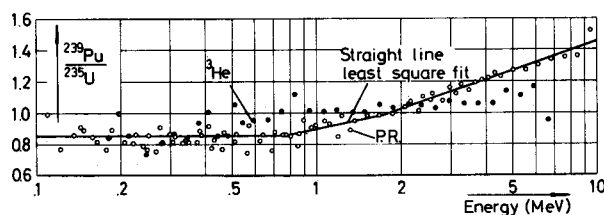


FIG. 5. Ratio of measured  $^{239}\text{Pu}/^{235}\text{U}$  fission spectra.

The ratio of the  $^{239}\text{Pu}$  to  $^{235}\text{U}$  spectra are shown in Fig. 5. Both techniques indicate that the  $^{239}\text{Pu}$  spectra are harder than the  $^{235}\text{U}$  spectra but the proton-recoil measurements reveal larger differences between the two fission spectra. The proton-recoil ratio contains data (from overlapping energy ranges of different counters) that are not taken into account in the representation of the spectra (Figs 4, 6 and Table II).

The measured spectra have been fitted to Maxwellian energy distributions,  $N_E(E) \sim \sqrt{E} e^{-E/T}$ , by a straight-line least square fit through the experimental values  $\ln(N_E(E)/\sqrt{E})$ . It can be seen from Fig. 6 that the experimental spectra in a large part of the measured energy range are quite well represented by Maxwellian distributions. The measurements show in most cases fewer neutrons between about 1 and 2 MeV and more neutrons somewhat above 2 MeV than the Maxwellian distributions. This might be a real discrepancy because in this energy range the measurements are thought to be quite reliable and because it is reflected in both techniques. For energies above 6 MeV the three measured proton-recoil spectra lie generally below the Maxwellian distribution, but it should be pointed out that the experimental uncertainty is already large in this region. The average energies  $\bar{E}_L = 1.5 \cdot T = -1.5/A$  calculated from the slope  $A$  of the straight-line Maxwell fit are listed in Table III. Two fitting intervals were chosen: the whole measured energy range and the range from 1.5 to 7 MeV only. For the reasons given above (delayed neutrons and inelastic scattering) and because systematic errors should be small here, the parameters deduced from this limited energy range should be better suited for comparisons.

The average energies deduced from numerical integration

$$\bar{E}_I = \frac{\sum E_i \cdot \chi_{E_i} \cdot \Delta E_i}{\sum \chi_{E_i} \cdot \Delta E_i}$$

are also listed in Table III. Above 7 MeV the  $^3\text{He}$  results have been extrapolated by the proton-recoil data (both normalized to equal neutrons between 0.5 and 6 MeV).

The  $\bar{E}_L$  values deduced from the limited energy range are generally higher than those from the whole energy range measured, though the difference of 1 - 2% is somewhat smaller than expected from the delayed neutrons and inelastic scattering effects. There is one exception, namely the  $^{252}\text{Cf}$  proton-recoil measurement. The flux values of the two or three points at the upper limit of the energy range are much too low compared to the Maxwell fit and compared to  $^{239}\text{Pu}$  (which agrees below 7 MeV very well with  $^{252}\text{Cf}$ ). Therefore, the  $^{252}\text{Cf}$  values above 7 MeV are suspected of unknown experimental errors. The generally good agreement between measured and Maxwellian spectra (at least above about 700 keV) is reflected in the relative small differences between the  $\bar{E}_I$  and the  $\bar{E}_L$  values.

The difference between the proton-recoil and the  $^3\text{He}$ - $\bar{E}_L$  values (range 1.5 - 7 MeV) amounts to 1% for  $^{252}\text{Cf}$  and to 3% for  $^{235}\text{U}$  and  $^{239}\text{Pu}$ , which is for  $^{235}\text{U}$  and  $^{239}\text{Pu}$  just outside the statistical but well within the estimated total error. But in contrast to  $^{235}\text{U}$  where the  $^3\text{He}$  measurements yield a 3% higher average energy, for  $^{239}\text{Pu}$  they give a 3% lower value as compared to the proportional counter measurements. Correspondingly, there is a very poor agreement in the ratios of the average energies between the

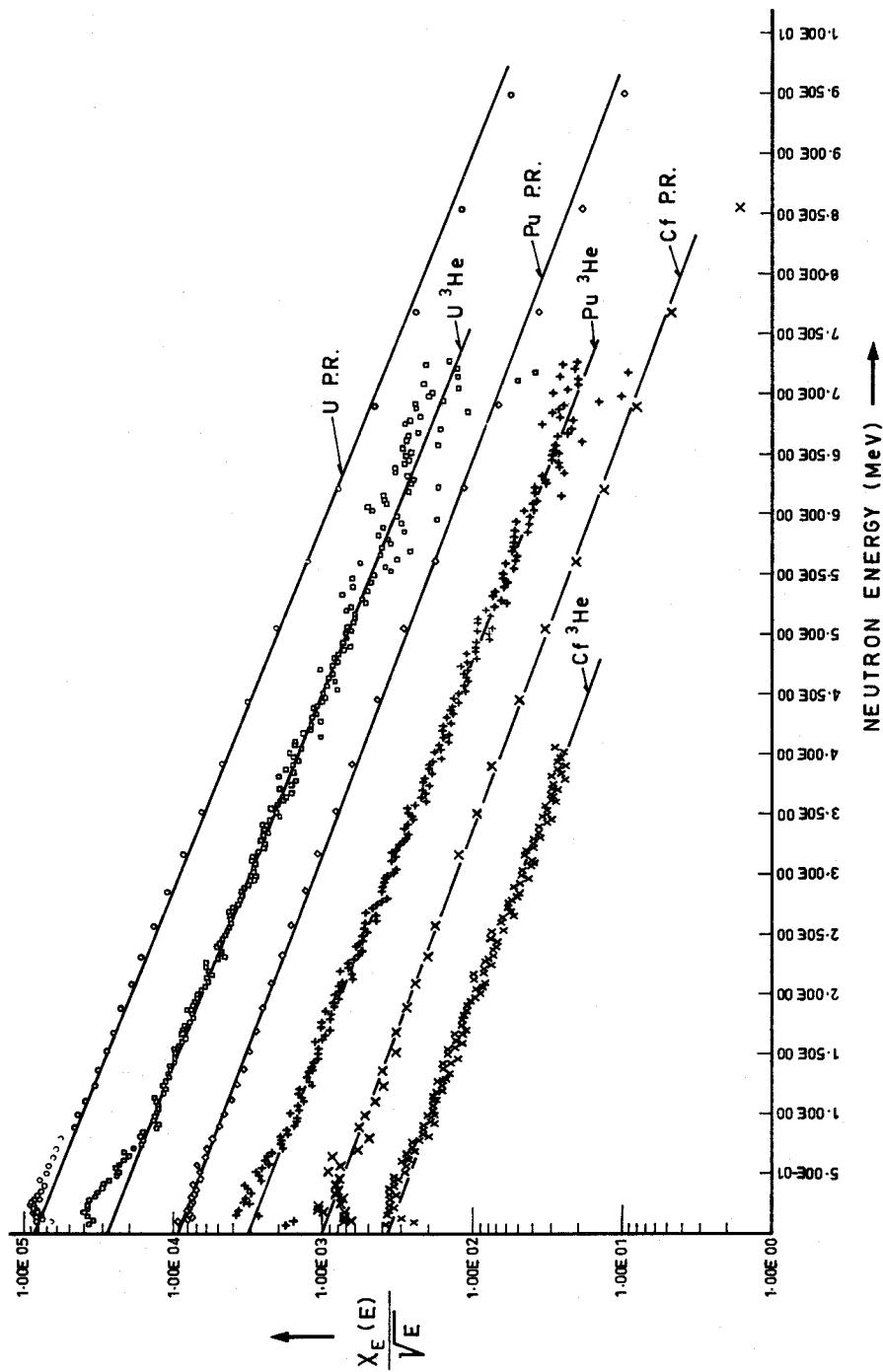


FIG. 6. Measured fission neutron spectra divided by  $\sqrt{E}$  fitted to Maxwellian distributions above 1.5 MeV.

TABLE III. AVERAGE FISSION NEUTRON ENERGIES, PRESENT INVESTIGATION

Isotope	Parameter (MeV)	Technique			
		Proton recoil		$^3\text{He}$ -spectrometer	
		Evaluated energy range		Evaluated energy range	
		0.1 - 10 MeV	1.5 - 7 MeV	0.1 - 7 MeV	1.5 - 7 MeV
$^{235}\text{U}$	$\bar{E}_L$	$1.932 \pm 0.012^a$	$1.956 \pm 0.013^a$	$1.970 \pm 0.017^a$	$2.020 \pm 0.025^a$
	$\bar{E}_I$	$1.946 \pm 0.12^b$		$2.000^c \pm 0.006^a$	$2.010^c \pm 0.007^a$
$^{239}\text{Pu}$	$\bar{E}_L$	$2.107 \pm 0.012^a$	$2.136 \pm 0.024^a$	$2.062 \pm 0.013^a$	$2.075 \pm 0.017^a$
	$\bar{E}_I$	$2.145 \pm 0.12^b$		2.02	
$^{252}\text{Cf}$	$\bar{E}_L$	$2.000 \pm 0.047^a$	$2.155 \pm 0.024^a$	$2.104^d \pm 0.018^a$	$2.130^d \pm 0.022^a$
	$\bar{E}_I$	$2.134 \pm 0.17^b$			
$\frac{^{239}\text{Pu}}{^{235}\text{U}}$	$\bar{E}_L$	$1.091 \pm 0.010^a$	$1.092 \pm 0.014^a$	$1.047 \pm 0.011^a$	$1.029 \pm 0.015^a$
	Ratios $\bar{E}_{RS}$	$1.106 \pm 0.015^a$			
	$\bar{E}_I$	$1.102 \pm 0.015^a$		1.06	
$\frac{^{252}\text{Cf}}{^{235}\text{U}}$	$\bar{E}_L$	$1.035 \pm 0.025^a$	$1.102 \pm 0.014^a$	$1.068 \pm 0.014^a$	$1.054 \pm 0.016^a$
	Ratios $\bar{E}_I$	$1.097 \pm 0.025^b$			

<sup>a</sup> Statistical error.<sup>b</sup> Estimated total error.<sup>c</sup>  $^3\text{He}$ -spectrometer with 200- $\mu\text{m}$  detectors.<sup>d</sup> Upper energy limit 4 MeV.

two techniques. Whereas the proton-recoil measurements yield values of 1.09 to 1.10 for the ratios of  $^{239}\text{Pu}$  and  $^{252}\text{Cf}$  average energies to  $^{235}\text{U}$  average energy (quite independent from energy range and method of evaluation), the corresponding ratios deduced from the  $^3\text{He}$  measurements are 1.03 to 1.06 ( $^{239}\text{Pu}/^{235}\text{U}$ ) and 1.06 ( $^{252}\text{Cf}/^{235}\text{U}$ ). No reasonable explanation has been found for this large discrepancy (a factor of two outside the statistical uncertainties) between the  $^3\text{He}$  and proton-recoil results. The results are at least consistent insofar as both techniques show that (1) the  $^{239}\text{Pu}$  spectra is definitely harder than that of  $^{235}\text{U}$  and (2) the  $^{252}\text{Cf}$  average energy is only about 1 to 3% higher than that of  $^{239}\text{Pu}$ .

Table IV compares the average energies deduced from the present measurements (in the energy range 1.5 - 7 MeV) with some more recently published values and with a combined average of earlier measurements compiled by Barnard et al. [3]. The proton-recoil  $^{235}\text{U}$  average energy is in excellent agreement, whereas the  $^3\text{He}$  value is about 3% higher than the combined average and most other values from differential measurements. On the other hand, the total error quoted here (6%) put the results of the activation measurements in disagreement with the present values. The  $^{239}\text{Pu}$  and  $^{252}\text{Cf}$  mean energies of both techniques are also in good agreement with the combined average (the proton-recoil  $^{239}\text{Pu}$  mean energy being 2%

TABLE IV. COMPARISON OF AVERAGE ENERGIES AND RATIOS OF AVERAGE ENERGIES, PRESENT INVESTIGATION AND PREVIOUS RESULTS

(Error margins are statistical uncertainties)

Isotope	Average energies (MeV)			Average energy ratios	
	$^{235}\text{U}$	$^{239}\text{Pu}$	$^{252}\text{Cf}$	$\frac{^{239}\text{Pu}}{^{235}\text{U}}$	$\frac{^{252}\text{Cf}}{^{235}\text{U}}$
Present investigation					
Proton-recoil	$1.956 \pm 0.013$	$2.136 \pm 0.024$	$2.155 \pm 0.024$	$1.092 \pm 0.014$	$1.102 \pm 0.014$
$^3\text{He}$ spectrometer	$2.020 \pm 0.025$	$2.075 \pm 0.017$	$2.130 \pm 0.022$	$1.028 \pm 0.015$	$1.054 \pm 0.016$
Combined average [3]	$1.95 \pm 0.015$	$2.085 \pm 0.015$	$2.13 \pm 0.03$	1.07	1.09
Barnard et al. [3] (TOF)	1.946	2.111		1.085	
Condé and During [4] (TOF)	1.86	2.01	2.085	1.08	1.12
Meadows [11] (TOF)			2.348		
Smith [12] (TOF)	1.95			$1.075 \pm 0.02$	
Zamyatnin [13] (TOF)			$2.22 \pm 0.05$		
Grundl [1] (activation)	2.20			$1.039 \pm 0.002$	
McElroy [2] (activation)	2.24				

higher), whereas the value of Meadows [11] lies outside our total experimental error limit. As regards the ratios of average energies, the proton-recoil values confirm the combined average and the other differential values, whereas the low  $^3\text{He}$  values favour the activation measurements of Grundl [1].

The measured spectra have also been compared with Watt distributions,  $\chi_E(E) \sim e^{-B \cdot E} \sinh(\sqrt{A \cdot E})$ . A noticeable improvement, as compared to a Maxwellian, is only achieved above about 7 MeV where the Maxwellian generally predicts values that are too large (Fig. 7). The best fit between 1 and 8 MeV to the proton-recoil data was achieved with  $B = 1.0 \text{ MeV}^{-1}$ ;  $A = 1.9 \text{ MeV}^{-1}$  for  $^{235}\text{U}$  and  $B = 0.95 \text{ MeV}^{-1}$ ,  $A = 2.0 \text{ MeV}^{-1}$  for  $^{239}\text{Pu}$ .

A comparison of the present measurements (integrated over broad energy intervals) with fission spectra representations used in fast reactor multigroup calculations and with spectra deduced from activation measurements is shown in Fig. 7. In the ABN set [14] and in the KEDAK file [15] the fission spectra are represented by Watt distributions (KEDAK:  $^{235}\text{U}$ ,  $B = 1.036$ ,  $A = 2.29 \text{ MeV}^{-1}$ ,  $\bar{E} = 1.98 \text{ MeV}$ ;  $^{239}\text{Pu}$ ,  $B = 1.0$ ,  $A = 2.0 \text{ MeV}^{-1}$ ,  $\bar{E} = 2.0 \text{ MeV}$ ), whereas Maxwell presentations with  $\bar{E} (^{235}\text{U}) = 1.95 \text{ MeV}$  and  $\bar{E} (^{239}\text{Pu}) = 2.115 \text{ MeV}$  are used in the ENDF/B file. The proton-recoil results support for both isotopes the ENDF/B representation, whereas the

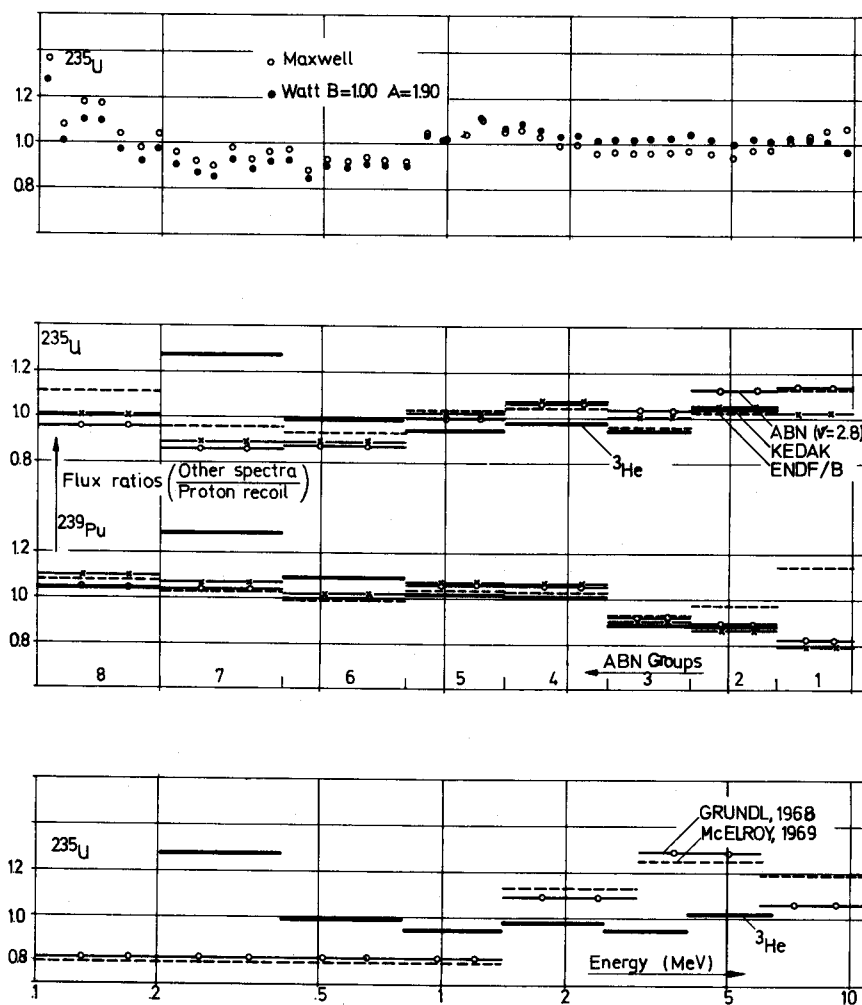


FIG. 7. Comparison of spectra from the present investigation, from activation measurements and of spectra used for multigroup reactor calculations.

$^3\text{He}$  results for  $^{239}\text{Pu}$  agree somewhat better with the ABN and KEDAK spectra. In reactor calculations performed at Karlsruhe [16] using the standard ABN fission spectrum for both  $^{235}\text{U}$  and  $^{239}\text{Pu}$   $k_{\text{eff}}$  is generally overestimated by 1 - 2% for U and underestimated by about the same amount for Pu assemblies. Using the ENDF/B representation these discrepancies are reduced for both types of assemblies by an amount that varies strongly from assembly to assembly, but averages to about 0.5% over a series of cores. Both  $^{235}\text{U}$  spectra deduced from foil activation measurements [1, 2] are considerably harder than the spectra measured here. The variation of

the ratios of the foil activation spectra to the proton-recoil  $^{235}\text{U}$  spectra by about 50% between about 1 and 4 MeV is thought to be well outside our experimental error.

A more recently performed investigation [17] has confirmed the observations of earlier measurements, that the fission spectra show some fine structure in the energy region between about 1 and 5 MeV. Although the energy resolution of the techniques used here should be sufficient to resolve this fine structure (60 keV for the  $^3\text{He}$ -spectrometer and about 8% for the proton-recoil counters), it was not observed in our measurements.

#### 4. CONCLUSIONS

The conclusion drawn from most previous microscopic measurements, that Maxwellian distributions describe the fission spectra quite well, as well as the values of average fission neutron energies deduced from these measurements are generally supported by the present investigation, whereas the high average energy of  $^{235}\text{U}$  fission neutrons deduced from activation measurements is in definite disagreement with our results.

An unexplained disagreement exists between the proton-recoil and the  $^3\text{He}$ -spectrometer values for the  $^{239}\text{Pu}/^{235}\text{U}$  average energy ratio. The high proton-recoil value agrees within the assumed error of 1 - 2% with most previous microscopic results, whereas the  $^3\text{He}$  value supports the low value deduced from activation measurements.

#### ACKNOWLEDGEMENTS

Our thanks are due to the staff of the FR-2 for their assistance, especially to Mr. Geipel, Mr. Hergert and Mr. Holub.

#### REFERENCES

- [1] GRUNDL, J., Nucl. Sci. Engng 31 (1968) 191.
- [2] McELROY, W., Nucl. Sci. Engng 36 (1969) 109.
- [3] BARNARD, E., FERGUSON, A.T.G., McMURRAY, W.R., VAN HEERDEN, I.J., Nucl. Phys. 71 (1965) 228.
- [4] CONDE, H., DURING, G., Ark. Fys. 29 (1965) 313.
- [5] OKRENT, D., LOEWENSTEIN, W.B., ROSSIN, A.D., SMITH, A.B., ZOLOTAR, B.A., KALLFELZ, J.M., Nucl. appl. Technol. 9 (1970) 454.
- [6] WERLE, H., KFK Rep. INR-4/70-25 (1970); Rep. ORNL-tr-2415.
- [7] BENJAMIN, P.W., KEMSHALL, C.D., BRICKSTOCK, A., Rep. AWRE 09/68 (1968).
- [8] BLUHM, H., Rep. KFK 1270/2 (1970) 121.
- [9] PATE, B.D., YAFFE, L., Can. J. Chem. 33 (1955) 15.
- [10] ALS-NIELSEN, J., Rep. CCDN-NW/6 (1967).
- [11] MEADOWS, J.W., Phys. Rev. 157 (1967) 157.
- [12] SMITH, A.B., Preprint, Argonne National Laboratory (1970); private communication.
- [13] ZAMYATNIN, Yu.S., Nuclear Data for Reactors (Proc. Conf. Helsinki, 1970), IAEA, Vienna (1970).
- [14] ABAGJAN, L.P., BAZAZJANC, N.O., BONDARENKO, I.I., NIKOLAEV, M.N., Rep. KFK-tr-144 (1964).
- [15] SCHMITT, J.J., Rep. KFK-120 (1968).
- [16] KIEFHABER, E., Gesellschaft für Kernforschung, private communication (1971).
- [17] NEFEDOV, V.N., Preprint, Atomic Reactor Research Institute Melekes (1969); private communication.



# FISSION NEUTRON SPECTRUM MEASUREMENT OF $^{252}\text{Cf}$

L. JÉKI, Gy. KLUGE, A. LAJTAI  
Central Research Institute for Physics,  
Hungarian Academy of Sciences,  
Budapest, Hungary

P.P. DYACHENKO, B.D. KUZMINOV  
Institute of Physics and Power Engineering,  
Obninsk, USSR

## Abstract

FISSION NEUTRON SPECTRUM MEASUREMENT OF  $^{252}\text{Cf}$ .

The spontaneous fission neutron spectrum of  $^{252}\text{Cf}$  was measured from 0.002 to 1 MeV by the time-of-flight technique. The experimental points fit a Maxwellian with  $T=1.3$  MeV.

The spontaneous fission neutron spectrum of  $^{252}\text{Cf}$  from 0.003 MeV to 15 MeV has been measured by MEADOWS [1] by time-of-flight technique using a hydrogenous liquid scintillator detector at the higher and a  $^6\text{Li}$ -lead glass scintillator at the lower neutron energies. Meadows pointed out that the low energy part of the experimental spectrum shows some deviation from the Maxwellian shape, while the agreement is excellent for the spectra above 0.5 MeV.

To study the discrepancies between this and newer experiments [3, 4] we have measured the energy spectrum of neutrons emitted in the spontaneous fission of  $^{252}\text{Cf}$  in the range 2 keV- 1 MeV.

A schematic drawing of the experimental apparatus is shown in Fig. 1. The energy of the fission neutrons was evaluated from the flight time measured over a given distance. The neutrons were detected with 7.6 cm diam. by 0.3 cm thick Nuclear Enterprises glass scintillator containing 7.3 % lithium enriched to 96 % in  $^6\text{Li}$ . The efficiency curve was taken from [1].

A  $^{252}\text{Cf}$  fission source rating  $1.7 \times 10^5$  fissions per minute on thin stainless steel foil, and later a  $^{252}\text{Cf}$

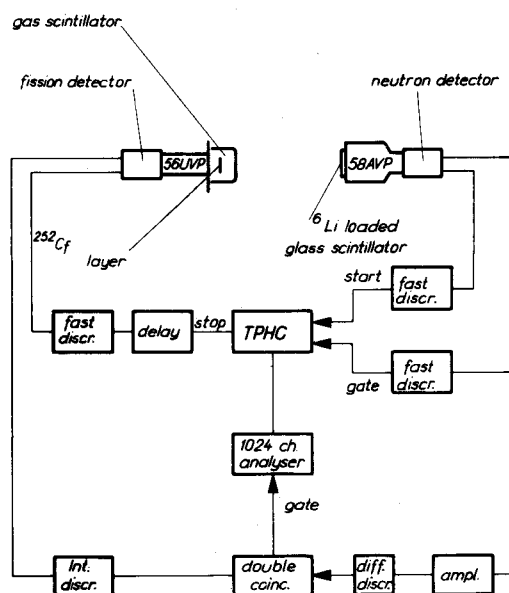


FIG. 1. Schematic drawing of the experimental apparatus.

source rating  $1.1 \times 10^6$  fissions per minute on thin platinum foil, was mounted in the centre of a gas scintillator cell 10 cm in diam. and 6 cm long. The gas scintillation counter contained a mixture of 80 % argon and 20 % nitrogen gas at a pressure of 1 atm. The gas scintillation counter was chosen to prevent the counting of other than fission events in view of the large background contribution from alpha, neutron and gamma radiation.

For measurements at 15.5, 30 and 57.5 cm flight paths the flight times up to 400 nsec were measured by a time-to-pulse height converter. Because of the high count rate of the fission detector, the neutron detector was used for triggering the time converter. The stop signal was provided by the fission detector. The limited signals from the fission detector were sent through a delay line of 400 nsec. The zero time was determined from the position of the prompt gamma ray peak, with a correction for the gamma ray flight time. The time scale was calibrated by recording

the position of this peak at different values of the delay varied by the use of calibrated delay lines. The channel time was 0.39 nsec. The time resolution, determined by the width of the prompt gamma ray, was 4.5 nsec. The time calibration, the detector pulse heights and bias levels were checked daily and, if necessary, adjusted.

The background sources arising when time-of-flight technique is used for measuring fission neutron energies were studied in detail elsewhere [2].

The random coincidence background was measured simultaneously in a given range of the spectrum by suppressing systematic events in this region with appropriate delays. The spectrum distortion due to the systematic random coincidences was calculated from the measured spectra.

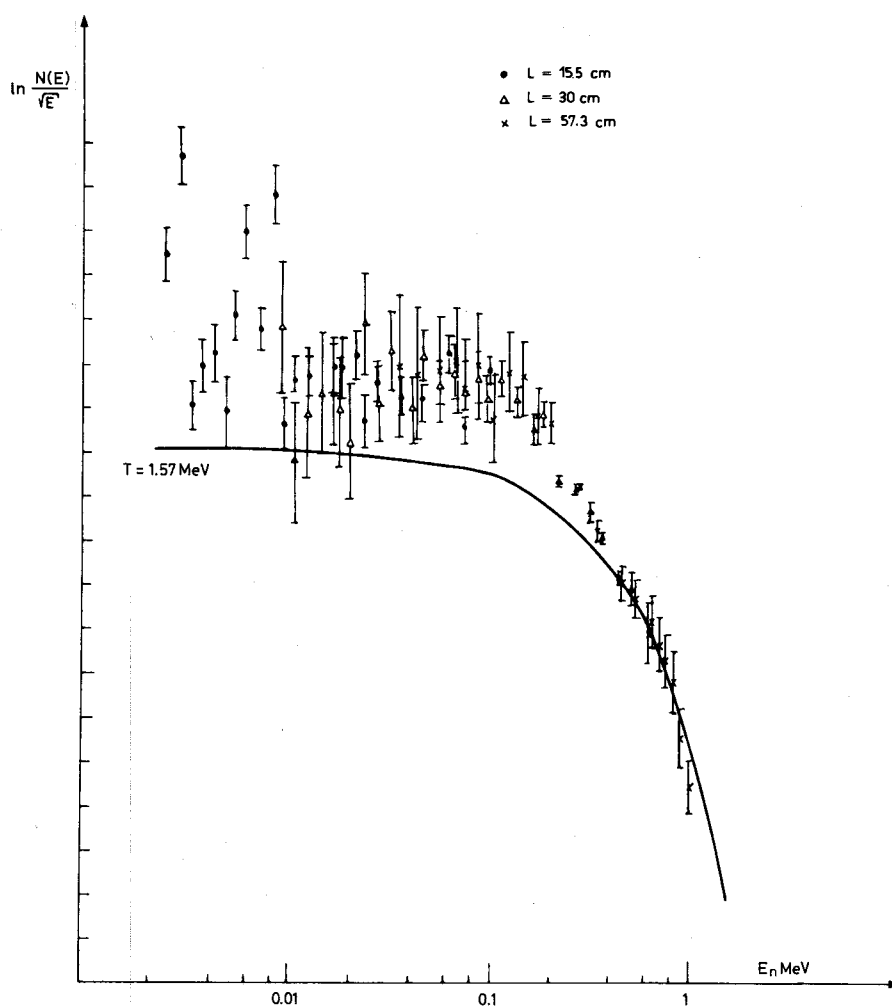
TABLE I. MEASURED RELATIVE INTENSITIES FOR NEUTRON SPECTRUM OF  $^{252}\text{Cf}$

A - 15.5 cm flight path; B - 30.0 cm flight path; C - 57.5 cm flight path.

$E_n$ /MeV/	N(E) arb.units	$\frac{\Delta N(E)}{N(E)}$ %/
0.0024	0.768	5.9 A
0.0027	1.019	6.4 A
0.0032	0.632	5.7 A
0.0036	0.742	6.0 A
0.0042	0.814	6.3 A
0.0046	0.752	7.7 A
0.0051	0.984	5.4 A
0.0059	1.271	5.7 A
0.0070	1.114	4.7 A
0.0080	1.621	6.7 A
0.0090	1.268	15.1 B
0.0092	1.034	5.6 A
0.0106	1.221	5.2 A
0.0106	1.021	14.8 B
0.0120	1.202	15.0 B
0.0122	1.321	4.9 A
0.0140	1.362	13.8 B
0.0160	1.460	12.1 B
0.0160	1.543	5.6 A
0.0175	1.477	12.4 B
0.0180	1.654	7.1 A
0.0195	1.435	13.2 B

TABLE I. cont.

$E_n$ /MeV/	$N(E)$ arb. units	$\frac{\Delta N(E)}{N(E)}$ /% /
0.0210	1.821	5.8 A
0.0230	1.653	6.0 A
0.0230	2.059	11.6 B
0.0270	1.854	8.7 B
0.0270	1.942	4.9 A
0.0320	2.275	9.1 B
0.0340	2.268	16.6 C
0.035	2.129	4.3 A
0.037	2.153	7.2 B
0.040	2.407	15.0 C
0.044	2.655	5.8 B
0.045	2.412	5.1 A
0.055	2.860	11.9 C
0.055	2.749	5.4 B
0.060	3.123	4.2 A
0.065	3.049	6.1 B
0.065	3.195	12.1 C
0.075	3.202	12.7 C
0.075	3.177	7.1 B
0.075	2.935	3.8 A
0.085	3.495	6.3 B
0.086	3.613	11.8 C
0.095	3.529	5.8 B
0.095	3.754	3.1 A
0.101	3.446	10.3 C
0.110	3.999	4.2 B
0.121	4.229	8.9 C
0.135	4.205	3.6 B
0.146	4.571	8.6 C
0.165	4.334	2.9 B
0.175	4.602	6.1 C
0.180	4.703	3.0 B
0.200	4.850	5.2 C
0.220	4.477	1.7 B
0.270	4.850	1.9 B
0.276	4.912	2.0 C
0.315	4.989	1.5 B
0.346	4.989	2.2 C
0.370	5.090	2.0 B
0.445	5.094	2.2 B
0.463	5.174	3.8 C
0.520	5.428	3.5 B
0.544	5.344	4.7 C
0.628	5.327	6.7 C
0.661	5.602	6.4 C
0.729	5.588	5.9 C
0.792	5.620	6.4 C
0.852	5.546	6.1 C
0.938	5.128	6.3 C
1.073	4.902	7.1 C

FIG.2. Measured fission neutron spectrum of  $^{252}\text{Cf}$ .

In order to reduce the scattered background, the detector was prepared from light material, using 0.1 cm aluminium and the window of the fission chamber from 0.03 cm aluminium. To measure the scattered neutron background, a 13 cm long brass cone was placed between the detectors for runs at 57.5 cm flight path and a cone 7 cm in length for other runs.

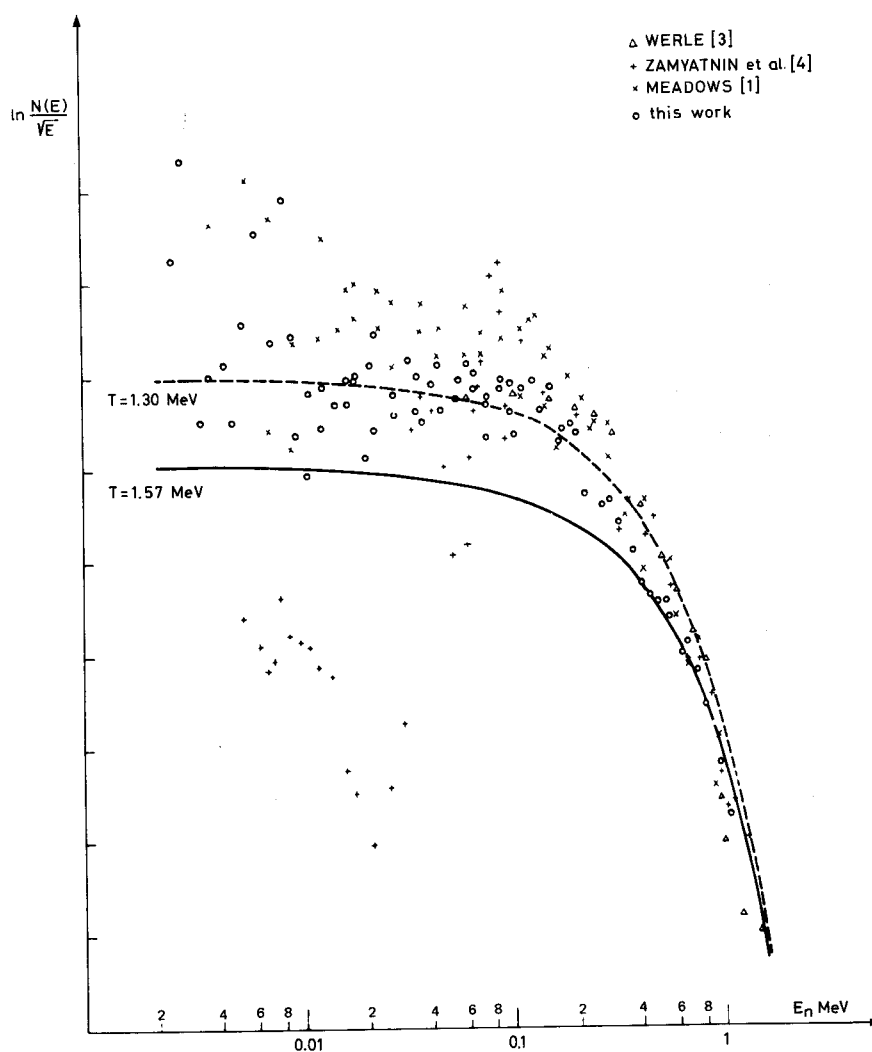


FIG.3. Comparison of different measurements (the data were normalized together in the energy range 0.7-1 MeV).

The background caused by the detection of delayed gamma rays was measured at 3.5 cm flight path and was normalized to the measured spectra taking into account the different solid angles and the number of fissions detected.

The results of the measurements are given in Table I and Fig. 2. The errors of each point are those of

purely statistical origin. It is hoped that measurements at 57.5 cm flight path which are still in progress will give the data a greater statistical accuracy.

A comparison of the different measurements can be seen in Fig. 3. The data were normalized together in the energy range 0.7 - 1 MeV. Two eye-guide Maxwellian curves with  $T = 1.57$  and 1.3 MeV are also plotted. Both Maxwellians were normalized together between 0.7 - 6 MeV. Taking the result of Fig. 3 and the earlier result of Ref. [1, 2] together, it can be seen that the experimental points fit quite closely a Maxwellian with  $T = 1.57$  MeV above 1 MeV and a Maxwellian with  $T = 1.3$  MeV at lower energies. Our measured data are in good agreement with the data of [1, 3].

A complete description of the experimental arrangements and the apparatus will be published in the KFKI-Report series.

#### REFERENCES

- [1] MEADOWS, J.W., Phys. Rev. 157 /1967/ 1076
- [2] JÉKI, L., KLUGE, GY., LAJTAI, A., Report KFKI-71-9 /1971/
- [3] WERLE, H., Report INR-4/70-25 /1970/
- [4] ZAMYATNIN, Y.S., KROSKIN, N.I., MELNIKOV, A.K., NEFEDOV, V.H., Proc. 2nd Conf. Nuclear Data for Reactors, /Helsinki, 1970/ IAEA Vienna 1970, Vol. II. p. 183.





# DELAYED NEUTRONS FROM SPONTANEOUS FISSION OF $^{252}\text{Cf}$

V. N. NEFEDOV, A. K. MELNIKOV, B. I. STAROSTOV  
Scientific Research Institute of Atomic Reactors,  
Melekess,  
Union of Soviet Socialist Republics

## Abstract

### DELAYED NEUTRONS FROM SPONTANEOUS FISSION OF $^{252}\text{Cf}$ .

The total neutron spectrum resulting from spontaneous fission of  $^{252}\text{Cf}$  has been measured by using the time-of-flight method with large path lengths. In addition, direct measurements were made by the delayed coincidence method to determine the number and time of emission of delayed neutrons. The results confirm earlier observations by the same authors of fission neutrons emitted about  $10^{-9}$ - $10^{-8}$  s after scission.

## INTRODUCTION

Earlier we indicated the existence of fission neutrons emitted approximately  $10^{-9}$ - $10^{-8}$  s after the moment of fission [1]. The energy spectrum of these neutrons, which will be referred to below as delayed neutrons, exhibits separate peaks at 0.085, 0.2, 0.45, 0.75, 1.2, 1.6 and 2.6 MeV [1,2] against a continuous spectrum of prompt fission neutrons.

To obtain additional data on delayed neutrons we used, in the work described here, the time-of-flight method with large path lengths to measure the total neutron spectrum resulting from spontaneous fission of  $^{252}\text{Cf}$ . Direct measurements were made by the delayed coincidence method to determine the number and time of emission of delayed neutrons.

### TOTAL NEUTRON SPECTRUM FROM SPONTANEOUS $^{252}\text{Cf}$ FISSION

The existence of delayed neutrons imposes special requirements on experimental measurements of fission neutron spectra. To obtain accurate data on delayed neutrons we must ensure rapid stopping of the fission fragments (in less than  $10^{-9}$  s) since the time of emission of delayed neutrons is  $10^{-9}$ - $10^{-8}$  s. Without rapid stopping of the fragments, no separate delayed neutron peaks could be observed: the energy resolution would be blurred as a result of averaging over all the directions of neutron escape from the flying fragments.

In measurements of fission neutron spectra by the time-of-flight method, the delayed neutron peaks are lower when individual groups are blurred owing to the long emission time of the delayed neutrons. Over short path lengths the individual groups will overlap, distorting the spectrum and reducing its mean energy. Hence measurements of fission neutron spectra by the time-of-flight method must be performed over large path lengths.

Bearing this in mind, we measured neutron spectra from spontaneous fission of  $^{252}\text{Cf}$  by the time-of-flight method over a 3.5-m path length.

The transit time was measured by means of a time-amplitude converter and the amplitude spectrum recorded on an AI-256 analyser.

The target was  $^{252}\text{Cf}$  deposited on Al backing 0.5 mm thick and 20 mm in diameter, giving  $7 \times 10^4$  fissions per second. The moments of fission were recorded from the light flashes produced in air by the fission fragments. The  $^{252}\text{Cf}$  target was set up 2 mm away from an FEU-36 photocathode. Figure 1 shows the amplitude spectrum of the fragment pulses recorded by the detector.

For recording the fission neutrons we used an FEU-63 photomultiplier with a  $100 \times 100$  mm plastic scintillator. In the course of the measurements the neutron recording threshold was checked periodically by means of a  $^{241}\text{Am}$  source with 59.6-eV gamma quanta energy.

To determine any effects deriving from the instruments, the measurements were performed over two path lengths, 3.5 and 2.7 m. The measurements showed that the peaks are displaced in proportion to the path length and consequently are not attributable to instrument effects.

Figure 2 shows a spectrogram of  $^{252}\text{Cf}$  spontaneous fission neutrons obtained over a 3.5-m path length in two days of continuous measurements.

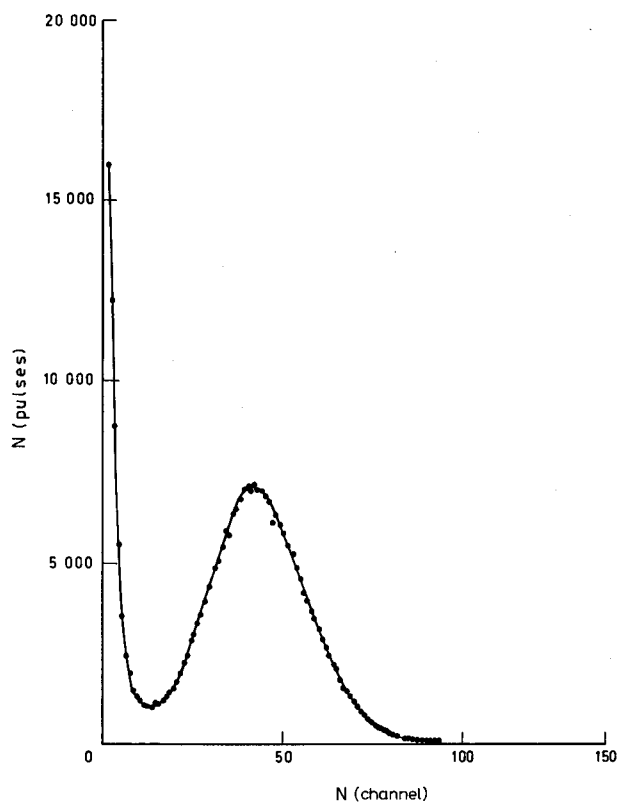
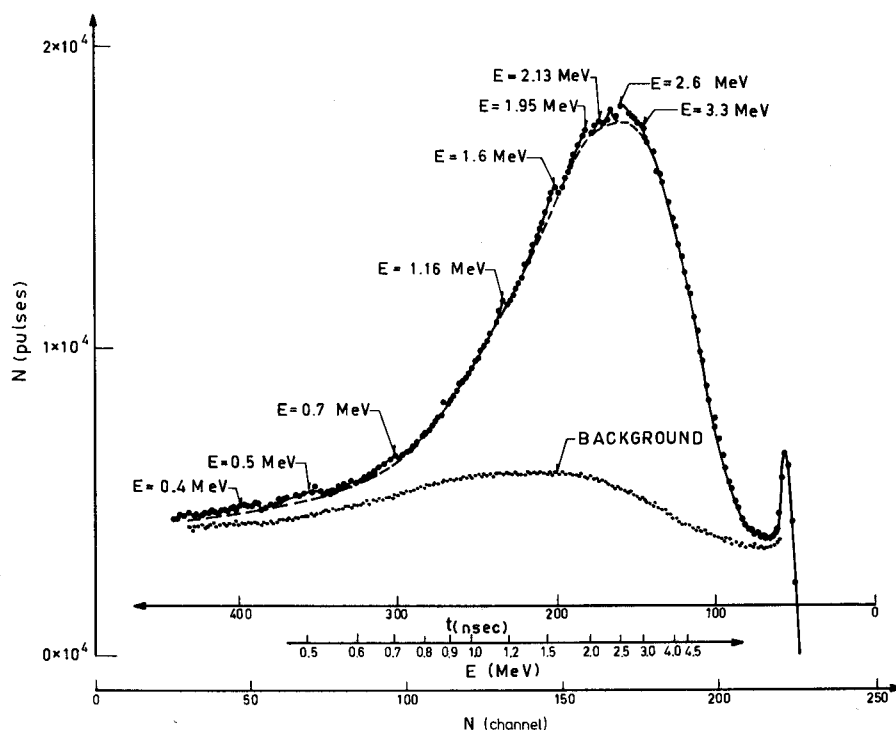


FIG. 1. Amplitude spectrum of  $^{252}\text{Cf}$  fission fragments.


 FIG. 2. Spectrogram of  $^{252}\text{Cf}$  spontaneous fission neutrons.

The spectrum exhibits separate peaks at 0.5, 0.7, 1.16, 1.6 and 2.6 MeV, which agrees with the data obtained in earlier work [1,2]. In addition, there are new peaks with energies of 2.13, 1.95 and 3.3 MeV. From Fig. 2 it can be seen that these peaks are in the form of steps with a smooth decay in the direction of larger time values. This configuration indicates that they are due to delayed neutrons. The length of the flat decay on the separate peaks is governed by the emission time of a given group of delayed neutrons; from it, therefore, we can find the emission time of these neutrons. To do this, we determine the time  $T$  taken for each peak to decay by half. To separate the peaks by extrapolation, we construct a smooth spectrum (the broken line). The emission times calculated in this way for delayed neutrons of different energy groups are shown in Table I.

For neutron groups with energies over 1.6 MeV it is more difficult to determine the emission time since the individual groups overlap; to separate them measurements over still greater path lengths are required. In addition, there may be groups of delayed neutrons with later emission times ( $>20$  ns). These would be virtually imperceptible in the time-of-flight measurements because of dispersion over a large number of channels. Therefore, to obtain more complete data on delayed  $^{252}\text{Cf}$  spontaneous fission neutrons, direct measurements were made by the method of delayed coincidences.

TABLE I. CALCULATED EMISSION TIMES FOR VARIOUS ENERGY GROUPS

No.	Energy of neutron group (MeV)	Emission time (s)
1	0.5	5-10
2	0.7	5-10
3	1.16	2-3
4	1.6	7-8

## MEASUREMENTS OF DELAYED NEUTRONS BY THE METHOD OF DELAYED COINCIDENCES

We placed the neutron detector close to a  $^{252}\text{Cf}$  target and measured the time distributions of the delayed coincidences between the instants of  $^{252}\text{Cf}$  fissions and the registration of fission neutrons by the neutron detector. The coincidences were recorded by AI-100 and AI-256 multichannel analysers. To convert the time distributions into amplitude distributions we used a time-amplitude converter [3].

When delayed neutrons are present the coincidence peak is asymmetrical in shape, broadening towards longer times; and this broadening is characterized by the emission time and the number of delayed neutrons emitted.

To obtain more reliable data, the measurements were performed in parallel on two installations employing different neutron detectors.

In the first experiment we used xenon-filled gas scintillation counters to record  $^{252}\text{Cf}$  fission fragments and the neutrons escaping during fission. The neutrons were recorded from fission events provoked by neutrons in a layer of metallic 95% enriched  $^{235}\text{U}$ , 0.025 mm thick and 24 mm in diameter.

The  $^{252}\text{Cf}$  target, with an intensity of  $4 \times 10^4$  fission/s, was a thin layer of  $^{252}\text{Cf}$  applied to an aluminium base 0.5 mm thick. The diameter of the  $^{252}\text{Cf}$  layer was 20 mm.

Both detectors were single stainless steel chambers. The design of the chamber and its geometrical dimensions are shown in Fig. 3. To fill the chamber with xenon we used a special device that purifies the gas during filling and in the course of the experiments [4]. Both halves of the chamber were scanned by FEU-53 photomultipliers through quartz glass.

To check the functioning of the electronics, the prompt coincidence peak (instrument peak) between  $^{252}\text{Cf}$  fission fragment pairs was recorded once every 24 hours. In measuring the prompt coincidence peak, the shutter mounted on the bellows rod (see Fig. 3) was moved aside to reveal an aperture in which the layer of  $^{252}\text{Cf}$  on its thin backing was located.

Most of the measurements were performed with a xenon pressure of 7 atm in the chamber. Figure 4 shows the results of measurements obtained over one month's continuous operation. The graph clearly shows

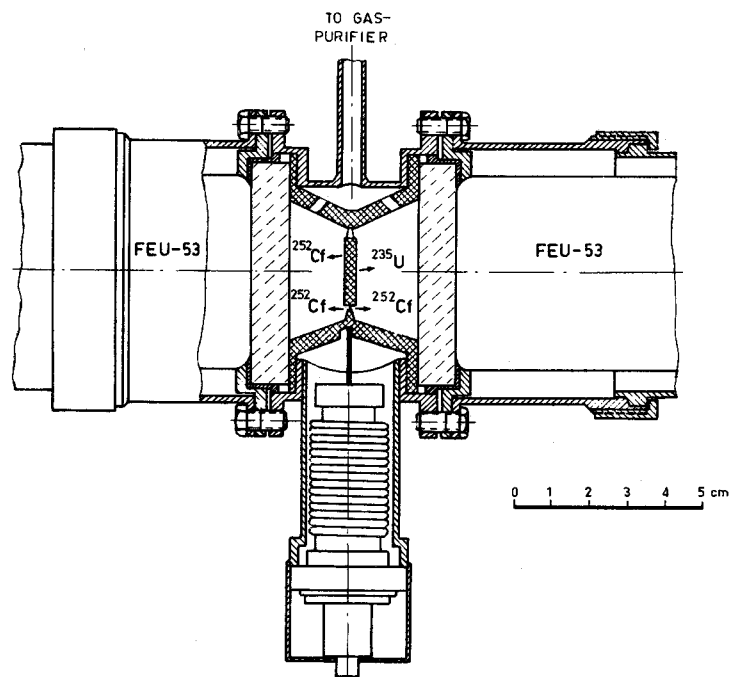


FIG. 3. Geometry of gas scintillation chamber.

several groups of delayed neutrons with different emission times. To check the effect on the results attributable to neutrons scattered from surrounding objects and components of the chamber, we carried out measurements with an additional scatterer — an iron ring of 55 mm internal diameter and  $25 \times 25$  mm thick attached to a side wall of the chamber. The measurements showed that effects due to scattered neutrons are negligible.

We also measured the delayed neutron yield with a gas pressure in the chamber of 0.1 atm, and these measurements confirmed our conclusion that the delayed coincidences are due to delayed neutrons. With a low gas pressure in the chamber the  $^{252}\text{Cf}$  fission fragments cover greater distances and strike the walls of the chamber. This considerably reduces the geometrical efficiency of recording the delayed neutrons emitted by these fragments. The anticipated reduction in the delayed neutron yield would be about 20-25%, and our experiment in fact showed a reduction of  $20 \pm 5\%$  in the number of delayed neutrons recorded.

After expanding the delayed coincidence curve (Fig. 4) by various exponents, we obtained the emission times and the yields for different delayed neutron groups that are shown in Table II.

The other neutron detector used a combination of a 13-mm thick silver strip and a  $50 \times 50$  mm plastic scintillator. The geometry of the experiment is shown in Fig. 5. The neutrons released in spontaneous fission of  $^{252}\text{Cf}$  were detected by recording the gamma quanta originating in the silver as a result of inelastic scattering and radiative capture of neutrons by the silver nuclei and the plastic scintillator. To eliminate delayed fission

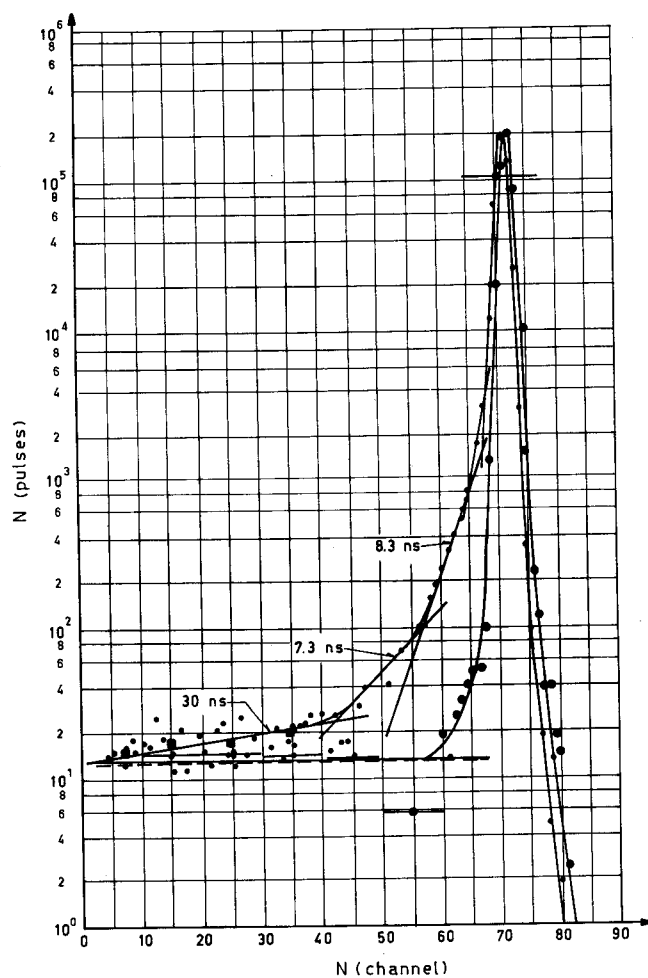


FIG. 4. Distribution of delayed coincidences:  
 . delayed coincidences of  $^{252}\text{Cf}$  fragments -  $^{235}\text{U}$  fragments;  
 o instrument peak.

TABLE II. EMISSION TIMES AND YIELDS FOR VARIOUS DELAYED NEUTRON GROUPS

No.	Emission time (ns)	Yield, as % of total number of neutrons emitted per fission event
1	$2.3 \pm 0.5$	$2.7 \pm 0.4$
2	$7.3 \pm 1$	$0.6 \pm 0.1$
3	$30 \pm 2$	$0.2 \pm 0.03$

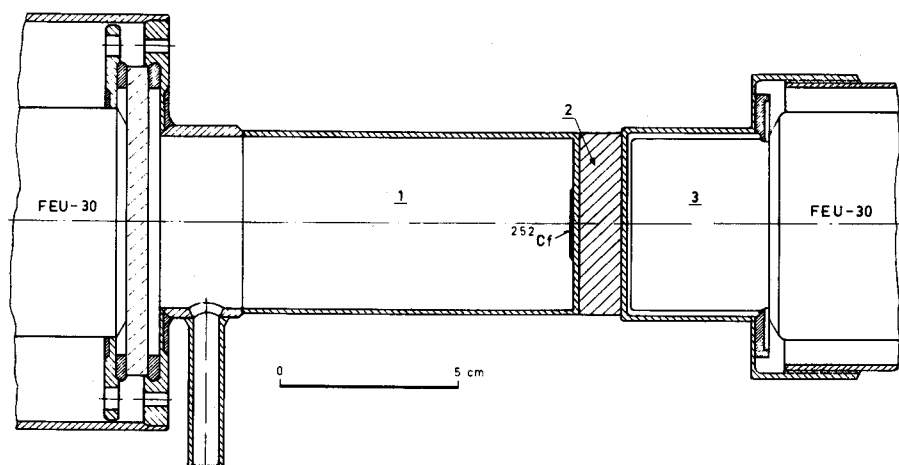


FIG. 5. Geometry of the experiment: 1. gas scintillation chamber; 2. silver strip; 3. plastic scintillator.

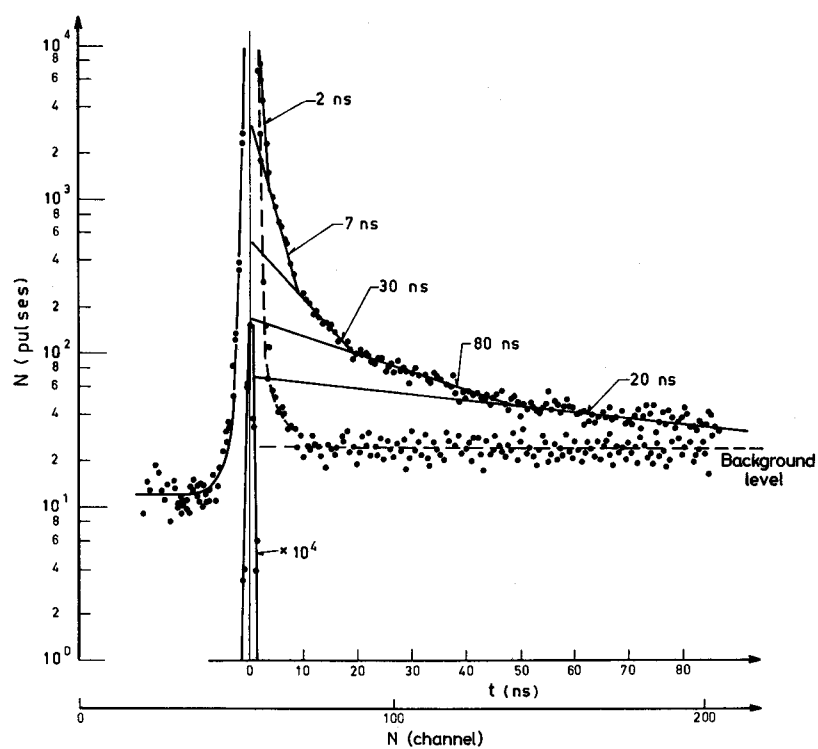


FIG. 6. Distribution of delayed coincidences:  
 • delayed coincidences of  $^{252}\text{Cf}$  fragments;  
 - neutron capture quanta in silver;

gamma quanta the gamma counting threshold was set at 2 MeV. To determine the background we replaced the silver strip by a lead strip 11 mm thick. Figure 6 shows the experimental curve obtained over two day's continuous measurement. After expansion the following emission times were obtained for the various groups of delayed neutrons:  $2 \pm 0.5$  ns,  $7 \pm 1$  ns,  $80 \pm 2$  ns,  $30 \pm 5$  ns and  $120 \pm 20$  ns. As in the previous experiments, groups were observed with emission times of 2.7 and 30 ns. Groups of delayed neutrons with emission times of 80 and 120 ns were also noted.

Thus, our experiments confirmed earlier data [1,2] and enabled us to obtain more complete information on the yield and emission time of delayed neutrons from spontaneous fission of  $^{252}\text{Cf}$ .

#### ACKNOWLEDGEMENTS

The authors wish to thank V. A. Kachalin for designing and setting up the electronic apparatus, and all the laboratory staff who helped to prepare and carry out these experiments.

#### REFERENCES

- [1] NEFEDOV, V. N., NILAR (Melekes Reactor Research Institute) preprint, P-52 (1969).
- [2] ZAMYATNIN, Yu. S., KROSHKIN, N. I., MELNIKOV, A. K., NEFEDOV, V. N., Nuclear Data for Reactors (Proc. Conf. Helsinki, 1970) 2, IAEA, Vienna (1970) 183.
- [3] BASOVA, B. G., KACHALIN, V. A., STAROSTOV, B. I., *Priborý Tekh. Éksp.* 4 (1970) 69.
- [4] KROSHKIN, N. I., KORMUSHKINA, G. A., STAROSTOV, B. I., SHIPILOV, V. I., *Gazovye scintilljacionnye detektory oskolkov delenija* (Gas scintillation detectors for fission fragments), NILAR preprint, P-59 (1971).



# DIFFERENCE OF MICROSCOPIC INTEGRAL CROSS-SECTION RATIOS IN THE $^{235}\text{U}$ AND $^{239}\text{Pu}$ THERMAL FISSION NEUTRON SPECTRA

A. FABRY

Reactor Study Department,

CEN/SCK,

Belgium

## Abstract

DIFFERENCE OF MICROSCOPIC INTEGRAL CROSS-SECTION RATIOS IN THE  $^{235}\text{U}$  AND  $^{239}\text{Pu}$  THERMAL FISSION NEUTRON SPECTRA.

For three threshold reactions commonly used in reactor dosimetry and whose energy coverage encompasses the range 1 - 10 MeV the differences of microscopic integral cross-section ratios measured in the  $^{239}\text{Pu}$  and  $^{235}\text{U}$  thermal fission neutron spectra are inconsistent with the current interpretation of the published ratios of the differential neutron spectra and tend to confirm earlier independent integral studies. The experiment is described and its difficulties outlined.

## INTRODUCTION

The much discussed inconsistencies [1-3] between microscopic integral cross-sections measured in thermal fission neutron spectra and the values obtained by convolution of the corresponding differential microscopic cross-sections with the current evaluation [4] of differential neutron flux spectra involve possible non-trivial errors in each of these three types of data. These uncertainties are of relevance to fast reactor technology. Of similar importance, but much more troublesome, are the inconsistencies observed in ratio measurements where essentially two neutron spectra are simply compared with each other:

- (a) Differential microscopic time-of-flight experiments performed with incident neutrons of energies ranging from 35 up to 400 keV and encompassing observed fission neutron energies from 0.3 to 8 MeV (or only part of this range) provide ratios of average energies  $\bar{E}_{x29}/\bar{E}_{x25}$  of the  $^{239}\text{Pu}$  to  $^{235}\text{U}$  fission neutron spectra of  $1.081 \pm 0.05$  [5],  $1.085 \pm 0.03$  [6],  $1.046 \pm 0.03$  [7] and  $1.075 \pm 0.02$  [8]. More particularly, the last and recent experiment has been designed and analysed in such a way as to determine specifically a direct ratio of spectra and average energies; it is therefore considered as the most appropriate one for discussion here.
- (b) The current interpretation of comparative microscopic integral cross-section measurements, on the other hand, provides ratios  $\bar{E}_{x29}/\bar{E}_{x25}$  of  $1.039 \pm 0.002$  [9] and  $1.026 \pm 0.005$  [10] ( $1.036 \pm 0.005$  Kovalev revised by Grundl [9]), while Bonner's [11] sphere integral-type experiments led to a value of approximately 1.041.

The ratio  $1.039 \pm 0.002$  is the most accurately and carefully assessed result of integral intercomparison between these two fission neutron spectra and should be compared with the differential figure of  $1.075 \pm 0.02$ . The

discrepancy is of real significance to fast reactor analysis and is a dramatic one because only relative measurements are involved in both the differential and integral approaches; in particular, it must be emphasized that detector cross-section uncertainties are unlikely here to contribute much to the disagreement.

As part of the CEN/SCK sustained program of integral cross-section measurements in fission and intermediate-energy standard neutron spectra, relative reaction rate ratios in the  $^{239}\text{Pu}$  and  $^{235}\text{U}$  thermal fission neutron spectra have been obtained and are described here. These 'double ratio' measurements have been designed specifically to provide a direct inter-comparison between the two neutron fields in such a way as to suppress (or at least minimize) all known sources of systematic errors; this has been possible by accepting low activation rates resulting in reduced statistical accuracy.

#### EXPERIMENTAL METHOD

The source-detector assembly displayed in Fig.1 is suspended by means of three thin stainless steel hypodermic tubings at the centre of a 50-cm diameter spherical cavity located close to the external edge of the BR1 horizontal graphite thermal column. The available thermal neutron flux is about  $3.5 \times 10^8 \text{ n} \cdot \text{cm}^{-2} \cdot \text{s}^{-1}$  at a reactor power level of 400 kW and is perfectly well thermalized: the gold-cadmium ratio at infinite dilution exceeds  $10^4$ .

The disc sources are in all cases unclad CBNM certified alloys of 0.1 mm thickness cut at a diameter of 19 mm; the content of fissile material in aluminium is 20 wt%; the uranium is enriched to 93% in  $^{235}\text{U}$  and the plutonium to 94% in  $^{239}\text{Pu}$ . The total macroscopic cross-sections in the cavity

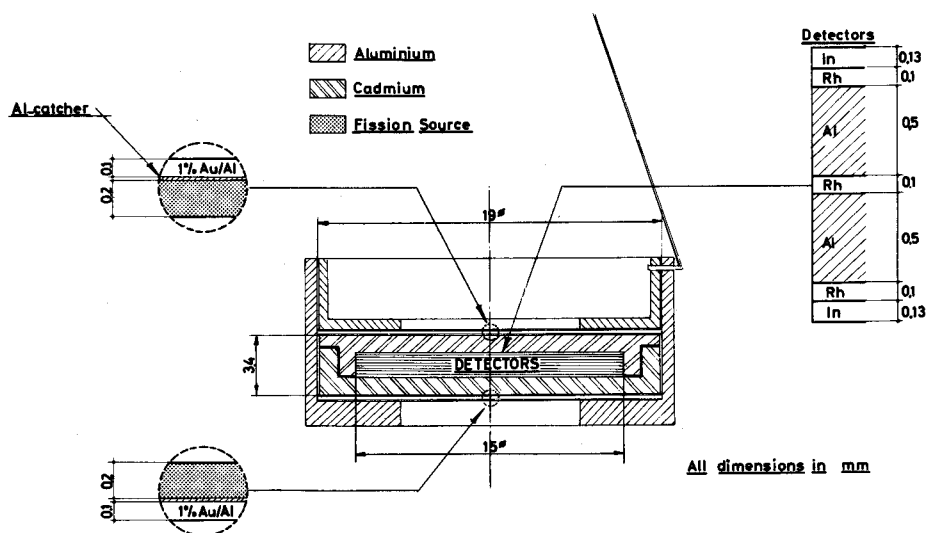


FIG. 1. Source-detector assembly.

Maxwellian thermal neutron flux (25°C temperature) are estimated respectively as 1.13 and 1.78 n/cm: for 90% enriched uranium metal this quantity would be about 30 n/cm. Four alloy discs are used for each irradiation, two of them constituting the upper (respectively lower) fission source; the total amount of fissile material in one irradiation is of the order of 75 mg. The homogeneity of the uranium alloys has been checked to be satisfactory within 1 - 1.5% by rotating them in thermal neutrons. The plutonium alloys have not been tested so extensively; however, for both plutonium and uranium irradiations two different sets of source stacks have been used, labelled A and B, and it may be inferred also from the corresponding results that the quality of plutonium alloys is comparable to that of enriched uranium alloys.<sup>1</sup> A total of eight irradiations of three hours each at reactor power level of 400 kW have been performed sequentially and are annotated chronologically from 1 to 8 (1: <sup>235</sup>U set A; 2: <sup>239</sup>Pu set A; 3: <sup>235</sup>U set B; 4: <sup>239</sup>Pu set B, ---); the flux profile is always the same, i.e. exponential start-up with a period of 20 s, stabilization for 3 hours and scram.

The detectors are activation foils of 15 mm diameter cut from commercial spectrographically pure aluminium, indium and rhodium sheets. The thicknesses are indicated in Fig.1 together with the order of stacking, which is the same for all irradiations. The nuclear reactions used, accepted half-lives and effective thresholds  $E_{\text{eff}}$  [12] in the <sup>235</sup>U fission spectrum are as follows:

<sup>103</sup> Rh(n, n') <sup>103m</sup> Rh	$T_{1/2} = 57 \text{ min}$	$E_{\text{eff}} = 0.9 \text{ MeV}$
<sup>115</sup> In(n, n') <sup>115m</sup> In	$T_{1/2} = 4.5 \text{ h}$	$E_{\text{eff}} = 1.1 \text{ MeV}$
<sup>27</sup> Al(n, p) <sup>27</sup> Mg	$T_{1/2} = 9.46 \text{ min}$	$E_{\text{eff}} = 4.7 \text{ MeV}$
<sup>27</sup> Al(n, $\alpha$ ) <sup>24</sup> Na	$T_{1/2} = 15.0 \text{ h}$	$E_{\text{eff}} = 7.3 \text{ MeV}$

The second reaction listed is the usual threshold reference foil used extensively for many years at this laboratory. Because the indium and rhodium reactions are expected to have similar energy responses in fission neutron spectra, the latter is not basically intended as a spectral index indicator, but its aim is twofold:

- (1) To protect the aluminium foils from any interfering activities induced by the indium foils (such effects have been observed in the past, likewise it has been shown that rhodium is neither sensitive to nor produces such cross-contaminations)
- (2) To check in each irradiation the reproducibility and magnitude of the axial fast flux gradient within the experimental volume.

The whole stack of foils fits exactly into a cadmium box coaxial with the fission sources. The cadmium thickness is in no place smaller than 1 mm in view of future irradiations of non-threshold foils, for which a measurable activity due to thermal neutron penetration has been observed at thicknesses equal to or smaller than 0.75 mm. The neutronic quality of this cadmium box has been checked as usual by a separate irradiation of 0.1-mm thick pure metallic gold foils at the centre of the cavity where the cadmium ratio is known.

<sup>1</sup> Weight per cent in CBNM alloys are guaranteed to within 1%. Extensive neutronic tests of CBNM alloys performed at CEN/SCK for a variety of isotopes and weight per cents have in almost all cases given excellent agreement with the nominal values (with the exception of some manganese-aluminium alloys for which absolute weight per cents disagree).

The two fission sources are intimately pressed into contact with this cadmium box; this provides both mechanical reproducibility and nearly  $2\pi$  exposures to the incident approximately isotropic thermal neutron flux. This flux is monitored by means of dilute gold foils (CBNM alloy 1% gold in aluminium) coaxial to and of the same diameter as the sources, from which they are protected by thin aluminium catchers.

The  $^{27}\text{Mg}$  and  $^{24}\text{Na}$  activities in the upper aluminium foil (Fig. 1) are measured by means of a Plastifluor  $\beta$ -counter; an anti-coincidence rejection set-up allows the background to be reduced to as low as 0.05 - 0.1 counts/s. The face of the foil exposed to the sensitive area of the counter is changed after each measurement; no noticeable difference has been observed. Corrections for  $^{24}\text{Na}$  contribution to the  $^{27}\text{Mg}$  count rate have been applied whenever necessary. In addition, the  $^{27}\text{Mg}$  gamma activity in the lower aluminium foil (Fig. 1) is measured by means of a calibrated  $3 \times 3$  in. NaI(Tl) spectrometer. This spectrometer is also used for detection of the  $^{115\text{m}}\text{In}$  335-keV isomeric transition gamma ray from both the upper and lower indium foils. The  $^{116\text{m}}\text{In}$  and  $^{114\text{m}}\text{In}$  competing capture activities are very small in these irradiations for cooling times ranging from 10 to 20 hours and do not contribute to the uncertainties of the final data, which are purely random. Sources of systematic errors like the photoactivation of  $^{115\text{m}}\text{In}$  and gamma-ray self-absorption have been studied previously and are negligible in this experiment. The isomeric transition in rhodium is completely converted and K X-rays are detected by means of a 2-in. diameter by 2-mm thick NaI(Tl) spectrometer. The three foils from each irradiation are alternatively counted, starting 1 hour after the scram and stopping at a cooling time of 4 hours. The interference from iridium impurities is insignificant.

In all measurements small corrections are applied for dead-time losses and decay during counting is also accounted for; all activities are reduced in counts/s per unit weight at scram for an infinitely long irradiation. The decays are always followed for two half-lives at least.

## ERRORS

The separation distance of 3.8 mm between the exposed faces of the two coaxial sources is the closest one ever used in this type of experiment and it probably precludes any precise interpretation of the data in terms of absolute integral cross-sections (i.e. use of absolute fluxes derived from the assessment of source intensity). Such an interpretation is not the subject of this work<sup>2</sup> where the emphasis is placed on double ratios, i.e. on the difference in reaction rate ratios when replacing  $^{235}\text{U}$  fission sources with  $^{239}\text{Pu}$  ones. Owing to the use of thin dilute alloy sources, such a substitution, conservative a priori from a strictly mechanical standpoint, is here also conservative in terms of effective source-detector distances  $\bar{Z}$ , defined [9] so that for a unit source of thickness  $T$ , radius  $R$  and a detector of thickness  $T'$ , radius  $R'$ , the flux effectively detected is simply  $1/4\pi\bar{Z}^2$ . A severe test of the neutronic equivalence and reproducibility of the source-detector assemblies is provided by the consideration of the ratio between the incident

<sup>2</sup> However, if carried out as a consistency check, such interpretation provides agreement to within 5 - 10% with previous work [13].

thermal neutron flux and the fast neutron flux within the irradiation cadmium box. This is illustrated in Table I, where the  $^{198}\text{Au}$  and  $^{115\text{m}}\text{In}$  activation rates are average values between the symmetric upper and lower foils (Fig. 1). If the 1% spread on alloy compositions is considered (gold monitor as well as fission sources) and the fact that a variation of 0.1 mm in the separation distance between the fission sources would induce a change of 3.5% in the indium-gold ratio is noted, it can be ascertained that the  $^{235}\text{U}$  and  $^{239}\text{Pu}$  source-detector assemblies should display an identical nuclear behaviour with respect to radial and axial fast flux spectrum gradients.<sup>3</sup> This homogeneity of the substitution is also supported by the data in Table II.

A firm discrepancy, however, is apparent between the gradients detected by rhodium and the computed ones. This might be due to intrinsic scattering effects within the source-detector assemblies; such effects may give rise to a difficult type of correction in integral fission spectrum cross-section measurements. However, owing to the equivalence of the  $^{235}\text{U}$  and  $^{239}\text{Pu}$  fission sources as discussed above, these corrections are presumed to cancel out in this double-ratio experiment and are not considered further.

Because the effective distances  $\bar{Z}$  are as small as about 2% of the cavity radius, it also results from earlier experiments [14, 15] and calculations [9, 14] that no corrections are to be applied here for neutron wall return backgrounds; an 'in vacuo' environment is achieved in practice.

Fast neutron leakage from the reactor core is known to produce negligible activation rates in this cavity. For completeness, this has again been verified by running the assembly with aluminium foils replacing the sources.

In conclusion, the very close separation distance between the sources, selected for performing these experiments with a total amount of fissile material as low as about 75 mg, provides optimum background conditions and ideal neutron field equivalence upon source substitution; the simple set-up used is still favourable in terms of fast flux gradient effects. As a consequence of these considerations, it turns out that no special correction has to be applied to the measured saturated activation rates when forming the double ratios. The statistical errors of the individual measurements have been propagated quadratically to provide the final errors.

## RESULTS

All reaction rate ratios obtained in the eight irradiations are presented in Table III with indium in the denominator, except for the data in columns 6 and 12 which, although seeming a priori redundant, provide in fact the most reliable information of this study because each figure only involves the counting of a single foil on a single equipment, i.e. reflects simply the straightforward unfolding of a radioactivity decay curve.

The rhodium and indium activation rates used when forming the ratios are always averaged over the three and two detectors respectively exposed (Fig. 1), which is done in accordance with Table II.

The individual errors quoted and the overall reproducibility have been accounted for when inferring errors on the mean ratios.

<sup>3</sup> Radial gradients are kept within reasonable limits, even for so close a geometry, by the choice of detector diameters smaller than 80% of source diameters.

TABLE I. NEUTRONIC REPRODUCIBILITY OF THE SOURCE-DETECTOR ASSEMBLIES

Source sets (see text)	Fission source $^{235}\text{U}$		Fission source $^{239}\text{Pu}$	
	Irradiation number	$\frac{115_{\text{In}}(n,n')^{115\text{m}}_{\text{In}}}{197_{\text{Au}}(n,\gamma)^{198}_{\text{Au}}}$ (a)	Irradiation number	$\frac{115_{\text{In}}(n,n')^{115\text{m}}_{\text{In}}}{197_{\text{Au}}(n,\gamma)^{198}_{\text{Au}}}$ (a)
A	1	$1.19, -4$ $\pm 1\%$	2	$1.76, -4$ $\pm 2\%$
B	3	$1.18, -4$ $\pm 1.5\%$	4	$1.78, -4$ $\pm 1.5\%$
A	5	$1.17, -4$ $\pm 1\%$	6	$1.80, -4$ $\pm 1\%$
B	7	$1.21, -4$ $\pm 1.5\%$	8	$1.77, -4$ $\pm 1\%$

(a) Ratio of activation rates of the indium detectors and the gold thermal neutron flux monitors (Fig. 1).

TABLE II. HOMOGENEITY OF THE SOURCE-DETECTOR ASSEMBLIES WITH RESPECT TO FLUX SPECTRUM GRADIENTS

REACTION	REACTION RATE RATIO (a)		
	UPPER/LOWER		
$^{115}\text{In}(n,n')^{115\text{m}}\text{In}$ $^{103}\text{Rh}(n,n')^{103\text{m}}\text{Rh}$ $^{27}\text{Al}(n,p)^{27}\text{Mg}$ $^{197}\text{Au}(n,\gamma)^{198}\text{Au}$ (c)	Fission source $^{235}\text{U}$	Fission source $^{239}\text{Pu}$	Expected from pure geometrical considerations
	0.998( $\pm 0.8\%$ )	0.998( $\pm 1\%$ )	1.000
	0.992( $\pm 1\%$ )	1.000( $\pm 1\%$ )	
	1.000 (b)	1.020( $\pm 3\%$ )	
	1.000( $\pm 1\%$ )	1.009( $\pm 1\%$ )	
REACTION RATE RATIO (a) AVERAGE(UPPER, LOWER)/CENTRE			
$^{103}\text{Rh}(n,n')^{103\text{m}}\text{Rh}$	Fission source $^{235}\text{U}$	Fission source $^{239}\text{Pu}$	Expected from pure geometrical considerations
	1.035( $\pm 1\%$ )	1.036( $\pm 1.5\%$ )	1.006

(a) See Fig. 1.

(b) Normalization.

(c) Ge(Li) measurements of the  $\gamma$  activities of the  $^{235}\text{U}$  fission discs ( $^{143}\text{Ce}$  and  $^{133}\text{I}$ ) also establish the real symmetry of the sources.

TABLE III. RELATIVE REACTION RATE RATIOS FOR  $^{235}\text{U}$  AND  $^{239}\text{Pu}$  THERMAL FISSION NEUTRON SPECTRA<sup>a</sup>

Fission source $^{235}\text{U}$					
Irradiation number	$\frac{^{27}\text{Al}(n,\alpha)^{24}\text{Na}}{^{115}\text{In}(n,n')}$	$\frac{^{27}\text{Al}(n,p)^{27}\text{Mg}}{^{115}\text{In}(n,n')}$		$\frac{^{103}\text{Rh}(n,n')^{103m}\text{Rh}}{^{115}\text{In}(n,n')}$	$\frac{^{27}\text{Al}(n,\alpha)^{24}\text{Na}}{^{27}\text{Al}(n,p)^{27}\text{Mg}}$ <sup>b</sup>
		$\gamma$ -counting	$\beta$ -counting		
1	$0.0364 \pm 2\%$	$0.0530 \pm 3\%$	$0.245 \pm 2\%$	$0.0606 \pm 1\%$	$0.149 \pm 3\%$
3	$0.0375 \pm 3\%$	$0.0525 \pm 6\%$	$0.244 \pm 2\%$	$0.0594 \pm 1\%$	$0.153 \pm 3.5\%$
5	$0.0353 \pm 3\%$	$0.0534 \pm 3\%$	$0.236 \pm 2\%$	$0.0604 \pm 1\%$	$0.150 \pm 3\%$
7	$0.0345 \pm 3\%$	$0.0510 \pm 3\%$	$0.239 \pm 2\%$	c	$0.144 \pm 3.5\%$
Mean	$0.0360 \pm 3\%$	$0.0525 \pm 3\%$	$0.241 \pm 2\%$	$0.0601 \pm 1\%$	$0.149 \pm 2\%$
Fission source $^{239}\text{Pu}$					
2	$0.0432 \pm 2\%$	$0.0568 \pm 3\%$	$0.276 \pm 5\%$	$0.0635 \pm 2\%$	$0.156 \pm 5\%$
4	$0.0419 \pm 3\%$	$0.0592 \pm 5\%$	$0.266 \pm 2\%$	$0.0640 \pm 1\%$	$0.157 \pm 3.5\%$
6	$0.0418 \pm 2\%$	$0.0549 \pm 4\%$	$0.264 \pm 2\%$	$0.0626 \pm 1\%$	$0.158 \pm 3\%$
8	$0.0422 \pm 2\%$	$0.0564 \pm 3\%$	$0.264 \pm 2\%$	c	$0.160 \pm 3\%$
Mean	$0.0423 \pm 2\%$	$0.0568 \pm 3.5\%$	$0.265 \pm 2\%$	$0.0633 \pm 1\%$	$0.158 \pm 1.5\%$

<sup>a</sup> See Fig. 1 and text.<sup>b</sup> Only  $\beta$ -counting data, see text.<sup>c</sup> X-ray spectrometer out of use at time of irradiation.

The definite increase of the rhodium over indium ratio when substituting  $^{239}\text{Pu}$  fission sources to  $^{235}\text{U}$  ones is totally unexpected and not understood so far; this ratio should be largely insensitive to the spectrum changes involved here.

The final double ratios most relevant to the intercomparison of the two fission neutron spectra are summarized in the second column of Table IV. For the unique case where a direct comparison with other integral measurements is possible, i.e. column 3, a rather good agreement is obtained within error bands.

The last two columns of Table IV allow a comparison between the present data and the values expected from the interpretation of the conflicting average energy ratios selected for consideration. This interpretation is done as follows: assuming a Maxwellian representation of fission neutron spectra for the consistency of the comparison, the double ratios  $\bar{\sigma}_i(\bar{E})/\bar{\sigma}_j(\bar{E})/\bar{\sigma}_i(\bar{E}_0)/\bar{\sigma}_j(\bar{E}_0)$  are computed as a function of the single parameter  $\bar{E}$  of the representation.  $\bar{E}_0$  is the average energy of the  $^{235}\text{U}$  thermal fission neutron spectrum for which an arbitrary realistic value is taken. The curve resulting for a given combination  $i, j$  is then interpolated at  $\bar{E}^* = (1.039 \pm 0.002) \bar{E}_0$  and  $(1.075 \pm 0.02) \bar{E}_0$ . The corresponding values and spreads of  $\bar{\sigma}_i(\bar{E}^*)/\bar{\sigma}_j(\bar{E}^*)/\bar{\sigma}_i(\bar{E}_0)/\bar{\sigma}_j(\bar{E}_0)$  are reported in columns 4 and 5 of the table.



TABLE IV. CROSS-SECTION RATIOS  $(\bar{\sigma}_i/\bar{\sigma}_j)_{x_{29}}/(\bar{\sigma}_i/\bar{\sigma}_j)_{x_{25}}$ 

(a) Detector combination i/j	Measurement		Implicated by integral data of reference (9) (b)	Implicated by differential data of reference (8) (b)
	This work	Literature (9) (16)		
$\frac{^{27}\text{Al}(n,p)^{27}\text{Mg}}{^{115}\text{In}(n,n')^{115\text{m}}\text{In}}$	$1.09 \pm 0.02^{(c)}$	--	$1.093 \pm 0.005$	$1.18 \pm 0.05$
$\frac{^{27}\text{Al}(n,\alpha)^{24}\text{Na}}{^{115}\text{In}(n,n')^{115\text{m}}\text{In}}$	$1.17 \pm 0.04$	--	$1.187 \pm 0.008$	$1.36 \pm 0.10$
$\frac{^{27}\text{Al}(n,\alpha)^{24}\text{Na}}{^{27}\text{Al}(n,p)^{27}\text{Mg}}$	$1.060 \pm 0.026$	$1.075 \pm 0.013$	$1.086 \pm 0.004$	$1.16 \pm 0.045$
$\frac{^{27}\text{Al}(n,\alpha)^{24}\text{Na}}{^{103}\text{Rh}(n,n')^{103\text{m}}\text{Rh}}$	$1.11 \pm 0.05$	--	$1.198 \pm 0.009$	$1.38 \pm 0.10$

(a) Detector with highest energy response always in numerator.

(b) See text.

(c) Weighted average between double ratios derived from  $\beta$  and  $\gamma$  measurements quoted in table III, i.e. respectively  $1.10 \pm 0.03$  and  $1.08 \pm 0.05$ .

The cross-section ratios measured so far are inconsistent with the implications of differential measurements and tend to support the previous independent integral studies.

#### ACKNOWLEDGEMENTS

The author is indebted to his colleagues M. Decoster and S. DeLeeuw for fruitful discussions during this experiment; he also thanks J.A. Grundl, of the National Bureau of Standards, for his pertinent advice, encouragement and criticism when writing this paper. He has appreciated the technical support of D. Langela and R. Sour for calculations and measurements likewise the help provided by F. Camps and R. Mermans in relation to the source-detector assembly. The flexibility displayed by the BR1 operation staff has allowed to complete the measurements under an optimum time schedule.

#### REFERENCES

- [1] GRUNDL, J.A., "Fission-neutron spectra: macroscopic and integral results", Neutron Standards and Flux Normalization, AEC Symposium Series 23 (1971).
- [2] SMITH, A.B., Some Remarks on Prompt-Fission-Neutron-Spectra, Rep. EANDC-147/A (1970).
- [3] McELROY, W.N., Implications of recent fission-average cross section measurements, Nucl. Sci. Engng 36 (1969) 109.
- [4] TERRELL, J., Fission neutron spectra and nuclear temperatures, Phys. Rev. 113 (1959) 527; Neutron yields from individual fission fragments, Phys. Rev. 127 (1962) 880.
- [5] CONDE, H., DURING, G., HANSEN, J., Fission neutron spectra, Ark. Fys. 29 (1966) 307.
- [6] BARNARD, E., FERGUSON, A.T.G., McMURRAY, W.R., VAN HEERDEN, I.J., Time-of-flight measurements of neutron spectra from the fission of  $^{235}\text{U}$ ,  $^{238}\text{U}$  and  $^{239}\text{Pu}$ , Nucl. Phys. 71 (1965) 228.
- [7] BELOV, L.M., BLINOV, M.V., KAZARINOV, N.M., KRIVOKHATSKIJ, A.S., PROTOPOPOV, A.M., Spectra of fission neutrons of  $^{244}\text{Cm}$ ,  $^{242}\text{Pu}$  and  $^{239}\text{Pu}$ , Soviet J. Nucl. Phys. 9 4 (1969) 421.
- [8] SMITH, A.B., Note on the prompt-fission neutron spectra of uranium-235 and plutonium-239, Nucl. Sci. Engng 44 (1971) 439.
- [9] GRUNDL, J.A., A study of fission-neutron spectra with high-energy activation detectors, Part II: Fission spectra, Nucl. Sci. Engng 31 (1968) 191 - 206.
- [10] KOVALEV, V.P., ANDREEV, V.N., NIKOLAEV, M.N., GUSEINOV, A.G., Comparison of neutron spectra in the fission of U233, U235, Pu239, Sov. Phys. JETP 6 (1958) 825.
- [11] BONNER, T.W., Measurements of neutron spectra from fission, Nucl. Phys. 23 (1961) 116.
- [12] GRUNDL, J.A., USNER, A., Spectral comparisons with high energy activation detectors, Nucl. Sci. Engng 8 (1960) 598.
- [13] FABRY, A., Test of the uranium-235 thermal fission spectrum representations by means of activation detectors, Nukleonik 10 (1967) 280.
- [14] FABRY, A., VANDEPLAS, P., "The generation of intermediate standard neutron spectra and their application in fast reactor physics", Fast Reactor Physics (Proc. Symp. Karlsruhe, 1967) 1, IAEA, Vienna (1968) 389.
- [15] FABRY, A., DECOSTER, M., MINSART, G., SCHEPERS, J.C., VANDEPLAS, P., "Implications of fundamental integral measurements of high energy nuclear data for reactor physics", Nuclear Data for Reactors (Proc. Conf. Helsinki, 1970) 2, IAEA, Vienna (1970) 535.
- [16] GRUNDL, J.A., private communication, 1971.

# MEASUREMENT OF THE AVERAGE FISSION CROSS-SECTION RATIO, $\bar{\sigma}_f(^{235}\text{U})/\bar{\sigma}_f(^{238}\text{U})$ FOR $^{235}\text{U}$ AND $^{239}\text{Pu}$ FISSION NEUTRONS

J. A. GRUNDL  
National Bureau of Standards,  
Washington, D.C.,  
United States of America

## Abstract

MEASUREMENT OF THE AVERAGE FISSION CROSS-SECTION RATIO,  $\bar{\sigma}_f(^{235}\text{U})/\bar{\sigma}_f(^{238}\text{U})$ , FOR  $^{235}\text{U}$  AND  $^{239}\text{Pu}$  FISSION NEUTRONS.

Average fission cross-section ratios,  $\bar{\sigma}_f(^{235}\text{U})/\bar{\sigma}_f(^{238}\text{U})$ , have been measured for  $^{235}\text{U}$  and  $^{239}\text{Pu}$  fission neutrons. A cavity fission source, a fission ionization chamber, and a redundant determination of fission foil weight ratios were employed for the measurements. The result for  $^{235}\text{U}$  fission neutrons is  $3.71 \pm 0.17$ , a value that confirms earlier integral microscopic results and is 12 to 20% discrepant with predictions based on differential microscopic data. The observed ratio of average cross-section ratios,  $\chi_{49}/\chi_{25}$ , is  $0.970 \pm 0.012$ . This value represents a departure from unity that is less than one-half of that predicted by differential microscopic data. The measurements described remain in progress.

Long-standing and basic integral detector measurements with fission spectrum neutrons remain discrepant with predictions based on differential data [1,2,3]. This paper presents an informal report of experiments in progress which substantiate the integral detector results. Average fission cross section ratios,  $\bar{\sigma}_f(^{235}\text{U})/\bar{\sigma}_f(^{238}\text{U})$ , were measured for  $^{235}\text{U}$  and  $^{239}\text{Pu}$  fission neutrons with a fission ionization chamber and a cavity fission source.

## THE EXPERIMENT

The cavity fission neutron source operates at the center of a cubic cavity 30 cm on a side within the thermal column of the NBS Research Reactor. At the cavity center, fission source disks of  $^{235}\text{U}$  or  $^{239}\text{Pu}$  metal (15.9 mm diam. and  $\sim 0.1$  mm thick) are mounted on a light-weight aluminum capsule which is the housing for the fission chamber. The fission foil, mounted at the mid-plane of the fission chamber is a 12.7 mm diameter uranium oxide deposit on a 0.13 mm thick polished platinum disk. It is coaxial with the fission source disk and at a separation distance of 3.8 mm. In this tight geometry the flux gradient is 4% per 0.1 mm and source-detector assembly procedures must be kept strictly consistent; dimensions of the assembly are checked to  $\pm 0.02$  mm during changes of the source disk or the fission chamber foil.

The fission ionization chamber is of conventional design with the ion collectors subtending about 90% of the  $2\pi$  solid angle into which the fission fragments are emitted. The performance of the chamber may be described in terms of  $v_\alpha$  the maximum output pulse height for natural alpha particles. For the  $200 \mu\text{g}/\text{cm}^2$  uranium fission foils used in these measurements the valley between the maximum of the alpha pulse height distribution and the minimum of the fission fragment distribution extends from  $v_\alpha$

to  $4v$ , and the peak-to-valley ratio is 25. The fraction of the pulses between  $v$  and  $2v$  is 0.6%, an indication of the correction necessary to derive absolute fission rates from biased fission counting. Fission pulses are observed with a triple scaler arrangement which provides easily observable checks for noise and gain shifts.

The two fission foils employed for these measurements were oxide deposits of 99.7% enriched  $^{235}\text{U}$  and normal uranium. Foil weight ratios were determined by two independent methods: (a) fission counting in a thermal beam; and (b)  $2\pi$  alpha counting. The first method, based on the isotopic concentration of  $^{235}\text{U}$  in normal uranium, gave a uranium weight ratio of 1.068; the second method, based on the conventional alpha disintegration rate for normal uranium and the absolute disintegration rate determined by Smith and Balagna [4] for the  $^{235}\text{U}$  material, gave a uranium weight ratio of  $1.074$ . These determinations are regarded now as accurate to better than 3%.

Fission rates were observed in four basic arrangements: the  $^{235}\text{U}$  and normal uranium fission foils exposed separately to the  $^{235}\text{U}$  and  $^{239}\text{Pu}$  fission sources. A  $^{235}\text{U}$  fission rate was also obtained without a fission source disk. Run to run thermal neutron flux levels in the cavity were monitored with a commercial  $^{235}\text{U}$  fission chamber exposed to a beam taken off the front face of the thermal column. A triple scaler arrangement was also used to record pulses from this monitor chamber. Reproducibility of observed fission rates under identical conditions was better than 0.5%; for fission rate ratios, a spread of 1% appeared in the observed values.

## RESULTS

Two results are to be distinguished for this experiment: (a) an average fission cross section ratio for  $^{235}\text{U}$  fission neutrons, a benchmark for differential data; and (b) the ratio of cross section ratios for  $^{235}\text{U}$  and  $^{239}\text{Pu}$  fission neutrons, a basic ingredient in the discrepancy between differential and integral measurements. At present these two results are:

- (a)  $^{235}\text{U}/^{238}\text{U}$  fission cross section ratio for  $^{235}\text{U}$  fission neutrons

$$R_{5/8} = \frac{\bar{\sigma}_f(^{235}\text{U}, x_{25})}{\bar{\sigma}_f(^{238}\text{U}, x_{25})} = 3.71 \pm 0.17;$$

- (b) Ratio of cross section ratios between  $^{235}\text{U}$  and  $^{239}\text{Pu}$  fission neutrons

$$\frac{R_{5/8}(x_{49})}{R_{5/8}(x_{25})} = 0.970 \pm 0.012.$$

A list of contributing errors for each part of the measurement provides an insight into the experimental problems involved in these reaction rate measurements.

Error Source	(a) Cross Section Ratio	(b) Ratio of Ratios
counting statistics:	$\pm 0.3\%$	$\pm 0.4\%$
thermal column monitor		
stability:	0.6%	0.6%
source-detector		
position:	2%	0.7%
cavity position:	1.2%	0.5%
reactor background:	2%	0.6%
cavity return		
background:	2.5%	-
relative detector		
efficiency:	0.3%	-
intrinsic source-		
detector scattering:	1.5%	-
foil weight ratio:	2%	-
rms sum:	$\pm 4.7\%$	$\pm 1.3\%$

Most of the partial errors greater than 1% reflect the limited effort put into this measurement thus far. Within existing capabilities they can be reduced to the 1% level and below.

It is appropriate to mention the question of cavity return since this problem often leads to misgivings regarding the reliability of cavity fission spectrum measurements in general. The return flux of fission source neutrons from the graphite surrounding the cube-shaped cavity (30 cm on a side) gives rise to a fission detector background response which must be computed. A useful estimate of this return flux can be obtained from elementary diffusion theory. The latter gives a value of 0.75 for the reflection coefficient or albedo of a 34 cm diameter spherical void in graphite. The mean distance between the fission detector and the fission source is 0.64 cm in this experiment. Thus, the fraction of the flux at the detector which has been scattered back from the graphite is  $[(0.75 + 0.75^2 + 0.75^3 + \dots)(0.64/17)^2]$  or about 0.4%. This crude estimate is within a factor of two of the results obtained from multigroup neutron transport and Monte-Carlo computations [2,5]. Sixteen-group DSN transport calculations for example give a fission-neutron-return flux background of 0.80%. The transport calculations also have been checked against measured fission neutron flux traverses in a cavity [6]. Since the average fission cross section for  $^{238}\text{U}$  in the degraded return spectrum is only 30% of its value for pure fission neutrons, the return background for  $^{238}\text{U}$  is 0.24%. For  $^{235}\text{U}$  the average cross section for the return spectrum is a factor of 7.2 higher and the fission neutron return background is 5.7%.

#### CONCLUSIONS

Two other measured values for  $R_{5/8}$  are available. One was obtained by means of fission foil activation calibrated with monoenergetic neutron [2,7] and the other by means of fission track detectors calibrated in a

thermal neutron beam [3,6]. Independently measured values for  $R_{5/8}$  then are the present work,

$$(1) \quad R_{5/8} = 3.71 \pm 0.17 \quad (\text{fission ionization chamber, 34 cm diam. cavity})$$

and the previous measurements,

$$(2) \quad R_{5/8} = 3.78 \pm 0.18 \quad (\text{fission track recorders, 50 cm diam. cavity})$$

$$(3) \quad R_{5/8} = 3.85 \pm 0.23 \quad (\text{fission foil activation, 10 cm diam. cavity}).$$

Predicted values for  $R_{5/8}$  have a considerable range because of an accumulation of fission cross section and fission spectrum measurements. If one accepts the constraint on the  $^{235}\text{U}$  and  $^{238}\text{U}$  fission cross sections provided by the ratio measurements of Stein [8] and includes the  $^{235}\text{U}$  fission cross section results of White [9] and also the corrected Los Alamos counter telescope data for  $^{235}\text{U}$  [10], a predicted ratio of  $R_{5/8} = 4.5 \pm 0.2$  is obtained using the conventional Maxwellian description of the  $^{235}\text{U}$  fission spectrum. Other selections of fission spectrum shape, or cross sections that still take cognizance of relative measurements, may lower the predicted ratio to 4.2. Thus, a 10 to 20% disagreement exists between integral measurement and the predictions based on differential data. And this disagreement becomes worse if the cavity return background has been underestimated as is often suspected. Fission cross section evaluations and the results of other relevant integral measurements are given in References [1, 7, and 10]; interpretation and critical discussion of integral fission spectrum measurements may be found in References [3, and 11 through 14].

Predictions for the double ratio value above,  $0.97 \pm 0.012$ , which compares  $^{235}\text{U}$  and  $^{239}\text{Pu}$  fission spectra, may be obtained from differential spectrometer measurements of the two spectra [15-17], and from other integral measurements that have sampled the two spectra with various threshold activation detectors [2,3]:

$$\frac{R_{5/8}(X_{49})}{R_{5/8}(X_{25})} = 0.92 \pm 0.02 \quad \text{differential spectrometry}$$

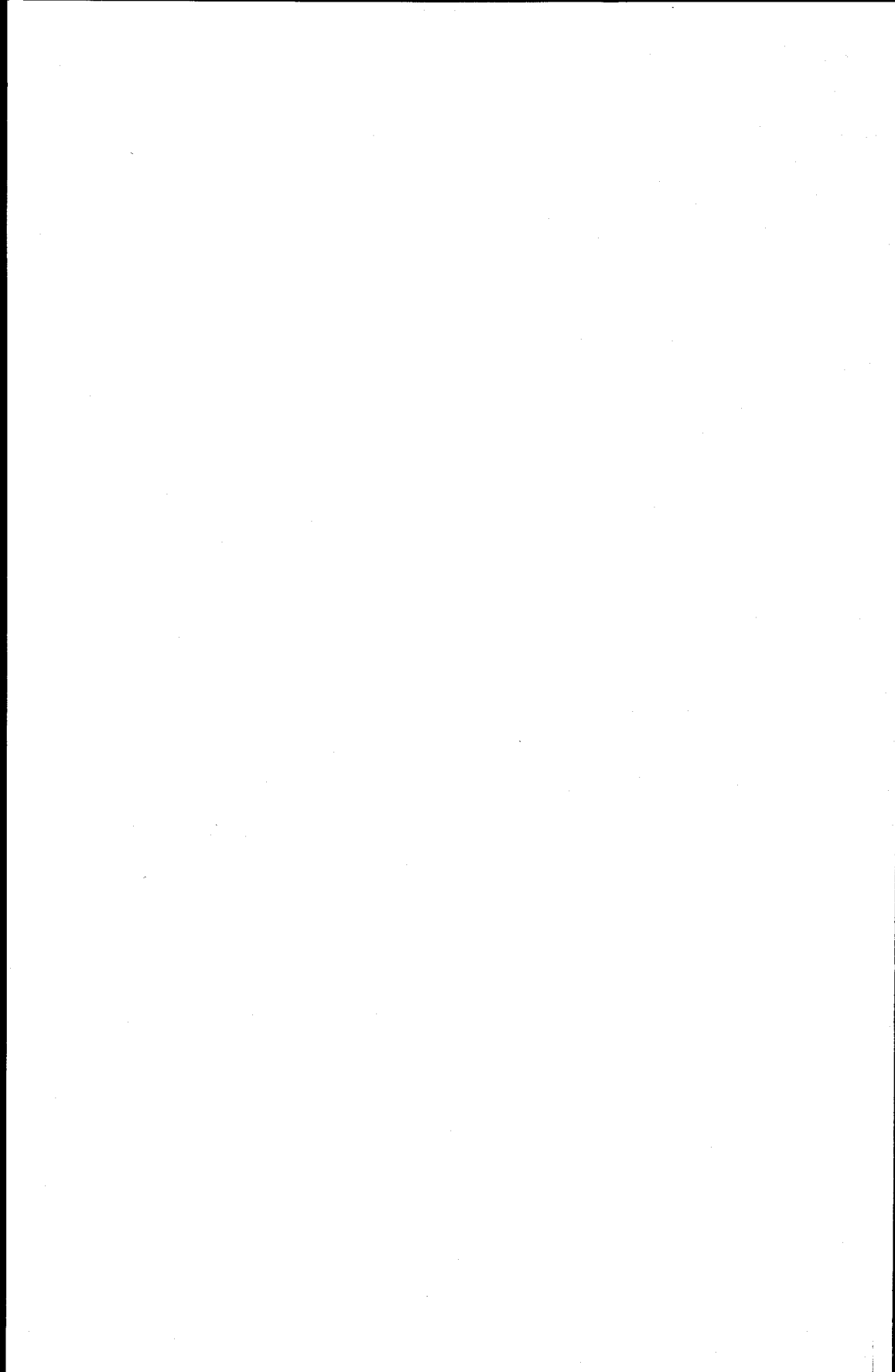
$$\frac{R_{5/8}(X_{49})}{R_{5/8}(X_{25})} = 0.96, \pm 0.005 \quad \text{integral detectors}$$

It is apparent that the differential data predict a departure from unity for the ratio of  $R_{5/8}$  values which is more than twice that observed in this and other integral measurements. On the face of it this discrepancy is not very large. However, since cross section uncertainties are not significant for the integral detector results and equivalently, detector efficiency problems are not important for the time-of-flight differential results, the disagreement is a firm one.

#### REFERENCES

- [1] GRUNDL, J. A., Fission-Neutron Spectra: Macroscopic and Integral Results, in "Neutron Standards and Flux Normalization", Proceedings of a Symposium, Argonne, Illinois, CONF-701002 (1970).

- [2] GRUNDL, J. A., A Study of Fission-Neutron Spectra With High-Energy Activation Detectors--Part II, Fission Spectra, Nucl. Sci. Engng. 31 (1968) 191.
- [3] FABRY, A., DE COSTER, MINSART, G., SHEPERS, J. C., VANDEPLAS, P., Implications of Fundamental Integral Measurements on High-Energy Nuclear Data for Reactor Physics, in "Nuclear Data for Reactors", Conf. Proceedings, Helsinki (1970).
- [4] SMITH, H. L., BALAGNA, J. P., A Method of Assay of  $^{235}\text{U}$ ,  $^{238}\text{U}$  and  $^{237}\text{Np}$  Fission Foils, in Conf. on "Neutron Cross Sections and Technology", Washington, D.C., (1966).
- [5] GRUNDL, J. A., Cavity Fission Spectra, Trans. Am. Nucl. Sci. 5 (1962) 381.
- [6] FABRY, A., Nukleonik 10 (1967) 280. FABRY, A. and VANDEPLAS, P., Standard Neutron Spectra for the Fast Energy Range, Progress Rep. at the Euratom Dosimetry Working Group, Brussels-June (1967).
- [7] GRUNDL, J. A., Nucl. Sci. Engng. 30 (1967) 39.
- [8] STEIN, W. E., SMITH, R. K., GRUNDL, J. A., Relative Fission Cross Sections of  $^{238}\text{U}$ ,  $^{237}\text{Np}$ , and  $^{235}\text{U}$ , in Conf. on "Neutron Cross Sections and Technology, Washington, D.C. (1966).
- [9] WHITE, P. H., J. Nucl. Energy 19 (1965) 325.
- [10] DAVEY, W. G., Selected Fission Cross Sections for  $^{232}\text{Th}$ ,  $^{233}\text{U}$ ,  $^{234}\text{U}$ ,  $^{235}\text{U}$ ,  $^{236}\text{U}$ ,  $^{237}\text{Np}$ ,  $^{238}\text{U}$ ,  $^{240}\text{Pu}$  and  $^{242}\text{Pu}$ , Nucl. Sci. Engng. 32 (1968) 35-45.
- [11] CAMPBELL, C. G., ROWLANDS, J. L., The Energy Spectrum of Prompt Fission Neutrons, 14th EACRP Meeting, Stockholm (1971).
- [12] SMITH, A. B., Note on Prompt Fission Neutron Spectra of  $^{235}\text{U}$  and  $^{239}\text{Pu}$ , EANDC(US)-153L (1970).
- [13] LUBITZ, C. R., STEWART, L., Remarks on the Neutron-Induced Fission Spectrum, EANDC(US)-139L.
- [14] McELROY, W. N., Implications of Recent Fission-Averaged Cross-Section Measurements, Nucl. Sci. Engng. 36 (1969) 109.
- [15] BARNARD, E., FERGUSON, A. T. G., McMURRAY, W. R., VAN HEERDEN, I. J., Nucl. Phys. 71 (1965) 228.
- [16] CONDÉ, H., DURING, G., HANSEN, J., Ark. Fys. 29 (1966) 307.
- [17] SMITH, A. B., Nucl. Sci. Engng. 44 (1971) 439.





# INTEGRAL CHECK OF THE FISSION NEUTRON SPECTRUM THROUGH AVERAGE CROSS-SECTIONS FOR SOME THRESHOLD REACTIONS

I. KIMURA, K. KOBAYASHI, T. SHIBATA

Research Reactor Institute,  
Kyoto University,  
Osaka, Japan

## Abstract

INTEGRAL CHECK OF THE FISSION NEUTRON SPECTRUM THROUGH AVERAGE CROSS-SECTIONS FOR SOME THRESHOLD REACTIONS.

Average cross-sections for some threshold reactions were measured in the core of the Kyoto University Reactor (KUR) and with a fission plate of enriched uranium. Making use of these results and energy-dependent cross-section data, an integral check of the fission neutron spectrum was carried out. The results support the authenticity of the forms given by earlier workers.

## 1. INTRODUCTION

Precise knowledge of cross-sections for threshold reactions is required not only from the standpoints of using them as fast neutron detectors in reactors; of the evaluation of radiation effects, such as swelling of reactor materials, by helium or hydrogen gas produced by these reactions; and of the calculation of the fuel cycle in detail, but also from that of the integral examination of neutron energy spectra, especially of fission neutrons.

In more recent years the expression of the fission neutron spectrum has become the subject of discussion [1-4]. It has been pointed out in particular that the shape of the fission neutron spectrum obtained with threshold detectors exhibits significant deviation from the earlier data [5-9], as shown in Fig. 1. While Bresesti et al. [10] concluded that the Watt spectrum [5] is the most appropriate representation of the  $^{235}\text{U}$  fission spectrum for the threshold foils that they considered, very recently Smith confirmed that the fission spectrum is reasonably consistent with the earlier data [11]. Thus from the standpoint of reactor design it is most essential to settle this problem definitely.

The present paper discusses from this point of view the results of our measurements of average cross-sections for some threshold reactions, most of which have been already reported [12-14] and the rest will be published soon, although they provide only an indirect integral check of the problem.

## 2. EXPERIMENTAL

Average cross-sections for threshold reactions were measured in the core of the KUR (Kyoto University Reactor, 5 MW, 90 ~ 93% enriched uranium-fuelled and light water moderated) and with a fission plate of 90% enriched uranium set at the thermal neutron facility of the KUR.

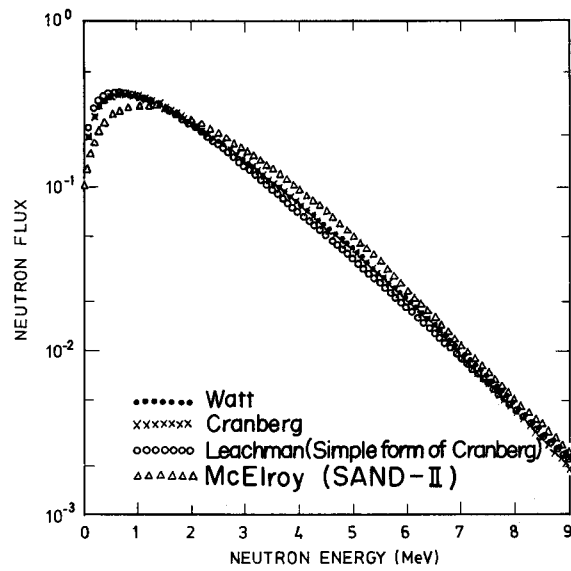
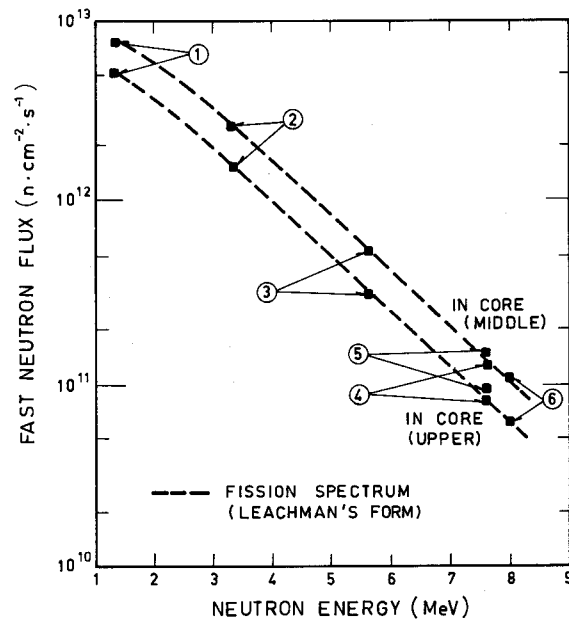


FIG.1. Four representations of the fission neutron spectrum.

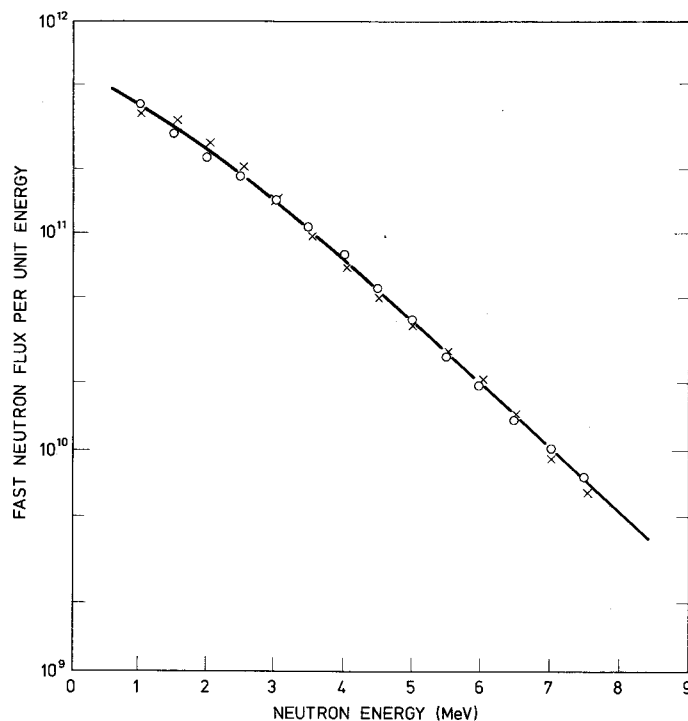


- |   |  |
|---|--|
| ①: $^{103}\text{Rh}(n, n')^{103m}\text{Rh}$ | ②: $^{58}\text{Ni}(n, p)^{58}\text{Co}$      |
| ③: $^{27}\text{Al}(n, p)^{27}\text{Mg}$     | ④: $^{24}\text{Mg}(n, p)^{24}\text{Na}$      |
| ⑤: $^{56}\text{Fe}(n, p)^{56}\text{Mn}$     | ⑥: $^{27}\text{Al}(n, \alpha)^{24}\text{Na}$ |

FIG.2. Integral flux of fast neutrons in the KUR core above the effective threshold energy, measured with threshold reactions.

The energy spectrum of fast neutrons above about 1 MeV in the core was found to be close to that of fission neutrons, as seen in Figs 2 - 4. The details are given in a previous paper [13].

The sample foils were fixed by adhesive tape on to an aluminium holder (middle position) inserted into the fuel element, as shown in Fig. 5. The  $^{58}\text{Ni}(n,p)^{58}\text{Co}$ ,  $^{24}\text{Mg}(n,p)^{24}\text{Na}$  and  $^{27}\text{Al}(n,\alpha)^{24}\text{Na}$  reactions were used for fast neutron flux monitoring during the irradiation of the samples. To obtain the average cross-sections for these reactions, calculations were performed by Hughes' method [15] with the Maxwellian fission neutron spectrum given by Leachman and the energy-dependent cross-sections taken from EUR-119e [16] to give the values in Table I. Fast neutron fluxes for the core and



ooo: Spectral analysis by  $^{103}\text{Rh}(n,n')^{103\text{m}}\text{Rh}$ ,  
 $^{115}\text{In}(n,n')^{115\text{m}}\text{In}$ ,  $^{58}\text{Ni}(n,p)^{58}\text{Co}$ ,  $^{27}\text{Al}(n,p)^{27}\text{Mg}$ ,  
 $^{24}\text{Mg}(n,p)^{24}\text{Na}$ ,  $^{56}\text{Fe}(n,p)^{56}\text{Mn}$  and  $^{27}\text{Al}(n,\alpha)^{24}\text{Na}$

xxx: Spectral analysis by  $^{103}\text{Rh}(n,n')^{103\text{m}}\text{Rh}$ ,  
 $^{115}\text{In}(n,n')^{115\text{m}}\text{In}$ ,  $^{58}\text{Ni}(n,p)^{58}\text{Co}$ ,  $^{27}\text{Al}(n,p)^{27}\text{Mg}$ ,  
 $^{24}\text{Mg}(n,p)^{24}\text{Na}$  and  $^{27}\text{Al}(n,\alpha)^{24}\text{Na}$

—: Fission spectrum (Leachman's form)

FIG. 3. Fast neutron spectrum in the KUR core obtained by the associated Laguerre expansion method.

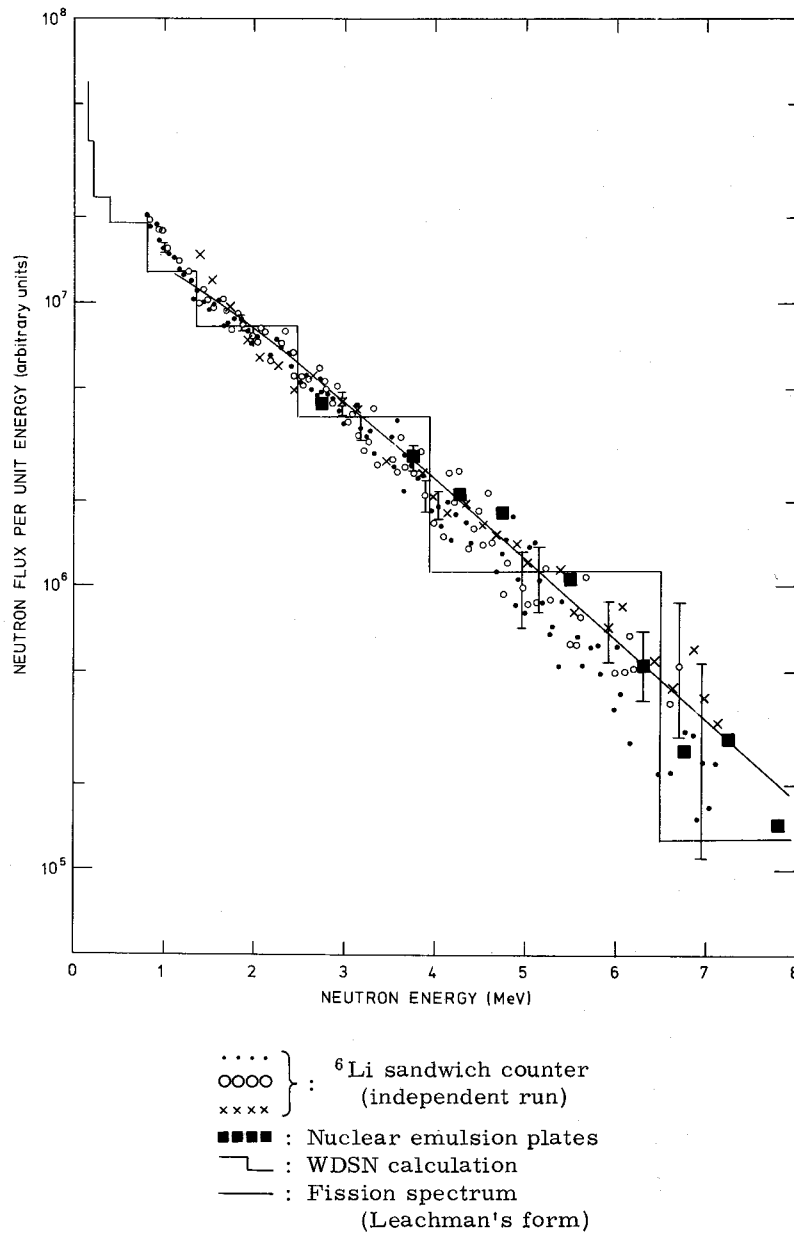


FIG.4. Fast neutron spectrum in the core of the KUR.

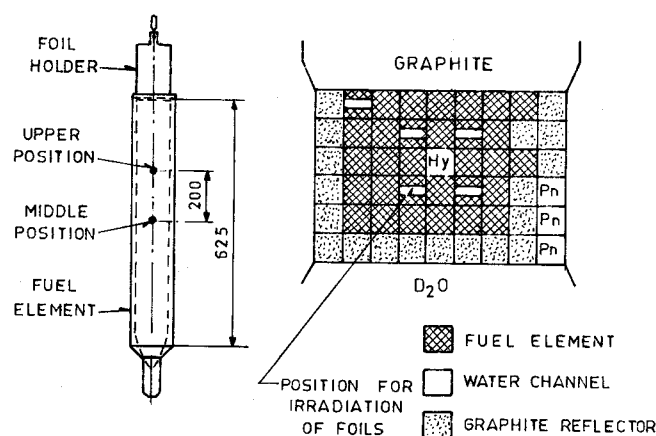


FIG. 5. Positions of foil irradiation in the KUR core.

TABLE I. NUCLEAR DATA FOR THRESHOLD REACTIONS SELECTED AS MONITORING DETECTORS

Reaction	Half-life of product	Average cross-section <sup>a</sup> (mb)	Detector and measured gamma ray
$^{58}\text{Ni}(n, p)^{58}\text{Co}$	71.3 d	104	1.5 in. NaI(Tl) and Ge(Li), 810 keV
$^{24}\text{Mg}(n, p)^{24}\text{Na}$	15 h	1.4	1.5 in. NaI(Tl) and Ge(Li), 1.37 MeV
$^{27}\text{Al}(n, \alpha)^{24}\text{Na}$	15 h	0.63	1.5 in. NaI(Tl) and Ge(Li), 1.37 MeV

<sup>a</sup> Present values calculated by 'Hughes' method using cross-section data from EUR-119e [16] and Leachman's fission spectrum [8].

for the fission plate measured with the above reactions agreed within 2% and 3% respectively. If instead of Leachman's we take the SAND-II fission neutron spectrum, the average cross-sections mentioned above are larger by 35, 20 and 18% respectively.

The fission plate (31 cm diam., 10.44 mm total thickness) used was composed of 90% enriched uranium oxide dispersed into an aluminium matrix and clad with aluminium plate [17]. The total amount of  $^{235}\text{U}$  contained was 1002 grams. The fission plate was placed in the thermal neutron irradiation facility of the KUR [18], where pure Maxwellian neutrons thermalized through a 140-cm thick heavy-water layer were available. The fast neutron flux at the centre of the surface of the fission plate was about

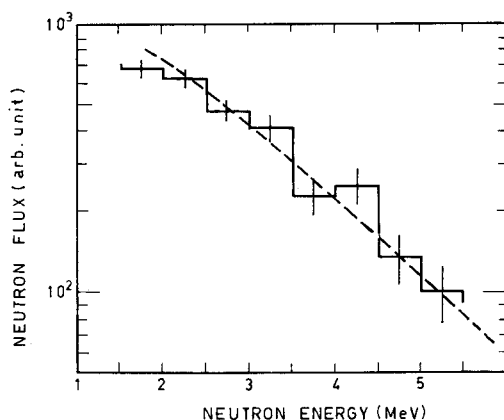


FIG. 6. Fast neutron spectrum obtained by nuclear emulsion plates (1000 tracks). The dotted line represents Leachman's fission spectrum.

$2.5 \times 10^9 \text{ n} \cdot \text{cm}^{-2} \cdot \text{s}^{-1}$  when the KUR was operating at its full power of 5 MW. The  $^{58}\text{Ni}(n, p)^{58}\text{Co}$ ,  $^{24}\text{Mg}(n, p)^{24}\text{Na}$  and  $^{27}\text{Al}(n, \alpha)^{24}\text{Na}$  reactions were also used for fast neutron flux monitoring. The fast neutron spectrum in front of the fission plate was measured with nuclear emulsion plates, Fuji ET-6B, 100  $\mu\text{m}$  thick. A preliminary result is given in Fig. 6.

The errors incurred in the course of the present work have been examined. These errors comprise (1) statistical errors, (2) errors deriving from the monitor flux, and (3) a systematic error. The amount of the second type of error, arising from dispersions occurring in each monitor flux, was found to be 2% for the core and 3% for the fission plate. As factors contributing to the systematic error we have considered the operating condition of the gamma-ray detector, the imprecision of the irradiation, waiting and counting, deviations in location between the samples and the monitor foils, changes in neutron flux during irradiation, errors in determining the weight of the foils, and so forth. The value of 5% attributed to the systematic error has usually been determined from the results of the above error analysis and from the results of several independent measurements.

### 3. RESULTS AND DISCUSSIONS

#### 3.1. $^{46}\text{Ti}(n, p)^{46}\text{Sc}$ , $^{47}\text{Ti}(n, p)^{47}\text{Sc}$ and $^{48}\text{Ti}(n, p)^{48}\text{Sc}$ [13]

As shown in Tables II - IV, the results for the core of the KUR and for the fission plate agree reasonably, but the data hardly allow any comment on the shape of the fission neutron spectrum.

TABLE II. COMPARISON OF FISSION AVERAGE CROSS-SECTIONS FOR THE  $^{46}\text{Ti}(n, p)^{46}\text{Sc}$  REACTION

Cross-section (mb)	Reference, given in Ref. [13]
$11.2 \pm 0.6_3$	Present (reactor)
$10.8 \pm 0.6_1$	Present (fission plate)
8.2	Mellish (reactor)
8.0	Roy (preferred)
10	Durham (reactor)
11.1	Comera (reactor)
$17 \pm 3$	Niese (reactor)
$9.0 \pm 0.1$	Hogg (reactor)
$12.8 \pm 0.6$	Boldeman (fission plate)
$12.6 \pm 0.4$	Köhler (reactor)
$10.2 \pm 0.4$	Bresesti (fission plate)

TABLE III. COMPARISON OF FISSION AVERAGE CROSS-SECTIONS FOR THE  $^{47}\text{Ti}(n, p)^{47}\text{Sc}$  REACTION

Cross-section (mb)	Reference, given in Ref. [13]
$19.0 \pm 1.2$	Present (reactor)
$17.3 \pm 0.9_0$	Present (fission plate)
0.42	Mellish (reactor)
18	Durham (reactor)
$18 \pm 3$	Niese (reactor)
$15 \pm 0.6$	Hogg (reactor)
$22 \pm 1.5$	Boldeman (fission plate)
$13.2 \pm 1.0$	Köhler (reactor)

TABLE IV. COMPARISON OF FISSION AVERAGE CROSS-SECTIONS FOR THE  $^{48}\text{Ti}(n, p)^{48}\text{Sc}$  REACTION

Cross-section (mb)	Reference, given in Ref. [13]
$0.29_4 \pm 0.02_3$	Present (reactor)
$0.27_2 \pm 0.05_2$	Present (fission plate)
0.15	Mellish (reactor)
0.53	Durham (reactor)
$0.44 \pm 0.08$	Niese (reactor)
$0.25 \pm 0.01$	Hogg (reactor)
$0.21 \pm 0.016$	Boldeman (fission plate)
$3.3 \pm 0.2$	Köhler (reactor)

3. 2.  $^{28}\text{Si}(n, p)^{28}\text{Al}$ ,  $^{29}\text{Si}(n, p)^{29}\text{Al}$  and  $^{30}\text{Si}(n, \alpha)^{27}\text{Mg}$  [13]

As shown in Tables V - VII, no comment can be made here either.

TABLE V. COMPARISON OF FISSION AVERAGE CROSS-SECTIONS FOR THE  $^{28}\text{Si}(n, p)^{28}\text{Al}$  REACTION

Cross-section (mb)	Reference, given in Ref. [13]
$4.9_0 \pm 0.3_2$	Present (reactor)
4.0	Roy (preferred)

TABLE VI. COMPARISON OF FISSION AVERAGE CROSS-SECTIONS FOR THE  $^{29}\text{Si}(n, p)^{29}\text{Al}$  REACTION

Cross-section (mb)	Reference, given in Ref. [13]
$2.9_8 \pm 0.1_7$	Present (reactor)
2.7	Roy (preferred)



TABLE VII. COMPARISON OF FISSION AVERAGE CROSS-SECTIONS FOR THE  $^{30}\text{Si}(n, \alpha)^{27}\text{Mg}$  REACTION

Cross-section (mb)	Reference, given in Ref. [13]
$0.13_0 \pm 0.02_0$	Present (reactor)
$0.15 \pm 0.02$	Niese (reactor)

3. 3.  $^{51}\text{V}(n, \alpha)^{48}\text{Sc}$ ,  $^{64}\text{Zn}(n, p)^{64}\text{Cu}$ ,  $^{92}\text{Mo}(n, p)^{92\text{m}}\text{Nb}$  and  $^{93}\text{Nb}(n, 2n)^{92\text{m}}\text{Nb}$  [13]

The results for these reactions are shown in Tables VIII-XI.

TABLE VIII. COMPARISON OF FISSION AVERAGE CROSS-SECTIONS FOR THE  $^{51}\text{V}(n, \alpha)^{48}\text{Sc}$  REACTION

Cross-section (mb)	Reference, given in Ref. [13]
$0.021_7 \pm 0.001_3$	Present (reactor)
0.08	Hughes (fission plate)
0.016	Saeland (reactor)
0.035	Roy (preferred)

TABLE IX. COMPARISON OF FISSION AVERAGE CROSS-SECTIONS FOR THE  $^{64}\text{Zn}(n, p)^{64}\text{Cu}$  REACTION

Cross-section (mb)	Reference, given in Ref. [13]
$35.5 \pm 2.8$	Present (reactor)
$37.4 \pm 3.0$	Present (fission plate)
44	Mellish (reactor)
39	Roy (preferred)
28	Passell (reactor)
31	Durham (reactor)
$27 \pm 1.6$	Boldeman (fission plate)
$26.9 \pm 1.2$	Rau (reactor)

TABLE X. COMPARISON OF FISSION AVERAGE CROSS-SECTIONS FOR THE  $^{92}\text{Mo}(n, p)^{92m}\text{Nb}$  REACTION

Cross-section (mb)	Reference, given in Ref. [13]
$6.0_0 \pm 0.4_3$	Present (reactor)
$6.0_4 \pm 0.4_5$	Present (fission plate)
1.3	Mellish (reactor)
2.6	Roy (preferred)
6.0	Hogg (reactor)
$6.2 \pm 0.4$	Boldeman (fission plate)
$6.74 \pm 0.27$	Rau (reactor)
$5.75 \pm 0.25$	Bresesti (fission plate)

TABLE XI. COMPARISON OF FISSION AVERAGE CROSS-SECTIONS FOR THE  $^{93}\text{Nb}(n, 2n)^{92m}\text{Nb}$  REACTION

Cross-section (mb)	Reference, given in Ref. [13]
$0.43_2 \pm 0.03_3$	Present (reactor)
$0.40_2 \pm 0.03_4$	Present (fission plate)
0.33	Fabry (reactor)

3. 4.  $^{204}\text{Pb}(n, n')^{204m}\text{Pb}$  and  $^{204}\text{Pb}(n, 2n)^{203}\text{Pb}$  [13]

The results for these reactions are shown in Tables XII and XIII.

TABLE XII. COMPARISON OF FISSION AVERAGE CROSS-SECTIONS FOR THE  $^{204}\text{Pb}(n, n')^{204m}\text{Pb}$  REACTION

Cross-section (mb)	Reference, given in Ref. [13]
$18.9 \pm 2.0$	Present (reactor)
22	Durham (reactor)
$15.3 \pm 0.7$	Köhler (reactor)

TABLE XIII. COMPARISON OF FISSION AVERAGE CROSS-SECTIONS FOR THE  $^{204}\text{Pb}(n, 2n)^{203}\text{Pb}$  REACTION

Cross-section (mb)	Reference, given in Ref. [13]
$1.9_0 \pm 0.1_8$	Present (reactor)
3.3	Roy (preferred)
5.0	Durham (reactor)

3.5.  $^{103}\text{Rh}(n, n')^{103\text{m}}\text{Rh}$ 

Our preliminary result of the average cross-section for this reaction measured with the fission plate five times independently agrees satisfactorily with the value calculated with the energy-dependent cross-section obtained by ourselves [19] and Leachman's fission spectrum. The result is given in Table XIV. Ribon [25] examined the data for this reaction and concluded that Butler and Santry's value, 710 mb, might be recommended as the average cross-section, but the present value is not in reasonable agreement with this value.

TABLE XIV. COMPARISON OF FISSION AVERAGE CROSS-SECTIONS FOR THE  $^{103}\text{Rh}(n, n')^{103\text{m}}\text{Rh}$  REACTION

Cross-section (mb)	Reference
$560 \pm 7$	Present (fission plate)
$558 \pm 32$	Present calculation with the cross-section by the authors [19] and Leachman's fission spectrum.
638	Present calculation with the cross-section by the authors [19] and SAND-II fission spectrum.
$566 \pm 17$	Kanda et al. [20] (fission plate).
$716 \pm 40$	Butler and Santry [21] (from energy-dependent cross-section).
589	Fabry [22] (reactor).
1093	Beckurts and Wirtz [23]
$535.8$	Roy [24] (reactor).

3.6.  $^{115}\text{In}(n, n')^{115\text{m}}\text{In}$ 

As a result of improving the accuracy of the cross-section data for this reaction, it has become one of the important reactions in fast neutron measurements and could also be useful as an integral check of the fission neutron spectrum. Our preliminary result for the average cross-section for this reaction measured with the fission plate four times independently agrees satisfactorily with the value calculated with the energy-dependent cross-section by ourselves [19] and Leachman's fission spectrum, as seen in Table XV. The agreement with the earlier data is reasonable.

TABLE XV. COMPARISON OF FISSION AVERAGE CROSS-SECTIONS FOR THE  $^{115}\text{In}(n, n')^{115\text{m}}\text{In}$  REACTION

Cross-section (mb)	Reference
$175 \pm 2$	Present (fission plate).
$177 \pm 10$	Present calculation with the cross-section by the authors [19] and Leachman's fission spectrum.
212	Present calculation with the cross-section by the authors [19] and SAND-II fission spectrum.
$174 \pm 6$	Kanda et al. [20] (fission plate).
$177 \pm 6$	Breesti et al. [10]
179	Zijp [26]
171	Beckurts and Wirtz [23]
170	Fährmann [27]

3.7.  $^{27}\text{Al}(n, p)^{27}\text{Mg}$ 

Our preliminary result for the average cross-section for this reaction measured with the fission plate five times independently agrees satisfactorily with the value calculated with the energy-dependent cross-section in EUR-119e [16] and Leachman's fission spectrum, as seen in Table XVI.

TABLE XVI. COMPARISON OF FISSION AVERAGE CROSS-SECTIONS FOR THE  $^{27}\text{Al}(n, p)^{27}\text{Mg}$  REACTION

Cross-section (mb)	Reference
$3.4 \pm 0.1$	Present (fission plate).
3.34	Present calculation with the cross-section in EUR-119e and Leachman's fission spectrum.
4.48	Present calculation with the cross-section in EUR-119e and SAND-II fission spectrum.
3.5	Beckurts and Wirtz [23]
$3.4 \pm 0.38$	Alexander [28]
$2.9 \pm 0.5$	Boldeman [29]
3.83	Brownell [30]
$3.5 \pm 0.2$	Beaugé [31]

3. 8.  $^{232}\text{Th}(n, f)$  [12]

When the absolute fission yield of  $^{140}\text{Ba}$  is normalized to 7.64%, as recommended by Bresesti et al. [32], the average cross-section for this reaction measured in the core of the KUR becomes  $67 \pm 6$  mb; this was compared with earlier data and the value calculated with the energy-dependent cross-section in BNL-325 (2nd edition, Supplement 2) and four expressions of the fission neutron spectrum. The present result agrees with those obtained with Watt, Cranberg and Leachman's formulae for the fission spectrum within the experimental error, as shown in Table XVII.

TABLE XVII. COMPARISON OF FISSION AVERAGE CROSS-SECTIONS FOR THE  $^{232}\text{Th}(n, f)$  REACTION

Cross-section (mb)	Reference
$67 \pm 6$	Present (reactor)
71.6	Present calculation with the cross-section in BNL-325 (2nd ed., Suppl. 2) and Watt's fission spectrum.
70.9	Present calculation with the cross-section in BNL-325 (2nd ed., Suppl. 2) and Cranberg's fission spectrum.
68.6	Present calculation with the cross-section in BNL-325 (2nd ed., Suppl. 2) and Leachman's fission spectrum.
85.0	Present calculation with the cross-section in BNL-325 (2nd ed., Suppl. 2) and SAND-II fission spectrum.
71.9	Bresesti et al. [33]
28	Beckurts and Wirtz [23]
69	Fabry [22]

3.9.  $^{232}\text{Th}(n, 2n)^{231}\text{Th}$  [14]

As shown in Table XVIII, the present result agrees reasonably with Phillips' value [36], and the calculated value with the cross-section in the UKAEA library [34] and Leachman's fission spectrum.

3.10.  $^{237}\text{Np}(n, f)$ 

When the absolute fission yield of  $^{140}\text{Ba}$  is assumed to be 5.6%, which is the average of the values given by Nambodiri [37], Von Gunten [38], Köhler [39], Bennett [40] and McElroy [41], the average cross-section for this reaction measured with the fission plate becomes  $1.33 \pm 0.11$  barns; this is compared with the earlier data in Table XIX. Since two groups of energy-dependent cross-sections exist for this reaction [42, 43], an integral check of the fission neutron spectrum cannot be made without first determining the cross-section.

TABLE XVIII. COMPARISON OF FISSION AVERAGE CROSS-SECTIONS FOR THE  $^{232}\text{Th}(n, 2n)^{231}\text{Th}$  REACTION

Cross-section (mb)	Reference
$12.5 \pm 0.84$	Present (reactor)
13.1	Present calculation with the cross-section in the UKAEA library [34] and Leachman's fission spectrum.
14.7	Present calculation with the cross-section by Butler and Santry [35] and Leachman's fission spectrum.
15.5	Present calculation with the cross-section in the UKAEA library [34] and SAND-II fission spectrum.
17.4	Present calculation with the cross-section by Butler and Santry [35] and SAND-II fission spectrum.
$12.4 \pm 0.6$	Phillips [36] (reactor).

TABLE XIX. COMPARISON OF FISSION AVERAGE CROSS-SECTIONS FOR THE  $^{237}\text{Np}(n, f)$  REACTION

Cross-section (barn)	Reference
$1.33 \pm 0.11$	Present (fission plate).
1.32	Present calculation with the cross-section by Grundl [42] and Leachman's fission spectrum.
1.43	Present calculation with the cross-section by Grundl [42] and SAND-II fission spectrum.
1.17	Present calculation with the cross-section by Davey [43] and Leachman's fission spectrum.
1.28	Present calculation with the cross section by Davey [43] and SAND-II fission spectrum.
1.323	Zijp [44]
1.460	Fabry [22]
1.367	Grundl [1]

## 4. CONCLUSION

The integral check of the fission neutron spectrum with values of average cross-sections for some threshold reactions obtained in the core of the KUR and with the fission plate performed so far suggests the authenticity of the forms given by earlier workers.

## REFERENCES

- [1] GRUNDL, J.A., Nucl. Sci. Engng 31 (1968) 191.
- [2] FABRY, A., Nukleonik 10 (1967) 280.
- [3] McELROY, W.N. et al., Nukleonik 36 (1969) 15.
- [4] McELROY, W.N., Nukleonik 36 (1969) 109.
- [5] WATT, B.E., Phys. Rev. 87 (1952) 1037.
- [6] CRANBERG, L. et al., Phys. Rev. 103 (1956) 662.
- [7] FRYE, G.M., GAMMEL, J.H., ROSEN, L., Rep. LA-1670 (1954).
- [8] LEACHMAN, R.B., Int. Conf. peaceful Uses atom. Energy (Proc. Conf. Geneva, 1955) 15, UN, New York (1956) 331.
- [9] BARNARD, E., FERGUSON, A.T.G., McMURRAY, W.R., VAN HEERDEN, I.J., Nucl. Phys. 71 (1965) 228.
- [10] BRESESTI, A.M. et al., Nucl. Sci. Engng 40 (1970) 331.
- [11] SMITH, A.B., Nucl. Sci. Engng 44 (1971) 439.
- [12] KOBAYASHI, K., KIMURA, I., Ann. Repts, KURRI, 3, 84 (1970).
- [13] KIMURA, I., KOBAYASHI, K., SHIBATA, T., J. nucl. Sci. Technol. 8 (1971) 59.
- [14] KOBAYASHI, K., HASHIMOTO, T., KIMURA, I., J. nucl. Sci. Technol. (in press).
- [15] HUGHES, D.J., Pile Neutron Research, Addison-Wesley Publ. Co. (1953) 96.
- [16] LISKIN, H., PAULSEN, A., Rep. EUR-119e (1963).
- [17] KANDA, K. et al., Neutron Energy Converter, to be published.
- [18] KANDA, K., KAWAMOTO, T., Standard Thermal Neutron Field in KUR Heavy Water Facility, Rep. KURRI-TR-59 (1969) 2.
- [19] KIMURA, I., KOBAYASHI, K., SHIBATA, T., J. nucl. Sci. Technol. 6 (1969) 485.
- [20] KANDA, K., CHATANI, H., SHIBATA, T., Ann. Repts, KURRI, 4 (in press).
- [21] BUTLER, J.P., SANTRY, D.C., Proc. Conf. Neutron Cross Sections and Technology, NBS Spec. Publ. 299, 2 (1968) 803.
- [22] FABRY, A., Proc. Conf. Radiation Measurements in Nuclear Power, Institute of Physics and Physical Society, London (1966) 245.
- [23] BECKURTS, K.H., WIRTZ, K., Neutron Physics, Springer Verlag (1964).
- [24] VOGT, E.W., CROSS, W.G., unpublished data quoted by ROY, J.C. et al., Rep. AECL-1994 (1964).
- [25] RIBON, P., Rep. DRP/MPNF/714/69 (1969).
- [26] ZIJP, W.L., Rep. RCN-37 (1965).
- [27] FÄHRMANN, K., Rep. ZfK-RN27 (1964).
- [28] ALEXANDER, K.F., Rep. ZfK-RN23 (1964).
- [29] BOLDEMAN, J.W., J. nucl. Energy A/B 18 (1964) 417.
- [30] BROWNELL, G.L. et al., Neutron Dosimetry (Proc. Symp. Harwell, 1962) 1, IAEA, Vienna (1963) 51.
- [31] BEAUGÉ, R., Neutron Dosimetry (Proc. Symp. Harwell, 1962) 2, IAEA, Vienna (1963) 3.
- [32] BRESESTI, M. et al., J. inorg. nucl. Chem. 29 (1967) 1189.
- [33] BRESESTI, M. et al., Neutron Dosimetry (Proc. Symp. Harwell, 1962) 1, IAEA, Vienna (1963) 27.
- [34] NORTON, S., STORY, J.S., UKAEA Nuclear Data Library, Rep. AEEW-M 802, M 824 (1967/1968).
- [35] BUTLER, J.P., SANTRY, D.C., Can. J. Chem. 39 (1961) 689.
- [36] PHILLIPS, J.A., J. nucl. Energy A/B 7 (1958) 215.
- [37] NAMBOODIRI, M.N., J. inorg. nucl. Chem. 30 (1968) 2305.
- [38] VON GUNTEN, H.R., Actinides Rev. 1 (1969) 275.
- [39] KÖHLER, W., Atomkernenergie 15 (1970) 263.
- [40] BENNETT, M.J., Phys. Rev. 156 (1967) 1277.
- [41] McELROY, W.N. et al., Trans. Am. nucl. Soc. 13 (1970) 868.
- [42] GRUNDL, J.A., Nucl. Sci. Engng 30 (1967) 39.
- [43] DAVEY, W.G., Nucl. Sci. Engng 26 (1966) 149.
- [44] ZIJP, W.L., Rep. RCN-Int-63-085 (1963).



# THE INFLUENCE OF FISSION NEUTRON SPECTRA ON INTEGRAL NUCLEAR QUANTITIES OF FAST REACTORS

E. KIEFHABER, D. THIEM  
Kernforschungszentrum Karlsruhe,  
Karlsruhe,  
Federal Republic of Germany

## Abstract

THE INFLUENCE OF FISSION NEUTRON SPECTRA ON INTEGRAL NUCLEAR QUANTITIES OF FAST REACTORS.

A few preliminary results on the influence of fission neutron spectra on important integral quantities of fast critical assemblies were reported previously. The scope of those studies was limited for two reasons: (i) only a small number of integral quantities for a few assemblies had been studied; and (ii) the various forms used previously for the energy dependence of the fission spectrum were of limited accuracy. In the present work the forms of the fission spectra are taken from the KEDAK and ENDF/B libraries. The various forms are compared with each other and with our 'standard' fission spectrum generally used in our calculations, which belongs to  $\nu = 2.8$  of the Russian ABN set of group constants. The influence of the different forms on calculated integral quantities for fast critical assemblies and on important characteristics of large fast power reactors is investigated. Some implications for the programs used to calculate flux distributions are outlined. Important conclusions of the present study are summarized at the end of the paper.

## 1. COMPARISON OF DIFFERENT FISSION NEUTRON SPECTRA

The forms of the fission spectra have been taken from two evaluated nuclear data files, the KEDAK and ENDF/B libraries.

The KEDAK fission spectra are described by a 'Watt' -type expression:

$$\chi(E) = c \cdot \exp(-aE) \cdot \sinh\sqrt{bE}$$

with the normalization constant  $c$  given by

$$c = 2a\sqrt{a/\pi b} \cdot \exp(-b/4a)$$

(see also Ref. [1]).

The parameters in the library for  $^{235}\text{U}$  and  $^{239}\text{Pu}$  are:

Material	1/a	a	b
$^{235}\text{U}$	0.965	1.036269	2.29
$^{239}\text{Pu}$	1.0	1.0	2.0

(see Ref. [1] p. 16, Ref. [2] p. H40 for  $^{235}\text{U}$ ; Ref. [1] p. 20 and Ref. [2] p. J42 for  $^{239}\text{Pu}$ ).



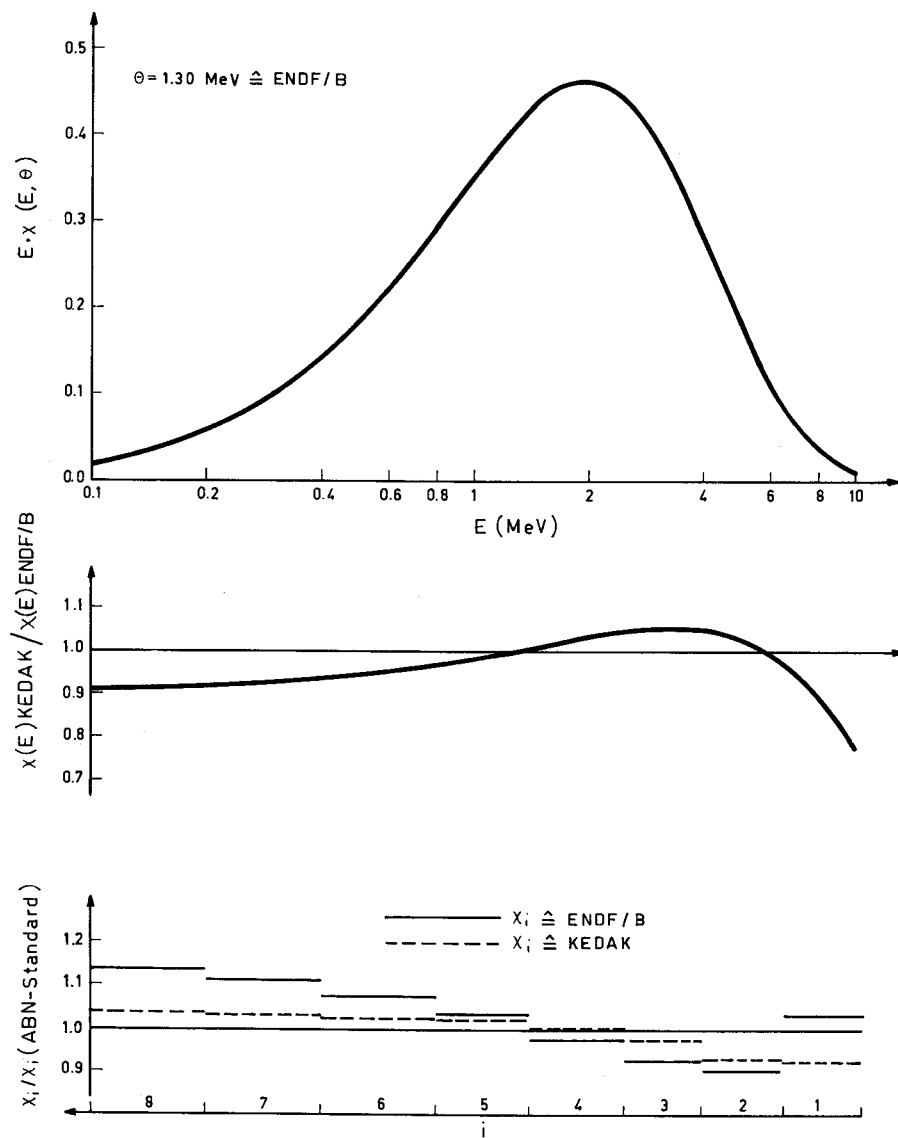


FIG. 1. The fission spectrum of  $^{235}\text{U}$  for thermal neutron-induced fission.

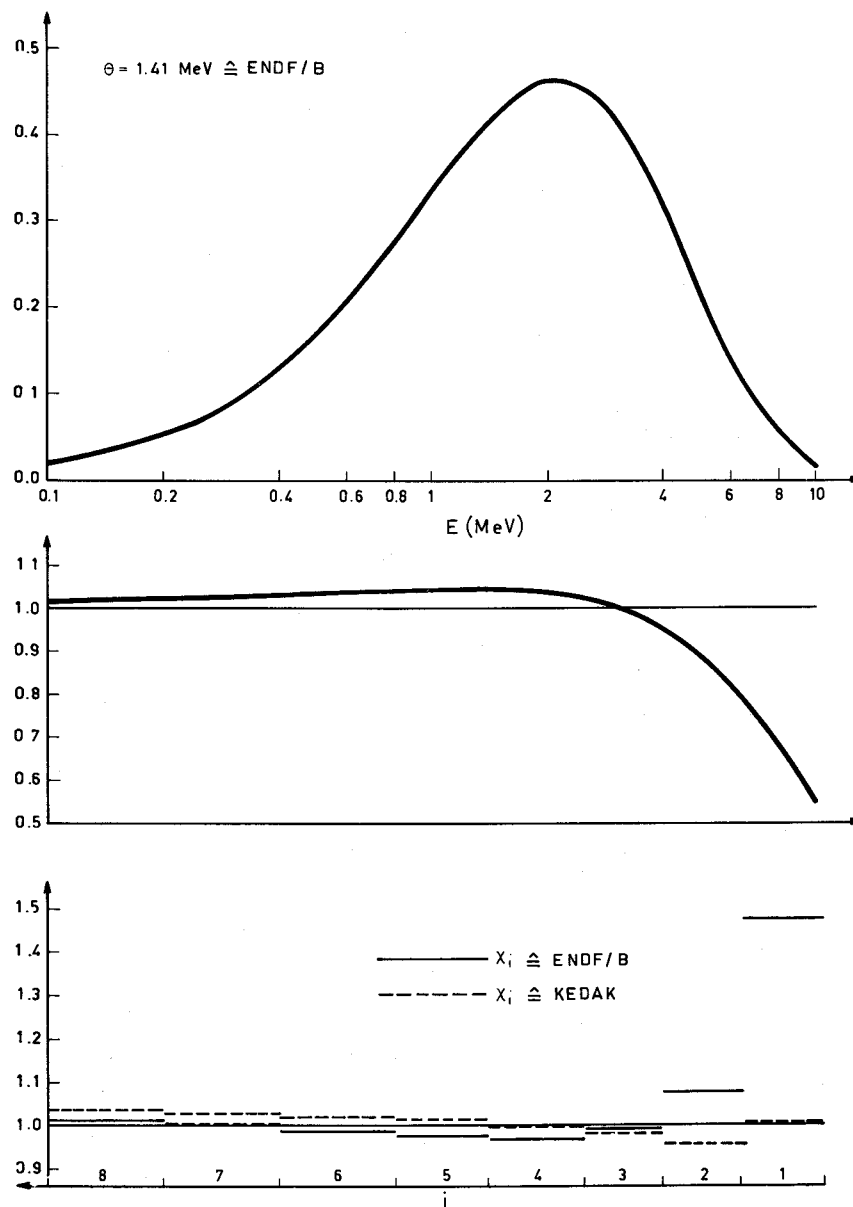


FIG. 2. The fission spectrum of  $^{239}\text{Pu}$  for thermal neutron-induced fission.

The ENDF/B fission spectra are described by a Maxwellian

$$\chi(E) = (2/\theta \sqrt{\pi\theta}) \cdot \sqrt{E} \cdot \exp(-E/\theta)$$

The parameter  $\theta$  depends on the energy  $E'$  of the neutron that induces the fission, but for our purposes we may use the parameters given for thermal fission because for all cases considered here the median energy of the fission-inducing neutrons is below about 0.5 MeV and the increase in  $\theta$  with increasing energy  $\Delta\theta/\Delta E'$  is only about 1% per 1 MeV (see Ref. [6] p. H41). The following values have been used:

$$\begin{aligned} {}^{235}\text{U}: \theta &= 1.30 \text{ MeV} \\ {}^{239}\text{Pu}: \theta &= 1.41 \text{ MeV} \end{aligned}$$

For  ${}^{238}\text{U}$  we used a value of  $\theta = 1.35$  MeV. This value was deduced from the measurements of Barnard et al. [3] who determined the  $\theta$ -values at incident neutron energies of 2.086 and 4.908 MeV. As in the work of Barnard, we assumed a linear dependence of  $\theta$  on  $\bar{\nu}$ , the average number of neutrons per fission. We applied our values of  $\bar{\nu}$  taken from KEDAK. For most of the assemblies considered in this study the average value of  $\bar{\nu}$  ( ${}^{238}\text{U}$ )  $\approx 2.85$ . An interpolation of Barnard's results [3] gives  $\theta$  ( ${}^{238}\text{U}$ )  $\approx 1.35$  MeV. From Terrell's formula (given in the report of Barnard [3])

$$\theta \approx 0.50 + 0.43\sqrt{\bar{\nu} + 1}$$

one would obtain  $\theta = 1.344$ . The good agreement with the value we have chosen may be fortuitous.

These parameters have been used to calculate the various fission spectra. For the application in multigroup calculations the group values

$$\chi_i = \int_{E_i}^{E_{i+1}} \chi(E) dE \quad i=1, 11$$

have been determined. They are given in Table I, together with our normally used 'standard' fission spectrum, which belongs to  $\nu = 2.8$  of the Russian ABN set [4]. In our calculations of group values  $\chi_i$  the neutrons emitted with energies above 10.5 MeV have been included in group 1 and those with energies below 10 keV in group 11 for the sake of simplicity.

The ENDF/B fission spectrum for  ${}^{235}\text{U}$  is shown in Fig. 1, together with a comparison with the corresponding KEDAK fission spectrum. In the lower part of this figure the group values  $\chi_i$  determined from the ENDF/B and KEDAK data are compared with those of our ABN 'standard' fission spectrum belonging to  $\nu = 2.8$ . Figure 2 shows the analogous figures for  ${}^{239}\text{Pu}$ .

From Fig. 1 it can be seen that, except for the region of very high energies, the KEDAK spectrum for  ${}^{235}\text{U}$  is somewhat 'harder' than the corresponding ENDF/B spectrum and both are softer than our 'standard' fission spectrum. Figure 2 shows that for  ${}^{239}\text{Pu}$  the KEDAK spectrum is generally 'softer' than the 'standard' fission spectrum, whereas the ENDF/B spectrum is definitely 'harder'. Thus, for the most interesting

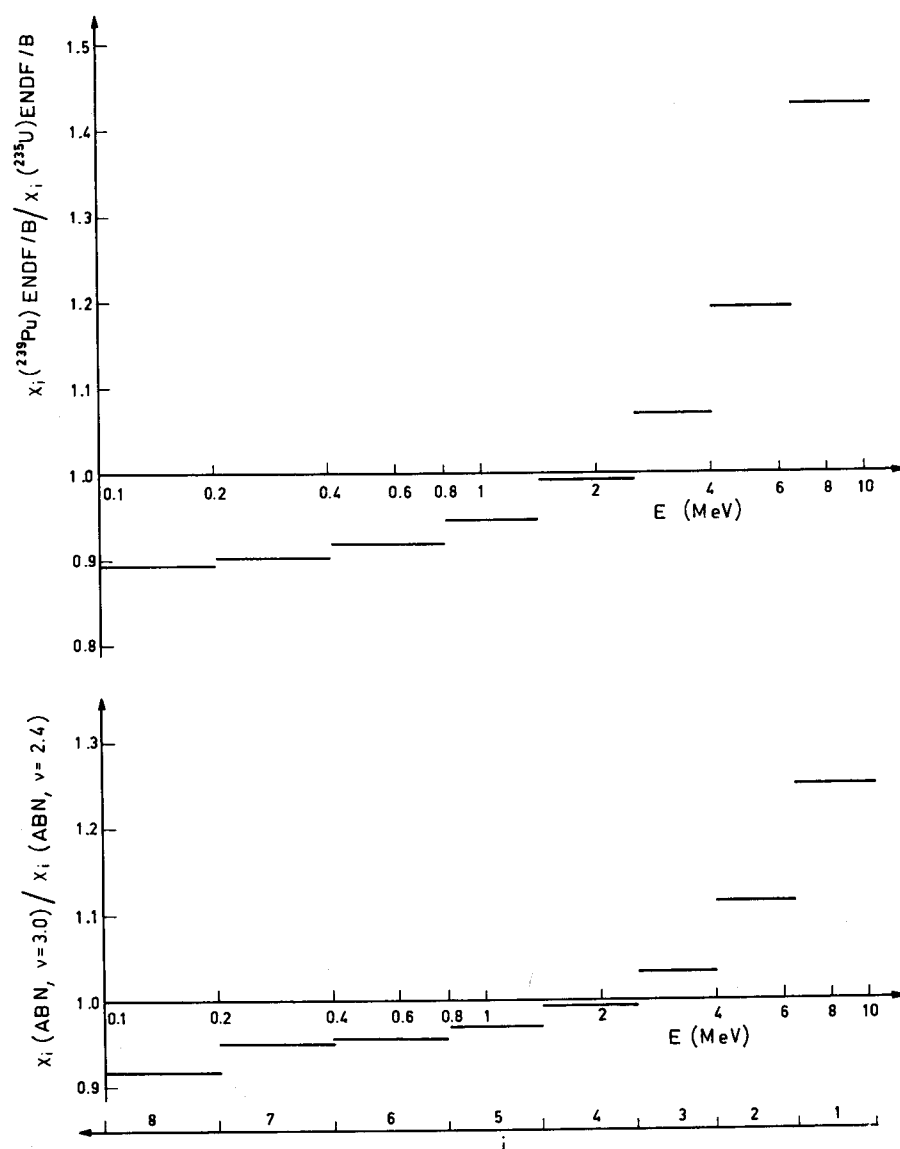


FIG.3. Comparison of various forms of fission spectrum  $\chi_i = \int_{\Delta E_i} \chi(E) dE$ .

energy range from 0.2 to 5.0 MeV the ENDF/B spectra show the largest deviations compared to our standard fission spectrum, that for  $^{235}\text{U}$  being the softest and that for  $^{239}\text{Pu}$  being the hardest of the fission spectra studied here.

The differential fission neutron spectra measurements of Werle [5] for thermal neutron-induced fission of  $^{235}\text{U}$  and  $^{239}\text{Pu}$  support the ENDF/B description. Therefore, the ENDF/B fission spectra are considered by us to be representative for the real difference between the  $^{235}\text{U}$  and  $^{239}\text{Pu}$  fission spectra. The ratio of both fission spectra is shown in the upper part of Fig. 3.

In the Russian ABN set the fission spectrum is given for different values of  $\nu$ , the average number of fission neutrons per fission. For fast criticals and fast power reactors the average  $\nu$  is generally somewhat below 3.0 for  $^{239}\text{Pu}$  and somewhat higher than 2.4 for  $^{235}\text{U}$  (probably even above 2.5). The lower part of Fig. 3 gives the ratio of the ABN fission spectra belonging to  $\nu = 2.4$  and  $\nu = 3.0$ . From a comparison with the upper part of the same figure it can be concluded that the difference between the  $^{235}\text{U}$  and  $^{239}\text{Pu}$  fission spectra is not sufficiently well represented by the  $\nu$ -dependence, as assumed in the ABN set.

## 2. INFLUENCE OF DIFFERENT FISSION NEUTRON SPECTRA ON CALCULATED INTEGRAL QUANTITIES OF FAST CRITICAL ASSEMBLIES

### 2.1. Influence on criticality

Table II gives the criticality differences obtained by using instead of the 'standard' fission spectrum the KEDAK and the ENDF/B fission spectra. The results have been determined by fundamental-mode homogeneous diffusion calculations. As nuclear data basis we have used the group constants of the MOXTOT set [6]. (Some few test calculations have shown that the influence of the fission spectrum on the criticality is even somewhat more pronounced in two-dimensional calculations, probably because the resulting change of the leakage probability or the space dependence of the flux shape is not accounted for by a corresponding change of the buckling in the fundamental-mode calculations.) The fission spectrum used corresponds in every case to the main fissionable isotope of the special assembly considered. With the ENDF/B data the maximum criticality decrease is about 0.009, the maximum criticality increase about 0.006. The criticality difference observed in Table II is generally of the same order of magnitude as other corrections, e. g. heterogeneity or transport corrections, which are applied in order to determine best theoretical criticality values. Thus the criticality correction caused by the deviation of the appropriate fission spectrum from the 'standard' fission spectrum is of the same importance as other commonly applied corrections.

From Table II it can be noted that replacing the 'standard' fission spectrum by the KEDAK fission spectrum gives for plutonium assemblies an opposite sign of the criticality differences than that obtained upon replacement by the ENDF/B fission spectrum. This is due to the fact mentioned before that for  $^{239}\text{Pu}$  the KEDAK fission spectrum is 'softer', whereas the ENDF/B fission spectrum is 'harder' than our 'standard'

TABLE II. CRITICALITY DIFFERENCES  $\Delta k$  CAUSED BY USING FISSION SPECTRA DIFFERENT FROM THE 'STANDARD' FISSION SPECTRUM  
Results of fundamental mode diffusion calculations for homogeneous mixtures using the MOXTOT set.

Assembly	Main fissionable isotope	$k_{\text{eff}}$ (KEDAK) - $k_{\text{eff}}$ (Standard)	$k_{\text{eff}}$ (ENDF/B) - $k_{\text{eff}}$ (Standard)
SUAK U1B	$^{235}\text{U}$	-0.0033	-0.0054
SUAK UH1B		-0.0013	-0.0011
ZPRIII-10		-0.0037	-0.0062
ZPRIII-25		-0.0051	-0.0091
SNEAK-3A1		-0.0016	-0.0027
SNEAK-3A2		-0.0013	-0.0021
ZPRIII-48	$^{239}\text{Pu}$	-0.0015	+0.0030
ZEBRA-6A		-0.0011	+0.0024
SNEAK-5C		-0.0018	+0.0034
ZPRIII-55		-0.0032	+0.0064

fission spectrum. The most pronounced difference occurs for the  $k_{\infty}$  experiment ZPR III-55 where the criticality difference obtained when using the ENDF/B instead of the KEDAK data amounts to about 0.01 in  $k_{\text{eff}}$ .

For a few test cases the influence of the fission spectrum of  $^{238}\text{U}$  has also been studied. We have chosen such critical assemblies where the fission in  $^{238}\text{U}$  is of relatively large importance: for the uranium assembly ZPRIII-25 about 27% of the neutron production stems from  $^{238}\text{U}$  and 73% from  $^{235}\text{U}$ ; for the plutonium assembly ZPR III-55 more than 20% of the neutron production stems from  $^{238}\text{U}$ , about 75% from  $^{239}\text{Pu}$  and the rest from  $^{235}\text{U}$  and the higher plutonium isotopes. The criticality values of the assemblies studied are known to be sensitive to the form of the fission spectrum. As a modified fission spectrum we have used a weighted average of the corresponding fission spectra: for ZPRIII-25  $^{235}\text{U}$  (73%) and  $^{238}\text{U}$  (27%) and for ZPRIII-55  $^{239}\text{Pu}$  (75%) and  $^{238}\text{U}$  (25%) (the contributions of  $^{235}\text{U}$  and the higher plutonium isotopes have been neglected in this case). The criticality differences  $\Delta k$  obtained with these modified fission spectra compared with the results obtained with the corresponding pure fission spectra of the appropriate main fissionable isotope are  $\Delta k = +0.0023$  for ZPRIII-25 and  $\Delta k = -0.0021$  for ZPRIII-55. Even these criticality differences are of the order of other more familiar criticality corrections. Thus for some particular assemblies even the effect of the  $^{238}\text{U}$  fission spectrum has to be taken into account for a precise criticality determination. This statement holds at least as long as the differences in the temperatures for the Maxwell distributions are as large as assumed at present:  $\theta(^{235}\text{U}) = 1.30$  MeV,  $\theta(^{238}\text{U}) = 1.35$  MeV,  $\theta(^{239}\text{Pu}) = 1.41$  MeV.



## 2.2. Influence on reaction rate ratios

Besides the criticality, one is also interested in the reaction rate ratios for fast zero-power assemblies because these quantities provide additional possibilities of testing the quality of the basic neutron cross-sections. Of course, one is mainly interested in those reaction rates that are relevant for the neutron balance, i. e. for neutron production or loss processes. It is evident that a change in the fission spectrum will cause the largest effect for those reactions that have a threshold in the MeV region. Here the fission process in  $^{238}\text{U}$  is the most important one. Replacing our 'standard' ABN fission spectrum by the ENDF/B representations, the fission rate ratio  $R_f^8/R_f^5$  decreased by about 5-6% for U-fuelled and increased by about 2.5-3.5% for Pu-fuelled assemblies. Moreover, noticeable variations in this ratio are even observed if the  $^{238}\text{U}$  contribution to the fission spectrum is taken into account appropriately.

For ZPRIII-25 a mixed fission spectrum composed of  $^{235}\text{U}$  (73%) and  $^{238}\text{U}$  (27%) leads to a 1% increase of the ratio  $R_f^8/R_f^5$  as compared to the result obtained for a pure  $^{235}\text{U}$  fission spectrum. For ZPRIII-55 we used a mixed fission spectrum composed of  $^{239}\text{Pu}$  (75%) and  $^{238}\text{U}$  (25%) instead of a pure  $^{239}\text{Pu}$  fission spectrum and obtained a decrease of 1% for the  $R_f^8/R_f^5$  ratio.

All other important reaction rate ratios remain nearly unchanged for the changes of the fission spectrum under consideration. Especially for the important ratios  $\alpha^5 = R_c^5/R_f^5$ ,  $R_c^8/R_f^5$ ,  $R_f^9/R_f^5$ ,  $\alpha^9 = R_c^9/R_f^9$ ,  $R_c^8/R_f^9$ ,  $R_f^0/R_f^9$ ,  $R_c^0/R_f^9$  the changes are smaller than 1% for the assemblies considered here. This change is much smaller than that caused by the uncertainties in the corresponding basic nuclear data. Only if those errors in the above-mentioned reaction rate ratios, which are caused by basic cross-section uncertainties, can be reduced below 1%, must the influence of the fission spectra on these reaction rate ratios be taken into account.

## 2.3. Influence on material worth and substitution experiments

For two assemblies (ZPRIII-25 and ZPRIII-48) we have studied the influence of the various forms of the fission neutron spectrum on the central material worth. Such an effect may be important if the reactivity of a plutonium ( $^{239}\text{Pu}$ ) sample in a uranium ( $^{235}\text{U}$ ) core has to be determined or vice versa. In both cases the fission spectrum of the sample is different from that of the surrounding medium, an effect that usually has been neglected up to now and cannot be taken into account in most of the existing perturbation codes. The net perturbation effect for the central material worth is composed of three terms: production, absorption and degradation. Our test calculations have shown that the production term is changed by about 2% for ZPRIII-25 and by about 1% for ZPRIII-48 if we use the fission spectrum for  $^{239}\text{Pu}$  instead of that for  $^{235}\text{U}$  (both taken from ENDF/B). For the assembly ZPRIII-48 the production term is larger than the net perturbation effect by a factor of about 1.5 for  $^{239}\text{Pu}$  and about 2.0 for  $^{235}\text{U}$ . Therefore we have to expect that errors of the order of a few per cent (probably up to 5%) may arise by neglecting the difference between the fission spectrum of the sample and that of the surrounding core material.

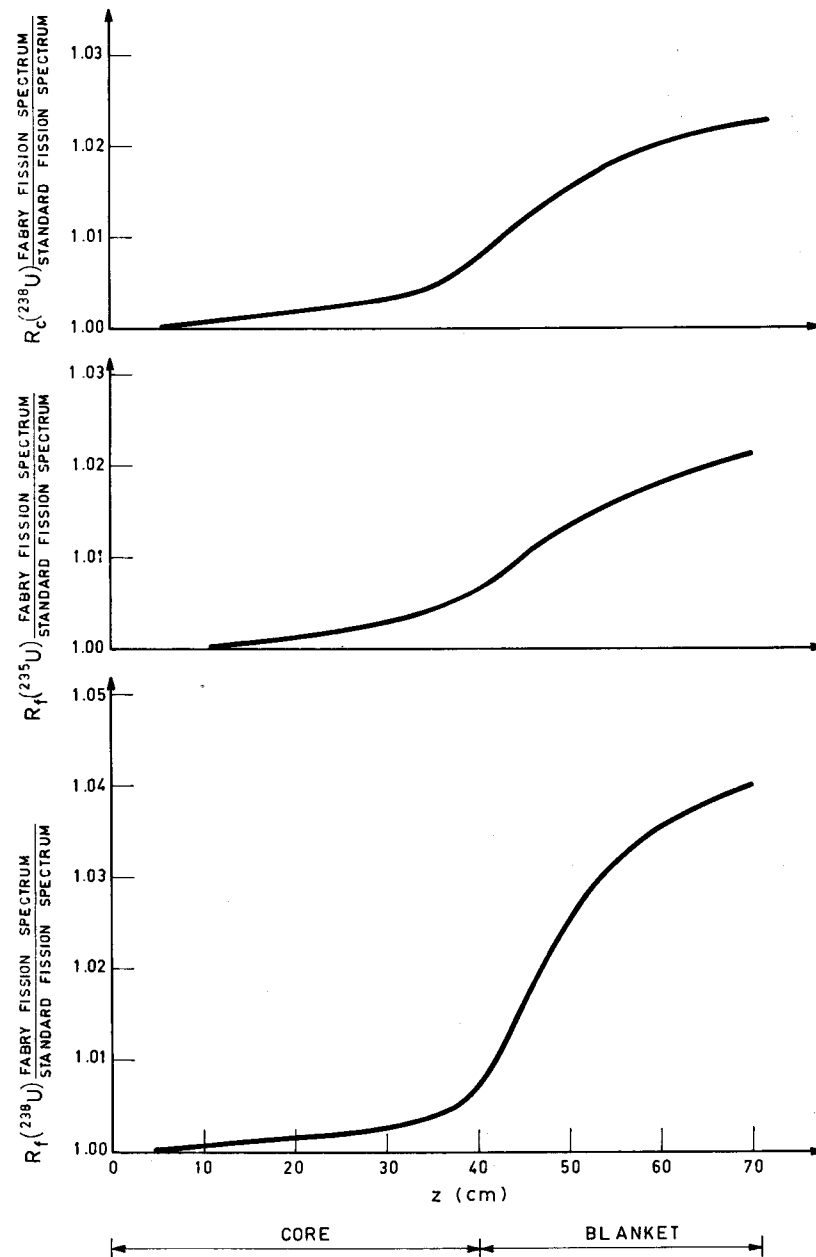


FIG. 4. Influence of Fabry's fission spectrum on the axial reaction rate traverse in SNEAK 3A2.

From the preceding discussion it is evident that in the case of substitution experiments errors of the same order as for the material worth may arise when the effect of differences in the fission spectra is neglected. In these experiments, e.g., a uranium zone is successively replaced by a plutonium zone [7]. From the results of successive substitution steps one tries to extrapolate to the results that would correspond to a full core with the composition of the substituted zone. Direct numerical calculations to determine the reactivity effect caused by the differences in the fission spectra of the substituted and the surrounding zone could not be performed up to now because the appropriate codes were not available. However, from the criticality calculations mentioned in section 2.1 one may conclude that for the extrapolated results of a fully substituted core criticality errors of up to 0.01 may arise if the differences in the fission spectra of the substituted and the original core zone are neglected.

#### 2.4. Influence on reaction rate traverses

In Ref. [8] it has been shown that the form of the fission spectrum has some influence on the shape of reaction rate traverses too, apart from the influence on the absolute magnitude of central reaction rates or central reaction rate ratios discussed in section 2.2. The result of the earlier work for the SNEAK 3A2 assembly [8] is redrawn here in Fig. 4. The Fabry fission spectrum used for Fig. 4 is based on results of integral measurements for the temperature of the  $^{235}\text{U}$  thermal neutron fission spectrum [9]. This fission spectrum is 'harder' than our 'standard' fission spectrum and therefore considerably harder than the ENDF/B  $^{235}\text{U}$  fission spectrum, which in the present work is considered to be the most realistic representation of the differential measurements. The ENDF/B  $^{235}\text{U}$  fission spectrum has been used to obtain the results of Fig. 5.

With the 'harder' spectrum used for Fig. 4 all the three reaction rate traverses studied ( $R_c(^{238}\text{U})$ ,  $R_f(^{235}\text{U})$ ,  $R_f(^{238}\text{U})$ ) show an increase of 0.7% in the outer part of the core region (all traverses are normalized at the core centre). In the blanket region  $R_c(^{238}\text{U})$  and  $R_f(^{235}\text{U})$  are increased by about 2% and  $R_f(^{238}\text{U})$  by about 4%.

In Fig. 5 the corresponding results with the 'softer' ENDF/B  $^{235}\text{U}$  fission spectrum are shown. In the outer part of the core the three reaction rate traverses studied are lower by about 0.7% than those calculated with the 'standard' fission spectrum. In the blanket region the traverses for  $R_c(^{238}\text{U})$  and  $R_f(^{235}\text{U})$  are decreased by about 2.5% and for  $R_f(^{238}\text{U})$  by about 4%.

It is probably interesting that even the discrepancies between the shape of the traverses determined with the  $^{235}\text{U}$  ENDF/B and  $^{235}\text{U}$  KEDAK fission spectrum are not too small: for the case studied here the traverses with the KEDAK spectrum are in the outer part of the core region about 0.5% and in the blanket region up to 1.5% higher than those calculated with the ENDF/B spectrum.

The present results indicate that for the precise determination of the reaction rate traverses including the power traverse it will be necessary to take into account the appropriate form of the fission spectrum if discrepancies in the shape between theory and experiment of the order of 1% in the core region and/or several per cent in the blanket region become

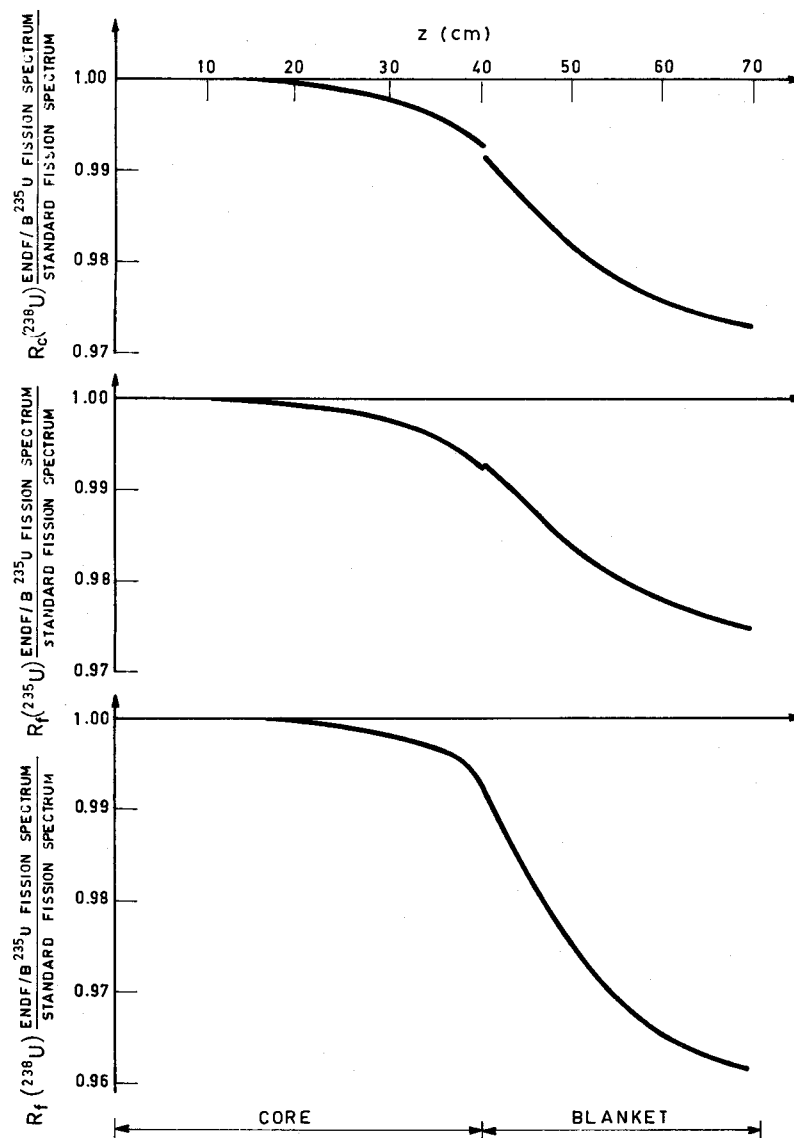


FIG. 5. Influence of the ENDF/B  $^{235}\text{U}$  fission spectrum on the axial reaction rate traverse in SNEAK 3A2.

relevant. The possible effect of using different fission spectra in the core ( $^{235}\text{U}$ ) and blanket region ( $^{238}\text{U}$ ) could not be studied because an appropriate code is not available at the moment.

### 3. INFLUENCE OF OTHER NUCLEAR DATA UNCERTAINTIES ON THE CRITICALITY OF FAST CRITICAL ASSEMBLIES

The importance of a precise knowledge of the appropriate fission spectrum must be judged in the context of the other current uncertainties in the nuclear data. We will discuss here only two examples of uncertainties, namely the fission and the inelastic scattering cross-sections of  $^{238}\text{U}$ .

The following results will show the sensitivity of the criticality on certain changes in the nuclear data. As the first change (CI of Table III) we study an increase in the  $^{238}\text{U}$  fission cross-section by 5%. Then the inelastic scattering cross-section of  $^{238}\text{U}$  is changed from the values used in the MOXTOT set [6] to the ABN values. In the first step (CII) for the energy range from 1.4-10.5 MeV (groups 1-4) and in the second step (CIII) from 0.05-1.4 MeV (groups 5-9). In addition to the change in the inelastic scattering cross-section of  $^{238}\text{U}$  we considered also a change in the corresponding scattering probabilities, i. e. of the energy distribution of the neutrons scattered inelastically by  $^{238}\text{U}$ . Instead of the probabilities determined for the MOXTOT set [6] we use those of the ABN set for the next two changes: Change CIV concerns the energy range between 1.4-6.5 MeV (groups 2-4) and CV the energy range between 0.05-1.4 MeV (groups 5-9). For case CVI the changes CII and CIII are applied simultaneously, i. e. the cross-section for inelastic scattering by  $^{238}\text{U}$  is changed in the whole energy range from the MOXTOT to the ABN values. The same is done for the inelastic scattering probabilities in case CVII, which is a combination of CIV and CV. For case CVIII, finally, all data for the inelastic scattering on  $^{238}\text{U}$  are changed from the MOXTOT to the ABN values.

Before discussing the results it is probably useful to mention that the changes considered here are reasonably realistic. Pitterle et al. [10] have increased their  $^{238}\text{U}$  fission cross-section by about 6% over Pitterle's earlier evaluation [11], for which a reasonable agreement with the corresponding data of the MOXTOT set exists. The modified data are similar to the ABN data. Kallfelz et al. [12] have shown that a possible reduction of the inelastic scattering cross-section by an amount between 15-30% would improve the agreement between theory and experiment for integral quantities, as, e. g., the criticality of the fission rate ratio  $R_f^8/R_f^5$  for a series of fast critical assemblies. Pitterle [11] changed the parameter  $\gamma$ , which via the 'effective temperature'  $\theta = \sqrt{E/\gamma A}$  determines the inelastic scattering probabilities of  $^{238}\text{U}$ , from  $\gamma = 0.099 \text{ MeV}^{-1}$  [11] to the new value  $\gamma = 0.0685 \text{ MeV}^{-1}$  [10]. For the MOXTOT set  $\gamma = 0.16 \text{ MeV}^{-1}$  has been used to calculate the inelastic scattering probabilities for  $^{238}\text{U}$  in the 'continuum' range of residual nucleus levels.

The difference in the inelastic scattering probabilities between the MOXTOT and ABN data is similar to the difference that results when the parameter  $\gamma$  is changed from 0.16 to 0.099  $\text{MeV}^{-1}$ . Therefore all changes considered here are within the range of the present uncertainties or within the range of suggested modifications of the nuclear data.

TABLE III. CRITICALITY DIFFERENCES  $\Delta k$  CAUSED BY CHANGES IN THE NUCLEAR DATA OF  $^{238}\text{U}$ 

Assembly	CI	CII	CIII	CIV	CV	CVI	CVII	CVIII
	$\sigma_f \times 1.05$	$\sigma_{\text{inel}}^{\text{Gr. 1-4}}$ MOXTOT → ABN	$\sigma_{\text{inel}}^{\text{Gr. 5-9}}$ MOXTOT → ABN	$P_{\text{inel}}^{\text{Gr. 2-4}}$ MOXTOT → ABN	$P_{\text{inel}}^{\text{Gr. 5-9}}$ MOXTOT → ABN	CII+CIII CIV+CV	CIV+CV	CII+CIII+ CIV+CV
SUAK U1B	+0.0064	+0.0038	-0.0055	+0.0019	-0.0065	-0.0016	-0.0048	-0.0059
SUAK UH1B	+0.0049	-0.0023	-0.0032	-0.0020	-0.0039	-0.0055	-0.0060	-0.0112
ZPRII-10	+0.0061	+0.0069	-0.0039	+0.0031	-0.0053	+0.0030	-0.0024	+0.0009
ZPRII-25	+0.0073	+0.0146	+0.0019	+0.0071	+0.0004	+0.0165	+0.0075	+0.0243
SNEAK-3A1	+0.0037	+0.0015	-0.0010	+0.0005	-0.0013	+0.0006	-0.0007	-0.0001
SNEAK-3A2	+0.0036	+0.0009	-0.0011	+0.0002	-0.0014	-0.0002	-0.0012	-0.0013
ZPRII-48	+0.0037	+0.0027	-0.0001	+0.0016	+0.0002	+0.0026	+0.0018	+0.0043
ZEBRA-6A	+0.0033	+0.0009	-0.0005	+0.0008	-0.0003	+0.0005	+0.0005	+0.0010
SNEAK-5C	+0.0030	+0.0035	+0.0004	+0.0017	+0.0005	+0.0039	+0.0022	+0.0060
ZPRII-55	+0.0058	+0.0130	+0.0033	+0.0069	+0.0041	+0.0163	+0.0113	+0.0275

All criticality differences  $\Delta k$  given in Table III are based on fundamental-mode homogeneous diffusion calculations using the MOXTOT set as nuclear data basis. The results should be compared with those given in Table II. With respect to the absolute  $\Delta k$  values each of the changes CI to CV of Table III has about the same importance as the differences in the fission spectrum representations. From cases CVI and CVII it can be seen that the uncertainties in the magnitude of the inelastic scattering cross-section as well as that of the inelastic scattering probabilities are somewhat more important with respect to the criticality than the changes in the form of the fission spectrum. Case VIII in particular demonstrates the large effect of the inelastic scattering data for  $^{238}\text{U}$  on the criticality of most of the fast assemblies included in our study. If the uncertainties assumed for case VII are realistic, then a precise determination of the inelastic scattering data of  $^{238}\text{U}$  is of high priority.

#### 4. INFLUENCE OF THE DIFFERENT FISSION NEUTRON SPECTRA ON IMPORTANT CALCULATED QUANTITIES OF LARGE FAST POWER REACTORS

##### 4.1. Influence on criticality and critical mass

Besides the influence of different fission neutron spectra on the calculation of fast critical assemblies discussed before, it is important to study the influence on the calculation of large fast power reactors. As test example of a large fast power reactor we have chosen the simplified model suggested by Baker, which was used for a world-wide intercomparison study. The details of the specifications may be found in the recently published report [13] on the results of this intercomparison of nuclear reactor calculations. The main features of the reactor model are as follows: spherical model with a core radius of 84.196 cm and a spherical annular blanket of 45.72 cm thickness. The fuel is mixed  $\text{PuO}_2\text{-UO}_2$ . Sodium is used as coolant and stainless steel for the structure and cladding material. Three versions have been studied with somewhat different fuel compositions:

- (A) Only  $^{239}\text{Pu}$  and  $^{238}\text{U}$ , no fission products, no higher plutonium isotopes
- (B)  $^{239}\text{Pu}$  plus  $^{238}\text{U}$  plus 10% fission product pairs, no higher plutonium isotopes
- (C)  $^{239}\text{Pu}$ ,  $^{240}\text{Pu}$  and  $^{238}\text{U}$  plus 10% fission product pairs,  $^{239}\text{Pu}$ :  $^{240}\text{Pu}$  = 1:0.5.

In the first column of Table IV the criticality differences are given that arise if the fission spectra for  $^{235}\text{U}$  and  $^{239}\text{Pu}$  (ENDF/B form) are used instead of our 'standard' fission spectrum. The reactor composition has been kept constant in this case. The fuel enrichment has been adjusted so that the original criticality value  $k_{\text{eff}} = 1.0000$  is attained. The corresponding absolute changes in critical mass of fissile material ( $^{239}\text{Pu}$ ) are given in the second column. The third column shows the relative changes of the critical fissile mass that were necessary to re-establish the criticality.

The largest absolute criticality change is about 0.007, which causes a change of the critical mass of somewhat more than 1%, corresponding in this case to about 11 kg of  $^{239}\text{Pu}$ . This change occurs if we use the  $^{235}\text{U}$  fission spectrum instead of our standard fission spectrum. Using the  $^{239}\text{Pu}$  fission spectrum, which is more appropriate in this case because

TABLE IV. VARIATION IN NUCLEAR CHARACTERISTICS OF LARGE FAST POWER REACTORS CAUSED BY USING FISSION SPECTRA DIFFERENT FROM THE 'STANDARD' FISSION SPECTRUM

Case	Fission spectrum	Changes in nuclear characteristics			
		$\Delta k$ (%)	$\Delta M(^{239}\text{Pu})$ (kg)	$\Delta M/M$ (%)	$\Delta \text{BR}$
A	$^{235}\text{U}$	-0.60	+10.57	+1.10	-0.015
	$^{239}\text{Pu}$	+0.32	- 5.68	-0.59	+0.008
B	$^{235}\text{U}$	-0.57	+10.22	+0.98	-0.012
	$^{239}\text{Pu}$	+0.28	- 5.00	-0.48	+0.007
C	$^{235}\text{U}$	-0.67	+10.98	+1.14	-0.015
	$^{239}\text{Pu}$	+0.29	- 4.72	-0.49	+0.007

the fissionable material is plutonium and which is closer to our standard fission spectrum than the  $^{235}\text{U}$  fission spectrum, the resulting changes are smaller in absolute magnitude, although of alternate sign. For this more realistic change the criticality difference is about 0.003, the change in critical mass about 0.6%, equivalent to somewhat less than 6 kg of  $^{239}\text{Pu}$  for these simplified cases with about 1000 kg total fissile mass. The main reason for the criticality differences is the change of the fission and production rate in the fertile materials  $^{238}\text{U}$  and  $^{240}\text{Pu}$  with fission thresholds in the high energy range.

#### 4.2. Influence on breeding performance

The most important quantity next to the critical mass is the breeding performance of a power reactor. Column 4 of Table IV shows that changes in the breeding ratio of up to 0.015 may be caused by changes in the form of the fission spectrum. The change in the breeding ratio is mainly caused by the adjustment of the enrichment that is necessary to bring the reactor with modified fission spectrum back to criticality. The ratio of reaction rates per atom  $R_c^8/R_f^9$  is changed by at most 0.5% upon changing the fission spectrum. For the corresponding fission rate ratio  $R_f^8/R_f^9$  changes similar to those mentioned in section 2.2 for the fast critical assemblies have been observed, i. e. -5.3% for the  $^{235}\text{U}$  fission spectrum and +2.3% for the  $^{239}\text{Pu}$  fission spectrum. The adjustment of the enrichment causes very small variations in the reaction rate ratios per atom, generally one order of magnitude smaller than the variations caused by using different forms of the fission spectrum.

#### 5. INFLUENCE OF OTHER NUCLEAR DATA UNCERTAINTIES ON CRITICALITY, CRITICAL MASS AND BREEDING PERFORMANCE

The influence of nuclear data uncertainties on criticality and breeding performance may be judged on the basis of the intercomparison study by Baker and Hammond [13] already mentioned. Excluding those sets of



group constants that still used the old KAPL values for  $\alpha$  ( $^{239}\text{Pu}$ ) in the resonance region, we found the following maximum deviations between the most extreme cases appearing in the intercomparison. For the criticality difference:  $\Delta k \approx 0.04$ , for the critical mass about 7.5% equivalent to 73 kg of  $^{239}\text{Pu}$  and 0.10 for the physical breeding ratio. For version B of the reactor model considered here the most extreme values for the total breeding gain are 0.160 and 0.268 (see Table 21 of Ref. [13]) if those group-constant sets still using the old and too low Kapl- $\alpha$  ( $^{239}\text{Pu}$ ) values are excluded. The corresponding average value is 0.206 for the total breeding gain of version B, which has the lowest total breeding gain of the three versions that formed the basis of the study by Baker. The deviation from the average value of about  $\pm 0.05$  for the extreme cases is much larger than the deviation caused by changes in the fission spectrum. The amount of  $\pm 0.05$  represents about 25% of the average value for the total breeding gain and will lead to a similar deviation in the doubling time, i. e. the time necessary for a reactor to produce a surplus of fissile mass equal to its own inventory. It should be mentioned that similar changes of 0.12-0.15 for the breeding ratio or the breeding gain have been observed at Karlsruhe when using the recently established MOXTOT set instead of the SNEAK or NAPPMB sets used formerly [14, 15].

From a comparison of the differences discussed in the preceding section with those obtained when the fission spectrum is changed it seems to us that for the physics prediction of large fast power reactors the form of the fission spectrum is not the most important uncertainty that exists in the nuclear data field at present.

## 6. IMPLICATIONS FOR THE COMPUTER PROGRAMS USED TO CALCULATE FLUX DISTRIBUTIONS

Table II illustrates the importance of taking into account the appropriate fission spectrum for each material composition. To do this correctly it will be necessary to modify the diffusion and transport codes in such a way that they are able to handle at least a composition-dependent fission spectrum. Even more desirable would be an isotope-dependent fission spectrum and as ultimate refinement an isotope-dependent fission matrix that also takes into account the dependence of the fission spectrum on the energy of the fission-inducing neutron (probably most important for  $^{238}\text{U}$ ). As a good first approximation a composition-dependent fission spectrum is presumably sufficient. This may be obtained by a calculation prior to the flux calculation if reliable values for the neutron production in the various isotopes are available. Otherwise an iteration procedure has to be applied. The indicated modification of the codes calculating the flux distribution seems to be necessary because otherwise one will not be able to calculate very accurately the nuclear characteristics of, e. g., an assembly like SNEAK 3B2 with an inner plutonium zone and an outer uranium driver zone in the core region.

For small cores reflected by natural or depleted uranium, i. e. mainly  $^{238}\text{U}$ , an influence of the different fission spectra in core and blanket may be important too. It seems worthwhile to study whether an effect on the reaction rate traverses, e. g. the fission traverse of  $^{238}\text{U}$ , can be observed by using the appropriate different fission spectra for different material

compositions. If a cell arrangement for a fast zero-power assembly contains platelets of both  $^{235}\text{U}$  and  $^{239}\text{Pu}$  of about equal amounts or of enriched fuel and natural (or depleted) uranium, then also the heterogeneity codes like ZERA [16] should probably be able to take into account a composition-dependent fission spectrum.

An isotope-dependent fission spectrum may probably be desirable for the calculation of a power reactor, which at the beginning may have  $^{235}\text{U}$  as main fissionable isotope and during the power production produces  $^{239}\text{Pu}$  according to its breeding properties, although it may turn out that in the burn-up calculations an approximate treatment of the variation of the form of the fission spectrum during the reactor lifetime may be sufficiently accurate.

The implications for the codes used in perturbation calculations have already been mentioned in section 2.3.

## 7. CONCLUSIONS

Our studies confirm that the difference in the form of the fission spectrum for  $^{235}\text{U}$  and  $^{239}\text{Pu}$ , as obtained in differential spectrum measurements, cannot be represented reasonably well by the  $\nu$ -dependence given, e.g., in Terrell's formula and, e.g., assumed in the Russian ABN set.

For the calculation of fast critical assemblies we have found criticality changes of up to 1% upon changing the form of the fission spectrum from our 'standard' form to the forms that are more appropriate for the individual assemblies considered.

The reaction rate ratios that are important for the neutron balance are rather insensitive to the form of the fission spectrum with the only exception of the fission rate ratio  $R_f(^{238}\text{U})/R_f(^{235}\text{U})$  or  $R_f(^{238}\text{U})/R_f(^{239}\text{Pu})$ . This ratio is changed by several per cent when the form of the fission spectrum is changed.

For some special assemblies it also seems important to take into account the contribution of the  $^{238}\text{U}$  fission spectrum to the total fission spectrum of the fuel mixture (either  $(^{235}\text{U} + ^{238}\text{U})$  or  $(^{239}\text{Pu} + ^{238}\text{U})$ ). Criticality changes slightly above 0.2% and changes of the fission rate ratio  $R_f(^{238}\text{U})/R_f(^{235}\text{U})$  of about 1% have been found when the  $^{238}\text{U}$  contribution has been properly taken into account.

Generally the criticality changes that have been obtained when the form of the fission spectrum is changed within reasonable limits are of the same order of magnitude as the criticality changes that result from various corrections usually applied, e.g. the transport ( $S_N$ ) correction, the heterogeneity correction etc. This shows that the form of the fission spectrum is of the same importance as these corrections, which usually need rather complicated and/or time-consuming computations. Therefore the appropriate form of the fission spectrum should be taken into account for accurate and reliable nuclear calculations.

At the present state of knowledge of nuclear data it seems impossible for us to draw definite conclusions from the analysis of fast critical assemblies on the correctness of the fission spectra used for this analysis. However, we have found that when using appropriately the ENDF/B forms for  $^{235}\text{U}$  and  $^{239}\text{Pu}$  instead of our 'standard' fission spectrum the agreement between theory and experiment for the criticality is improved. With our

'standard' form we have found in our analysis of a series of fast criticals using the MOXTOT set [6] that  $^{235}\text{U}$ -fuelled assemblies are generally predicted supercritical, whereas  $^{239}\text{Pu}$ -fuelled assemblies are predicted subcritical. These discrepancies are reduced by using the more reasonable ENDF/B forms of the fission spectra.

For fast power reactors the form of the fission spectrum is in most cases less important than for fast criticals. But the test of the nuclear data and methods of calculations that should subsequently be used for the calculation of power reactors can only be performed by comparing the experimental results obtained in fast criticals with the corresponding theoretical results. The reliability of the nuclear data used for the power reactor design can therefore only be judged on the basis of checking the experimental results of a variety of different fast criticals. This fact explains why the fission spectrum is more important for the calculation of fast power reactors than one would assume from its direct influence on the nuclear characteristics of fast power reactors.

The effect of nuclear data uncertainties on the design of large fast breeder reactors has been studied by several authors (see, e.g., Refs [17, 18]). One major concern is for the design of the early-generation fast breeder power plants. Here the uncertainties in the nuclear data and the resulting uncertainties in the predicted reactor parameters as e.g., criticality or reactivity coefficients will cause economic disadvantages. The costs of the power plant will increase because of the increased flexibility of the core design, which is necessary in order to counterbalance the effects of uncertainties in the predicted reactor parameters. Probably at the same time the maximum total power output cannot be attained because the optimum conditions for the power production cannot be reached. Furthermore, an extrapolation from early demonstration power reactors to large power plants with an output of at least 1000 MW(e) will be affected by uncertainties in the nuclear data (even if the results derived from critical assemblies are taken into account). This leads us to the second concern: The uncertainties in the nuclear data cause uncertainties in the long-term potential of fast breeders as, e.g., the doubling time or the long-term power generating costs. Usually a criticality uncertainty  $\Delta k$  of  $\pm 1\%$  caused by the combined effects of all nuclear data uncertainties is considered to be tolerable at present. Table IV shows that a criticality difference of about this magnitude is caused just by replacing the  $^{239}\text{Pu}$  fission spectrum by the  $^{235}\text{U}$  fission spectrum (ENDF/B forms). If the uncertainty in the fission spectrum is only allowed to cause a criticality uncertainty smaller than  $\pm 0.2\%$ , which seems reasonable for an accepted total criticality uncertainty of  $\pm 1\%$  caused by a combination of all nuclear data uncertainties, this would mean that the temperatures of the corresponding Maxwell distributions of the fission spectra have to be determined with an absolute uncertainty smaller than  $\pm 0.02$  MeV. This fact demonstrates more drastically than Table IV or the discussion in section 4 that the fission spectrum should be determined with rather high accuracy because it is only one of a long list of important nuclear data.

It is probably worth mentioning that the form of the fission spectrum is also of some importance with respect to irradiation effects on fuel elements and structural materials caused by high-energy neutrons.

The studies presented in this paper have shown that the form of fission neutron spectrum plays an important role in neutron physics calculations of fast critical assemblies and large fast power reactors. At present, however, one specific difficulty exists: most existing codes for nuclear calculations assume that the fission spectrum is the same for all regions or compositions of the reactor. Probably this assumption is too crude and may give rise to difficulties in the interpretation of material worth or substitution experiments, as explained in more detail in section 2.3. It may turn out that in special cases even in heterogeneity codes like ZERA [16] it will be desirable to use different fission spectra for the different fuel platelets.

In the analysis of fast critical assemblies and in the nuclear design calculations of large fast power reactors a variety of important nuclear data is involved. The fission spectrum is only one of several nuclear data that are important in the high-energy range and are still uncertain to some extent. Other uncertainties in the nuclear data field are the inelastic scattering cross-section and the fission cross-section of  $^{238}\text{U}$  for the calculation of criticality or critical mass and the capture cross-section of  $^{238}\text{U}$  for the determination of the breeding properties of power reactors. To draw more definite conclusions with respect to the reliability of these other data it is highly desirable to know the form of the fission spectra of the different isotopes rather accurately.

#### ACKNOWLEDGEMENT

The authors would like to thank Mr. J. Braun for his support in the numerical work.

#### REFERENCES

- [1] Reactor Physics Constants, Rep. ANL-5800.
- [2] SCHMIDT, J.J., Rep. KFK 120, EANDC-E-35 "U" (1966).
- [3] BARNARD, R. et al., Nucl. Phys. **71** (1965) 228.
- [4] ABAGJAN, L.P. et al., Rep. KFK-tr-144 (1964).
- [5] WERLE, H., BLUHM, H., Fission-neutron spectra measurements of  $^{235}\text{U}$ ,  $^{239}\text{Pu}$  and  $^{252}\text{Cf}$ , to be published in J. nucl. Energy.
- [6] KIEFHABER, E. et al., Rep. KFK 969, EANDC(E)-118 "U" (1970).
- [7] HELM, F., Rep. KFK 975 (1969).
- [8] KIEFHABER, E., Rep. KFK 1314 (1970).
- [9] FABRY, A., personal communication, Feb. 1970.
- [10] PITTERLE, T.A. et al., "Evaluation of modifications to ENDF/B version II data", Third Conf. Neutron Cross Sections and Technology, Knoxville, 1971.
- [11] PITTERLE, T.A., Nuclear Data for Reactors (Proc. Conf. Helsinki, 1970) **2**, IAEA, Vienna (1970) 687.
- [12] KALLFELZ, J.M., ZOLOTAR, B.A., SEHGAL, B.R., Rep. ANL-7610 (1970) 224-32.
- [13] BAKER, A.R., HAMMOND, A.D., Calculations for a Large Fast Reactor, TRG Rep. 2133(R) (1970).
- [14] EISEMANN, E., private communication, to be published in KFK 1310.
- [15] ENGELMANN, P., HAFELE, W., "The base program of the DeBeNeLux fast breeder project", Int. Conf. peaceful Uses atom. Energy (Proc. Conf. Geneva, 1971) **5**, IAEA, Vienna (1972) 63.
- [16] WINTZER, D., Reps KFK 633, SM101/13, EUR 3677e (1967), KFK 743, EUR 3725d (1969).
- [17] GREEBLER, P., et al., Significance of Neutron Data Uncertainties to Fast Reactor Economics and Power Plant Design, Rep. GEAP-5635 (1968).
- [18] ZARITSKI, S.M., TROYANOV, M.F., Int. Conf. Physics of Fast Reactor Operation and Design, BNES, London, 1969, translated from the Russian as KFK-tr-301.

# PROMPT FISSION NEUTRON SPECTRA

Gy. KLUGE

Central Research Institute for Physics,  
Budapest, Hungary

## Abstract

### PROMPT FISSION NEUTRON SPECTRA.

Some of the main features of the present theoretical understanding of the fission neutron spectra are discussed. The effect of a possible centre-of-mass anisotropy and the validity of Terrell's  $T(\bar{v})$  relation are discussed. Results of some calculations on the prompt fission neutron spectra are given.

## 1. INTRODUCTION

The main purpose of this paper is to give a short survey of the present state of the theory of the emission of prompt fission neutrons. The topic is a very large one and is of great importance both for 'pure' nuclear physics and for reactor physics and design. The large amount of experimental data and observations of the pre-1965 period and also most 'macroscopic' measurements of the ensuing period were surprisingly well interpreted by Terrell's considerations [1]. (The terms microscopic and macroscopic are used in a similar sense to that in nuclear physics, i. e. the first term is used in connection with the individual fragment nuclei, while the second refers to the totality of fission reactions.) However, understanding of such new observations as the saw-tooth dependence of the average number of prompt neutrons on the fragment mass, or the interpretation of the more sophisticated 'microscopic' measurements, including those with higher excitation energies, have revealed the need for an extension and detailing of the earlier theoretical interpretations. (It is a pity that not much has happened in this field.)

The need seems to be twofold: the interpretations of the microscopic spectra, the possible existence of more detailed characteristics of scission neutrons and the understanding of emission processes at higher excitation energies on the one hand, and the deviations and some new observations on the characteristics of the measured spectra on the other require new considerations to solve the possible contradictions and new attempts to clarify the situation in a unified manner. I should like to make a small contribution in this direction by reviewing the present status of understanding.

### Remarks on the experimental situation

There seems to have been no significant progress in the microscopic measurement of neutron spectra from low-energy fission, not even in the interesting but rather difficult problem of scission neutrons, since the important measurements of various authors published between 1962 and 1965 [2-6]. This is not the case for fission induced by particles of higher energy (e. g. Refs [7-11]), alone an enumeration of the results

would go beyond the scope of this review. The practical need for better nuclear data has stimulated a number of authors to carry out neutron energy spectra measurements, partly with new techniques, partly over an extended energy range, or just to confirm earlier data or such newly observed phenomenon as the detection of peaks or some excess in the low-energy part of the fission neutron spectra [12-24].

## 2. BASIC CONCEPTS ON EMISSION SPECTRA

The contradictions in the conclusions drawn from experiments and the attempts to understand the best way of extracting information from measured spectra make it necessary to develop or revise Terrell's conclusions by tracing all the approximations made, whether consciously or not, in evaluating the experimental data. The energy and angular distributions of prompt fission neutrons measured in the laboratory frame of reference are described partly as a sum of contributions of neutrons emitted from flying fragments and, as an assumed possibility for the case of low-energy fission, partly by the contributions of 'central' or 'scission' neutrons, i. e. neutrons emitted before or just at the instant of scission of the fissioning nucleus. The investigation of neutrons of the latter kind is being carried out by studying the deviation between experimentally determined and calculated spectra, assuming only neutrons from the fully accelerated fragments in the calculations. In the course of such calculations one tries to determine the spectrum form in the frame of reference of the fully accelerated fragments and then transforms them into the laboratory system for possible comparison with the experimental data.

It has to be emphasized that the determination of the centre-of-mass (c. m.) spectra is physically of basic importance and at the same time a most difficult task. There may be a lot of different spectra, depending on such characteristics of the individual fragments as the initial excitation energy  $E^*$ , number of neutrons and protons,  $N, Z$ , spins and so on. Only those spectra  $\varphi_{c.m.}(\epsilon, \vartheta, E^*, N, Z, E_k)$  retaining parameters that are thought to be the most important will be considered.

In the first approximation  $\epsilon$  and  $\vartheta$  are the energy and the angle characterizing the direction of the emission of the neutrons in the c. m. system.  $E_k$ , the kinetic energy of the fragment, seems to be included only formally, but it connects the total and excitation energies of the fragments through the relation  $E_{\text{total}} = E_k + E^*$ . The total spectra of neutrons in the c. m. system could be described by

$$N(\epsilon, \vartheta) d\epsilon d\vartheta = \sum_{N, Z} \int_{E^*} \rho(E^*, E_k, N, Z) \varphi_{c.m.}(\epsilon, \vartheta, E^*, N, Z, E_k) dE d\epsilon d\vartheta$$

The  $\rho$ -function gives the frequency of occurrence of the fragment with the given characteristics.

These spectra must be transformed individually into the laboratory system according to the kinetic energy of the given fragment. The connection between the centre-of-mass neutron energy,  $\epsilon$ , and that in the laboratory system is the well-known relation

$$E = E_f + \epsilon + 2\sqrt{E_f\epsilon} \cos \vartheta$$

where  $E_f$  is the fragment kinetic energy per nucleon ( $E_k/A$ ), or more precisely the energy of a neutron moving with the velocity of the fragment.

Even if the c. m. spectrum forms for different fragments show strong similarity, rather large differences have been observed in the laboratory system in at least some characteristic spectrum parameters. Let the transformed spectra be  $\phi(E, \theta, E^*, N, Z, E_f)$ . Then the total spectrum of neutrons can be given as

$$N(E, \theta) dE d\theta = \sum_{N, Z} \int_{E^*} \rho(E^*, E_k, N, Z) \phi(E, \theta, E^*, N, Z, E_f) dE^* dE d\theta$$

The next approximation is the replacement of the  $N, Z$  pair by  $A$ , which implies an imaginary averaging over the different  $N, Z$  on the condition that  $A = N + Z$ . Then

$$N(E, \theta) dE d\theta = \sum_A \int_{E^*} \rho(E^*, E_k, A) \phi(E, \theta, E^*, A, E_f) dE^* dE d\theta$$

In Terrell's 'classical' consideration the sum over  $A$  is ignored by using one or several representative fragments and so the weighting function is reduced to the distribution probability of the different excitation energies, or in other words to the probability distribution of the fragment temperatures

$$N(E, \theta) dE d\theta = \int_T p(T) \phi(E, \theta, T) dT dE d\theta$$

As the transformation from the c. m. to the laboratory system is independent of  $T$ , formulas in the c. m. and laboratory systems are similar.

The further approximation used to be to neglect the  $p(T)$  distribution by using only one of their  $T$  values.

In our work [25] we investigated another possible approximation, namely replacement of the initial energy distributions of the individual fragments by an average value, again in principle by an averaging

$$N(E, \theta) dE d\theta = \sum_A \rho(\bar{E}^*, \bar{E}_k, A) \phi(E, \theta, \bar{E}^*, A, E_f) dE d\theta$$

In this case  $\rho(E^*, E_k, A)$  becomes an expression proportional to

$$\nu(A) \cdot y(A)$$

Beyond the problems of averaging and of transforming from the c. m. to the laboratory system, the basic problem is the adequate description of the neutron cascades emitted from the individual fragments, i. e. the calculation of the functions  $\varphi_{c.m.}(\epsilon, \vartheta, E^*, N, Z)$  or  $\varphi_{c.m.}(\epsilon, \vartheta, E^*, A)$ . These

functions ought to be determined in a detailed Hauser-Feshbach calculation, but the enormous quantity of calculations involved makes it necessary to find reasonable simplifications.

One approximation, based on the compound reaction theory, is the assumption of isotropic, or at least symmetric angular distribution about  $90^\circ$ . This can be realized by a general function  $\varphi(\epsilon, E^*, A) \cdot (1 + b \cos^2 \theta)$ . A number of different assumptions and approximations exist for  $\varphi(\epsilon, E^*, A)$ . The most often used are the following:

$$(a) \quad \varphi_{c.m.}(\epsilon, E^*, A) \sim \epsilon \cdot \sigma_A^c(\epsilon) \cdot \omega_{A-1}(E^* - B_n - \epsilon)$$

where  $\sigma_A^c(\epsilon)$  is the cross-section of formation of a compound nucleus A of excitation  $E_i$  by a neutron of energy  $\epsilon$ ;  $\omega_{A-1}(E^* - B_n - \epsilon)$  is the density of nuclear energy levels in the final nucleus with mass number A-1, and  $B_n$  is the binding energy of a neutron.

From this an evaporation spectra of the form  $\epsilon \exp(-\epsilon/T)$  is derived in the case of one neutron emission with the assumption of a constant  $\sigma_A^c$ . In this case, and in this case only, does the T parameter have some real, immediate relation to the nuclear temperature, although on the other hand the validity of the derivation for neutron energies  $\epsilon \ll \bar{\epsilon}$  or  $\epsilon \gg \bar{\epsilon}$  is rather questionable. (However, in the latter case, at small residual excitation energies the exact level densities could show a similar functional form up to energies where the use of level-densities becomes meaningless.)

(b) The Maxwellian approximation

$$\varphi_{c.m.}(\epsilon, E^*, A) \sim \epsilon^{1/2} \exp(-\epsilon/T)$$

is supported by two special reasons. One is the general  $1/\sqrt{\epsilon}$  behaviour of the inverse cross-sections at low energies, the other is the theoretical reasoning of Le Couteur and Lang's studies [26], according to which a spectrum of the neutron cascade emission from a nucleus having a distribution of the initial excitation energies can be approximated tolerably well by a Maxwellian spectrum and there is a simple relation between the T parameter of the spectrum and the average initial excitation energy.

(c) The numerical results of 'exact' cascade calculation [25], which also seem to reproduce the experimentally observed spectra rather well.

(d) Phenomenological spectrum forms such as that of Bowman et al. [2].

In sum, we can draw the conclusion that until recently the best theoretical established spectrum form is the Maxwellian one. This form automatically takes into account the spread in the initial excitation energies, so giving a reasonable simplification in the very complicated calculations. For experimental tests these spectrum forms have to be transformed into the laboratory system and averaged for the different fragments and excitation energies.

### 3. SCISSION NEUTRONS

Comparison of the measured and calculated total angular and energy spectra indicates that there are extra neutrons with isotropic angular



distribution in the laboratory system (Refs [2-6]). It appears that about 10-15% of all prompt neutrons belong to this 'central group' of neutrons and their average energy is somewhat greater than that of the prompt neutrons generally. It assumed that they are emitted about the instant of the scission and they are therefore referred to as 'scission' neutrons.

In 1965 Sargent et al. were unable to demonstrate the existence of scission neutrons in photofission of  $^{232}\text{Th}$ . As an attempt to clarify the problem of the reality of the scission neutrons, or at least of some of their properties, it has been shown in Ref. [25] that one cannot exclude the possibility that this central component of neutrons might arise as a consequence of insufficiently precise evaluation of the experimental data.

#### 4. ENERGY SPECTRA OF FISSION NEUTRONS

If the centre-of-mass emission spectrum is isotropic, the laboratory energy spectrum for a given  $E_f$  is

$$N E dE = \int_{(\sqrt{E}-\sqrt{E_f})^2}^{(\sqrt{E}+\sqrt{E_f})^2} \varphi(\epsilon) / 4\sqrt{E_f} \cdot \epsilon d\epsilon$$

If the emission spectra of neutrons is of Maxwellian type, one gets the Watt distribution:

$$N(E) dE = (e^{-E_f/T} / \sqrt{\pi E_f T}) \cdot e^{-E/T} \cdot \sinh(2\sqrt{E E_f}/T)$$

This Watt distribution with its simple average  $E_f$  (0.75 MeV) does not fit the experimental data, indicating a c.m. emission spectrum, broader than a single Maxwellian and hence possibly the necessity for a more realistic averaging process for the different  $E_f$  values, as suggested in Ref. [1]. Moreover, c.m. spectra are better represented by a sum of two Maxwellian distributions of different average energy and thus the laboratory spectra can be viewed as a sum of at least four Watt distributions, the result of which is close to a Maxwellian distribution. See Ref. [1].

Note that the same situation is valid for the case of c.m. evaporation spectra, i.e. the sum of evaporation spectra transformed into laboratory system can be approximated rather well by one Maxwellian spectrum [18]. These observations confirm the considerations of the first part of this paper.

#### Effect of a c.m. anisotropy on the energy spectra

One has to take into account also the effect of a possible anisotropy of the c.m. fission neutron spectrum [27]. Here we quote Terrell's result for a spectrum

$$\varphi_{c.m.}(\epsilon, \vartheta) = \varphi_{c.m.}(\epsilon) (1 + b \cos^2 \vartheta)$$

Then the laboratory spectrum is

$$N(E)dE = \int \frac{\varphi(\epsilon)[1 + b(E - E_f - \epsilon)^2 / 4\epsilon E_f]}{4(\epsilon E_f)^{1/2}(1 + b/3)} d\epsilon$$

It can be observed that an anisotropy of this type causes a perturbation in the energy spectra, but for low energies leaves the  $E^{1/2}$  dependence unchanged, even allowing for the possibility of a fit to a Maxwellian with changed  $T$  and with not so good overall agreement.

The main effect of an anisotropy with  $b > 0$  is twofold:

(a) A decrease in the neutron yield between 0.7 and 3 MeV

(b) An increase elsewhere at the expense of the average energy.

Thus in principle the anisotropy can cause the effect observed by Meadows and other authors, namely a surplus number of neutrons at low energies relative to a Maxwellian fit at other energies. This possibility was not verified until recently.

## 5. TERRELL'S $T(\nu)$ RELATION

An inadequate averaging process can cause deviations in some of the experimental data from the simple form of the relation between the average neutron energy and the average number of neutrons proposed by Terrell. From the relation between the laboratory and c. m. neutron energies one gets for the averaged values of these energies

$$\bar{E} = \bar{E}_f + \bar{\epsilon}$$

where

$$\bar{\epsilon} \sim \bar{T} = \langle \bar{E}_f^{1/2} / a^{1/2} \rangle_{AV} \sim [(\bar{\nu} + 1) E_0 / 2a]^{1/2}$$

$\bar{T}$  is an averaged, representative value of the parameters of the assumed evaporation spectra, and  $a$  is an average of the different level-density parameters

$$\bar{E}_f = \bar{E}_f^* - B_n - \bar{\epsilon} \sim (\bar{\nu} + 1)E_0/2$$

where  $\bar{\nu}$  and  $E_0$  are the average number and the average excitation energy change per emitted neutron, respectively.

For the value of  $E_f$  Terrell obtained  $0.78 \pm 0.02$  and later  $0.74 \pm 0.02$  MeV. The fact that  $E_f$  remains essentially unchanged for a wide range of  $Z$  and  $A$ , although the total fragment kinetic energy divided by the total number of nucleons  $E_f = E_k/A = 0.121Z^2/A^{4/3}$  increases with  $Z$ , may be connected with the compensating decrease of the mass ratio with increasing  $Z$  [1].

However, these considerations seem to stray too far from the exact averaging process by a  $\rho(E^*, E_k, N, Z) \cdot \varphi_{c.m.}(\theta, \varphi, E^*, N, Z)$  distribution.

We can state that Terrell's  $T(\nu)$  expression for the  $T$  parameters of the laboratory energy spectra

$$\bar{E} = 3/2 T \sim a + b\sqrt{\bar{\nu} + 1}$$

is a rough general guide and is probably a good expression for the case of different excitations of the same fissioning nuclei if the fragment mass yields and the kinetic energy distributions do not change drastically with the variations of the excitation. On the other hand, a too precise test of this expression for different fissioning nuclei seems to be meaningless.

## 6. SPECTRA AT HIGHER EXCITATION ENERGIES

The study of the  $T(\bar{\nu})$  relation leads directly to the problem of investigating neutron spectra at higher excitation energies (above 10 MeV). Despite the experimental difficulties, a considerable number of such experiments on fission neutrons have been carried out [7-11]. The 'microscopic' information of great importance, such as the dependence of average neutron energies on the fragment mass, has been obtained, but in general this gives no direct information for the evaluation of the total neutron spectra.

The theoretical considerations should be similar to those for the case of low excitation energies, but the problem of the poorly known dependence of the previously mentioned weighting functions and that of the characteristics of the spectrum shapes of the neutron cascade processes make them especially difficult.

After these short remarks I should like to turn back to a discussion of the problem of the evaluation of experimental neutron spectra of fissioning nuclei at lower excitation energies.

## 7. RESULTS OF SOME NEW CALCULATIONS

Though we cannot speak of a basic progress in the theoretical understanding of neutron spectra, the comparisons of results of different approximate calculations can give some guide for further studies.

On the basis of the approximations described in the first part of this paper we have made some pure theoretical calculations in the c.m. system of fragments, with the assumption of different spectrum types. By using realistic c.m. average energies and weighting functions for spontaneous fission of  $^{252}\text{Cf}$  and for the thermal fission of  $^{235}\text{U}$  we have obtained total neutron spectra in numerical forms.

What conclusions can be drawn from this calculation?

(1) All the total spectra could be described rather well by a simple Maxwellian spectrum, but the fits in different energy intervals give different values of  $T$  (see Table I).

(2) As mentioned by Meadows, the effect of anisotropy seems to be the most probable cause of the extra neutrons at low energies relative to the Maxwellian distribution (see Figs 1-5) but for more precise conclusions more detailed investigations are needed.

TABLE I. T VALUES OF VARIOUS BASIC SPECTRA FOR VARIOUS ENERGY RANGES

Energy range (MeV)	T for different basic spectra				
	MAX.	MAX-AN.	BOW	BOW-AN	CAS:
<sup>252</sup> Cf					
0.003 - 15	1.405 ± 0.007	1.384 ± 0.005	1.458 ± 0.003	1.435 ± 0.006	
0.5 - 15	1.374	1.385 ± 0.007	1.446	1.457 ± 0.003	
1 - 15	1.365	1.375 ± 0.006	1.442	1.453	
0.003 - 10	1.449 ± 0.008	1.391 ± 0.010	1.473	1.430 ± 0.009	
0.59 - 10	1.410	1.402 ± 0.020	1.458	1.470 ± 0.003	
With scission neutrons					
1.2 - 10	1.397	1.388 ± 0.020	1.453	1.466	
0.003 - 7.5	1.496 ± 0.009	1.422 ± 0.012	1.478 ± 0.005	1.405 ± 0.013	1.50 ± 0.007 <sup>a</sup>
0.5 - 7.5	1.445	1.458 ± 0.009	1.451	1.463 ± 0.005	1.46 ± 0.006 <sup>a</sup>
1 - 7.5	1.422	1.437	1.439	1.452	1.45 ± 0.005 <sup>a</sup>
0.003 - 6	1.521	1.424 ± 0.015	1.481 ± 0.006	1.390 ± 0.016	
0.5 - 6	1.470	1.482 ± 0.009	1.450	1.461 ± 0.006	1.306 ± 0.021
1 - 6	1.450 ± 0.006	1.466	1.435	1.448	1.268
0.003 - 2	1.671 ± 0.007	1.295 ± 0.040	1.592 ± 0.003	1.249 ± 0.044	
0.5 - 2	1.599 ± 0.007	1.595	1.579 ± 0.014	1.582 ± 0.010	1.938 ± 0.025
1.2 - 2	1.560	1.574	1.510 ± 0.017	1.527 ± 0.016	1.861 ± 0.027
0.003 - 1	1.741 ± 0.005	1.063 ± 0.050	1.594 ± 0.004	1.006 ± 0.050	
0.59 - 1	1.667	1.615 ± 0.004	1.656	1.613 ± 0.004	2.123 ± 0.018
<sup>235</sup> U					
0.003 - 15	1.342 ± 0.005		1.288 ± 0.008		

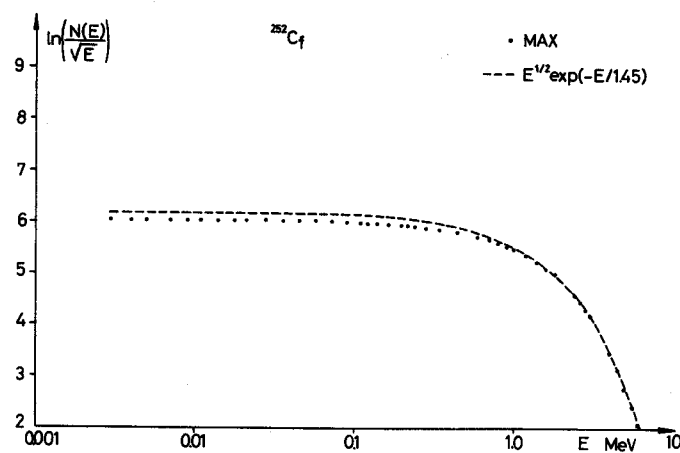
<sup>a</sup> With the spectrum of Ref.[2] averaged from 0° up to 85° only.

FIG. 1. Comparison of the sum of Maxwellians (MAX) and a single Maxwellian fit from 1 to 10 MeV.

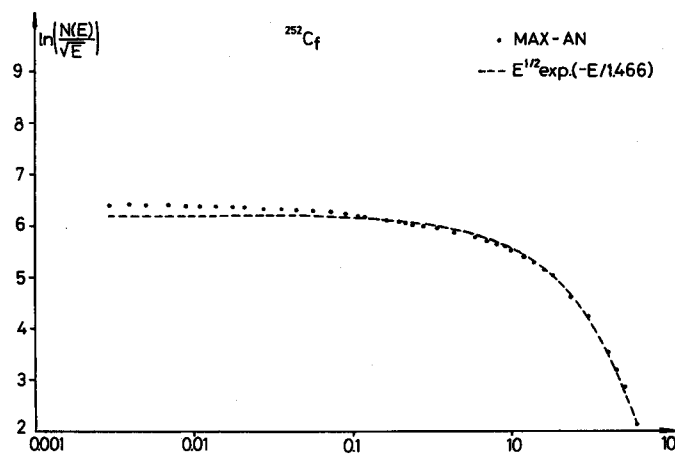


FIG. 2. Comparison of the sum of anisotropic Maxwellians  $\phi_M(\epsilon) (1 + 0.4 \cos^{16}\theta)$  (MAX-AN) and a single Maxwellian fit from 1 to 10 MeV.

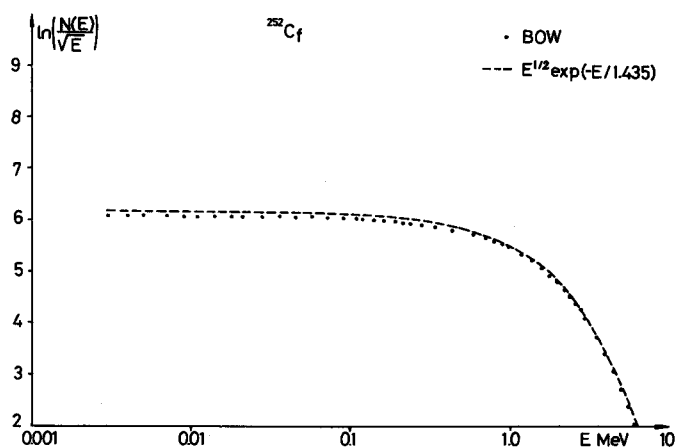


FIG. 3. Comparison of the sum of spectra from Ref. [2] (BOW) and a single Maxwellian fit from 1 to 10 MeV.

(3) The calculations direct attention to some possibilities of understanding the deviations in the values of spectrum temperatures obtained by the different authors for different energy ranges.

(4) The deviations in the experimental data from a single Maxwellian could indicate a description with two Maxwellians of different  $T$  parameters.

The conclusions with respect to the energy and angular distribution of neutrons are summarized in a paper to be published in Physics Letters [25]. Because of the lack of energy-angular distribution data below 0.5 MeV, the theoretical calculations likewise refer to neutron energies above 0.5 MeV.

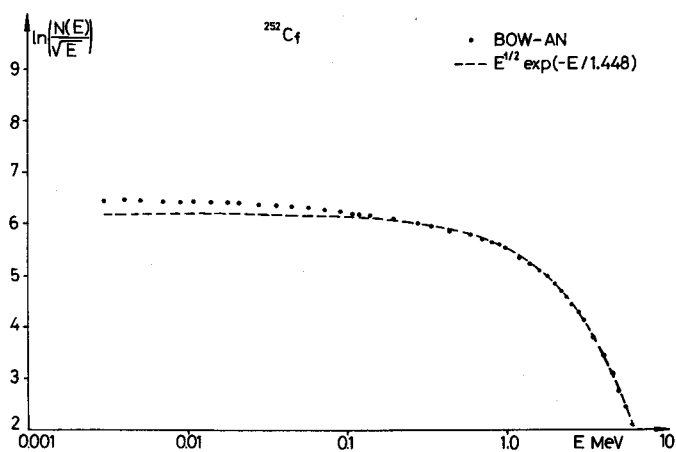


FIG. 4. Comparison of the sum of spectra from Ref. [2] with an anisotropic term  $1 + 0.4 \cos^{16} \theta$  (BOW-AN) and a single Maxwellian fit from 1 to 10 MeV.

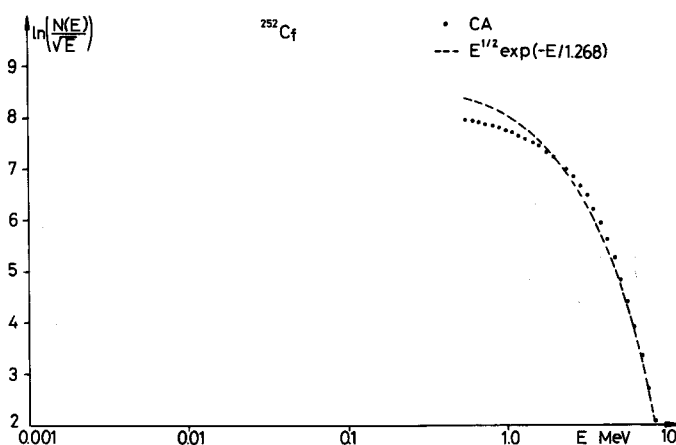


FIG. 5. Comparison of the sum of spectra from detailed cascade calculations [25] (CA) and a single Maxwellian fit from 1 to 10 MeV.

## 8. CONCLUSIONS

After this review of only some of the main features of the present situation of the fission neutron spectra, it must be stated that this paper is far from being a comprehensive or complete one. The intention has been to point out some interesting aspects of the problem that may have some actuality and should be settled in a more definite way. From this point of view we should keep in mind that both nuclear fission itself and neutron emission from fission reactions are very complex processes and the

simplifications that arise out of this complexity have only a limited range of validity. On this basis the following comments can be made on the subject.

(1) From the theoretical point of view similar experiments to those of Bowman et al., Skarsvåg and Bergheim, and others, but over extended energy ranges and for specific fragment excitations and kinetic energies, would be of great importance and could give more decisive information on the problem of a possible c.m. anisotropy, or on the problem of the existence of scission neutrons.

(2) Energy spectrum measurements with proper precision over extended energy intervals also would be very informative, if special care would be given to the accuracy of

- (a) the detection of fragments of all kinds and different kinetic energies
- (b) the proper averaging for the different angles (these remarks may not apply to earlier measurements)
- (c) the more detailed spectrum analysis not only by deducing an overall T parameter for the spectra but also by evaluating it for definite energy ranges
- (d) the effect of the different background problems [28].

(3) More spectrum measurements of fission of higher energies are required for the experimental study of  $T(\bar{\nu})$  relations. Perhaps these desires are too unrealistic at present, but results of this type would greatly help theoreticians to escape from the stagnation into which work on the solution of the problem of fission neutron spectra has fallen.

## REFERENCES

- [1] TERRELL, J., Phys. Rev. 113 (1959) 527; Physics and Chemistry of Fission (Proc. Symp. Salzburg, 1965) 2, IAEA, Vienna (1965) 3.
- [2] BOWMAN, H.R. et al., Phys. Rev. 126 (1962) 2120.
- [3] SKARSVÅG, K. et al., Nucl. Phys. 45 (1963) 72.
- [4] KAPOOR, S.S. et al., Phys. Rev. 131 (1963) 283.
- [5] SARGENT, C.P. et al., Phys. Rev. B137 (1965) 89.
- [6] MILTON, J.C.D. et al., Physics and Chemistry of Fission (Proc. Symp. Salzburg, 1965) 2, IAEA, Vienna (1965) 39.
- [7] SCHMITT, H.W. et al., Phys. Rev. Lett. 16 (1966) 1008; Phys. Rev. 172 (1968) 1213.
- [8] CHEIFETZ, E. et al., Phys. Rev. Lett. 21 (1968) 36.
- [9] BURNETT, S.C. et al., Phys. Rev. Lett. 21 (1968) 1350.
- [10] CHEIFETZ, E. et al., Phys. Rev. C2 (1970) 256.
- [11] BISHOP, C.J. et al., Nucl. Phys. A150 (1970) 129.
- [12] FABRY, A., Nukleonik 10 (1967) 280.
- [13] BOYCE, D.A. et al., Rep. AERE-PR/NP 14 (1968).
- [14] GRUNDL, J.A., Nucl. Sci. Engng 31 (1968) 191.
- [15] McELROY, W.N., Nucl. Sci. Engng 36 (1969) 15, 109.
- [16] BATCHELOR, R. et al., Rep. AERE 055/69.
- [17] OKRENT, D. et al., Nucl. Appl. Techn. 9 (1970) 454.
- [18] MEADOWS, J.W., Phys. Rev. 157 (1967) 1076.
- [19] BOSCHUNG, P. et al., Helv. phys. Acta 42 (1969) 225.
- [20] WERLE, H., Rep. INR-4/70-25 (1970).
- [21] ZAMYATNIN, Y.S. et al., Nuclear Data for Reactors (Proc. Conf. Helsinki, 1970) 2, IAEA, Vienna (1970) 183.
- [22] JÉKI, L. et al., Nuclear Data for Reactors (Proc. Conf. Helsinki, 1970) 2, IAEA, Vienna (1970) 87.
- [23] ALMÉN, E. et al., Nuclear Data for Reactors (Proc. Conf. Helsinki, 1970) 2, IAEA, Vienna (1970) 93.

- [24] SMITH, A.B., Rep. EANDC/USA/-153/L (1971).
- [25] KLUGE, Gy., Physics and Chemistry of Fission (Proc. Conf. Vienna, 1969), IAEA, Vienna (1969) 927; and to be published in Phys. Letters.
- [26] Le COUTEUR K.J., LANG D.W., Nucl. Phys. 13 (1959) 32; LANG, D.W., Nucl. Phys. 53 (1964) 113.
- [27] HILL, D.L., WHEELER, J.A., Phys. Rev. 89 (1953) 1102.
- [28] JÉKI, L. et al., Rep. KFKI-71-9 (1971).



# REMARKS ON NEUTRON FISSION RELATED TO THE RELATIVE IMPORTANCE OF THE SYMMETRIC AND ASYMMETRIC FISSION MODES

Ghislaine DE LEEUW-GIERTS, S. DE LEEUW  
Laboratoires du CEN,  
Mol-Donk,  
Belgium

## Abstract

REMARKS ON NEUTRON FISSION RELATED TO THE RELATIVE IMPORTANCE OF THE SYMMETRIC AND ASYMMETRIC FISSION MODES.

Any comparison between experimental mean energies of neutron-induced fission spectra and theory were up to now performed without taking into account the existence of the two different fission modes: a symmetric and an asymmetric one. The paper shows that the discrepancy observed with Terrell's laws could reasonably be explained if the physical characteristics of the neutrons emitted during symmetric and asymmetric fission were not the same; if neutrons emitted during symmetric fission were not emitted by the fully accelerated fission fragments but at the moment of scission with the spectral characteristics found for the scission neutrons of thermal fission.

Theoretical neutron fission spectra have been extensively compared to experimental results in the case of thermal neutron fission characterized by an almost purely asymmetric fission mode, theory being based in this case on the hypothesis of the emission of neutrons by the fully accelerated fission fragments. Discrepancies between experimental neutron fission results and Terrell's  $\bar{E}(\bar{\nu})$  law and the existence of scission neutrons with spectra of rather large mean energies, together with discrepancies observed in charged particle fission between theory and experimental results, especially when neutron binding energies are involved, have led us to consider neutron fission as a superposition of the two fission modes with a relative importance related to the valley to peak ratio of the fragment mass distribution, at least for small variations of their ratio. Taking into account the nature of discrepancies observed, a reasonable distinction between the two fission modes as far as the emitted neutrons concerned is their emission mode.

Most of the discrepancies vanish if one adopts the following hypothesis:

"Neutrons emitted during the symmetric fission mode are not emitted by the fully accelerated fission fragments, but at the moment of scission."

There are no measurements to verify this hypothesis directly, as could be done by the determination of the angular fission neutron distribution emitted during a pure symmetric fission process, but it is possible to test its validity indirectly by comparing experimental  $\bar{E}$  values for neutron fission with  $\bar{E}$  calculated values using the following statements related to the hypothesis:

(1) Neutrons emitted during the symmetric fission mode are analogous to scission neutrons that have an evaporation spectrum with large mean energy.

(2) The mass yield before neutron emission  $Y(M^*)$  is a sum of two components, a symmetric  $Y_s(M^*)$  and an asymmetric  $Y_a(M^*)$  one. Thus:

$$Y(M^*) = Y_a(M^*) + Y_s(M^*)$$

The fractions of symmetric and asymmetric fission are then defined by

$$F_{a,s} = \frac{\int Y_{a,s}(M^*) dM^*}{\int Y(M^*) dM^*}$$

where

$$F_a + F_s = 1$$

(3)  $\bar{\nu}$  may be decomposed as follows:

$$\bar{\nu} = \bar{n}_a F_a + \bar{n}_s F_s$$

where  $\bar{n}_a$  and  $\bar{n}_s$  are the mean number of neutrons emitted respectively for 100% asymmetric and symmetric binary fission, i. e.

$$\bar{n}_{a,s} = 2 \frac{\int n_{a,s}(M^*) Y_{a,s}(M^*) dM^*}{\int Y_{a,s}(M^*) dM^*}$$

$n_a(M^*)$  and  $n_s(M^*)$  being the number of emitted neutrons associated to mass  $M^*$  for the asymmetric and symmetric component respectively. In the  $\bar{E}$  determination,  $\bar{n}_s$  was taken as constant and equal to 7.5 [1].

(4) The fission spectrum is represented by the superposition of two distributions, one due to the neutrons emitted during symmetric fission and the other to asymmetric fission.

$$\bar{\nu} \chi(E) = \bar{n}_a F_a \chi_a(E) + \bar{n}_s F_s \chi_s(E)$$

the different  $\chi(E)$  being normalized to 1. The mean energy is given by

$$\bar{E} = \frac{\bar{n}_a F_a}{\bar{\nu}_a} \bar{E}_a + \frac{\bar{n}_s F_s}{\bar{\nu}_s} \bar{E}_s \quad (1)$$

Putting  $p_a = \bar{n}_a F_a / \bar{\nu}_a$  and  $p_s = \bar{n}_s F_s / \bar{\nu}_s$  then  $p_a + p_s = 1$ .

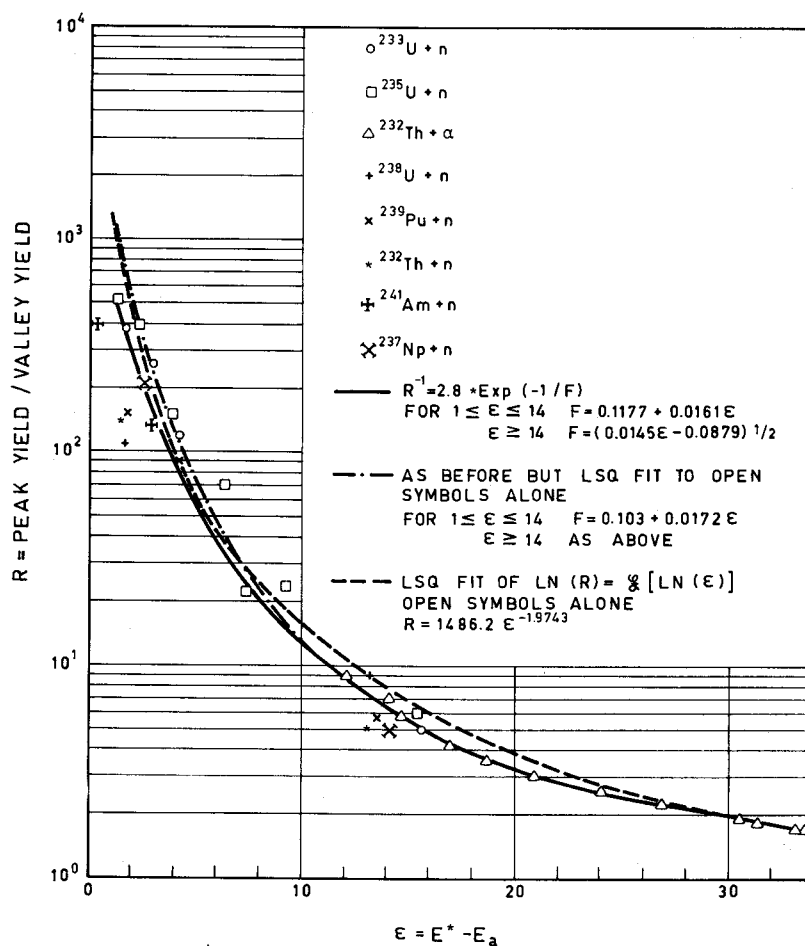


FIG.1. Comparison of peak to valley ratios.

$\bar{E}_a$  is the mean energy of the neutron spectrum issued from asymmetric fission for which Terrell's theory is admitted

$$\bar{E}_a = (0.746 + 0.646 \sqrt{\bar{n}_a + 1}) \text{ MeV}$$

$\bar{E}_s$  is the mean energy of the scission neutron spectrum. A constant value of 3 MeV [2] was assumed in the  $\bar{E}$  calculations.

(5) Fast neutron fission mass yields being very scarce,  $F_a$  and  $F_s$  were determined in two different ways, once from peak to valley ratios and once from valley yields for 200% binary fission.

(a) Peak to valley ratios from Refs [3-11] are shown in Fig. 1, together with possible least square fits. The fit adopted is given by the relation

$$R^{-1} = 2.8 \exp(-1/F)$$

where for

$$1 \leq E^* - E_a \leq 14 \quad F = 0.1177 + 0.0161 (E^* - E_a)$$

and

$$E^* - E_a \geq 14 \quad F = [0.0145 (E^* - E_a) - 0.0879]^{\frac{1}{2}}$$

with  $E^*$ : excitation energy

$E_a$ : activation energy for fission [12].

This fit is in agreement with the results of Turkevich et al. [13] and at high excitation energies gives a result quite similar to that obtained by Jones et al. [14]. The dashed line is given for comparison with Ref. [4]. It seems that a unique curve for all fissile isotopes can hardly be accepted at lower excitation energies, where the curve is probably not smooth at all. It is clear that these fits report only an overall trend of the valley to peak ratios.

(b) Experimental valley yields are reported in Fig. 2 as a function of excitation energy. The solid line fits the experimental results from Ref. [15] (squares) and Ref. [16] (open dots) by the procedure of Ref. [15]. The dashed line refers to first chance fission alone. To determine  $F_s$  one assumes a normal distribution curve for  $Y_s$  with a full width at half maximum equal to  $W_s$ . Its surface equals  $1.06 Y_v W_s$  if  $Y_v$  is the valley yield in per cent. The values of  $F_s$  so deduced are given for a total yield normalized to 200% by:

$$F_s = \frac{1.06 Y_v W_s}{200} \quad (2)$$

or

$$F_s = \left[ 2 R_0 \left( \frac{k}{1.06} \frac{W_a}{W_s} + 1 \right) \right]^{-1} \quad (3)$$

with  $R_0$ : peak to valley ratio corrected for the amount of symmetry products in the peak region

and  $k$ : form factor  $\sim 1$ .

Using both formulae it should be possible to deduce  $W_s$  from the experimental yield curves. In practice such an estimate is impossible because its extreme sensitivity to experimental inaccuracies. Errors of several hundred per cent are legion at low excitation energies, only at higher excitation energies ( $E_n \approx 14$  MeV) are the results better.

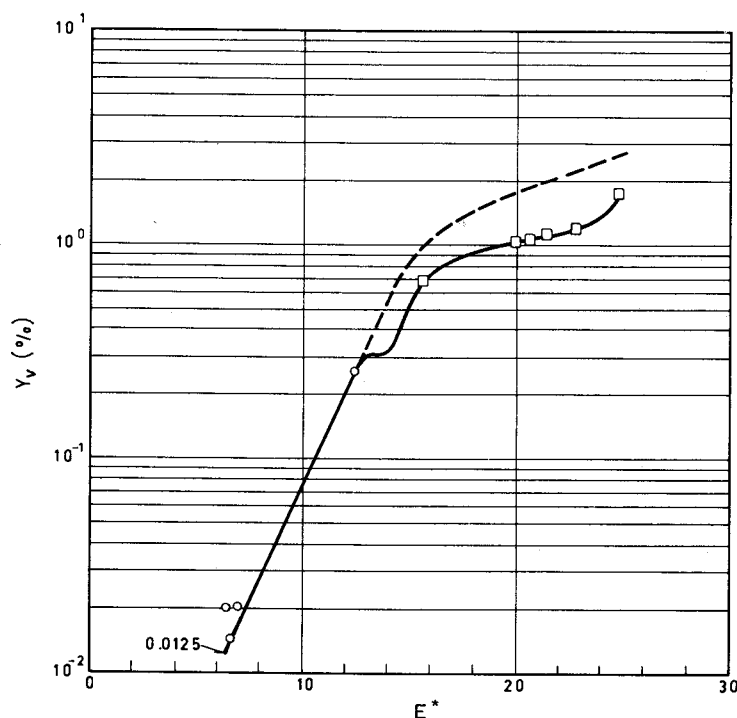


FIG. 2. Experimental valley yields as a function of excitation energy  $E^*$ .

To analyse the consistency of experimental and calculated  $\bar{E}$  values,  $\bar{E}$  values were determined by means of relation (1) and the above-mentioned statements for  $^{235}\text{U}$ . The results are compared in Fig. 3 with experimental  $\bar{E}$  values of several fission spectra. A trial and error procedure was used in which we assumed  $F_{\text{sth}}$  for thermal neutron fission, calculated  $W_{\text{sth1}}$  from relation (3) with  $R$  determined from Fig. 1 and corrected to obtain  $R_0$  and  $W_a = W_{\text{ath}}$  from the experimental data; or alternatively used relation (2) with  $Y_v$  from Fig. 2.

To calculate the  $\bar{E}$  values of the  $^{235}\text{U}$  fission spectra as a function of the incident neutron energy or corresponding experimental  $\bar{\nu}$  values,  $F_{\text{sth}}$  was taken as equal to 0.0055 [17] and  $W_s = W_{\text{sth1}}$ . The  $\bar{E}$  values computed with relation (2) correspond to the upper dashed curve, those computed with relation (3) to the upper dot-dashed one.

To make sure that the assumed  $W_s$  values were not inconsistent with experimental data,  $Y_{\text{ath}}(M^*) + Y_s(M^*)$  and  $Y_{\text{exp}}(M^*)$  were compared. No evident inconsistency was found up to  $E_n \approx 6$  MeV, which does not necessarily mean that  $W_s$  is constant up to this energy but that within the experimental errors of the existing data a constant value did not lead to inconsistencies. On the other hand, the 14-MeV yield data could not be fitted with that  $W_s$  value. The largest value that could be adopted was  $W_{s14\text{MeV}} \approx \frac{1}{2} W_{\text{sth}}$ . The lower dot-dashed and dashed curves were obtained for the new  $W_s$  value, corresponding to  $F_{\text{sth}} = 0.00275$ .

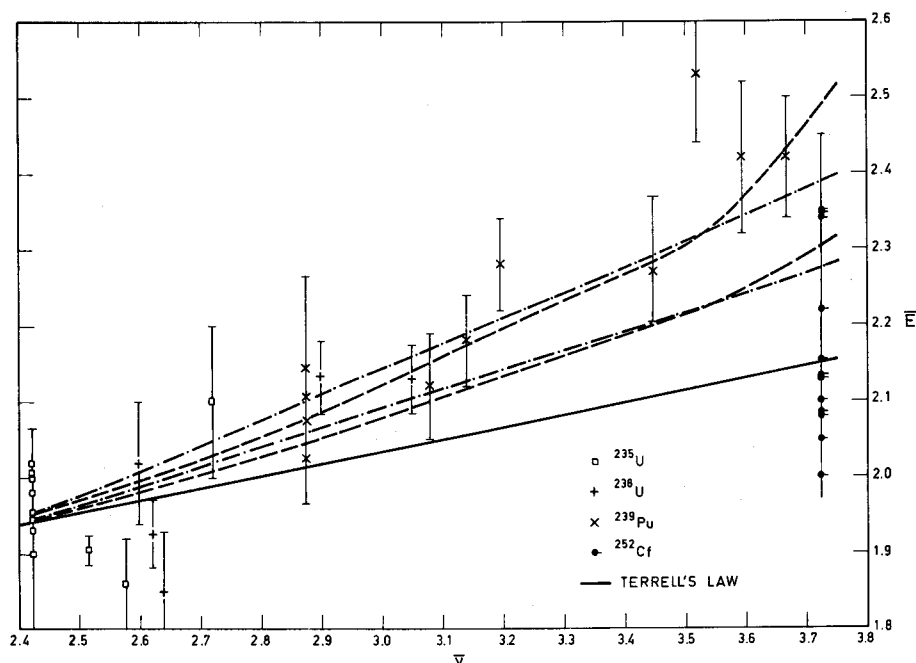


FIG.3. Comparison of  $\bar{E}$  values from Eq.(1), experimental  $\bar{E}$  values and Terrell's law.

Above about  $E_n = 6$  MeV the true result should be somewhat between the two sets, reaching the lower curve at 14 MeV. In this energy region, however, first chance fission is competitive and though this is not accounted for, no great confidence can be given to the results obtained there. The  $\bar{\nu}$  in Fig.3 are obtained from the best least square fit to the data of Refs [18-20] and the experimental points are from Refs [21-25]. The solid line gives Terrell's law [26, 27].

#### CONCLUSION

Although the  $\bar{\nu}_s$  and  $\bar{E}_s$  values used are somewhat arbitrary, the general trend of the curves of Fig.3 indicates that a symmetric fission component should be taken into account for intercomparison of experimental and theoretical results and that it is a possible explanation for the discrepancies observed between experimental  $\bar{E}$  values and Terrell's law, reinforcing the previously formulated hypothesis. Its introduction into theoretical evaluations on measurements, such as the determination of fragment mass distribution by the time-of-flight method, could give better agreement between theory and results.

Since  $\bar{\nu}_s$  and  $\bar{E}_s$  are difficult to determine experimentally, more precise values for theoretical use can be indirectly derived if more fragment mass distributions and  $\bar{E}_X(E_n)$  are available.

## REFERENCES

- [1] PLASIL, E., FERGUSON, R.L., SCHMITT, H.W., Physics and Chemistry of Fission (Proc. Symp. Vienna, 1969), IAEA, Vienna (1969) 505.
- [2] KAPOOR, S.S. et al., Phys. Rev. 131 (1965) 283.
- [3] CORYELL, C.D., SUGARMAN, N., Eds, Radiochemical Studies: The Fission Products, NNES Div. 4, 9, McGraw-Hill, New York (1951).
- [4] VON GUNTEN, H.R., Act. Rev. 1 (1969) 275.
- [5] D'YACHENKO, P.P. et al., Soviet J. nucl. Phys. 6 (1968) 6.
- [6] BURNEY, L.R., SCADDEN, E.M., J. inorg. nucl. Chem. 27 (1965) 1183.
- [7] APALIN, V.F. et al., Nucl. Phys. 55 (1964) 249.
- [8] FORD, G.P., GILMORE, J.S., Rep. LA-1997.
- [9] KATCOFF, S., Nucleonics Handbook of Nuclear Research Technology, McGraw-Hill, New York.
- [10] TURKEVICH, A., NIDAY, J.B., Phys. Rev. 81 (1952) 1.
- [11] HICKS, H.G. et al., Phys. Rev. 128 (1962) 700.
- [12] VANDENBOSCH, R., SEABORG, G.T., Phys. Rev. 110 (1958) 2.
- [13] TURKEVICH, A. et al., Phys. Rev. 89 3 (1953) 552.
- [14] JONES, W.H. et al., Phys. Rev. 99 (1955) 184.
- [15] FORD, G.P., LEACHMAN, R.B., Phys. Rev. 137 4B (1965) B82b.
- [16] MEADOWS, J.W., Phys. Rev. 177 (1969) 1817.
- [17] MILTON, J.C.D., FRASER, J.S., Can. Forum Physics 40 (1962) 1633.
- [18] SOLEILHAC, M. et al., J. nucl. Energy 23 (1969) 257.
- [19] MATHER, D.S., BAMPTON, P.F., AWRE Rep. 044/71.
- [20] MATHER, D.S., BAMPTON, P.F., AWRE Rep. 086/70.
- [21] COPPOLA, M., KNITTER, H.H., Z. Phys. 232 (1970) 286.
- [22] KNITTER, H.H. et al., Z. Phys. 244 (1971) 358.
- [23] KNITTER, H.-H., COPPOLA, M., ISLAM, M.M., AHMED, N., JAY, B., "Fission neutron energy spectra induced by fast neutrons on  $^{238}\text{U}$ ,  $^{235}\text{U}$  and  $^{239}\text{Pu}$ ", these Proceedings.
- [24] WERLE, H., BLUHM, H., "Fission-induced spectra measurements of  $^{235}\text{U}$ ,  $^{239}\text{Pu}$  and  $^{252}\text{Cf}$ ", these Proceedings.
- [25] SMITH, A.B., "Fission neutron spectra: Perspective and suggestion", these Proceedings.
- [26] TERRELL, J., Phys. Rev. 113 (1958) 2.
- [27] TERRELL, J., Phys. Rev. 127 (1962) 3.





## CONCLUSIONS AND RECOMMENDATIONS

After listening to the papers and subsequent discussion the meeting reached consensus on a number of points, which are reflected in recommendations formally adopted in the final session. These notes attempt to place these recommendations in context. The framework of these recommendations is to be found in the paper by A. B. Smith at the beginning of these Proceedings and much detailed supporting argument is to be found there. The recommendations fall into three classes, viz. those directed particularly at the microscopic area, those directed at the macroscopic area and those of a more general nature.

### MICROSCOPIC MEASUREMENTS

It was recognised that just as there was a need for standard cross-sections such as those for scattering of neutrons by hydrogen or carbon so it would be of value if there were a well-measured and documented fission spectrum to act as a standard in this field. It was essential that the standard spectrum should be measurable by as many of the standard techniques as possible. Two candidates were considered, viz. the spontaneous fission of  $^{252}\text{Cf}$  and the fission of  $^{235}\text{U}$  by thermal neutrons. It did not seem possible that either would completely satisfy everyone's needs. For time-of-flight systems  $^{252}\text{Cf}$  had to be contained in a fission chamber with the attendant complexity of corrections for environmental scattering. On the other hand, it could be used in the absence of reactor or accelerator neutron sources. There was also a problem of its availability. It was felt that  $^{235}\text{U}$  was widely available in whatever quantity required. The agreed solution was for both to be regarded as standards.

#### Recommendations

1. We recommend that the fission neutron spectrum of  $^{235}\text{U}$  arising from fission induced by neutrons below 150 keV should be regarded as a standard. High priority should be given to its precise determination over an energy range from a few keV up to above 10 MeV. The experimental data should be made available in tabular form, including estimated errors. We suggest it would be valuable to make strictly comparable measurements of the fission neutron spectra of other elements such as  $^{239}\text{Pu}$  at the same incident neutron energy and under essentially identical experimental conditions to those used for the 'standard' measurements. The point by point ratios of the unknown to the standard would constitute valuable data.
2. High priority should be given to the determination of the  $^{252}\text{Cf}$  fission neutron spectrum to the best possible precision over an energy range from a few keV up to at least 10 MeV and to relate them to the  $^{235}\text{U}$  standard. The quality of the results should be such as to make it a 'standard' fission neutron spectrum.

The results presented by Holmqvist at this meeting, together with analyses of other results both at this meeting and from the published literature, convinced the participants that the simple Maxwellian form could not be regarded as a satisfactory representation of the fission neutron spectrum. This representation is very poorly grounded in theory. The meeting accepted that a more complex representation would be required but that it would be premature to suggest one. Instead it was felt that for the present a purely numerical representation of experimental results would be best. The meeting therefore resolved that:

3. It is recognised that a simple Maxwellian form does not satisfactorily fit all observed fission spectra.

One consequence of this is that it cannot be regarded as satisfactory to measure a part of the fission spectrum and extrapolate using a Maxwellian shape. As a result we recommend:

4. The shape of the fission neutron spectra of  $^{235}\text{U}$ ,  $^{238}\text{U}$ ,  $^{239}\text{Pu}$  — and, if possible, higher Pu isotopes — as a function of incident neutron energy should be studied. The fission neutron spectra should be measured over the entire fission neutron energy range from a few keV to  $\approx 10$  MeV. Techniques that specifically identify the observed neutrons as being of fission origin should be used in order to avoid distorting the fission neutron spectrum by elastically and inelastically scattered neutrons. The experimental data should be made in tabular form including the estimated errors.

There was considerable discussion on sources of systematic error in microscopic measurements. It was realized that few results had been fully corrected for multiple scattering in the sample and its environment. The calibration of the efficiency of detection systems as a function of neutrons energy as well as obtaining a reliable energy scale were also recognised as major problems. In time-of-flight methods the dangers due to delayed gamma rays, which could have half-lives of between nanoseconds and microseconds, were pointed out and the need for neutron detectors insensitive to these gamma rays was accepted. The results reported to date give no indication of a dependence of the spectrum on the angle between the incident neutron and the outgoing fission neutron. Nevertheless, because of neutron fragment and fragment-fission-neutron correlations, the possibility of this was recognised as existing. Dr. Knitter pointed out recent measurements of angular correlations that showed a greater angular dependence than had hitherto been supposed.

Arising from concern in these areas, the following recommendations were made:

5. Measurement systems employed in microscopic-fission spectrum experiments should be well calibrated, using a controlled monoenergetic neutron source and a standard such as hydrogen or carbon or other methods of equivalent accuracy, e. g. associated radioactivity or associated particle counting manganese bath, etc. The calibration should be inclusive of corrections for multiple processes and other perturbations.

6. Angular distribution measurements of fission neutrons relative to the direction of the incident neutron seem necessary as anisotropies of unknown magnitude may arise from a number of underlying causes, viz.

- (a) effect of anisotropic fission fragment angular distribution
- (b) effect of a possible anisotropy in emission of neutrons from the fission fragments in the centre-of-mass systems
- (c) some possible systematic errors in the neutron spectrum measurements.

7. Particular attention should be paid to measurements of the low-energy parts of the  $^{252}\text{Cf}$ ,  $^{235}\text{U}$  and other fission spectra where, in some experiments, the major departures from a simple Maxwellian shape have been suggested. To carry out time-of-flight measurements in the low-energy part of the  $^{252}\text{Cf}$  spectrum, a detector of well-known efficiency and smooth energy dependence from 1 - 200 keV, insensitive to gamma rays below 2 MeV, is required.

Although the meeting concentrated mainly on empirical measurements, the desirability of a theoretical understanding was strongly felt and therefore:

8. It is recommended that a theoretical understanding of the shape of fission spectra and that of  $\bar{\nu}(E_n)$  are very desirable in the long-term. To achieve this, multiparameter investigation of neutron spectra versus fragment mass,  $\bar{\nu}(A)$  and fission fragment mass distributions as a function of incident energy should be encouraged.

However, on one theoretical point this meeting sounded a note of caution. This was concerned with Terrell's  $T(\bar{\nu})$  formula. If we abandon a representation in terms of  $T$ , this becomes less useful. The considerable scatter of points round the theoretical line was not accepted as being purely random. The meeting therefore proposed:

9. The limited validity of Terrell's  $T(\bar{\nu})$  formula must be recognized concerning the possible differences in connection with:

- (a) the different type of fission reactions
- (b) the different excitation energies.

Notwithstanding this, however, in the absence of any empirical data the broad predictions of Terrell's formula must be regarded as the best available for applied use.

Although it should by now be standard practice, it was felt to be worth emphasizing that to reach and be of use to the reactor community data must be incorporated in appropriate compilations and evaluations. The meeting therefore adopted the following recommendation:

10. It is recommended that data on fission neutron spectra should be transmitted by the experimenter to his local nuclear data centre in numerical form as measured. A hard copy should be sent to the Nuclear Data Section of the IAEA who should correlate them and, at an appropriate time, issue a compilation and review. A detailed technological description of the experimental apparatus should be given and the environment described. A tabulation of the important parameters of the experiment should accompany the data. A clear account should be given of the corrections already applied to the data.

### Macroscopic Measurements

It was the analysis of integral experiments that first suggested that our knowledge of the fission neutron spectrum might not be as good as had been believed. However, the large body of relevant experiments comprised many complex measurements that required for their interpretation numerous different cross-sections. Recognising the extremely confused state of the interpretation of these experiments (see, e. g., the paper by Campbell and Rowlands in these Proceedings) the meeting proposed that for the immediate future there should be some concentration on the very simplest integral experiments. It was therefore recommended that:

11. Fundamental microscopic integral cross-sections ( $\chi_A$  is the thermal fission spectrum of isotope A)

(1)  $\bar{\sigma}_f(\chi_{235}, {}^{238}\text{U})$  and  $\bar{\sigma}_f(\chi_{235}, {}^{235}\text{U})$ ,  $\bar{\sigma}_f(\chi_{252}, {}^{238}\text{U})$  and  $\bar{\sigma}_f(\chi_{252}, {}^{235}\text{U})$  should be determined to an accuracy of  $\pm 2-3\%$ , preferably at more than one laboratory.

(2)  $\bar{\sigma}_f(\chi_{235}, {}^{238}\text{U})$  and  $\bar{\sigma}_f(\chi_{235}, {}^{235}\text{U})$  should be determined in an alternative approach, using pulsed-source and fast timing techniques for background reduction.

These are difficult measurements to the suggested precisions but this is considered to be the minimum requisite to giving a meaningful comparison with microscopic data.

There are a number of areas of nuclear data where important uncertainties have masked critical analysis as it relates to fission neutron spectra. It is appreciated that these are by no means the only shortcomings. It has been pointed out that improper computational procedures, ignoring dependence of spectra on incident neutron energy, lack of homogeneity of composition etc. all contribute to the confused analytical situation. Nevertheless it seemed important to get some of these important cross-sections right and so it was proposed:

12. To enable a more reliable interpretation of important integral measurements, absolute fission cross-section measurements are required for the following:

(a)  ${}^{238}\text{U}$ :  $E_n = 500 \text{ keV} - 1.3 \text{ MeV}$ ;  $\Delta\sigma = \pm 10\text{mb}$   
 $E_n = 1.3 - 2.0 \text{ MeV}$  ( $\Delta E = \pm 25 \text{ keV}$ );  $\frac{\Delta\sigma}{\sigma} = \pm 3\%$   
 $E_n > 2.0 \text{ MeV}$ ;  $\frac{\Delta\sigma}{\sigma} = \pm 2\%$

(b)  ${}^{235}\text{U}$ :  $E_n > 100 \text{ keV}$ ;  $\frac{\Delta\sigma}{\sigma} = \pm 2\%$

In view of the fact that the  ${}^{235}\text{U}$  fission cross-section serves as basic standard for the majority of fission and capture cross-section measurements, it is highly recommended that the second IAEA Panel on Neutron Standard Reference Data (to be held in November 1972) consider the  ${}^{235}\text{U}$  fission cross-section as one of the main discussion items.

(c)  ${}^{239}\text{Pu}$ :  $E_n > 100 \text{ keV}$   $\frac{\Delta\sigma}{\sigma} = \pm 2\%$

13. Measurements on  $^{238}\text{U}$  inelastic scattering should be extended above 1.5 MeV. Cross-sections for individual levels should be reported wherever possible; otherwise cross-sections over small energy intervals (250-500 keV) would be acceptable. If the degree of angular anisotropy is shown to be small ( $\approx 10 - 20\%$ ), then energy spectra at one angle (preferably  $55^\circ$ ) would suffice.

14. It is recognized that in some circumstances it will be necessary to use detectors based on the  $^6\text{Li}(n, \alpha)\text{T}$  reaction, e. g. Li glass, or sandwich detectors. The group is concerned that this cross-section is still inadequately known above 100 keV. For some applications especially below 100 keV, it is necessary to know the triton angular distribution.

Another 'simple' integral experiment suggested is to measure the age to the indium resonance of  $^{252}\text{Cf}$  fission neutrons in water. Harris has pointed out that a 10% change in age corresponds to a 200 keV change in average fission neutron energy about 2 MeV. (Besides, it was noted that this method, when applied to Pu and  $^{235}\text{U}$ , also gives good values for the ratios of average fission neutron energies.) It was therefore proposed that:

15. The age of  $^{252}\text{Cf}$  fission neutrons to indium resonance in  $\text{H}_2\text{O}$  should be determined to at least  $\pm 0.5 \text{ cm}^2$  using an ideal point source.

Many of the experimental worries were seen to be common to integral and differential measurements, e. g. concern over the effects of the environment. This gave rise to proposals:

16. In fission-neutron studies, careful attention should be given to spectral purity and a controlled environment.

17. Wherever possible, detectors employed for both differential and integral measurements should be carefully calibrated with a controlled mono-energetic neutron source. Foils used should be retained and made available for subsequent study and exchange.

The latter part of this resolution was given considerable importance.

#### GENERAL COMMENTS

In all kinds of experiments the participants recognized the need for the fullest criticism and assessment. This could only take place if a detailed account of the procedures were made widely available. In all scientific journals there is pressure to reduce the length of papers, which leads to the exclusion of much experimental detail whose importance might only be appreciated on reanalysis. The conclusion was that two-tier publication was inevitable, i. e. a detailed laboratory report accompanied by a brief article in the open literature. It was appreciated that some smaller institutions might have difficulties with this procedure. Perhaps this is an area in which the Agency could assist. The formal resolution of the meeting was:

18. More detailed information on the experimental equipment and the environment should be provided, together with the assumptions used for the analysis of the experiments and (including) the assessment of the corresponding corrections and errors.

## LIST OF PARTICIPANTS

### MEMBERS

ABRAMSON, D. (Mme)	Centre d'Etudes Nucléaires de Cadarache, St. Paul-lez-Durance, France
BERTIN, A.	Centre d'Etudes de Limeil, Boite Postale 27, 94 Villeneuve St. Georges, France
DE LEEUW-GIERTS, Ghislaine	Laboratoires du CEN, Mol - Donk, Belgium
FABRY, A.	Laboratoires du CEN, Mol - Donk, Belgium
FERGUSON, A. T. G. (Chairman)	AERE Harwell, Didcot, Berks., United Kingdom
GRUNDL, J. A.	Nuclear Radiation Division, US Department of Commerce, National Bureau of Standards, Washington, D. C. 20234, United States of America
HOLMQVIST, B.	AB Atomenergi, S-611 00 Studsvik, Nyköping, Sweden
ISLAM, M.	Bureau Central de Mesures Nucléaires, EURATOM, Steenweg Op Retie, Geel, Belgium
JÉKI, L.	Central Research Institute of Physics, P.O. Box 49, Budapest 114, Hungary

KIEFHABER, E.	Kernforschungszentrum Karlsruhe, Postfach 3640, 75 Karlsruhe, Federal Republic of Germany
KLUGE, Gy.	Central Research Institute of Physics, P.O. Box 49, Budapest 114, Hungary
KNITTER, H. -H.	Bureau Central de Mesures Nucléaires, EURATOM, Steenweg Op Retie, Geel, Belgium
NEFEDOV, V. N.	Scientific Research Institute of Atomic Reactors, Melekess, USSR
SMITH, A. B. (Chairman)	Argonne National Laboratory, 9700 South Cass Avenue, Argonne, Ill. 60439, United States of America
STEWART, L.	Los Alamos Scientific Laboratory, P.O. Box 1663, Los Alamos, N. Mex. 87544, United States of America
WERLE, H.	Kernforschungszentrum Karlsruhe, Postfach 3640, 75 Karlsruhe, Federal Republic of Germany

## SCIENTIFIC SECRETARIES

HJÄRNE, L.	Division of Research and Laboratories, IAEA
SCHMIDT, J. J.	Division of Research and Laboratories, IAEA



# HOW TO ORDER IAEA PUBLICATIONS

Exclusive sales agents for IAEA publications, to whom all orders and inquiries should be addressed, have been appointed in the following countries:

UNITED KINGDOM Her Majesty's Stationery Office, P.O. Box 569, London S.E.1  
UNITED STATES OF AMERICA UNIPUB, Inc., P.O. Box 433, New York, N.Y. 10016

In the following countries IAEA publications may be purchased from the sales agents or booksellers listed or through your major local booksellers. Payment can be made in local currency or with UNESCO coupons.

ARGENTINA Comisión Nacional de Energía Atómica, Avenida del Libertador 8250, Buenos Aires  
AUSTRALIA Hunter Publications, 58 A Gipps Street, Collingwood, Victoria 3066  
BELGIUM Office International de Librairie, 30, avenue Marnix, Brussels 5  
CANADA Information Canada, 171 Slater Street, Ottawa, Ont. K1A 0S 9  
C.S.S.R. S.N.T.L., Spálená 51, Prague 1  
Alfa, Publishers, Hurbanovo námestie 6, Bratislava  
FRANCE Office International de Documentation et Librairie, 48, rue Gay-Lussac, F-75 Paris 5<sup>e</sup>  
HUNGARY Kultura, Hungarian Trading Company for Books and Newspapers, P.O.Box 149, Budapest 62  
INDIA Oxford Book and Stationery Comp., 17, Park Street, Calcutta 16  
ISRAEL Heiliger and Co., 3, Nathan Strauss Str., Jerusalem  
ITALY Agenzia Editoriale Commissionaria, A.E.I.O.U., Via Meravigli 16, I-20123 Milan  
JAPAN Maruzen Company, Ltd., P.O.Box 5050, 100-31 Tokyo International  
NETHERLANDS Martinus Nijhoff N.V., Lange Voorhout 9-11, P.O.Box 269, The Hague  
PAKISTAN Mirza Book Agency, 65, The Mall, P.O.Box 729, Lahore-3  
POLAND Ars Polona, Centrala Handlu Zagranicznego, Krakowskie Przedmiescie 7, Warsaw  
ROMANIA Cartimex, 3-5 13 Decembrie Street, P.O.Box 134-135, Bucarest  
SOUTH AFRICA Van Schaik's Bookstore, P.O.Box 724, Pretoria  
Universitas Books (Pty) Ltd., P.O.Box 1557, Pretoria  
SWEDEN C.E.Fritzes Kungl. Hovbokhandel, Fredsgatan 2, Stockholm 16  
U.S.S.R. Mezhdunarodnaya Kniga, Smolenskaya-Sennaya 32-34, Moscow G-200  
YUGOSLAVIA Jugoslovenska Knjiga, Terazije 27, Belgrade

Orders from countries where sales agents have not yet been appointed and requests for information should be addressed directly to:



Publishing Section,  
International Atomic Energy Agency,  
Kärntner Ring 11, P.O.Box 590, A-1011 Vienna, Austria

